

Some pages of this thesis may have been removed for copyright restrictions.

If you have discovered material in AURA which is unlawful e.g. breaches copyright, (either yours or that of a third party) or any other law, including but not limited to those relating to patent, trademark, confidentiality, data protection, obscenity, defamation, libel, then please read our [Takedown Policy](#) and [contact the service](#) immediately

**THE ANTI-DIABETIC COMPOUND METFORMIN:
EFFECTS UPON BILE SALT ABSORPTION AND
VASCULAR COMPLIANCE.**

DALE CARTER

Doctor of Philosophy

THE UNIVERSITY OF ASTON IN BIRMINGHAM

October 2000

This copy of the thesis has been supplied on condition that anyone who consults it is understood to recognise that its copyright rests with its author and that no quotation from the thesis and no information derived from it may be published without proper acknowledgement.

Summary

The Anti-diabetic Compound Metformin: Effects upon Bile Salt Absorption and Vascular Compliance.

**Dale Carter
Doctor of Philosophy
2000**

The anti-diabetic drug, metformin, has been shown to reduce the incidence of macrovascular complications in type 2 diabetic patients, often associated with a lowering of total plasma cholesterol concentrations. This thesis has investigated potential mechanisms through which metformin might produce these effects. The possibility that metformin reduces cholesterol concentrations by reducing the intestinal re-uptake of bile salts was examined in anaesthetised rats with ^{14}C sodium glycocholate introduced into jejunal or ileal segments of small intestine. Subsequent monitoring of the appearance of ^{14}C sodium glycocholate in plasma and bile showed that metformin (250mg/kg) produced different effects on bile salt absorption in the ileal and jejunal regions. Metformin significantly reduced the movement of ^{14}C glycocholate from the ileum into bile and hepatic portal, arterial, and venous plasma. Conversely, metformin increased ^{14}C glycocholate uptake from the jejunum.

In human Caco-2 enterocyte preparations cultured on polyester membranes in transwell plates, metformin (10^{-2} M) significantly inhibited active transfer of ^{14}C sodium glycocholate from the apical to basolateral chamber. Integrity of monolayer preparations was confirmed using the non-transportable marker ^3H mannitol. Metformin (10^{-2} M) increased mannitol flux into the basolateral chamber implying an alteration of membrane integrity. The inhibitory effect of metformin on ^{14}C glycocholate transfer in conjunction with increased mannitol flux implies a specific effect upon bile salt transport.

To investigate whether metformin could reduce the onset of macrovascular disease, normal mice received a high cholesterol (5%) diet for nine months with and without metformin (250mg/kg). Thoracic aortic compliance was assessed using a sensitive modification of the Mulvany and Halpern myograph. Metformin significantly increased contractile responses and produced a leftward shift in the dose-response to noradrenaline. Metformin also increased tissue relaxation in response to acetylcholine at high concentrations. Microscopic examination of thoracic aorta determined no cholesterol deposition in any experimental group. Furthermore, plasma cholesterol concentrations actually decreased following chronic cholesterol feeding.

Investigation of the effects of metformin upon ^{14}C sodium glycocholate uptake and transfer has identified a specific ileal effect to reduce bile salt re-uptake. This effect may provide a basis for lowering circulating cholesterol concentrations through the tightly regulated feedback mechanisms that exist between lumenally absorbed cholesterol, cholesterol derived from *de novo* synthesis, and the circulating pool of bile salts derived from these sources. Chronic administration of metformin improved aortic compliance in mice.

Type 2 Diabetes Mellitus Cholesterol Thoracic Aorta Caco-2 Dimethylbiguanide

I would like to dedicate this thesis to Mum, Dad, Adrian, Sam, and Tigger. Many thanks for all the support and assistance, both financial and emotional, over the last three years. I hope this makes you proud. Last but certainly not least my love and appreciation goes to Emily for the support, confidence building and encouragement she has given me throughout this project.

Acknowledgements:

My extended thanks go primarily to my supervisors Dr Clifford J Bailey (Pharmaceutical Sciences, Aston University) and Dr Harry C S Howlett (Lipha-Merck Pharmaceuticals) for their invaluable advice, monitoring, and direction, without which, this thesis would not have been possible.

I would also like to thank Mrs Sue Turner (Aston University) for her excellent technical advice, support, and assistance over the past three years.

Many thanks also to Dr Ariëns and Kristina for the opportunity to visit Leeds General Infirmary, and their guidance and assistance during the Factor XIII assays.

I would also like to thank Mr Melvin Gamble, Mr Brian Burford, for their excellent assistance and tutorship, Mr Kevin Hughes and Mr Derek Stirling for their assistance and advice.

Finally, I would like to thank all my family and friends for their unwavering support particularly Emily whose encouragement and understanding has made the last three years possible.

List of Contents:

Title Page		1
Summary		2
Dedication		3
Acknowledgements		4
List of Contents		5
List of Figures		9
List of Tables		14
Chapter One:	Introduction	15
1.1	Diabetes Mellitus	16
1.2	NIDDM and associated conditions	18
1.2.1	Insulin resistance	19
1.2.2	Sites of Insulin resistance	21
1.2.2a	Liver	21
1.2.2b	Muscle	23
1.2.3	Hyperinsulinaemia	24
1.2.4	Obesity	24
1.2.5	Role of increased free fatty acids and the regulation of glycogen synthesis in NIDDM	25
1.3	Lipoprotein Homeostasis	27
1.3.1	Lipoprotein metabolism in NIDDM	33
1.4	Atherogenesis and NIDDM	35
1.4.1	Haemostatic Factors	39
1.5	Cholesterol Homeostasis	40
1.5.1	Cholesterol within Enterocytes	42
1.6	Bile Salts	44
1.6.1	Synthesis	44
1.6.2	Function	49
1.6.3	Transport	49
1.7	Treatment Regimens in NIDDM	53
1.7.1	Dietary Therapy	53
1.7.2	Anti-diabetic Agents	53
1.7.2a	Alpha-glucosidase Inhibitors	54
1.7.2b	Sulphonylureas	54
1.7.2c	Thiazolidinediones	55
1.7.2d	Insulin Therapy	55
1.7.3	Metformin	56
1.7.3a	Glucose Lowering Action	56
1.7.3b	Effects upon Lipids and Lipoproteins	57
1.7.3c	Vascular Effects	59
1.7.3d	Contraindications	60
1.7.3e	Hypotheses for Metformin's Cholesterol lowering effect	61
1.8	Aims and Objectives	62

Chapter Two:	Materials and Methods	64
2.1	<i>In vivo</i> Studies	65
2.1.1	Animal Care and Preparation	65
2.1.2	Radiolabel Preparation and Administration	66
2.1.3	Sample Collection #1	66
2.1.4	Surgical Manipulation	67
2.1.5	Sample Collection #2	68
2.2	Thin Layer Chromatography	68
2.3	Chronic Cholesterol Feeding Studies	70
2.3.1	Arterial Compliance Studies	71
2.3.1a	Study #1	71
2.3.1b	Mulvany and Halpern Multimyograph (Study #2)	72
2.4	Histology	74
2.4.1	Cryotomy	74
2.4.2	Enzymatic Cholesterol Determination	75
2.5	Determination of Total Plasma Cholesterol	77
2.6	Factor XIII Analysis	78
2.6.1	Factor XIII Activity Assay	78
2.7	<i>In vitro</i> Studies	81
2.7.1	Everted Intestinal Sacs	81
2.8	Cell Culture	85
2.8.1	L6 Skeletal Muscle Cell Culture	85
2.8.1a	Supplements and Media	85
2.8.1b	L6 Muscle Cell Maintenance and Propagation	86
2.8.1c	L6 Cell Seeding	87
2.8.1d	Uptake of 2-Deoxy-D-[1,2- ³ H]-Glucose by L6 Muscle Cells	87
2.8.2	Caco-2 Cell Culture	88
2.8.2a	Caco-2 Media and Supplements	88
2.8.2b	Maintenance and Propagation	89
2.8.2c	Seeding Transwell Inserts	90
2.8.2d	Long-term Storage of Caco-2 Cells	91
2.8.2e	Propagation of Cells from Long-term Storage	91
2.8.2f	Bile Salt Transport Studies	92
2.8.2g	Determination of Monolayer Integrity	93
2.8.3	The A7r5 Smooth Muscle Cell Line	94
2.8.3a	Cell Maintenance and Propagation	94
2.8.3b	Petri Dish Studies	95
2.8.3c	Uptake of 2-Deoxy-D-[1,2- ³ H]-Glucose by A7r5 Smooth Muscle Cells	95
2.8.4	Intracellular Calcium Image Analysis	96
2.8.4a	Drug Perfusion	97
2.8.4b	Apparatus	97
2.8.4c	Fluorescence λ	98
2.9	Statistical Analyses	100
2.9.1	Student's 't'-Test	100
2.9.2	Analysis of Variance and post-tests	100

Chapter Three:	The Effect of Metformin on Bile Salt Absorption: <i>In Vivo</i> and <i>In Vitro</i> Studies	102
3.1	Introduction: <i>In vivo</i>	103
3.2a	Results: <i>In vivo</i>	113
3.2b	The Effects of Metformin on ¹⁴ C Sodium Glycocholate Transfer in the Ileum and Jejunum	113
3.3	Introduction: <i>In vitro</i>	119
3.4	Results: <i>In vitro</i>	120
3.5	Discussion	145
Chapter Four:	Bile Salt Transport in the Caco-2 Epithelial Cell Line	156
4.1	Introduction	157
4.2	Results	163
4.3	Discussion	196
Chapter Five:	The Effect of Metformin and Cholesterol on the Compliance of Aortic Smooth Muscle	202
5.1	Introduction	203
5.1.1	Smooth Muscle	203
5.1.2	Endothelium	205
5.1.3	Hyperpolarisation	207
5.1.4	Endothelin	210
5.2	How Diabetes and its Associated Conditions Affect Vascular Function	213
5.3	Atherosclerosis	219
5.4	Results	225
5.4.1	Vascular Compliance Study #1	225
5.4.2	Vascular Compliance Study #2	228
5.4.3	Factor XIII Activity Assay	232
5.4.4	Total Plasma Cholesterol Assay	233
5.4.5	Uptake of 2-Deoxy-D-[1,2- ³ H]-Glucose by L6 Skeletal Muscle and A7r5 Smooth Muscle Cells	236
5.4.6	Calcium Imaging in Skeletal and Smooth Muscle Cells	237
5.4.7	Histology of Aortic Vessels	240
5.5	Discussion	269
5.5.1	Second Messenger Systems	272
5.5.2	Smooth Muscle Relaxation	277
5.5.3	Mechanisms through which Metformin may influence Vascular Responses	283
Chapter 6:	General Discussion	298
6.1	The Hypothesis behind this Study	299
6.2	Summary of Results	300
6.3	Hypotheses for the Cholesterol Lowering Effect of Metformin	302
6.4	Concluding Remarks	317

List of References		319
Appendices		351
Appendix I	Photographs of L6, Caco-2, and A7r5 Cells, Vascular Compliance Apparatus, Histological Stains of Thoracic Aorta from Vascular Compliance Studies, and Transmission Electron Micrographs of Mouse Thoracic Aorta	352
Appendix II	Physiological Buffers and Staining Protocols	360

List of Figures:

Figure		Page
1.1	Diagrammatic representation of the Glycogen Cycle and the influence of Free Fatty Acids on Glycogen metabolism	25
1.2	The role increased Free Fatty Acids play in potentiating hyperglycaemia	26
1.3	Diagrammatic representation of Cholesterol synthesis and absorption in intestinal epithelia	43
1.4	The <i>Classic</i> and <i>Acidic</i> pathways of Bile Salt synthesis	47
1.5	The Oxidative side chain pathway of Bile Salt synthesis	48
2.1	Representation of the Transwell culture system	92
3.1	Representation of Bile Acid transport through Ileal enterocytes	110
3.2.1	Effect of metformin in the Ileum on uptake and secretion of ^{14}C Sodium Glycocholate into hepatic bile	125
3.2.2	Effect of metformin on plasma ^{14}C content at 180 minutes following Ileal administration of ^{14}C Sodium Glycocholate	126
3.2.3	Effect of metformin on tissue ^{14}C content at 180 minutes following Ileal administration of ^{14}C Sodium Glycocholate	127
3.3.1	Effect of metformin in the Jejunum on uptake and secretion of ^{14}C Sodium Glycocholate into hepatic bile	128
3.3.2	Effect of metformin on plasma ^{14}C content at 180 minutes following Jejunal administration of ^{14}C Sodium Glycocholate	129
3.3.3	Effect of metformin on tissue ^{14}C content at 180 minutes following Jejunal administration of ^{14}C Sodium Glycocholate	130
3.3.4	Effect of metformin on tissue and luminal bolus ^{14}C content following administration of ^{14}C Sodium Glycocholate to Ileum and Jejunum	131
3.4.1	Effect of metformin on carotid artery plasma ^{14}C content over 60 minutes following Ileal administration of ^{14}C Sodium Glycocholate	132
3.4.2	Effect of metformin on tissue ^{14}C content at 60 minutes following Ileal administration of ^{14}C Sodium Glycocholate	133
3.4.3	Effect of metformin on carotid artery and hepatic portal vein plasma ^{14}C content at 30 and 60 minutes following Ileal administration of ^{14}C Sodium Glycocholate	134

3.5.1	Effect of metformin on carotid artery plasma ¹⁴ C content over 60 minutes following Jejunal administration of ¹⁴ C Sodium Glycocholate	135
3.5.2	Effect of metformin on carotid artery and hepatic portal vein plasma ¹⁴ C content at 30 and 60 minutes following Jejunal administration of ¹⁴ C Sodium Glycocholate	136
3.5.3	Effect of metformin on tissue ¹⁴ C content at 60 minutes following Jejunal administration of ¹⁴ C Sodium Glycocholate	137
3.5.4	Effect of metformin on tissue wall and luminal bolus ¹⁴ C content following administration of ¹⁴ C Sodium Glycocholate to Ileum and Jejunum	138
3.6.1	Acute effect of metformin on percentage transfer of ¹⁴ C Sodium Glycocholate by everted Ileal intestinal sacs (20mmol/l study)	139
3.6.2	Acute effect of metformin on percentage transfer of ¹⁴ C Sodium Glycocholate by everted Ileal intestinal sacs (10mmol/l study)	140
3.6.3	Acute effect of metformin on percentage transfer of ¹⁴ C Sodium Glycocholate by everted Ileal intestinal sacs (10mmol/l study 2)	141
3.6.4	Acute effect of metformin on percentage fluid transfer by everted Ileal intestinal sacs	142
3.7.1	Acute effect of metformin on percentage transfer of ¹⁴ C Sodium Glycocholate by everted Jejunal intestinal sacs (5mmol/l study)	143
3.7.2	Acute effect of metformin on percentage fluid transfer by everted Jejunal intestinal sacs	144
4.1.1	Effect of metformin on ³ H mannitol flux across Caco-2 monolayers from the apical chamber of transwell inserts	172
4.1.2	Effect of metformin on ³ H mannitol flux across Caco-2 monolayers into the basolateral chamber of transwell inserts	173
4.1.3	Effect of metformin on ³ H mannitol content of Caco-2 monolayers cultured on transwell inserts	174
4.1.4	Effect of metformin on ¹⁴ C Sodium Glycocholate transport across Caco-2 monolayers from the apical chamber of transwell inserts	175
4.1.5	Effect of metformin on ¹⁴ C Sodium Glycocholate transport across Caco-2 monolayers into the basolateral chamber of transwell inserts	176
4.1.6	Effect of metformin on ¹⁴ C Sodium Glycocholate content of Caco-2 monolayers cultured on transwell inserts	177
4.2.1	Acute effect of metformin and ouabain on ³ H mannitol flux across Caco-2 monolayers from the apical chamber of transwell inserts	178
4.2.2	Acute effect of metformin and ouabain on ³ H mannitol flux across Caco-2 monolayers into	

	the basolateral chamber of transwell inserts	179
4.2.3	Acute effect of metformin and ouabain on ^3H mannitol content of Caco-2 monolayers cultured on transwell inserts	180
4.2.4	Acute effect of metformin and ouabain on ^{14}C Sodium Glycocholate transport across Caco-2 monolayers from the apical chamber of transwell inserts	181
4.2.5	Acute effect of metformin and ouabain on ^{14}C Sodium Glycocholate transport across Caco-2 monolayers into the basolateral chamber of transwell inserts	182
4.2.6	Acute effect of metformin and ouabain on ^{14}C Sodium Glycocholate content of Caco-2 monolayers cultured on transwell inserts	183
4.3.1	Effect of unlabelled glycocholic acid on the transfer of ^3H mannitol and ^{14}C Sodium Glycocholate across Caco-2 monolayers cultured on transwell inserts	184
4.3.2	Comparison of the effect of unlabelled Glycocholic acid on the flux of ^3H mannitol across Caco-2 monolayers cultured on transwell inserts versus controls	185
4.3.3	Comparison of the effect of unlabelled Glycocholic acid on the transport of ^{14}C Sodium Glycocholate across Caco-2 monolayers cultured on transwell inserts versus controls	186
4.4.1	Reverse transfer of ^3H mannitol and ^{14}C Sodium Glycocholate across Caco-2 monolayers cultured on transwell inserts	187
4.4.2	Comparison of the apical to basolateral flux versus the basolateral to apical flux of ^3H mannitol across Caco-2 monolayers cultured on transwell inserts	188
4.4.3	Comparison of the apical to basolateral flux versus the basolateral to apical flux of ^{14}C Sodium Glycocholate across Caco-2 monolayers cultured on transwell inserts	189
4.5.1	Acute effect of metformin and ouabain on ^3H mannitol flux across Caco-2 monolayers from the apical chamber of transwell inserts (^{14}C D-glucose studies)	190
4.5.2	Acute effect of metformin and ouabain on ^3H mannitol flux across Caco-2 monolayers into the basolateral chamber of transwell inserts (^{14}C D-glucose studies)	191
4.5.3	Acute effect of metformin and ouabain on ^3H mannitol content of Caco-2 monolayers cultured on transwell inserts (^{14}C D-glucose studies)	192
4.5.4	Acute effect of metformin and ouabain on ^{14}C D-glucose transport across Caco-2 monolayers from the apical chamber of transwell inserts	193

4.5.5	Acute effect of metformin and ouabain on ¹⁴ C D-glucose transport across Caco-2 monolayers into the basolateral chamber of transwell inserts	194
4.5.6	Acute effect of metformin and ouabain on ¹⁴ C D-glucose content of Caco-2 monolayers cultured on transwell inserts	195
5.1.1	Chronic effect of cholesterol feeding on the contraction of murine thoracic aorta (study #1)	242
5.1.2	Chronic effect of metformin and cholesterol feeding on the contraction of murine thoracic aorta (study #1)	243
5.1.3	Comparison of the chronic effects of metformin and cholesterol feeding on the contraction of murine thoracic aorta to noradrenaline (study #1)	244
5.2.1	Chronic effect of metformin treatment on monthly food consumption values in mice fed a high cholesterol diet (study #1)	245
5.2.2	Chronic effect of metformin treatment on the average food consumption values per mouse per day (study #1)	246
5.2.3	Chronic effect of metformin treatment on mean body weight values between weeks 1 and 33 in mice fed a high cholesterol diet (study #1)	247
5.2.4	Chronic effect of metformin treatment on weekly body weight values in mice fed a high cholesterol diet (study #1)	248
5.3.1	Contraction of murine thoracic aorta in response to noradrenaline (study #2)	249
5.3.2	Chronic effect of cholesterol feeding on the contraction of murine thoracic aorta in response to noradrenaline (study #2)	250
5.3.3	Chronic effect of metformin and cholesterol feeding on the contraction of murine thoracic aorta in response to noradrenaline (study #2)	251
5.3.4	Comparison of the chronic effects of a standard rodent diet, a high cholesterol diet, and metformin with a high cholesterol diet on the contraction of murine thoracic aorta in response to noradrenaline (study #2)	252
5.3.5	Comparison of the chronic effects of a standard rodent diet, a high cholesterol diet, and metformin with a high cholesterol diet on the relaxation of murine thoracic aorta in response to acetylcholine (study #2)	253
5.4.1	Effect of chronic metformin treatment on monthly food consumption values in mice fed a high cholesterol diet (study #2)	254
5.4.2	Effect of chronic metformin treatment on the average food consumption values per mouse per day (study #2)	255

5.4.3	Effect of chronic metformin treatment on mean body weight values between weeks 1 and 36 in mice fed a high cholesterol diet (study #2)	256
5.4.4	Effect of chronic metformin treatment on weekly body weight values in mice fed a high cholesterol diet (study #2)	257
5.5.1	Chronic effect of metformin treatment on Factor XIII activity levels in mice fed a high cholesterol diet (study #1)	258
5.5.2	Chronic effect of metformin treatment on Factor XIII activity levels in mice fed a standard diet and a high cholesterol diet (study #2)	259
5.6.1	Metformin and insulin stimulated (individual treatments) uptake of 2-DG in L6 cells: 24h	260
5.6.2	Metformin and insulin stimulated (combined treatments) uptake of 2-DG in L6 cells: 24h	261
5.7.1	Effect of insulin on 2-DG uptake in A7r5 cells: 24h	262
5.7.2	Effect of metformin on 2-DG uptake in A7r5 cells: 24h	263
5.7.3	Effect of metformin and insulin (combined treatments) on 2-DG uptake in A7r5 cells: 24h	264
5.7.4	Effect of metformin and insulin (combined treatments) on 2-DG uptake in A7r5 cells: 24h	265
5.7.5	Effect of metformin and insulin (combined treatments) on 2-DG uptake in A7r5 cells: 24h	266
5.7.6	Effect of metformin and insulin (combined treatments) on 2-DG uptake in A7r5 cells: 24h	267
5.8.1	Acute effects of metformin and noradrenaline on intracellular calcium levels in A7r5 cells	268b
5.8.2	Acute effect of metformin on intracellular calcium levels in A7r5 cells	268c
5.8.3	Acute effects of metformin and noradrenaline on intracellular calcium levels in L6 cells	268d
6.1	Diagrammatic representation of the possible modes of action of metformin in the Intestine	315
6.2	Diagrammatic representation of the possible modes of action of metformin on the vascular system	316
a	Photograph of a confluent monolayer of Caco-2 cells derived from a human adenocarcinoma, $\times 10$	352
b	Photograph of a confluent monolayer of Caco-2 cells derived from a human adenocarcinoma, $\times 40$	352
c + d	Photographs of the multimyograph system	353

e	Photograph of a cryostat section of thoracic aorta (12µm) from a mouse fed a high cholesterol diet with metformin, × 10 H + E	354
f	Photograph of a cryostat section of thoracic aorta (12µm) from a mouse fed a high cholesterol diet with metformin, × 40 H + E	354
g	Photograph of a cryostat section of thoracic aorta (12µm) from a mouse fed a standard rodent diet × 10 H + E	355
h	Photograph of a cryostat section of thoracic aorta (12µm) from a mouse fed a standard rodent diet × 40 H + E	355
i	Photograph of a cryostat section of thoracic aorta (12µm) from a mouse fed a high cholesterol diet × 10 H + E	356
j	Photograph of a cryostat section of thoracic aorta (12µm) from a mouse fed a high cholesterol diet and stained for cholesterol × 10	356
k	Photograph of a cryostat section of mouse thoracic aorta (12µm) stained with Sudan III + IV, × 40	357
l	Photograph of a cryostat section of mouse thoracic aorta (12µm) stained with Oil Red O, × 40	357
m	Transmission electron micrograph of an endothelial cell of mouse thoracic aorta stained with lead citrate and uranyl acetate, × 15.000	358
n	Transmission electron micrograph of an endothelial cell and the luminal surface of mouse thoracic aorta stained with lead citrate and uranyl acetate, × 12.000	358
o	Photograph of a confluent monolayer of A7r5 smooth muscle cells derived from the thoracic aorta of embryonic rat × 40	359
p	Photograph of a confluent cluster of A7r5 vascular smooth muscle cells derived from the thoracic aorta of embryonic rat, incubated with Fura-2 and excited using the fluorescence ratio 360:380nm, × 40	359

List of Tables:

Table

1	Percentage recovery in hepatic bile of ¹⁴ C Sodium Glycocholate when administered to the Ileum and Jejunum in the presence and absence of metformin	119
2	Total plasma cholesterol levels in mice chronically fed a high cholesterol diet in the presence and absence of metformin	233

Chapter One:

Introduction

Chapter One: Introduction

1.1 Diabetes Mellitus:

Diabetes mellitus can be summarised as a condition of overt hyperglycaemia associated with a multitude of factors related to impaired metabolism of carbohydrate and fat. The origins of this condition arise from a contribution of genetic and environmental factors. The condition is precipitated by a deficiency of insulin secretion or resistance to the physiological effect of insulin (DeFronzo, 1997).

There are two main types of diabetes mellitus. Insulin-dependent diabetes mellitus (IDDM) also known as type 1, and non-insulin-dependent diabetes mellitus (NIDDM), also known as type 2. The introduction to this thesis will focus upon type 2 diabetes, reviewing how this disease may predispose the patient to life-threatening complications. The main focus of this thesis, however, will be directed towards one specific anti-diabetic drug used in the treatment of type 2 diabetes, dimethylbiguanide (metformin). In specific, this thesis will investigate how metformin can improve life expectancy of type 2 diabetic patients independently of glycaemic control, via its effects on lipoprotein parameters and on vascular compliance.

NIDDM is characteristically associated with hyperglycaemia, the patient probably having already passed through a prodromal period of impaired glucose tolerance (IGT) prior to definitive diabetes. These conditions are the result of

defects in insulin action and abnormalities of insulin secretion. Impaired insulin action, or insulin resistance, is usually accompanied by a compensatory increase in insulin secretion limiting the extent of hyperglycaemia. As the diabetic condition progresses, both insulin resistance and insulin deficiency become apparent. It is generally recognised that a variety of genetic and environmental factors confer upon an individual a susceptibility to become less sensitive to the acute metabolic effects of insulin, eventually giving rise to a condition of insulin resistance (DeFronzo, 1997).

Slight hyperglycaemia, a consequence of tissue resistance to insulin's effects, causes the pancreatic β cells to attempt to 'compensate' for the insulin resistance by secreting increasing amounts of insulin (DeFronzo, 1997). The increased levels of insulin secreted may lead to hyperinsulinaemia. This may continue for a lifetime, however in individuals who are genetically susceptible, and whose β cells display limited adaptive capacity for insulin secretion, then a point is reached where insulin secretion falls due to exhaustion of the β cell population. This usually occurs when the fasting glucose concentration exceeds 140 mg/dl or approximately 7.8mmol/l (DeFronzo, 1997). At this point hepatic glucose output (HGO) begins to increase, due to both insulin resistance at the hepatic level and falling insulin levels. HGO makes a major contribution to fasting hyperglycaemia (DeFronzo *et al.*, 1989). According to Scheck *et al.* (1991), insulin resistance in skeletal muscle is one of the most important sites for impaired glucose uptake in individuals with NIDDM. Insulin resistance (to the metabolic effects of insulin)

is, however, common in both tissue types and serves to potentiate elevated blood glucose levels (DeFronzo, 1997).

NIDDM accounts for up to 85% of all cases of diabetes worldwide and is associated with premature mortality as a result of its microvascular and macrovascular complications (Weir and Leahy, 1994). The prevalence of NIDDM is increased in people who are obese, those which are physically inactive and first-degree relatives of NIDDM sufferers. The problem of NIDDM is growing at an alarming rate and has been linked to industrialisation, affluence and an increased elderly population, making diabetes the fourth or fifth leading cause of death in most occidental societies.

1.2 NIDDM and associated conditions:

Individuals who suffer from NIDDM tend to have a variety of additional conditions associated with their diabetic state. Together this cluster of conditions is referred to as Syndrome X and consists of the following: -

- ❖ Insulin resistance
- ❖ Hyperinsulinaemia (initially)
- ❖ Hyperglycaemia
- ❖ Obesity (mainly visceral)
- ❖ Dyslipidaemia
- ❖ Atherosclerosis
- ❖ Coronary heart disease (CHD), the most common cause of death amongst diabetic patients.
- ❖ Pro-coagulant state

Not all of these conditions are necessarily present in a diabetic individual, however the presence of several of these factors is commonly seen in diabetic patients. The underlying feature of the proposed syndrome is believed to be insulin resistance, with hyperinsulinaemia and the other features occurring consequentially (Reaven, 1988). NIDDM itself, is a condition that leaves the sufferer susceptible to serious microvascular complications such as retinopathy, nephropathy, and neuropathy. Furthermore, the presence of syndrome X increases the prevalence of macrovascular disease in the diabetic individual.

1.2.1 Insulin resistance:

Insulin resistance is a common condition within the general population. Indeed evidence exists linking advancing age with a reduced sensitivity to insulin (DeFronzo, 1979). The majority of patients with IGT or NIDDM are insulin resistant, and initially the plasma insulin concentrations are raised. If, however, the pancreatic β cells are able to maintain the plasma glucose level within a 'normal range' then hyperglycaemia will not result. It is only when they are no longer able to sustain the increased levels of insulin secretion (which are required to compensate for the underlying insulin resistance) that hyperglycaemia appears (Reaven, 1988; Reaven *et al.*, 1989). Insulin resistance *per se* is probably present in the majority of individuals who are glucose intolerant, albeit at a mild level. There is a fine line between impaired glucose tolerance and overt diabetes, the latter may never develop and is ultimately dependent upon the magnitude of resistance to insulin and the adaptability of the β cells to compensate for this defect with hyperinsulinaemia.

There are two hypotheses for the progression of IGT to NIDDM as reviewed by DeFronzo (1997). The first hypothesis is that insulin resistance is the primary metabolic defect, and enhanced insulin secretion is merely a consequence of this. The second hypothesis involves the over secretion of insulin as the primary event, with insulin resistance as a consequence, presumably through down-regulation of insulin receptors. Indeed, there are arguments in support of both as to the origins of this disease, each as plausible as one another. Nevertheless we do not know for certain which metabolic defect precedes the development of type 2 diabetes, although the volume of evidence presently available suggests an initial defect of insulin resistance.

In a study by Taylor *et al.* (1992), some patients were seen to develop diabetes as a result of mutations in the insulin receptor gene. Such patients became severely resistant to insulin and consequently hyperinsulinaemic. This, according to Taylor *et al.* (1994), implies that both insulin resistance and hyperinsulinaemia commonly exist together and are instrumental in the progression of the disease. However, one of these factors alone can be a sufficient cause of diabetes and can be primary to hyperinsulinaemia in the development of NIDDM.

An alternative possibility in some individuals is that a primary defect of insulin secretion may be responsible for type 2 diabetes i.e. hypersecretion, as detailed by DeFronzo (1997). This is supported by the finding that hyperinsulinaemia in the fasting state and following a meal precede the development of insulin resistance in individuals with juvenile-onset diabetes. Insulin receptors may be down-regulated in insulin sensitive tissues as a result of excessive production of the

hormone. The net result is impaired glucose transport and glucose phosphorylation (Jeanrenaud, 1994; Del Prato *et al.*, 1994). There are, however, many hypotheses as to the primary cause of this insulin resistance, which is a characteristic feature of NIDDM; these will be discussed where relevant in the following paragraphs.

1.2.2 Sites of Insulin Resistance:

A characteristic feature of NIDDM is hyperglycaemia during both the fasting and postprandial state. The brain is responsible for the utilisation of approximately 50-60% of the glucose during the postabsorptive state. The use of glucose by the brain is insulin-independent and thus is not affected by the diabetic state (DeFronzo, 1997). In the non-diabetic state, secretion of insulin is stimulated above basal levels when glucose becomes available during a meal and the plasma glucose concentration rises above approximately 5.5mmol/l. Insulin normally prevents the production and release of glucose from the liver. However, in NIDDM this insulin signal is not generated due to insulin resistance and a blunted first phase release of the hormone. Thus, the liver continues to produce glucose when glucose is being absorbed from the intestine, contributing to the hyperglycaemia (DeFronzo, 1997).

1.2.2a Liver:

Hepatic glucose production (HGP) is regulated hormonally by the short-term actions of insulin and glucagon. The disposal of glucose by comparison is primarily under the control of insulin (Weir and Leahy, 1994). In the non-diabetic, HGP should under normal circumstances be suppressed by

hyperglycaemia (Revers *et al.*, 1984). However, in type 2 diabetes this normal autoregulation is impaired, i.e. the suppressive effect of hyperglycaemia on HGP is diminished. Indeed, glucose production by the liver is incremental as the state of diabetes worsens (DeFronzo, 1988). In addition to the suppressive effect of hyperglycaemia upon HGP, insulin normally inhibits HGP. Many subjects with NIDDM demonstrate fasting hyperinsulinaemia along with enhanced HGP leading to the conclusion that the liver has developed resistance to the metabolic actions of insulin (DeFronzo, 1997).

Glycogenolysis and gluconeogenesis account for glucose production from the liver (DeFronzo and Ferrannini, 1987; Cherrington *et al.*, 1987). Several studies, using radiolabelled gluconeogenic precursors have shown that gluconeogenesis accounts for over 90% of the increase in HGP in type 2 diabetes (Consoli *et al.*, 1989; Consoli *et al.*, 1990) and reflects impaired nutrient metabolism at various tissue sites.

In addition to insulin resistance, several mechanisms have been suggested to contribute to the increase in gluconeogenesis in type 2 diabetes. These include increased circulating levels of gluconeogenic precursors (such as lactate) (Consoli *et al.*, 1989), and hyperglucagonaemia (Baron *et al.*, 1987). These gluconeogenic precursors have become available to the liver due to disturbances in other areas of metabolism, themselves quite possibly a consequence of insulin resistance. Since insulin is known to regulate lipolysis, any reduction in the sensitivity to insulin will have widespread metabolic ramifications. An imbalance in the glucose-fatty acid cycle with increased free circulating fatty acid concentrations, results in increased fatty acid oxidation in the liver. This results in

preferential metabolism of free fatty acids (FFA) in place of glucose. In the liver excess FFA provides an energy source which facilitates gluconeogenesis and thereby potentiates hyperglycaemia.

1.2.2b Muscle:

Skeletal muscle is quantitatively the main site of insulin-mediated glucose disposal. As such, skeletal muscle is seen as the major site of impaired glucose uptake due to insulin resistance in diabetic patients (DeFronzo *et al.*, 1985). Hyperinsulinaemic clamp studies and forearm glucose uptake studies have demonstrated that insulin-stimulated glucose uptake is impaired in type 2 diabetic patients (DeFronzo, 1997). It has also been noted in various studies that basal glucose uptake may be increased in type 2 diabetic patients (Firth *et al.*, 1986; Gerich *et al.*, 1990). This can be attributed to the mass action effect of glucose, which is seen to promote passive uptake of glucose into cells (Best *et al.*, 1996).

The normal fate of glucose inside cells is altered in NIDDM patients. Little glucose is stored in the form of glycogen. This, together with impaired glucose oxidation, means that less glucose follows the normal metabolic routes for disposal (Felber *et al.*, 1987). Muscle glycogen synthase activity is also impaired and this decreases glycogen synthesis (DeFronzo, 1997). Consequently, gluconeogenesis occurs as a result of glucose being converted into other gluconeogenic precursors such as lactate, as mentioned previously (Avogaro *et al.*, 1996).

1.2.3 Hyperinsulinaemia:

The insulin resistance observed in obese non-diabetic individuals and those with IGT and the early stages of NIDDM is usually 'compensated' by enhanced insulin secretion (DeFronzo, 1988). This, at least initially, limits the extent to which metabolism is disturbed. It is important to note that both resistance to, and elevation of, plasma insulin levels are coexistent and important features commonly found in syndrome X. Although these complications are to be discussed individually it should be noted that the development of syndrome X would probably not occur, were it not for the loss of insulin sensitivity.

1.2.4 Obesity:

Obesity is highly prevalent amongst diabetic populations (Golay *et al.*, 1997). In many cases obesity reflects a sedentary lifestyle with excessive caloric intake (Flier, 1994). The incidence of diabetes increases with increased weight and particularly abdominal deposition of adipose tissue (Flier, 1994). Typically in obesity there exists insulin resistance, hyperinsulinaemia and increases in both lipogenesis and lipolysis. This increased turnover of abdominal lipids is a characteristic of obesity and supplies extra FFAs to the liver, thereby contributing to hepatic insulin resistance (Golay *et al.*, 1988) and HGO.

Increased lipid oxidation resulting from increased FFA concentrations, a prominent feature of the 'metabolic disorder' in obesity, is accompanied by a decrease in glucose oxidation and inhibition of glycogen synthesis, as predicted by the glucose-fatty acid cycle (Boden and Chen, 1995; Ferrannini *et al.*, 1983; Thiébaud *et al.*, 1982). The hyperinsulinaemia of obesity, due partly to increased

influx of nutrients and to compensation for increased insulin resistance, initially prevents glucose concentrations from rising to the extent of IGT and NIDDM. In susceptible individuals, however, who cannot maintain the increasing requirement for hyperinsulinaemia, then IGT and NIDDM can develop.

1.2.5 Role of increased FFAs and the regulation of glycogen synthesis in NIDDM:

The major pathway for the disposal of glucose under normal conditions is via glycogen synthesis and is summarised in the diagram below. Rises in plasma glucose and insulin levels stimulate glycogen synthesis and inhibit glycogen breakdown. This inhibitory capacity is removed during times of increased energy demand (Golay *et al.*, 1997).

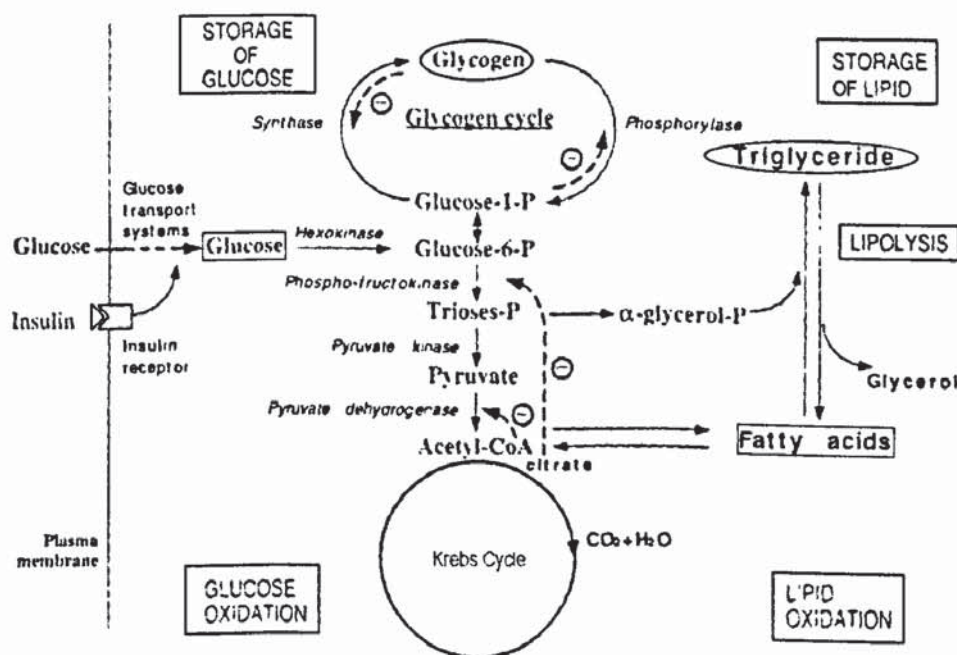


Figure 1.1 Adapted from Golay *et al.*, 1997.
Glycogen metabolism and influence of FFAs.

Glucose may be stored as glycogen or alternatively oxidised in the Krebs cycle. The oxidative pathway can be inhibited at two levels by increased oxidation of

FFAs (Randle *et al.*, 1963). Both glycogen mobilisation and glucose storage become inhibited through glycogen phosphorylase and synthase inhibition respectively as detailed by Golay *et al.* (1997).

Reaven (1995) has shown that lipolysis, a pathway regulated by insulin, is impaired in obesity and diabetes. This impairment of lipolysis results in increased circulating FFA concentrations, indicating resistance to the effects of insulin at the level of adipose tissue itself. Increased FFA levels may also increase HGP through gluconeogenesis, as discussed earlier (Blumenthal, 1983; Ruderman *et al.*, 1969). Elevated levels of FFA increases their uptake into cells resulting in lipid oxidation and stimulation of gluconeogenesis via pyruvate carboxylase and phosphoenolpyruvate carboxykinase, rate-limiting enzymes in gluconeogenesis (Williamson *et al.*, 1966; Ruderman *et al.*, 1969).

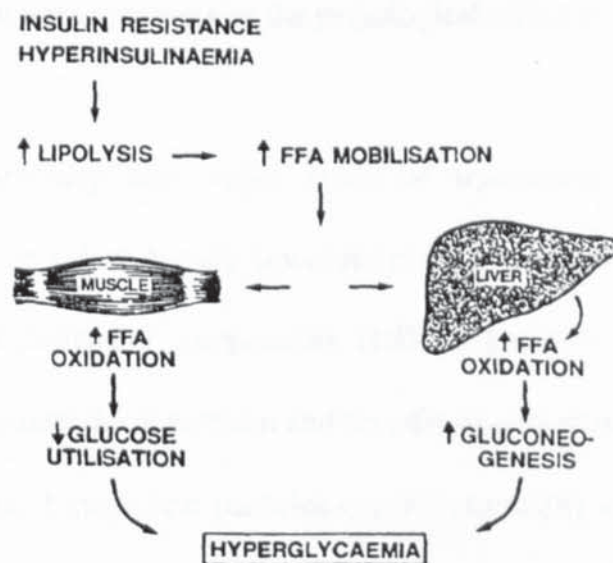


Figure 1.2 Adapted from DeFronzo, 1988.
The role of FFAs in potentiating hyperglycaemia.

Increased glucagon levels may also facilitate HGO through enhanced gluconeogenesis and glycogenolysis. Indeed, glucagon levels are frequently

elevated in type 2 diabetes (Matsuda *et al.*, 1992). Greater suppression of glycogenolysis than gluconeogenesis also leads to increased HGO due to the prevailing insulin resistance (Cherrington *et al.*, 1987). Thus, obesity and diabetes, in coexistence, appear to facilitate a progressive deregulation of the normal metabolic state.

1.3 Lipoprotein homeostasis:

To appreciate the ramifications of elevated cholesterol levels in the diabetic individual, it is important to understand the processes underlying the regulation of lipid metabolism in the non-diabetic. The following paragraphs are designed to elaborate the functional metabolic pathway of lipoprotein homeostasis. Insulin is central in regulating lipoprotein metabolism (Betteridge, 1997), and insulin resistance in type 2 diabetics confers a defect of insulin's role in regulating this metabolism, but not as strongly as the pathological effect on glucose homeostasis.

There are essentially four major types of lipoprotein particles, these are chylomicrons, very low-density lipoproteins (VLDL), low-density lipoproteins (LDL), and high-density lipoproteins (HDL). Together these subclasses of lipoproteins regulate the absorption and transfer of cholesterol and lipids between cells and tissues. Lipoprotein particles consist essentially of a hydrophilic outer coat of phospholipids, free cholesterol and apoproteins. The hydrophobic inner core comprises triglyceride and esterified cholesterol (Betteridge, 1997). The metabolic fate of the lipoprotein classes is strongly dependent upon the presence of apoproteins. Specific apoprotein types also play a defining role in the structure of these particles (Cooper, 1999).

As detailed by Betteridge (1997), lipoprotein metabolism can be summarised by three interrelated pathways. The exogenous pathway involves metabolism of chylomicron particles. Chylomicrons are formed following the absorption of dietary fat and cholesterol from the intestinal lumen following the digestive action of bile salts and digestive enzymes. The cholesterol and fat absorbed are enveloped within chylomicron particles following esterification, encompassing triglycerides and cholesterol esters. Chylomicrons are triglyceride-rich containing approximately 90% triglyceride, about 2% cholesterol esters with free cholesterol and phospholipids constituting a further 1% and 7% respectively (Miller and Small, 1987). Association of apoproteins occurs inside the intestinal enterocyte and includes Apo B₄₈, A-I, A-II and A-IV (Cooper, 1999). Chylomicron particles are then secreted from the enterocyte and enter the lymphatic circulation enroute to the thoracic duct where they enter the general circulation. Compositional changes occur on the surface of these chylomicron particles as a consequence of HDL interaction whereby they obtain apoproteins C and E and lose some apoprotein A (Cooper, 1999).

Once in the general circulation, chylomicron particles interact with the enzyme lipoprotein lipase (LPL), present on the surface of endothelial cells found in adipose tissue and a variety of muscle types. Apoprotein C II is essential for allowing the action of LPL (Miller and Small, 1987). LPL action hydrolyses the triglycerides into FFAs and glycerol. These products may be utilised as a metabolic fuel or re-esterified for storage within the cell (Levy, 1981).

The action of LPL generates remnant particles depleted of triglyceride with a modified lipid and apoprotein composition (Miller and Small, 1987). These remnant particles are richer in cholesterol and are avidly taken up by hepatocytes, via recognition of apo E (Havel and Hamilton, 1988). Transfer of extraneous surface components is believed to occur, forming new lipoproteins with characteristic features of HDL. This pathway may be a significant route via which HDL particles are formed (Cooper, 1999). Clearance of these chylomicron remnants is rapid, spending less than 30 minutes in the circulation in most individuals (Cooper, 1999).

The endogenous pathway of lipoprotein metabolism involves VLDL particles. This pathway is very similar to the chylomicron pathway detailed above. VLDLs are triglyceride-rich lipoproteins synthesized by hepatocytes. They contain cholesterol from *de novo* synthesis or from uptake from the plasma and endogenously derived triglyceride (Miller and Small, 1987). Their apoprotein constituents are apo B₁₀₀, C and E (Betteridge, 1997). Both cholesterol and insulin are required for the secretion of VLDL (Khan and Fungwe, 1990; Schonfeld, 1985). Insulin may also regulate several of the enzymes involved in the lipogenic pathway for synthesis of the triglyceride incorporated into VLDL. Once secreted VLDL particles interact with LPL, the affinity of this enzyme is linked to the triglyceride content of the lipoprotein subclass (Cooper, 1999). The triglyceride content of VLDL particles accounts for approximately 65% of their total mass (Miller and Small, 1987).

VLDL remnant particles (IDL) are generated following LPL action. Surface components may again be transferred to HDL particles (Eisenberg, 1984). The remnant particles formed contain less triglyceride, have lost some surface apo C and are denser than the original VLDL particles (Faergeman and Havel, 1975).

The VLDL particles may undergo triglyceride depletion forming intermediate-density lipoprotein (IDL) and, subsequently, LDL particles (Kane, 1983). During this process most of the cholesterol remains within the lipoprotein particle. Thus as triglyceride is removed the proportion of cholesterol increases, such that LDL constitutes the major cholesterol rich lipoprotein subclass in the circulation (Betteridge, 1997). Alternatively, VLDL remnants may be removed directly by the liver. The liver removes the vast majority of VLDL remnants in the rat accounting for the low levels of LDL in this species, in humans most VLDL remnants are converted to LDL (Cooper, 1999).

LDL particles are essentially remnants of VLDL and are triglyceride depleted (Levy, 1981). The contribution made by LDL particles to cholesterol homeostasis has been reviewed by Brown and Goldstein, (1986). Essentially, the LDL particle interacts with its specific LDL receptor. The receptor-lipoprotein complex then becomes internalised by endocytosis with the subsequent formation of an endocytic vesicle. Proton pumps in the membrane of this vesicle lower the intravesicular pH causing the LDL receptor to dissociate from the LDL particle. The dissociated LDL receptor then returns to the cell surface, while the LDL particle becomes hydrolysed by the action of enzymes following fusion with

lysosomes. During the hydrolytic process, protein is degraded to amino acids while esterified cholesterol is converted to free cholesterol.

The LDL receptor pathway has two distinct functions: one to catabolise plasma LDL, the second to deliver free cholesterol to cells (Gianturco and Bradley, 1987). Indeed, cholesterol feeding is known to suppress the synthesis of hepatic LDL receptors while reduced cholesterol synthesis results in increased receptor activity (Brown and Goldstein, 1983). Modification (by oxidation) may render these lipoproteins susceptible to uptake via the scavenger receptor, ultimately leading to the progression of atherosclerosis. Unlike the classic LDL receptor pathway, the scavenger receptor is not down-regulated. The process of atherogenesis is discussed in subsequent paragraphs.

It is now understood that free cholesterol, when delivered to cells, represses the *de novo* synthesis of cholesterol within these cells. The pathway regulating cholesterol homeostasis is covered in relative detail later in this chapter.

High-density lipoproteins constitute several distinct subclasses of this lipoprotein fraction. Such lipoproteins are seen as being protective, in that they participate in reverse cholesterol transport removing cholesterol from peripheral tissues and returning it to the liver (Eisenberg, 1984). HDL particles may be synthesised by the liver and intestine and appear structurally disc shaped. Their conversion to spherical HDL particles (in plasma) is dependent upon the enzymes LCAT (lecithin cholesterol acyltransferase) and CETP (cholesterol ester transfer protein) (Cooper, 1999). HDL particles are also formed from redundant surface

components transferred during triglyceride depletion of other lipoprotein subclasses such as VLDL, or associations between phospholipids and apoproteins (Patsch and Gotto, 1987). The HDL precursor molecules contain low amounts of cholesterol and are composed of phospholipids and apolipoproteins.

Through the action of LCAT and CETP larger and more complex HDL molecules are formed (Eisenberg, 1984). The mature form of HDL contains a core of cholesteryl esters; the conversion to mature HDL is facilitated by the presence of apo-AI (Cooper, 1999). The cholesterol ester formed within the core of HDL particles can be transferred to VLDL and LDL particles via CETP or delivered directly to the liver (Fielding and Fielding, 1982; Gwynne, 1989). This transfer capability permits the HDL particles to continually operate a reverse transport mechanism.

Several subclasses of HDL exist, notably HDL₂, and HDL₃. As detailed by Eisenberg (1984), HDL₂ particles may contain three-fourfold more cholesteryl and triglyceride molecules than the HDL₃ subfraction, and are twice as effective in carrying triglyceride as HDL₃. I will not discuss the conversionary pathway in detail since it lies outside the focus of this thesis. Nevertheless, conversion between these different subclasses can occur in either direction. Ultimately, these subclasses of HDL differ in their size and density and in their ability to transport cholesterol.

The incidence of coronary arterial disease (CAD) and CHD is strongly associated with elevated cholesterol levels. An inverse relationship exists between the

incidence of CAD, CHD, and HDL cholesterol levels due to its role in reverse cholesterol transport (Gordon *et al.*, 1989). The HDL₂ subfraction is specifically associated with the protective effect against CAD and CHD risk (Patsch and Gotto, 1987). A relative lowering of all lipoprotein subclasses infers no greater risk on the health of the individual, however, a concomitant lowering of HDL in association with increased LDL levels may be life-threatening.

1.3.1 Lipoprotein metabolism in NIDDM:

Type 2 diabetes is associated with an increase in the frequency of lipid and lipoprotein abnormalities, with characteristic dyslipidaemia often being present prior to definitive diabetes (Laakso, 1995). The insulin resistance in type 2 diabetes, particularly at the level of the liver, often confers a defect in insulin's normal inhibitory action on VLDL secretion (Cummings *et al.*, 1995). This effect leads to hypertriglyceridaemia caused by excessive VLDL levels. Cummings *et al.* (1995) has suggested that the higher VLDL concentration may be an effect of enhanced cholesterol and triglyceride synthesis, possibly as a consequence of increased nutrient flux to the liver.

Associated defects in the lipoprotein profile include elevated levels of LDL (Howard *et al.*, 1987) and reduced levels of HDL. HDL cholesterol concentrations tend to be between 25-30% lower in type 2 diabetics, this reduction being attributable to a lower HDL₂ subfraction (Bagdade, 1997). Taken together, the altered lipid profile characteristic of diabetes predisposes the individual to a threefold increase in the risk of cardiovascular disease compared

to non-diabetics (Kannel and McGee, 1979). Additional risk factors such as a sedentary life style may further advance this risk.

In type 2 diabetes the VLDL profile is characterised by an over-production of triglyceride-rich VLDL particles (Taskinen *et al.*, 1986). In addition, impaired removal of these particles leads to their elevation in plasma (Taskinen, 1990). As a result, type 2 diabetic patients display abnormally large VLDL₁ particles (triglyceride-rich), and smaller VLDL₂ particles. Taskinen (1990) has commented that insulin has far reaching effects on all lipoprotein fractions and that any specific defect in this system, such as in VLDL metabolism, would have ramifications in subsequent pathways. Thus, changes in the composition of VLDL particles may predispose the individual to atherosclerosis (Howard and Howard, 1994).

Impairment in the rate of LDL clearance exists in some NIDDM patients (Howard *et al.*, 1987). This situation is worsened by the concomitant elevation in LDL levels commonly observed in diabetes. The majority of LDL produced in NIDDM patients comes from the triglyceride-rich pool of VLDL particles (Taskinen, 1990). Insulin has been shown to stimulate LDL binding in fibroblasts and is known to regulate the normal metabolism of lipoproteins. Thus, the prevailing hyperinsulinaemia and insulin resistance in type 2 diabetes may be intimately involved in the defective clearance of LDL (Chait *et al.*, 1979).

HDL concentrations within plasma are dependent upon the normal degradation of VLDL particles. VLDL catabolism is initiated by interaction with LPL; any

defect in LPL activity or resistance of LPL to insulin action would lower HDL levels. As reviewed by Bagdade (1997), insulin regulates the activity of LPL and hepatic lipase (HL). LPL levels are reduced in NIDDM patients resulting in raised triglyceride levels due to impaired clearance of triglyceride from VLDL. This indirectly influences the formation of HDL and the reverse cholesterol transport process, since these particles are generated during this clearance process.

HL is known to influence the metabolism of HDL; in type 2 diabetes the activity of this enzyme is increased (Kasim *et al.*, 1987). Thus, a reduced HDL concentration may be attributed to enhanced activity of HL leading to increased HDL clearance. In addition, Taskinen (1990) has provided evidence that reverse cholesterol transport by HDL may be impaired due to an increased proportion of cholesterol and triglyceride within these particles. This prevents the normal function of cholesterol transfer via CETP between HDL and the LDL classes.

1.4 Atherogenesis and NIDDM:

Macrovascular and microvascular complications are common in type 2 diabetes. Mortality rates from CHD range from two-four times greater in diabetics compared to non-diabetics (Laakso and Lehto, 1997). In addition, a cluster of risk factors exists in type 2 diabetes linked with increased cardiovascular risk, as discussed previously (syndrome X).

Factors other than vessel occlusion may occur in blood vessels from type 2 diabetes. These are detailed by Laakso and Lehto (1997), and ultimately impair

the elasticity of the vessel wall. Medial layer calcification may induce such effects along with increased levels of connective tissue such as collagen and fibronectin. While the above conditions may influence the elasticity of the vessel, occlusion of the vessel lumen is seen as life-threatening and represents an advanced stage in the atherosclerotic process.

The abnormal distribution of lipoproteins in diabetes is seen as a major event in the progression of atherosclerotic vascular disease (Lopes-Virella *et al.*, 1997). Foam cell formation from macrophages, proliferation of endothelial cells and monocyte interactions are believed to be a consequence of modified lipoproteins, in particular LDL.

An initiating event in the progression of atherosclerosis is the adhesion of monocytes to a damaged endothelial cell layer (Ross, 1986). These monocytes then migrate into the subendothelial space and differentiate into macrophages. Here macrophages may be presented with, and internalise modified lipoproteins leading to their development into foam cells. Receptors for LDL molecules exist on the surface of macrophages, however uptake of LDL via this route is not seen as significant. It is uptake of these lipoproteins via the scavenger receptor, following their modification (by oxidation or acetylation), which is believed to result in significant cholesterol accumulation (Goldstein *et al.*, 1979). The scavenger receptor, unlike the classical LDL receptor, is not down-regulated in the presence of cellular cholesterol leading to unregulated cholesterol deposition. Diets rich in cholesterol and fat may lead to the generation of VLDL particles rich in cholesterol. Such particles may be internalised by the LDL receptor (via

apo E interaction) leading to intracellular cholesterol accumulation (Brown and Goldstein, 1986).

The immune system is believed to play an important role in the progression of atherosclerosis. Lymphocytes and foam cells once activated release cytokines, which serve to attract additional cells (Lopes-Virella *et al.*, 1997). The net result of mediator release is an inflammatory reaction with associated cell migration and proliferation. Monocyte chemotactic protein is a cytokine released by macrophages in the subendothelial space, this is a potent attractor for other monocytes (Clemmons, 1997). The production of this factor is increased by oxidised LDL (Cushing *et al.*, 1990). Indeed, oxidised LDL also acts as a monocytic attractant (Quinn *et al.*, 1987).

Arguably one of the most significant events in the progression of arterial lesions into fatty plaques is the migration and subsequent proliferation of smooth muscle cells into the medial and intimal layers (Ross, 1986). Expression of fibronectin is important in smooth muscle cell migration and proliferation (Lopes-Virella *et al.*, 1997). Proliferation of muscle cells is induced by mitogens secreted from plaque cells. Fox *et al.* (1987) describes how platelet-derived growth factor (PDGF) is secreted by a number of cell types including endothelial cells, macrophages and smooth muscle cells. Both endothelial cells and macrophages play an important role in PDGF production during early lesion formation. PDGF is one of the most potent growth factors in non-proliferating cells (Lopes-Virella *et al.*, 1997). Platelets are also a source of this mitogen; platelets become attached to the damaged endothelial cell layer where they release this substance, inducing further

platelet adherence and cell proliferation. Many other cytokines may be secreted during atherogenesis, too many to list individually. Nevertheless, such mediators are presumed to play multifactorial roles, as with PDGF, in the progression of this disease. The exact mechanisms by which these mediators operate are slowly becoming apparent. Several of these factors are only released by damaged or activated cells and may be a consequence of the diabetic state.

A relatively new concept in the role of immune cells in atherogenic progression is provided by Lopes-Virella *et al.* (1997). According to these authors, autoantibody production may be triggered by modified LDL molecules leading to immune complex generation. These immune complexes are avidly internalised via Fc receptors on the surface of macrophages and facilitate foam cell generation. The formation of immune complexes is believed to occur predominantly within the subendothelial space following LDL modification. Evidence is provided that LDL uptake via immune complexed LDL is significantly greater than native LDL. In addition, degradation of IgG-complexed LDL has been shown to be impaired leading to cholesterol accumulation (Lopes-Virella *et al.*, 1997).

LDL particles modified by glycation have been identified in plasma of diabetic patients (Lopes-Virella *et al.*, 1997). The uptake of glycated LDL was, according to the preceding authors, relative to the degree of glycation. Uptake of this modified lipoprotein is not via the scavenger receptor, but a receptor of lower affinity. In addition, advanced glycation end products have been identified on LDL (AGE-LDL). As with oxidised LDL, foam cell formation occurs following uptake of glycated LDL. Cross-linking of these AGEs may occur with structural

proteins or LDL itself, leading to their entrapment in the intimal or medial layers. This may facilitate oxidation of LDL already present or release of free radicals. Indeed, diabetics display a propensity to glycate proteins such as collagen, this may increase the chances of lipoprotein oxidation through trapping of these lipoproteins in the collagen matrix (Brownlee *et al.*, 1985). Immune reactions have been generated to LDL molecules following minor modifications. Although initially mild, these reactions become more severe. This provides an example of how the immune system may propagate atherosclerotic disease.

Risk factors for CHD have been listed previously and account for a large proportion of mortality in type 2 diabetics. Other factors intimately linked with the diabetic state, such as syndrome X, may also facilitate the progression of atherogenesis.

Conflicting evidence exists with regard to glycation of lipoproteins. However, as detailed previously in this chapter, glycated LDL is taken up by macrophages and may indeed be atherogenic (Lopes-Virella *et al.*, 1997). HDL molecules may display an impaired ability to accept cholesterol from peripheral cells and tissues due to cholesterol and triglyceride loading (Taskinen, 1990; Duell *et al.*, 1990). In addition, HDL molecules may also undergo glucosylation and are cleared at an abnormal rate in guinea pigs (Witztum *et al.*, 1982).

1.4.1 Haemostatic factors:

Type 2 diabetes mellitus is associated with an imbalance of some haemostatic factors. Decreased fibrinolysis is associated with diabetes due to increased levels of platelet activator inhibitor-1 (PAI-1) and reduced levels of tissue plasminogen

activator (tPA) (Jokl and Colwell, 1997). The contribution such factors make in the clotting cascade is discussed in more detail in chapter 5. Nevertheless, a pro-coagulant state in the presence of diabetes is seen as a major risk factor in arterial disease. It becomes apparent from the evidence presented that many factors present in diabetes may accelerate or exacerbate the atherosclerotic process. It is not within the scope of this thesis to categorise all factors that may facilitate atherogenesis, rather to provide an overview of the origins of atherosclerosis and ultimately its end points.

1.5 Cholesterol Homeostasis:

Cholesterol plays a fundamental structural role in all cells and is the origin of all steroid hormones. Strict regulation of cholesterol levels occurs at a cellular level ensuring that the rate of cholesterol absorption is equal to its rate of excretion (Stange and Dietschy, 1985).

The two main enzymes responsible for regulating cholesterol synthesis and availability are HMG-CoA reductase and acyl-coenzyme A: cholesterol acyltransferase (ACAT). These enzymes are closely involved in cholesterol biosynthesis and esterification, respectively. HMG-CoA reductase activity determines the rate of cholesterol synthesis in both liver and intestine (Stange *et al.*, 1981).

The intestinal mucosa plays a significant role in the synthesis and delivery of cholesterol. As reviewed by Nguyen *et al.* (1994), it is the only site where cholesterol may be absorbed, and as stated is involved in its synthesis. In addition, it is a route along which derivatives of cholesterol may be excreted

(Turley and Dietschy, 1988). Dietary fat and cholesterol are absorbed into intestinal cells through the action of bile salt micelles. Uptake of triglyceride and cholesterol and their packaging into chylomicrons has been discussed in preceding sections and will not be reiterated here.

Stange and Dietschy (1985) provide evidence for differential rates of cholesterol synthesis along the length of the intestine. According to these authors, the highest rates of cholesterol synthesis, with the exception of liver, occurs in the stomach, duodenum, and terminal ileum, respectively. The mid-region of the small intestine is thought to be the site where most cholesterol absorption occurs, as such synthetic rates were found to be lowest in this region. The levels of HMG-CoA reductase are believed to be higher in the ileum than jejunum (Stange and Dietschy, 1985). Despite this, the jejunum is regarded as the site where most cholesterol synthesis occurs due to the greater mucosal thickness of this region. The activity of HMG-CoA reductase is believed to be tightly regulated. According to Stange *et al.* (1980), regulation of this enzyme may occur via the LDL receptor pathway in smooth muscle cells and via HDL and VLDL receptors in hepatocytes. Experiments performed by the above authors in a cell culture model determined that LDL could significantly attenuate the activity of HMG-CoA reductase. When utilising intestinal crypt and villous cells, cholesterol feeding resulted in a marked diminution of enzyme activity in the jejunum. The effect in the ileum was less pronounced but nevertheless significant (Stange *et al.*, 1981).

Esterified cholesterol constitutes a form that is metabolically inactive (Vlahcevic *et al.*, 1999). In a study by Stange *et al.* (1983), cholesterol feeding increased the activity of the enzyme ACAT significantly in the jejunum, but little effect was observed in the ileum. Under normal conditions, the activity of the enzyme along the length of intestine is very similar with slightly higher activity in the jejunum compared with ileum. These same authors provide a model detailing cholesterol synthesis, uptake, and excretion within intestinal cells (figure 1.3).

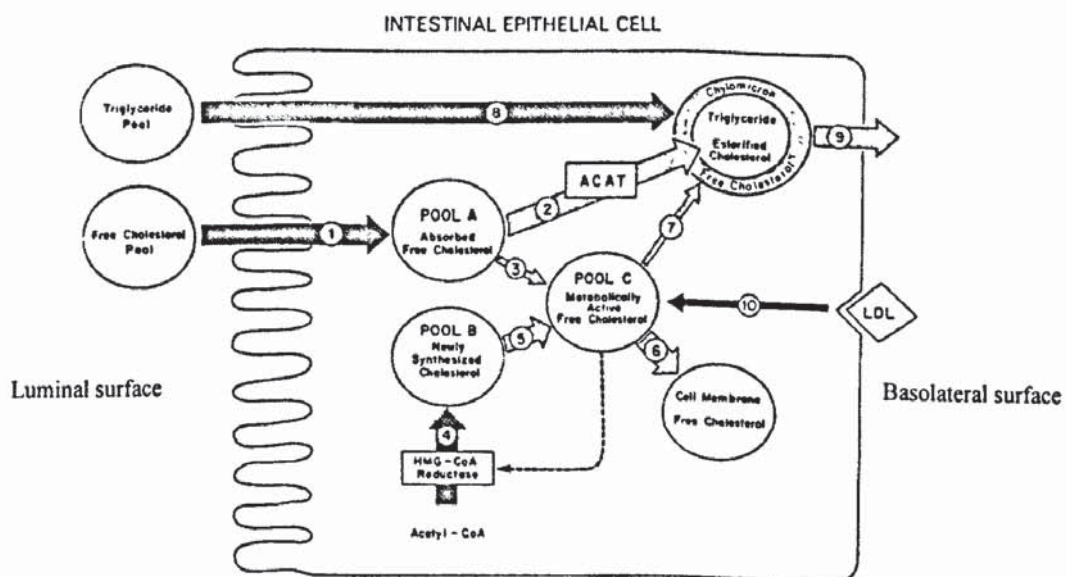
Esterification of cholesterol must take place for its incorporation into lipoprotein particles. ACAT is seen as the major mucosal enzyme responsible for this esterification (Forester *et al.*, 1983). As with HMG-CoA reductase, the activity of ACAT may be tightly controlled via phosphorylation and substrate supply.

1.5.1 Cholesterol within Enterocytes:

Stange *et al.* (1983) provide a model for intracellular cholesterol pools within intestinal cells. These authors based their model on evidence that the first pool (A) is formed from the absorption of dietary cholesterol and as such exists in an unesterified form. This pool is predominantly the target for the enzyme ACAT which esterifies cholesterol for incorporation into chylomicrons. Cholesterol feeding results in increased ACAT activity and may be a reflection of increased substrate availability. Pool B is derived from *de novo* synthesis. Inducing increased cholesterol synthesis by, for example, cholestyramine administration resulted in no increase in ACAT activity, suggesting independent pools may exist, and with the synthesised pool (B) not being a substrate for ACAT activity.

Evidence is also provided for a lack of feedback inhibition between pools A and B, since cholesterol feeding does not significantly alter the rate of cholesterol synthesis within intestinal cells. Some contribution exists, however, between pools A and C providing cholesterol for membrane synthesis. Most cholesterol in pool C is derived from the pool of newly synthesised cholesterol (pool B); a small proportion is also available from the uptake of lipoproteins such as LDL. Thus, the level of cholesterol in pool C is crucial due to the output of cholesterol into cell membrane synthesis and chylomicron coats. This pool inhibits HMG-CoA reductase activity limiting further cholesterol synthesis. Evidence is also provided indicating that cells located in the crypts of villi in both the proximal and distal intestine accounted for approximately 70% of cholesterol synthetic activity. In those mature jejunal cells involved in cholesterol absorption, then synthesis rates were depressed.

Figure 1.3 Adapted from Stange *et al.*, 1983.
Cholesterol synthesis and absorption in intestinal epithelia.



Cholesterol can only be excreted from the body as a constituent of bile (Hofmann, 1994a). The bile salt pool is tightly regulated and is intimately linked

to the cholesterol biosynthetic pathway. Taurocholate feeding results in reduced activity of the enzyme HMG-CoA reductase (Nguyen *et al.*, 1994). In several additional studies, bile salt feeding was seen to reduce the activity of both HMG-CoA reductase and 7 α -hydroxylase, as reported by Duckworth *et al.* (1991). It has long been proposed that bile salts can regulate their own production by negative feedback (Goldstein and Brown, 1990). Evidence now exists that bile salts directly repress the activity of one or more enzymatic steps via specific nuclear receptors. This model would allow bile salts to specifically target intestinal and hepatocytic cells in modulating cholesterol flux into bile. This hypothesis is discussed in more detail in chapter 3.

1.6 Bile Salts:

In humans, bile is formed in the liver and stored in the gallbladder between meals. In the rat, no gallbladder exists therefore bile is secreted directly into the intestinal lumen via the bile duct in response to feeding. Thus, the rat provides a convenient model for direct measurement of the rate of bile production and the concentration of components within hepatic bile. The biliary pathway serves both as a vehicle for bile acids to facilitate the digestion and absorption of dietary fat and fat-soluble vitamins and provides a route for excretion of substances including cholesterol and xenobiotics (Hofmann, 1994a).

1.6.1 Synthesis:

Bile acids are the products of cholesterol metabolism (Bahar and Stolz, 1999). Bile consists of cholesterol, bile salts, bilirubin, bile alcohols, and lecithin. In

order for cholesterol to be excreted, it must undergo modification to render the molecule water-soluble. This conversionary process begins in the liver.

The term “bile salts” bears reference specifically to a group of compounds that undergo conjugation with sulphate (bile alcohols) or with taurine or glycine amino acids (bile acids) (Hofmann, 1994a). The processes by which cholesterol is converted to bile acids occur in the liver and involves a multitude of enzymatic steps as detailed in figures 1.4 and 1.5 (Vlahcevic *et al.*, 1999).

Briefly, there are two distinct pathways through which cholesterol may be modified and converted to bile acids. The first pathway is termed the *neutral pathway*. This is seen as the ‘classical’ pathway and involves manipulation of the steroid nucleus prior to any side chain modifications (Vlahcevic *et al.*, 1996). The second pathway involves modification of the steroid side chain before any nuclear modifications have occurred and is termed the *acidic pathway*, as detailed by Vlahcevic *et al.* (1999).

The enzyme responsible for driving bile acid synthesis in the *neutral pathway* occurs solely in the liver and is a cytochrome P450 termed 7 α -hydroxylase (Russell and Setchell, 1992). The *acidic pathway* involves a mitochondrial enzyme termed 27-hydroxylase. This enzyme introduces a hydroxyl group at position 27 of the carbon ring, with subsequent steps involving hydroxylation at position 7 of the steroid ring. The two most predominant bile acids, chenodeoxycholic acid and cholic acid, are synthesised in approximately equal ratios via the *neutral pathway* (Vlahcevic *et al.*, 1999). Bile acids and alcohols are characterised by the presence of hydroxyl groups at positions 3 and 7 of the

steroid nucleus. The terminal side chain group on bile alcohols is a hydroxyl group on carbon C₂₄ or C₂₇ (Hoshita, 1985). In bile acids the terminal group is a carboxyl group. The specific reactions involved in both the *neutral* and *acidic pathways* are summarised in figures 1.4 and 1.5.

The enzyme responsible for driving bile salt synthesis via the *acidic pathway* is a mitochondrial sterol 27-hydroxylase. Chenodeoxycholic acid is the predominant end product of this pathway (Vlahcevic *et al.*, 1996). The same enzyme is also involved in the latter stages of bile salt formation, utilising the products of the *neutral pathway* following manipulation of the steroid nucleus (see figure 1.5).

Regardless of origin, the final step in bile acid formation involves conjugation of the molecule with either taurine or glycine (Vlahcevic *et al.*, 1999). Conjugated bile acids constitute the vast majority of bile acids secreted, with the amide linkage between the amino group of the amino acid with the carboxyl group of the bile acid (Hofmann, 1994a). In addition, the bile acids may be conjugated with a variety of alternative molecules, as detailed by Hofmann *et al.* (1992a). This conjugation step results in increased solubility of the bile acid at pH values found in the intestinal lumen (Vlahcevic *et al.*, 1991). In addition, conjugation also results in ionisation of the molecule, and this in turn prevents its passive absorption in the biliary tract (Hofmann and Mysels, 1988). Due to the higher pH conditions that exist in hepatic bile, bile acids exist in their ionised form in this region.

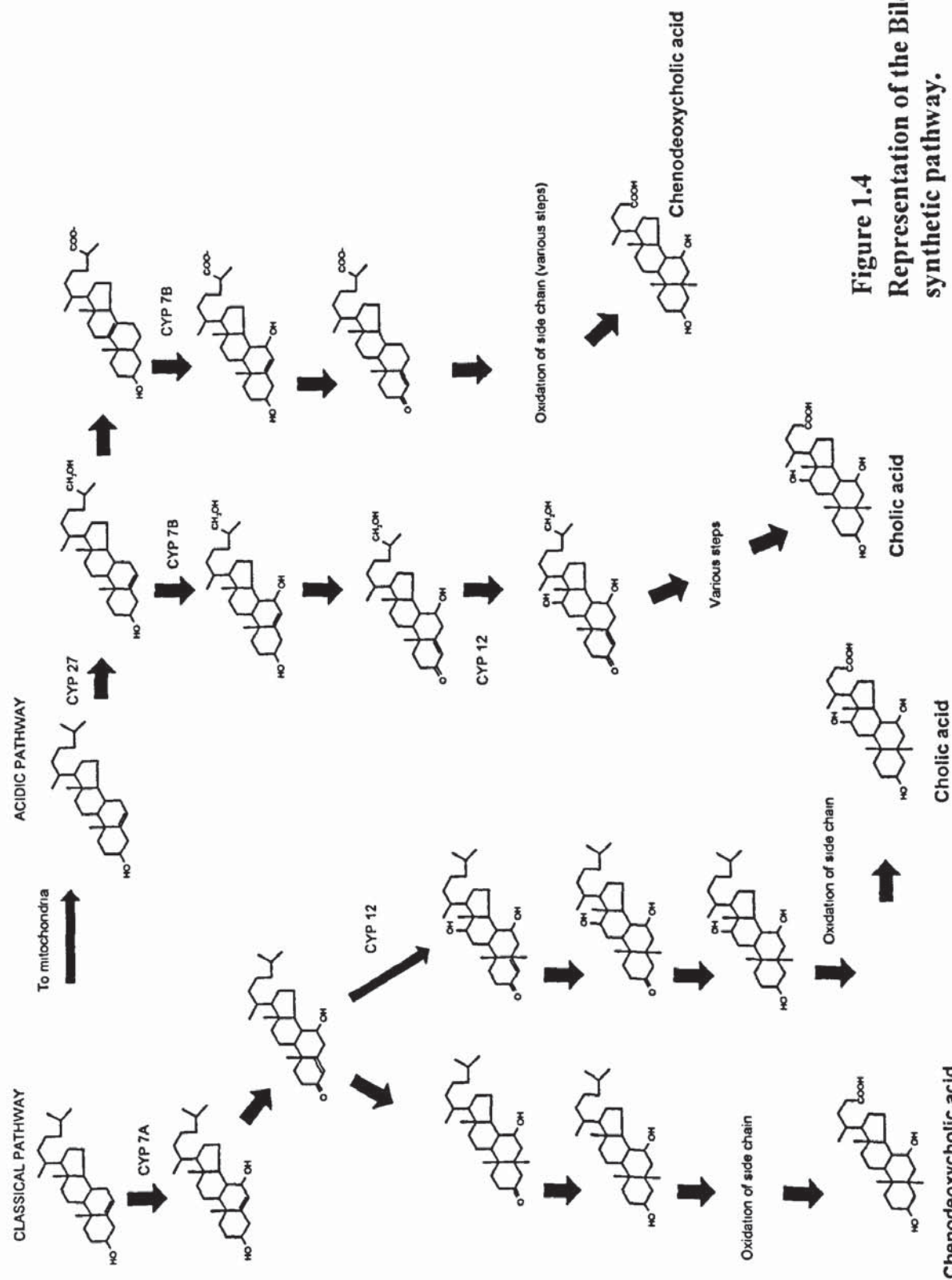


Figure 1.4
Representation of the Bile salt
synthetic pathway.

Adapted from Vlahcevic *et al.*, 1999.

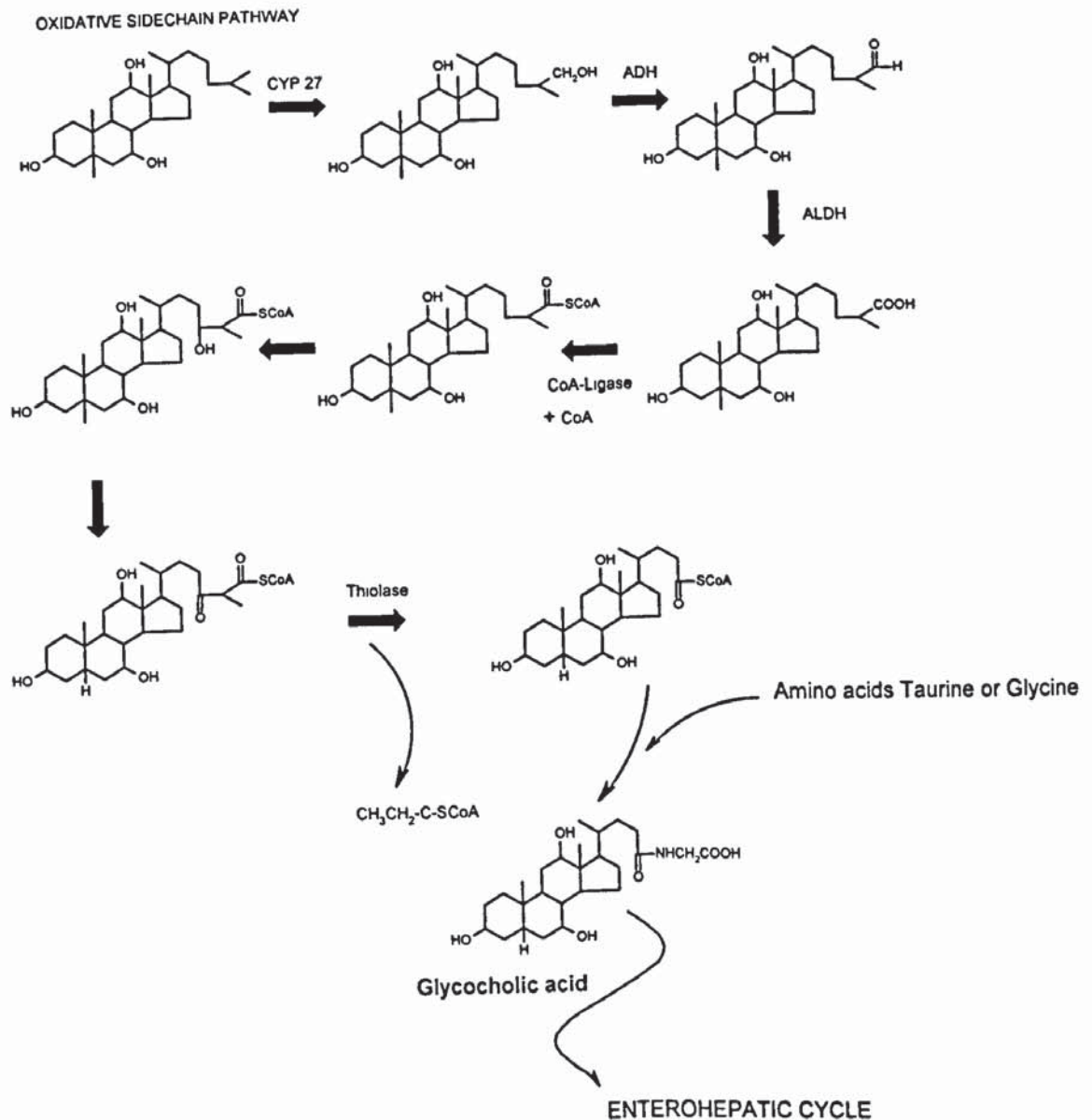


Figure 1.5

Representation of the Oxidative side chain pathway of Bile salt synthesis.

Adapted from Vlahcevic *et al.*, 1999.

CYP27 = sterol 27 hydroxylase
 ADH/ALDH = alcohol/aldehyde dehydrogenase
 CYP 7A = 7 alpha hydroxylase
 CYP 12 = 12 alpha hydroxylase
 CYP 27 = sterol 27 hydroxylase
 CYP 7B = oxysterol 7 alpha hydroxylase

1.6.2 Function:

Bile salts are 'detergent-like' in nature, and their role in micellar lipid dispersal in the intestine is well established. Bile salts exist predominantly as monomers. However, a concentration is reached, termed the critical micellar concentration, where these bile salt monomers associate with one another forming the aforementioned micelles (Donovan, 1999). In addition, a critical micellisation pH also exists. This can be defined as a narrow pH range above which bile salts exist in their micellar form, being freely soluble. Below this pH range they are poorly soluble (Hofmann and Mysels, 1988). Conjugation with taurine or glycine is believed to reduce this critical micellisation pH, resulting in conjugated bile acids being fully soluble at the pH in the small intestine (Hofmann and Mysels, 1988).

As stated, this micellar formation is critical in permitting the absorption of fat-soluble vitamins along with dietary fats and cholesterol which, according to Hofmann and Mysels (1988), is achieved high up in the small intestine. Lipids are by nature hydrophobic, their absorption from micelles and across the enterocyte is limited by the presence of an unstirred water layer and by the enterocyte membrane. According to Borgström *et al.* (1985), the unstirred water layer acts as a barrier between the contents of the intestinal lumen and the brush-border membrane of the enterocyte, thus creating a concentration gradient.

1.6.3 Transport:

Bile acids are secreted into the small intestine in response to hormonal and nervous mechanisms in humans (Spellman *et al.*, 1979; Rock *et al.*, 1981), similar mechanisms are likely to operate in rats. All bile acids/salts undergo an

enterohepatic circulation, in which they are reabsorbed along the length of the small intestine and returned to the liver. This reabsorption process is highly efficient with approximately 95% of bile acids being reclaimed via this route.

Passive uptake of ionised conjugated molecules from the intestinal lumen is however, generally slow. At the pH levels found in the small intestine, the majority of conjugated bile acids exist in an ionised state and thus reabsorption is limited (Amelsberg *et al.*, 1996). Conjugation with taurine or glycine means that these conjugated bile acids can only be actively recovered via specific transporters. If, however, the amino acid groups become detached from the bile acid molecule via bacterial deconjugation, or bile acids are secreted in an unconjugated form, then these uncharged molecules can readily traverse the lipid bilayer of intestinal cells (Dietschy, 1968).

Previous studies have demonstrated that bile acids are actively absorbed in the ileum against a concentration gradient. The ileal mechanism is sodium-dependent and most active in the distal ileal region (Dietschy *et al.*, 1966; Lack and Weiner, 1961; Playoust and Isselbacher, 1964). Unconjugated bile acids may be absorbed passively along the entire length of the small intestine via ionic and non-ionic diffusion (Stiehl, 1995). This pathway is believed to operate independently of the ileal system (Holt, 1964).

According to Bahar and Stolz (1999), passive/facilitated jejunal absorption of bile acids may account for 50% of taurocholate transport in the rat. The ileal transport system is believed to preferentially favour trihydroxy bile acids such as glycocholate (Bahar and Stolz, 1999), whilst uptake in the jejunum diminishes as

the number of hydroxyl groups increase (Stiehl, 1995). The presence of a highly specific transport pathway for bile acids in the terminal ileum is believed to permit almost complete reabsorption of bile acids and prevent their progression into the colon. Any bile salts that pass into the colon may undergo bacterial modification and may induce electrolyte and water secretion into the colon, leading to diarrhoea. Indeed, Mekhjian *et al.* (1971) found that both conjugated and unconjugated bile acids (3-5mmol/l) induced the secretion of water and sodium ions into the colon. Binder and Rawlins (1973) later confirmed these observations.

Once absorbed, bile acids must pass through the enterocyte, across the basolateral membrane and into the portal circulation. In the circulation bile acids exist predominantly bound to albumin (99% binding for dihydroxy and 70% binding for trihydroxy acids) (Roda *et al.*, 1982). Binding of bile acids to plasma proteins appears to reduce their renal filtration and urinary excretion (Craddock *et al.*, 1998). These bound bile acids are removed from the circulation by the liver during their first pass, the process being 70-90% efficient (Bahar and Stolz, 1999). Any bile acids escaping this first pass clearance are recirculated to the liver and subsequently extracted.

In rat predominantly taurine conjugation of cholic acid occurs (Elliot, 1985). Such conjugated bile acids cannot be absorbed passively due to their protonation. However, preliminary evidence exists that the tight junctions between intestinal cells may become more open during digestion, allowing the paracellular transfer

of bile acids (Madara, 1989). Such an effect may increase the rate of uptake of the majority of bile acids (Hofmann, 1994b).

Any bile acids not recovered by the active transporter of the ileum will pass into the large intestine and colon. Here bacterial modification of bile acids occurs and involves the lysis of the amide bond between the amino and bile salt. Alternatively, they may cause dehydroxylation and oxidation of the hydroxyl groups (Elliot, 1985). As stated, this deconjugation results in unconjugated bile acids which may be absorbed passively depending upon their surface charge. Such products of bacterial modification are termed secondary bile acids and are returned to the liver and reconstituted before undergoing a further enterohepatic cycle.

The cellular transport mechanisms involved in the transfer of bile acids by the ileal and jejunal transporters are discussed in more detail in chapter 3. The experiments detailed in subsequent chapters have utilised a radiolabelled trihydroxy bile acid 1-¹⁴C glycocholic acid, prepared from cholic acid and 1-¹⁴C glycine. Such trihydroxy acids are characterised by the presence of three hydroxyl groups usually at positions 3, 7, and 12 of the steroid ring. Although in the rat taurocholic acid is the predominant conjugated bile acid, glycocholic acid was used throughout since this molecule is transported with similar efficiency to taurocholate despite not being a normal constituent of rat bile (Lack and Weiner, 1961).

1.7 Treatment regimens in NIDDM:

The regimen for treatment lies most fundamentally with attempting to normalise metabolism and control the hyperglycaemia whilst also attempting to rectify or correct the associated risk factors of the metabolic (insulin resistance) syndrome.

1.7.1 Dietary therapy:

Dietary management is the most fundamental method to control glycaemia in diabetic subjects. The currently recommended diet for such individuals consists of a high proportion of complex carbohydrate, low in fat with moderate amounts of protein (Crapo, 1994). Dietary measures are successful in less than 20% of NIDDM patients and rarely remains effective due to the progressive nature of the disease (UKPDS, 1995). An inherent problem with such a treatment is that compliance by the patient can be lacking, which can lead to the advancement of the hyperglycaemia and insulin resistance. Nevertheless, dietary restriction can reduce lipid and glucose levels in NIDDM, reducing cardiovascular risk factors (Crapo, 1994).

In addition to dietary management, exercise provokes a reduction in excessive glucose levels evident in diabetes. The beneficial effect of strenuous glycogen depleting exercise in NIDDM patients is an increase in both peripheral insulin sensitivity and non-insulin-mediated glucose disposal, which can persist for longer than 12 hours (Goodyear and Smith, 1994).

1.7.2 Anti-diabetic agents:

There are many agents currently used in the management and treatment of type 2 diabetes. It is not within the scope of this thesis to cover in detail each compound

or their class. However, their benefits to the diabetic patient will be mentioned briefly. Metformin, as a treatment, however, will be covered in detail since it is a major focus of this thesis. Metformin has become the most widely prescribed agent in the treatment of type 2 diabetes. This compound is associated with several beneficial side effects which significantly reduce mortality rates from micro- and macrovascular complications in the diabetic (UKPDS, 1998).

1.7.2a Alpha-glucosidase Inhibitors:

These compounds delay the absorption of glucose by slowing complex polysaccharide digestion. As such they produce a dose-related decrease in postprandial hyperglycaemia (Bailey, 1997b). In NIDDM patients these agents cause a reduction in the postprandial plasma insulin response and may improve basal blood glucose concentrations to a small extent. Interestingly, in patients with hypertriglyceridaemia alpha-glucosidase therapy can reduce serum triglycerides, possibly by decreasing VLDL synthesis (Clissold and Edwards, 1988). This may have important implications for the elevated triglyceride levels in NIDDM.

1.7.2b Sulphonylureas:

These oral anti-diabetic agents stimulate insulin secretion from the β cell (Bailey, 1997b). Sulphonylureas induce insulin secretion by closing ATP-sensitive K^+ -channels in the plasma membrane of the β cell (Bailey, 2000). Approximately 10-15% of NIDDM patients prove unresponsive to sulphonylureas in terms of glycaemic response, and are classed as primary failures (Balodimos *et al.*, 1966). In the same study, secondary failures accounted for around 25% of patients. This

may reflect a progressive loss of overall β cell function. Sulphonylureas have no profound effect on lipid metabolism. By reducing glucotoxicity, sulphonylureas may improve the sensitivity of tissues such as liver and muscle to insulin (Lebovitz, 1994), although they have no direct insulin-sensitising effect.

1.7.2c Thiazolidinediones:

Thiazolidinediones represent a group of anti-diabetic agents that potentiate the action of insulin on the metabolism of carbohydrate and lipids by stimulating the nuclear receptor PPAR γ (Day, 1999). They lower plasma insulin concentrations and increase insulin-stimulated glucose disposal and inhibit glucose production (Day, 1999). They increase glycogenesis and glycolysis in muscle, stimulate glucose oxidation and lipogenesis in adipose tissue and reduce gluconeogenesis in the liver (Hofmann *et al.*, 1991; Hofmann *et al.*, 1992b).

1.7.2d Insulin therapy:

Diabetic patients who fail to achieve adequate glycaemic control with diet and oral anti-diabetic drugs or those where diagnosis of the condition occurs too late, will eventually require exogenous insulin. It is seen by many as the last resort in treatment of type 2 diabetes and a means to suppress the advancement of the disease, rather than correct the underlying metabolic defects associated with the condition. Nevertheless, insulin therapy is equally as effective as alternative treatments in the prevention of microvascular complications associated with diabetes (Rosenzweig, 1994).

The decision to begin insulin therapy is dependent upon the symptoms experienced and the severity of hyperglycaemia that exists. The paradox of insulin therapy in the treatment of NIDDM is that it may further exacerbate the insulin resistance that already exists (since supra-optimal concentrations are required to induce a physiological effect). Hyperglycaemia can usually be improved by aggressive insulin therapy, which can overcome the insulin resistance and glucose toxicity, but usually leads to weight gain and an increased occurrence of hypoglycaemic episodes (Rosenzweig, 1994).

1.7.3 Metformin

Metformin, a member of the biguanide family of anti-diabetic agents, has proved equally effective and in some instances more effective than alternative oral treatment regimens for type 2 diabetes (UKPDS, 1995). Metformin is classed as an anti-hyperglycaemic agent since it lowers blood glucose concentrations without inducing hypoglycaemia; it does not stimulate insulin secretion (Bailey, 1992). However, the glucose lowering effects appear to require the presence of insulin (Wiernsperger and Bailey, 1999).

1.7.3a Glucose lowering action:

The glucose lowering effect of metformin is attributable to reduced HGO through suppression of gluconeogenesis and glycogenolysis, and an increase in glucose utilisation (Wiernsperger and Bailey, 1999). Metformin's effects in peripheral tissues include increased insulin-mediated glucose uptake, specifically in skeletal muscle, and oxidative glucose disposal in muscle and non-insulin-mediated glucose utilisation in the intestine (Bailey, 1992). Additionally, metformin may

also reduce fatty acid oxidation (Wiernsperger and Bailey, 1999). Metformin has been shown to improve the action of insulin via several mechanisms. These include increasing glucose transporter (GLUT 4) translocation to the plasma membrane, increasing tyrosine kinase activity in the insulin receptor, and increasing the activity of glycogen synthase (Howlett and Bailey, 1999). Importantly, metformin appears to improve the sensitivity of tissues, specifically liver, to the glucose lowering effect of insulin, thereby reducing the prevailing hyperglycaemia.

Metformin becomes heavily concentrated within cells of the intestinal tract (Wilcock and Bailey, 1994). This accumulation may be one thousandfold greater in the intestine compared with other tissues and may account for several of its effects. Metformin is excreted unchanged in urine with approximately 90% being cleared within twelve hours. It is poorly absorbed via the intestine, an effect which may be related to its ionisation and hydrophobicity (Bailey, 1992; Vidon *et al.*, 1988). Unlike insulin, metformin does not increase body weight and appears to impose a variety of beneficial effects in several different physiological systems in diabetic individuals.

1.7.3b Effects upon Lipids and Lipoproteins:

Type 2 diabetic patients characteristically demonstrate lipid and lipoprotein abnormalities, which can be partially redressed by metformin therapy. One primary cause of increased HGO in type 2 patients is elevated fatty acid concentrations. As detailed earlier in this chapter, these elevated fatty acids serve as substrates for hepatic metabolism and are oxidised preferentially to glucose.

According to Randle *et al.* (1963), elevated fatty acids inhibit the metabolism of glucose in muscle and stimulate gluconeogenesis, contributing to elevated glucose levels. The improvements in insulin-stimulated glucose disposal detailed earlier, along with effects of metformin on fatty acid oxidation, serve to lower the contribution of fatty acids to the generation of glucose.

The abnormal lipid profile in diabetic patients renders these individuals susceptible to a greater risk of CHD (Laakso and Lehto, 1997). Metformin has been shown to partially correct these lipid abnormalities. In studies performed by Cusi and DeFronzo (1998), metformin was shown to reduce triglyceride levels by as much as 25%. VLDL levels were also reduced to a similar level or in some instances by up to 50% (reviewed by Bailey, 1992). Metformin has also been shown to decrease the amount of cholesterol in VLDL particles favourably altering their composition (Schneider *et al.*, 1990). LDL levels, commonly elevated in diabetes, show a modest reduction following metformin therapy (Rains *et al.*, 1988; Rains *et al.*, 1989). In addition, HDL levels show a modest increase following metformin therapy (Janka, 1985). The correctional effect upon lipid profiles is also evident in non-diabetic individuals who demonstrate hypertriglyceridaemia and elevated cholesterols (Cusi and DeFronzo, 1998).

Metformin may also influence cholesterol metabolism at the level of cholesterol synthesis. Evidence exists that metformin can decrease the activity of HMG-CoA reductase and ACAT. The activity of these enzymes, involved in cholesterol synthesis and esterification, respectively, was suppressed by metformin in the intestine of diabetic rats. This suggests a mechanism by which metformin may

suppress cholesterol synthesis and storage (Scott and Tomkin, 1983; Ni Neill *et al.*, 1987). Similarly, metformin also reduced the absorption of cholesterol administered orally (Cusi and DeFronzo, 1998).

1.7.3c Vascular Effects:

Metformin also imposes beneficial effects on the vascular system with important implications in the development of atherosclerosis. Metformin has been shown to reduce several risk factors linked with cardiovascular disease. These include increasing the rate of fibrinolysis and reducing PAI-1 levels (Bailey, 1997a).

In a study by Bünting *et al.* (1986), metformin was shown to decrease the proliferation of vascular smooth muscle cells *in vitro*. This action of the drug is of significance not only in the diabetic but also in the non-diabetic. Conflicting data exist for a beneficial effect of metformin upon blood pressure and hypertension. It has been shown to reduce blood pressure in rat models of hypertension, but the majority of clinical data indicate little effect of the drug on blood pressure in normotensive patients. As discussed earlier, hyperinsulinaemia is a positive risk factor for cardiovascular disease, as is hypertension and obesity. Although metformin does not reduce hypertension in humans, its effects upon elevated lipoproteins and insulin resistance may increase insulin sensitivity in tissues such as vascular smooth muscle (Fantus and Brosseau, 1986).

This insulin-sensitising effect is effectively demonstrated at the level of the liver and reduced HGO following metformin therapy. If metformin imposed similar insulin-sensitising and growth-inhibiting effects in vascular tissue, this could contribute to a beneficial effect upon the vasculature reflected, possibly, by a

modest decrease in hypertension, blood pressure and, ultimately, the progression of central and peripheral vascular disease. Metformin may also influence vascular tone at the level of the endothelium. According to Cusi and DeFronzo (1998), metformin is associated with increased glucose transport, activity of tyrosine kinases, and the general vasodilatory response to L-arginine.

Type 2 diabetic patients often demonstrate abnormal haemostatic function (Jokl and Colwell, 1997). Elevated levels of PAI-1 are common in both diabetic and non-diabetic individuals with insulin resistance (Jokl and Colwell, 1997). Metformin is associated with reduced levels of t-PA and PAI-1 antigen in patients with peripheral vascular disease and fibrinolytic impairment (Montanari *et al.*, 1992).

1.7.3d Contraindications:

Serious side effects of metformin therapy are rare. Clear contraindications to therapy have been identified and if adhered to result in few deaths from this compound. Lactic acidosis, by far the most serious side effect, accounts for only 0.03 cases per 1000 patient-years of treatment (Bailey, 1997a). Gastrointestinal (GI) symptoms are a common minor side effect of metformin therapy. Symptoms include diarrhoea, vomiting, bloating, metallic taste, flatulence, and nausea (Cusi and DeFronzo, 1998). The GI symptoms can be alleviated by reducing the dose of metformin. Only in less than 5% of cases do these GI symptoms become intolerable for the patient and metformin has to be withdrawn. Malabsorption of vitamin B₁₂ is a further side effect of metformin treatment (Bailey, 1997a). In

some cases this may be overcome by calcium or cyanocobalamin supplementation.

1.7.3e Hypotheses for Metformin's Cholesterol lowering effect:

Although it is generally agreed that metformin can lower cholesterol levels by increasing HDL and lowering VLDL, it is unclear how the drug actually achieves this (Cusi and DeFronzo, 1998). The cholesterol lowering effect is predominantly seen in hypercholesterolaemic individuals with diabetes, however, it is also evident in non-diabetics suffering from elevated cholesterol levels (Bailey, 1992). This cholesterol stabilising effect is certainly advantageous and may help to lower the incidence of atherosclerosis among the diabetic population. One aim of this thesis is to account for the cholesterol lowering effect of metformin.

A hypothesis put forward by Scarpello *et al.* (1998) involves metformin inhibiting bile salt uptake in the small intestine, resulting in the passage of unabsorbed bile salts into the colon where they may induce diarrhoea or be excreted in the faeces. Bile salts are synthesized from cholesterol and are the major pathway through which cholesterol may be excreted from the body (Hofmann, 1994a). Increased excretion via the faecal route would result in a reduction in the circulating bile salt/acid pool and the subsequent synthesis of additional bile salts to replenish those lost through malabsorption. Thus, hepatic LDL receptors would be up-regulated to provide the precursor for bile salt synthesis, accounting for the reduction in plasma cholesterol levels evident following metformin therapy. An alternative hypothesis involves a direct action

of metformin upon the enzymes involved in cholesterol synthesis and esterification, as detailed earlier.

1.8 Aims and objectives of this thesis:

Type 2 diabetic patients commonly exhibit abnormal circulating concentrations of lipoproteins, which may contribute to the increased incidence of CHD in these patients. In particular, VLDL and LDL levels are often elevated in diabetes, whereas there may be a concomitant decrease in the HDL fraction (Cusi and DeFronzo, 1988).

Metformin, an anti-hyperglycaemic agent used in the treatment of type 2 diabetes, is frequently associated with a small reduction in the circulating levels of LDL cholesterol and sometimes a small increase in HDL cholesterol, especially in hypercholesterolaemic patients. Treatment of type 2 diabetic patients with metformin has also been reported to reduce the incidence of micro- and macrovascular complications (UKPDS, 1998).

Recent clinical evidence suggests that metformin may reduce the intestinal absorption of bile salts (Scarpello *et al.*, 1998). Bile salts are actively reabsorbed in the terminal region of the ileum and contribute to the tightly regulated pool of circulating cholesterol via their continued synthesis, secretion, and reabsorption. Thus, a reduction in the absorption of bile salts in the terminal small intestine may account for the modest fall in circulating total cholesterol levels in patients receiving metformin therapy. Moreover, the cholesterol lowering action of metformin may be related to the lower mortality rates from microvascular and

macrovascular complications compared with alternative oral anti-diabetic agents (UKPDS, 1998).

The aim of this thesis is to investigate the effect of metformin on bile salt absorption from the intestine and to evaluate potential mechanisms involved utilising whole animal, isolated tissue, and cultured cell models. In addition, studies have been undertaken to investigate the effect of chronic metformin therapy upon cholesterol deposition within aortic vessels, and upon the compliance of these vessels in response of vascular smooth muscle to the contractile influence of noradrenaline (NA) and the vasodilatory effect of acetylcholine (Ach).

Chapter Two:
Materials and Methods

Chapter Two: Materials and Methods

2.1 *In vivo* studies:

2.1.1 Animal Care and Preparation:

Male rats of the Wistar strain weighing between 150-250g were used throughout. Animals were fed a standard laboratory pellet diet (SDS Economy Rodent Breeder, Special Diet Services, Witham Essex, U.K.) and tap water *ad libitum*. Food was withheld for a period of 12h prior to commencement of procedures, while tap water remained available *ad libitum*. During the period when food was withheld, the animals were housed separately in a large metallic cage with wide mesh flooring to prevent coprophagy. The animal unit was air conditioned at $22\pm 2^{\circ}\text{C}$ with a regular lighting schedule of 12h light and 12h dark.

Prior to experimentation, the animals were weighed and injected intraperitoneally with Sagatal (sodium pentobarbitone, Rhône Mérieux, France) at a concentration of 60mg/kg. Once anaesthesia had been induced, a lateral midline incision was made into the abdomen and the intestine exposed. The bile duct was exposed by threading a suture (Mersilk 4/0 Ethicon Ltd, Edinburgh, U.K) around the jejunum, to retract the jejunum to the right, and expose the bile duct close to the liver. The bile duct was partially cut and cannulated with a pp10 cannula. The cannula was secured using a braided suture and bile subsequently collected. A 5cm region of distal ileum or proximal jejunum was selected and tied off at either end with ligatures. In the case of ileum, a region was selected 2-3cm proximal to

the ileo-caecal junction. For jejunum, a region 2-3cm distal from the ligament of Treitz was selected. Throughout the experiment the animal's temperature was continually monitored. The animal was maintained at approximately thermoneutrality using an angle poise lamp positioned approximately 30cm away, and by using tissue paper covering the abdomen.

2.1.2 Radiolabel Preparation and Administration:

Radiolabelled [1- ^{14}C] Glycocholic acid, sodium salt (Amersham U.K., specific activity 57mCi/mmol) at a concentration of 1 μCi was dissolved in a 1ml solution of unlabelled glycocholic acid (Sigma) at a concentration of 20mmol/l for administration to ileum and 8mmol/l for administration to jejunum. Drug treated animals received metformin (Sigma) at a concentration of 250mg/kg dissolved in the solution of unlabelled glycocholate/ ^{14}C sodium glycocholate. This solution was injected directly into the isolated region of intestine using a 5ml syringe and 25G needle. To assist the maintenance of body temperature, peritoneal muscle was closed at the site of surgical incision using artery clamps.

2.1.3 Sample Collection #1:

Bile samples from the biliary cannula and blood samples from tail vein were collected at 10-minute intervals over a 180-minute period. Blood samples were centrifuged upon collection and the plasma layer removed and stored at 4°C. Upon cessation of the experiment, samples of liver, ileum, jejunum, caecum, ascending colon and the luminal contents of the relevant segments of ileum or jejunum were collected. Tissues were weighed and placed in scintillation vials with 0.5ml of 1M sodium hydroxide (NaOH), heated to 60°C until dissolved,

mixed with 5ml of scintillation fluid (Optiphase 'Hisafe' III, Fisons) and vortex mixed. Bile and plasma samples (20µl) were mixed with 5ml scintillation fluid. All samples were counted for ^{14}C on a Packard 1600/1900 TR scintillation counter.

2.1.4 Surgical Manipulation:

A second series of similar experiments was performed using male Wistar rats weighing between 150-200g. Animals were starved and surgically manipulated as detailed in section 2.1.1. Additionally, the carotid artery was cannulated with a pp10 cannula and secured using ligatures. This was achieved by making a 2-3cm lateral incision through skin covering the ventral surface of the neck. Muscle covering the trachea was then blunt dissected and split longitudinally using scissors. The left carotid artery, running parallel to the trachea, was readily accessible.

Curved forceps were used to gently separate the vagus nerve from the left carotid artery along a length of approximately 2cm. A ligature was secured distally to the proposed site of incision to prevent backflow of blood. The carotid artery was then clamped proximally to the intended site of cannulation using an artery clamp and a small incision made into the artery. The vessel was cannulated through the incision using pp10 tubing and secured with a ligature. Prior to cannulation, the cannula tubing was passed over a 26G needle attached to a 5ml syringe containing heparin (Sigma, 50units/ml) to prevent blood clotting at the point of incision. Radiolabel was prepared and injected into ileal or jejunal regions as

detailed in section 2.1.2. Bile samples were collected at 10-minute intervals over a period of 60 minutes.

2.1.5 Sample collection #2:

Blood samples (150µl) were withdrawn from the carotid artery at 10-minute intervals, centrifuged, and plasma removed and stored at 4°C until conclusion of the experiment. Hepatic portal vein (HPV) samples were collected every 30 minutes over the duration of the experiment. Prior to experimentation, needles (25G) were soaked overnight in heparin (500units/ml) to prevent clotting upon incision into the HPV. The needle was inserted at a shallow angle along the direction of blood flow and approximately 200µl of blood withdrawn. Haemorrhage was prevented by the gentle application of pressure using a swab following removal of the needle. Blood samples were then centrifuged, and plasma removed and stored at 4°C until required. Bile samples were weighed at the end of the experiment and 20µl placed in 5ml scintillation fluid. Tissues were removed, weighed, and dissolved in 0.5ml NaOH (1M) before being mixed with scintillation fluid (5ml). All samples were counted for ^{14}C ; results are expressed as disintegrations per minute (dpm) per microlitre plasma/bile and per mg tissue.

2.2 Thin Layer Chromatography:

In order to confirm that the radiolabelled molecule collected in bile and plasma samples was the same as that introduced, i.e., intact glycocholate, thin layer chromatography (TLC) was performed. The method employed was derived from

routine procedures undertaken at Aston University to confirm the integrity of steroids and related compounds including bile salts.

Plasma sample (A) was obtained from the tail of an anaesthetised animal prior to bile salt administration and therefore contained no radiolabel. Sample B was collected from the HPV during bile salt absorption studies and contained 4.56dpm of ^{14}C glycocholate per microlitre plasma. Dilute radiolabel (0.1 μl diluted tenfold with serum) was added to sample A for comparison with sample B. Equal volumes of chloroform-methanol (50 μl) were added to plasma samples to precipitate protein. Samples were allowed to stand for 5 minutes and were then centrifuged for 60 seconds. The upper lipid layer was subsequently removed and stored at 4°C until required.

Preparation of the TLC plate involved stripping 1cm of silica powder from either side along the intended direction of solvent flow. A faint pencil line was drawn 2cm from the bottom of the plate and represented the point of origin of the samples. Plasma samples were spaced 6cm apart and from either side of the plate; the sample was introduced onto the silica in 0.5 μl aliquots and dried between applications using a hairdryer. Once dried, the plate was introduced into a covered glass container and placed vertically in 103ml solvent (64ml hexane, 35ml diethylether, 4ml acetic acid) which was allowed to travel vertically by capillary action for a period of 45 minutes. During this time solvent flow resulted in the separation of substances relative to their molecular weight. After 45 minutes the plate was removed and lipids identified in the presence of iodine

vapour. Separated fractions were marked with pencil and measured from the point of origin to the solvent front and their R_f values determined

The chromatography plate was divided into 1cm sections from which the silica was scraped using a razor blade and added to 5ml scintillation fluid. The vials were vortex mixed for 20 seconds and counted for ¹⁴C. The results demonstrated that virtually all radiolabel was located in the final band of silica in both samples. This suggests that the ¹⁴C sodium glycocholate recovered during absorption studies is the same as that initially added. Some streaking was observed in initial experiments and may be attributed to insignificant amounts of radiolabel being attached to plasma proteins of differing molecular weights.

2.3 Chronic Cholesterol Feeding Studies:

Sixteen male homozygous lean (HO) mice from the Aston colony used to breed the *ob/ob* mutants were initially used to study the chronic effect of metformin administration during consumption of a high cholesterol diet. Mice were maintained on a standard powdered diet (SDS Economy Rodent Breeder, Witham Essex, U.K.) supplemented with 5% cholesterol and 4% lard for a period of eight-nine months. The diet was prepared by mixing 40g melted lard with 50g powdered cholesterol (Sigma) and 910g standard powdered diet. This was then mixed with approximately 800ml tap water and dried overnight at 70°C. Animals were housed in plastic cages with the food and water available *ad libitum*. The animal unit environment was controlled at a temperature of 22°C ± 2°C with a regular 12h light-dark lighting schedule. The bedding of sawdust was changed weekly along with cages and water bottles. Animals were housed in two

experimental groups; eight controls and eight metformin treated animals. Drug treated animals were supplied with drinking water containing metformin at a concentration of 250mg/kg, the volume of water supplied was in excess of their normal drinking capabilities and was thus available *ad libitum*. Food was replenished every other day where necessary and animals were weighed weekly. At intervals throughout the experiment, tail vein blood samples were collected and plasma was separated by centrifugation and retained for determination of plasma cholesterol levels at a later date. After a period of eight months, the animals were anaesthetised with halothane and killed by cervical dislocation. Tissues (liver and aorta) were removed for histology (section 2.4) and arterial compliance studies.

2.3.1 Arterial Compliance studies:

2.3.1a Study #1:

A segment of thoracic aorta measuring approximately 2cm was removed and placed in chilled physiological salt solution (PSS) buffer (Palmer *et al.*, 1998; appendix II). Aorta was removed under careful dissection by inserting curved watchmaker's forceps under the vessel and carefully dissecting the fatty tissue surrounding the organ as it runs parallel with the vertebral column. Tissue was trimmed of any remaining fatty tissue under a dissecting microscope, and mounted horizontally between two wire triangles in order to quantify compliance. The tissue was placed into an organ bath containing PSS buffer prewarmed to 37°C, gassed with 5% CO₂ and 95% air. Aortic tissues were subjected to a resting tension of 1g and allowed to equilibrate for 60-90 minutes. Compliance was

determined using standard organ bath and compliance apparatus (electromed amplifiers, isometric transducers (Poiden UF1) and a BBC Goerz chart recorder). Vessel contraction was recorded following the addition of NA (bitartrate salt; Sigma; $3 \times 10^{-9} - 1 \times 10^{-6}$ M) directly to the organ bath. Results are expressed as percentage contraction to NA of the cholesterol fed group.

2.3.1b The Mulvany and Halpern based multimyograph (Study #2):

The above apparatus was leased from Danish Myotech Technologies (Aarhus, Denmark, model 610M; figures c + d, appendix I) in order to measure the compliance and responsiveness of large vessel resistance to contractile and relaxant agonists. Essentially, these experiments were a repeat of experiments in section 2.3.1a, using more sensitive apparatus, although some modifications were implemented in the light of the previous experiments.

Animals were divided into three experimental groups: a control group which received normal pellet diet and tap water; a cholesterol fed group which received high cholesterol diet (5% cholesterol, 4% lard w/w of diet) and tap water; and a drug treated group. The drug treated group received a high cholesterol diet and metformin in tap water at a dose of 250mg/kg. Animals were kept under identical conditions as in section 2.3 and subject to the same treatments. The experimental time period represented approximately eight-nine months. Unlike the previous set of experiments, blood samples were not removed from the tail during this trial.

In a preliminary part of the present study to assess the use of anaesthesia, it was discovered that inducing halothane anaesthesia in order to conduct cardiac

puncture influenced the functioning of the aortic vessel. Animals were therefore stunned and killed by cervical dislocation to alleviate this effect. Blood was obtained from the heart once cervical dislocation had been performed and this was used to determine cholesterol concentrations and clotting factors at a later date (sections 2.5 and 2.6 respectively). The excised vessel was immediately immersed in chilled PSS buffer and trimmed free of adherent connective tissue under a dissecting microscope. At this point a 0.5cm segment of the vessel was placed in 2.5% glutaraldehyde (Sigma) in 0.2M phosphate buffer for electron microscopy. In addition, a segment of vessel was also embedded in OCT (BDH) mounting compound for cryotomy. The remaining length of aorta was then divided into two sections approximately 0.5cm in length and carefully mounted onto the wire supports of the myograph system.

The tissue was subject to a resting tension of 1g throughout the experiment, which was measured using a micropositioner. Each tissue segment was placed in an individual organ bath, gassed continually with 5% CO₂ and 95% air, and maintained at 37°C. As in the initial experiments, a contractile dose-response curve was established in response to NA ($5 \times 10^{-9} - 1 \times 10^{-6}$ M). In addition, the ability of the vessel to relax in response to Ach was also investigated ($1 \times 10^{-9} - 1 \times 10^{-6}$ M). Vessel reactivity was recorded on a chart recorder (BBC Goerz) through a force transducer output. Results are expressed as a percentage contraction to NA of the control group, and a percentage relaxation to Ach of the maximally achieved contractile response.

Preliminary experiments were also performed to assess vessel compliance in the absence of a functional endothelial cell layer. During these experiments the vessel lumen was carefully rubbed using the tips of fine forceps to disrupt the endothelial cell layer, and the vessel subsequently contracted with NA. It became evident that vessel damage was occurring as the vessel lumen was rubbed, resulting in a diminished contractile response. It was subsequently decided to perform future experiments in the presence of the endothelial cell layer, to maintain tissue viability.

2.4 Histology:

Aortic samples removed from control and drug treated mice were subject to histological examination under light (Leitz Wetzlar microscope) and electron microscopy.

2.4.1 Cryotomy:

In order to quantify the presence of cholesterol and lipids in aortic samples, it was necessary to section samples using a cryostat since conventional histological procedures would result in lipid loss. Thoracic aorta was removed and immediately frozen (using dry ice) in OCT mounting compound onto a cryostat chuck. Once frozen the tissue was stored at -70°C wrapped in aluminium foil. Sectioning tissue involved attachment of the frozen specimen of tissue to a chuck of the cryostat using mounting compound. Once the tissue sample had equilibrated to the temperature within the cryostat chamber (approximately 60 minutes at -24°C), the sample could be sectioned either manually or mechanically.

Sections of tissue (12µm thickness) were delivered serially and attached to microscope slides (Sigma; aminoalkylsaline coated, or BDH; electrostatically charged) by capillary action. The sections were allowed to air dry overnight and were then stained for the presence of lipids using Oil red O or Sudan III and IV (appendix II). Cholesterol was determined using the enzymatic method described in section 2.4.2, and the perchloric acid-naphthoquinone (PAN) method (appendix II). For identification of aortic structure, traditional stains (Haematoxylin Gill III, Fisher; Carazzi's, see appendix II; and Eosin Y, 1% aqueous, Fisher) were used (Bancroft and Stevens). Since the PAN method (Adams, 1961) proved difficult to employ, and staining to an appreciable extent difficult to achieve, the enzymatic method (described below) for determining the presence of cholesterol was used routinely.

2.4.2 Enzymatic Cholesterol Determination:

Emis *et al.* (1977) described a method for the determination of total cholesterol and its esters within tissue. The method involves the production of hydrogen peroxide (H_2O_2) from free cholesterol following the enzymatic action of cholesterol oxidase. An insoluble brown complex is generated at sites of H_2O_2 production in the presence of 3,3'-diaminobenzidine tetrahydrochloride (DAB), the reaction being driven by peroxidase.

The overall reaction involves the production of cholesterol and fatty acid from cholesterol ester via the enzyme cholesterol ester hydrolase. Cholesterol in the presence of oxygen is converted to cholest-4-en-3-on and H_2O_2 by cholesterol oxidase enzyme. The H_2O_2 in the presence of DAB is converted by horseradish peroxidase to an insoluble brown coloured polymer.

Cholesterol esterase (from *Pseudomonas fluorescens*, 2mg/ml in 3.2M ammonium sulphate, 10units/mg) was purchased from Sigma along with cholesterol oxidase (from *Nocardia erythropolis*, 1mg/ml in 1M ammonium sulphate, 20units/mg) and DAB (tetrahydrochloride). Peroxidase (from horseradish, 10mg/ml in 3.2M ammonium sulphate, 250units/mg) was purchased from Boehringer Mannheim. All reagents were prepared freshly on the day of use, immediately prior to the experiment.

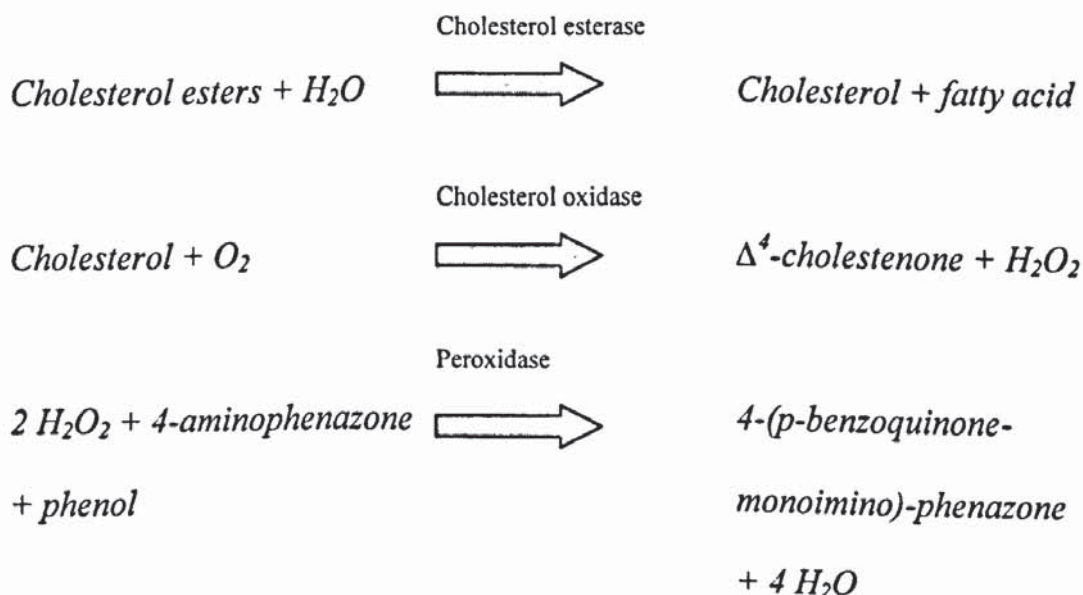
A solution of 0.1M phosphate buffer containing 1.4units/ml cholesterol esterase, 0.4units/ml cholesterol oxidase, 50units/ml peroxidase, 0.5mg/ml DAB, and 0.1% (v/v) triton X-100 was prepared. Frozen sections (12 μ m in thickness) were taken from aortic samples frozen at the time of the vascular response study (section 2.3.1b), attached to BDH Superfrost slides and air dried. Slides were rinsed initially in 0.1M phosphate buffer for 15 minutes and immersed in the incubation medium described above for 150 minutes. The medium was kept at 37°C throughout and masked from daylight using foil to prevent the photo-oxidation of DAB.

Slides were then washed in cold 0.1M phosphate buffer for 15 minutes to remove all traces of unreacted DAB. Sections were then counterstained with Carazzi's haematoxylin (appendix II), passed through 70% alcohol, 100% alcohol, and xylene before being mounted using DPX (Fisher). Observation of the sections under light microscopy revealed that no deposition of cholesterol was evident in the arterial wall (figures e-j, appendix I). The positive control (adrenal gland) stained very lightly with DAB. However, following counterstaining with

haematoxylin, this colouration was masked. The DAB complex was evident in small quantities in some fatty tissue surrounding the aortic structure (figure j, appendix I). This provides evidence that if cholesterol was present in the arterial wall it would have been visible by the formation of the DAB complex. Sections of aorta from all animals were counterstained with haematoxylin, mounted in DPX and photographs taken for structural reference.

2.5 Determination of Total Plasma Cholesterol:

Plasma samples from mice subject to high cholesterol feeding with and without metformin (section 2.3) were collected and stored at -20°C until required. Total cholesterol levels were measured utilising the CHOD-PAP method, as described below. The assay kit was purchased from Boehringer Mannheim and the reaction summarised below.



Cholesterol esters are hydrolysed by cholesterol ester hydrolase into free cholesterol. Free cholesterol is subsequently converted to cholestenone along with H₂O₂ by cholesterol oxidase. In the presence of aminophenazone, phenol,

and peroxidase, cholestenone is converted to a chromogen with a maximum absorption at 500nm (Allain *et al.*, 1974). The reactions were quantified using a spectrophotometer (LKB 4053 Ultrospec K) by the use of H₂O₂-dependent colour forming reactions. Plasma samples (20µl) were pipetted into the reagent solution (2ml) and mixed. A single blank was used for each experiment and consisted of reagent solution (2ml). All samples were incubated at 37°C for 5 minutes to facilitate the colour forming reaction and were read at 500nm within one hour.

2.6 Factor XIII Analysis:

During the cholesterol feeding studies (section 2.3), blood samples were collected by cardiac puncture from the mice following cervical dislocation. The blood was added to anticoagulant (tri-sodium citrate, 0.1M) in a ratio of 9:1, blood to anticoagulant. Samples were placed immediately on ice and subsequently centrifuged at 2560rpm for 30 minutes at 4°C (Baird and Tatlock Mark IV refrigerated centrifuge). Following centrifugation, plasma was separated from the pellet of blood cells and immediately stored at -20°C. Samples were assayed at a later date for the activity of factor XIII, a factor involved in the stabilisation of the fibrin clot. The procedure involves the conversion of fibrinogen to fibrin in the presence of the enzyme thrombin. The activity of factor XIII was then measured using the procedure detailed below.

2.6.1 Factor XIII Activity Assay:

Blood plasma samples obtained from experimental mice utilised in arterial compliance studies (2.3.1a and b) were used to determine the activity of factor XIII. Factor XIII was selected for study because it is a factor essential for fibrin

clot stabilisation (Muszbek *et al.*, 1996). It may also affect cross-linking of proteins in the vessel wall, which could alter compliance, and might contribute to beneficial vascular effects seen with metformin therapy. Being a guanidine, metformin might also alter factor XIII activity since metformin is known to increase fibrinolysis (Chakrabarti *et al.*, 1965). A disproportionate balance between fibrin clot formation and fibrinolysis may exist in diabetes (Jokl and Colwell, 1997). As such, plasma samples obtained during cardiac puncture were used to determine the activity of factor XIII in mice receiving a normal rodent diet and a high cholesterol diet with and without metformin.

Plasma samples were centrifuged at 4°C at 2560rpm to separate blood cells, and stored at -20°C until required. Assays for Factor XIII activity were performed by myself at Leeds General Infirmary, Unit of Molecular Vascular Medicine, where the assay is routinely used in human studies. The opportunity to undertake this work at Leeds was kindly made available courtesy of Professor Grant, and guidance provided in the procedures thanks to Dr Ariëns.

Mouse fibrinogen was purchased from Sigma chemicals and used in the microtiter assay along with 5-(biotinamido)pentylamine as substrates.

Mouse fibrinogen (100µl) was used to coat Nunc Immuno Maxisorp microtiter plates at 40µg/ml in TBS buffer (40mmol/l Tris-HCL, 140mmol/l NaCl and 0.02% (w/v) NaN₃, pH8.3) for 45 minutes at room temperature. The solution was discarded and the reaction blocked by the addition of 200µl TBS containing 1% BSA for 20 minutes at 37°C. Following this incubation, wells were washed twice

in 300 μ l TBS buffer. Plasma samples taken into 0.1M tri-sodium citrate buffer were diluted 1:10 with TBS buffer and 10 μ l of the dilute samples reverse pipetted in to the centre of each well in duplicate.

A reaction solution consisting of α -thrombin 1.11IU/ml (Sigma), 5-(biotinamido)pentylamine 1.11mmol/l (Pierce Chemical Company), DTT (Dithiothreitol) 0.56mmol/l (Sigma), and CaCl₂ 0.11M was prepared in TBS beforehand and kept on ice until required. This solution was delivered (90 μ l) into each well to initiate the cross-linking reaction, and incubated for 3 and 10 minutes. The reaction was stopped by the addition of 200 μ l 200mM EDTA after 3 minutes and 10 minutes. Wells were washed twice with 300 μ l TBS, and 100 μ l of 10 μ g/ml streptavidin-alkaline phosphatase (Sigma) in TBS containing 0.1% BSA added to each well and allowed to incubate for one hour at 37°C.

The assay works on the basis of coating wells of microtiter plates with fibrinogen. Coated fibrinogen in the presence of activated factor XIII becomes converted to fibrin monomers (Song *et al.*, 1994). Factor XIII becomes activated in the presence of thrombin and calcium. Incorporation of 5-(biotinamido)pentylamine occurs into adsorbed fibrin following commencement of the fibrinogen to fibrin conversion. Biotinylated products were detected by incubating with streptavidin-alkaline phosphatase and reading the absorbency at 405nm for *p*-nitrophenol. Absorbance was measured on a Titertek automated absorbance reader (Flow Laboratories).

2.7.1 Everted Intestinal Sacs:

Following the *in vivo* observation that bile salt transport could be influenced differently by metformin in ileum and jejunum, an *in vitro* model was established to examine the effects of metformin on bile salt transport in isolated everted intestinal sacs. Everted intestinal sacs have been used previously to study the transport characteristics of sugars, amino acids and bile salts (Caspary, 1971; Holt, 1964; Lack and Weiner, 1961; Caspary and Creutzfeldt, 1975).

The model utilised herein for bile salt transport was based on that of Lack and Weiner (1961), with additional methodology adapted from Wilson and Wiseman (1954).

Male rats of the Wistar strain weighing approximately 200g were used. Unlike the *in vivo* rat model, the decision was taken not to starve the animals prior to experimentation since the intestinal contents could be removed during the eversion process. Observations were also noted in the literature suggesting starvation may reduce mucosal and serosal fluid transfer compared to *ad-lib* fed animals (Perris, 1964). Thus, food and water were available *ad libitum*. Initially, animals were killed by stunning and cervical dislocation. However, the intestine is incredibly sensitive to shock. Since it appeared that this initial shock might induce massive vasoconstriction of the tissue, subsequent animals were killed by sodium pentobarbitone overdose.

Following pentobarbitone overdose, a midline incision was made into the abdomen and the intestine exposed. The whole of the small intestine was removed by severing the upper duodenum and the lower ileum. The intestinal tissue was separated from the attached mesentery by manual stripping, placed into Krebs-Henseleit buffer (appendix II) and allowed to equilibrate to room temperature. At this point, any excessive fatty tissue was removed along the site of mesenteric attachment.

The intestine was then secured to a glass rod (0.5cm diameter) using a ligature and the remaining tissue rolled over the secured site. The everted intestine was then returned into buffer at room temperature. To prevent damage to the intestinal mucosa, the everted tissue was placed onto filter paper discs saturated with 0.9% NaCl. Five centimetre regions of intestine were then measured, cut, and placed back into Krebs-Henseleit buffer.

A preweighed ligature was tied around one end of each sac. A second ligature, also preweighed, was tied loosely around the open end in preparation for tightening. The ligatures were bathed in buffer solution prior to weighing to allow saturation of the material. This was performed to prevent absorption of fluid by the ligatures and therefore avoid inaccurate quantitation of fluid uptake into the sac preparation. Each sac (plus the two ligatures) was weighed (W1) using a torsion balance. A blunt needle attached to a 1ml syringe was then introduced into the intestinal lumen and the second ligature secured over the needle. Approximately 0.5ml of solution (Krebs-Henseleit buffer containing unlabelled glycocholic acid at 10mmol/l for ileum and 5mmol/l for jejunum) was injected

into the sac. As the needle was removed from the lumen, the second ligature was tied securely and the sac was reweighed (W2).

The sac was then placed into a 50ml conical flask containing 15ml Krebs-Henseleit buffer with unlabelled glycocholic acid at the concentrations described above. In addition, metformin was present at a concentration of 1×10^{-3} M, 1×10^{-2} M and 5×10^{-2} M, where appropriate. Radiolabelled sodium glycocholate was also added to all flasks (1 μ Ci). The flasks were stoppered using 'suba-seals' and placed into a shaking water bath (37°C) maintained at approximately 90 oscillations per minute. The tissue was aerated continually for 90 minutes with 5% CO₂ and 95% air. Following 90 minutes incubation, each sac was removed from the bathing solution, blotted, and weighed (W3). Intestinal fluid contents were then removed using a 1ml syringe with a 26G needle attached. The weight of the tissue less the intestinal contents was then recorded (W4). A section of the intestinal sac wall was removed, weighed and dissolved in 0.5ml NaOH (1M) at 60°C for 30 minutes.

Triplicate samples (20 μ l) were removed from the solution bathing the intestinal sacs and the solution from within the lumen. Samples were added to 5ml scintillation fluid and counted for the presence of ¹⁴C. Results represent values of dpm per μ l solution or per mg tissue and are expressed as percentage of controls. Using the weights recorded throughout the experiment, it was possible to determine the serosal and mucosal fluid transfer, along with the volume of fluid

retained within the intestinal wall. The calculation is similar to that used by Perris (1964) and is as follows:

W1 = Weight of empty gut including two saturated ligatures

W2 = Weight of initial full gut including two saturated ligatures

W3 = Weight of full gut following 90 minute incubation including two saturated ligatures

W4 = Weight of final empty gut (contents removed) including two saturated ligatures

Mucosal fluid transfer (A) = $W3 - W2$

Gut fluid uptake (B) = $W4 - W1$

Serosal fluid transfer (C) = $A - B$

Initial wet weight of tissue = $W1 - \text{weight of ligatures}$

If A is > than B then C = serosal fluid uptake, with B value from mucosal surface.

If B is > than A then C = serosal fluid loss, with B value from serosal surface.

Parsons *et al.* (1958) originally described the terminology used above; i.e. serosal fluid transfer is the increase or decrease in the volume inside the sac following incubation. Mucosal fluid transfer is defined as the diminution in the volume of the mucosal fluid (fluid bathing the sac) over the incubation period. The gut fluid uptake represents the volume of fluid retained within the intestinal wall and may originate from either mucosal or serosal surfaces in this model. Results are expressed as the percentage fluid transfer in microlitres, of control values. These

calculations were made following each experiment and were introduced as a measure of the absorptive capacity of the intestinal tissue. Frequently, however, the absorptive function of the intestinal regions was influenced by the presence of metformin. In some instances, the results may not accurately reflect the true nature of the absorption capacity of the specified regions, due to the localised drug effect. This is discussed further in chapter 3.

2.8 Cell Culture:

2.8.1 L6 Skeletal Muscle Cell Culture:

2.8.1a Supplements and Media:

Sterile DMEM (Dulbecco's Modified Eagle Medium) was purchased from Gibco as 500ml solutions supplemented with 0.11g/l sodium pyruvate and 2500mg/l glucose. Medium was supplemented with foetal calf serum (FCS) at 5% for complete medium and 0.5% for serum-depleted medium. Antibiotic/antimycotic solution (100 ×, containing 100units/ml penicillin G sodium, 10mg/ml streptomycin sulphate, 25µg/ml amphotericin B as fungizone in 0.85% saline) and L-glutamine (2mmol/l) were also added. All supplements for L6 media were purchased from Gibco.

L6 skeletal muscle cells were originally derived from the thigh of newborn rats (Yaffe, 1968). They are used widely as a culture model for glucose uptake since the primary site for glucose uptake and utilisation *in vivo* occurs in skeletal muscle, and insulin resistance at the level of this tissue is a major contributory

factor to hyperglycaemia (Baron *et al.*, 1988). Studies characterising the L6 cell line and their suitability for glucose uptake and affinity for metformin have been performed by Bates (1999). Thus, the experiments described herein represent preliminary studies designed to confirm the findings of Bates (1999). Aseptic technique was employed for all cell culture studies.

2.8.1b L6 Muscle Cell Maintenance and Propagation:

The L6 cell line was sustained as a monolayer culture in 75cm³ culture flasks (Sarstedt). Monolayers were cultured in 20ml DMEM medium supplemented with 5% FCS, 1% antibiotic and L-glutamine (2mmol/l). Flasks were incubated at 37°C under 5% CO₂ and 95% air until confluent (Heraeus Instruments, Model BB6220). Cells were passaged at approximately 80% confluence.

All DMEM was aspirated from confluent flasks and discarded. Approximately 5ml of trypsin-EDTA (0.5g porcine trypsin, 0.2g EDTA, 4Na/l of HBSS; Sigma) was added to the flasks to detach cells. Flasks were agitated for approximately 10 minutes until all cells were visibly detached under an inverted microscope (Olympus CK 2, Olympus Optical Co. U. K.). The trypsinised cells were centrifuged (MSE Mistral 2000, Fisher Scientific Loughborough, UK) for 5 minutes at 1000rpm and the supernatant discarded. The cell pellet was resuspended with 10ml of fresh medium to obtain a cell suspension, and 1ml of this suspension was added to 20ml prewarmed DMEM in fresh culture flasks. Cell type, date, and passage numbers were recorded for each flask. Flasks were incubated for 3-4 days until confluent. The remaining cell suspension was used for subsequent experimentation.

2.8.1c L6 Cell seeding:

Trypsinised cells were seeded into 24 well plates (16mm wells containing 5×10^5 cells per ml medium) and grown to confluence for 2-Deoxy-D-[1,2- ^3H] glucose uptake experiments. Plates were serum-starved by the addition of DMEM supplemented with 0.5% FCS. Following serum starving, appropriate drugs were added onto cells for 24 hours prior to experimentation (metformin $10^{-5} - 10^{-3}$ M, insulin $10^{-9} - 10^{-6}$ M).

2.8.1d Uptake of 2-Deoxy-D-[1,2- ^3H] Glucose into L6 Muscle Cells:

In order to determine the uptake of glucose into muscle cells, a radiolabelled glucose analogue was used (2-deoxy-D-[1,2- ^3H] glucose, Amersham; Specific activity 60.0Ci/mmol). This labelled molecule is transported via the same route as traditional glucose but is not metabolised past the point of phosphorylation (Walker *et al.*, 1989). This pathway allows the determination of ^3H -2-DG once the muscle cells have been lysed. Details relating to the growth stages of these cells and their subsequent differentiation has been previously characterised by Bates (1999). L6 muscle cells *in vitro* differentiate into multinucleated myotubes following membrane fusion, mimicking the process of maturation occurring during muscle ontogenesis (Klip and Leiter, 1990). Over time these muscle cells align and eventually undergo differentiation and fusion into myotubes.

Plates of confluent serum-starved cells were washed with 1ml of glucose-free Krebs-Ringer buffer solution maintained at room temperature (appendix II). This solution was aspirated and discarded. A second solution of glucose-free Krebs buffer, containing the radiolabel 2-deoxy-D-[1,2- ^3H] glucose (7.4Kbq/ml,

0.2 μ Ci/ml) and 0.0162mg/ml unlabelled 2-DG (Sigma), was then added to each well at a volume of 1ml and incubated for 10 minutes at room temperature. The radiolabel solution was then aspirated from the wells and discarded. An ice-cold solution of glucose-free Krebs buffer was used to wash the cells of radiolabel and terminate glucose uptake. Cells were lysed by the addition of 0.5ml (1M) NaOH over a period of 60 minutes. Post-incubation, contents of each well were collected individually using a Gilson pipette and added to 5ml scintillation fluid. Samples were vortex mixed and counted for ^3H using a Packard 1600/1900 TR scintillation counter.

2.8.2 Caco-2 Cell Culture:

2.8.2a Caco-2 Media and Supplements:

Sterile DMEM was purchased from Gibco as 500ml solutions supplemented with 0.11g/l sodium pyruvate and 4500mg/l glucose. Medium was supplemented with FCS at 10% for complete medium. The following supplements were also added: Non-essential amino acids (Sigma, 5ml of a 10mM 100 \times solution). Antibiotic/antimycotic solution (100 \times , containing 100units/ml penicillin G sodium, 10mg/ml streptomycin sulphate, 25 μ g/ml amphotericin B as fungizone in 0.85% saline) and L-glutamine (2mmol/l). Hepes (Sigma, 2.45ml of a 1M solution) was also added. Complete medium for the subculture of Caco-2 cells was refrigerated at 5°C for up to 14 days.

All supplements, unless stated as sterile by the supplier, were filter sterilised and added directly to the medium. FCS was aliquoted into 25ml samples and stored at -20°C. The antibiotic solution was stored in 5ml aliquots at -20°C, whilst L-glutamine was prepared as a 200mmol/l stock and stored as 5ml aliquots at -20°C. Hepes buffer and non-essential amino acids were stored at 5°C.

2.8.2b Maintenance and Propagation:

Caco-2 cells were purchased from the European Culture Collection as a growing culture and are derived from a primary colonic tumour of a 72-year-old caucasian male (Fogh *et al.*, 1977). Medium covering confluent cells was aspirated and discarded. A solution of PBS-EDTA (Sigma, 5ml of 0.02% solution EDTA prepared in Ca^{2+} and Mg^{2+} -free buffer) prewarmed to 37°C was added to the culture flasks and allowed to stand for 5 minutes. The PBS-EDTA solution was aspirated, discarded, and 2ml trypsin-EDTA (Gibco, 2.5ml 1 × solution containing 0.5g trypsin, 0.2g EDTA, 4Na/l) was added to the flasks and incubated at 37°C for approximately 2 minutes. Following this incubation, the trypsin-EDTA solution was aspirated and flask(s) incubated for 5 minutes. Cells were disaggregated by sharp tapping of the flask.

A single cell suspension was obtained by adding 10ml fresh DMEM medium and repeat pipetting. The generation of single cells is essential to obtain an even distribution of the cells for subsequent seeding. Fresh flasks containing 9ml prewarmed complete DMEM (37°C) were seeded with 3ml of the trypsinised cell suspension. Flasks were incubated at 37°C under 5% CO_2 and 95% air until

confluent. Monolayers were passaged at approximately 80% confluence to facilitate the generation of single cell suspensions.

2.8.2c Seeding Transwell Inserts:

Caco-2 cells display many characteristics of ileocytes in the small intestine. They are epithelial in nature and form monolayers (Pinto *et al.*, 1983). Caco-2 cells exhibit a functional intact transport system for bile salts and many other actively transported molecules. The Caco-2 bile acid transporter is reportedly the same as the ileal bile acid transporter *in vivo* (Kanda *et al.*, 1998). These characteristics make them an ideal model to study the transport of specific molecules, in particular bile salts (Hidalgo and Borchardt, 1990). When seeding cell inserts, cells are passaged as detailed in section 2.8.2b. Following trypsinisation, the cell monolayer was resuspended in 11ml of complete medium and a single cell suspension obtained by repeated pipetting. A 1ml sample was removed into an eppendorf and used to determine the cell concentration. Trypan blue (100µl; Sigma) was added to 400µl of the cell sample and the cell concentration and viability determined using a haemocytometer. The cell concentration required for seeding inserts was 200,000 cells/ml.

Following cell concentration adjustments, 2ml of fresh complete medium was added to the basolateral side of each insert. Transwell inserts and plates were purchased from Corning (Corning Costar, Buckinghamshire, U.K. type 3452, pore size 3.0µm, growth area 4.7cm², insert diameter 24mm, polyester membrane) and were seeded at 200,000 cells/ml, i.e. 400,000 cells/insert. The cell suspension was then slowly added to the apical chamber of the insert (2ml),

and the cells observed using an inverted microscope. The plates were incubated at 37°C for 21 days to facilitate monolayer formation, with the medium in both the basolateral and apical chambers changed every other day. After 21 days incubation, the viability of the monolayer was determined visually using an inverted microscope. Prior to experimentation, 2.6ml Hanks Balanced Salt Solution (HBSS; Gibco) was added to the basolateral side of the inserts and 1.5ml added to the apical chamber.

2.8.2d Long-term Storage of Caco-2 Cells:

Caco-2 cells were frozen under liquid nitrogen for long-term storage. The cells were trypsinised and resuspended as described previously (section 2.8.2b). The cell suspension was centrifuged for 5 minutes at 1000rpm to pellet the cells. The supernatant was aspirated and the pellet resuspended in 3ml freezing medium (90% FCS, 10% Dimethyl sulphoxide, DMSO; Sigma). The pellet was gently resuspended in this medium and 1ml added to cryovials. The cells were frozen at a rate of approximately 1°C per minute and placed into the -70°C freezer overnight. Cryovials were then stored under liquid nitrogen.

2.8.2e Propagation of Cells from Long-term Storage:

Complete medium was prepared as before with 20% FCS. Fresh 25cm³ flasks containing 9ml prewarmed DMEM were used to resuspend the thawed cell suspension. Cells were thawed rapidly by partial submergence of cryovials in a warm water bath (37°C). Cells were gently resuspended and slowly added drop-wise into the culture medium of the 25cm³ flasks. Flasks were incubated undisturbed for 7 days at 37°C in 5% CO₂ and 95% air. Following incubation,

cells were passaged from one 25cm³ flask into two 75cm³ flasks, following the procedure detailed in section 2.8.2b.

2.8.2f Bile Salt Transport Studies:

Caco-2 cells were seeded onto Transwell cell inserts (section 2.8.2c) and allowed to form a monolayer for 21 days. Following 21 days incubation, medium in both the basolateral and apical chambers was substituted for HBSS, 2.6ml and 1.5ml respectively.

Figure 2.1
Representation of the Transwell culture system.



24 mm Transwell

Radiolabelled bile salt (0.1µCi ¹⁴C sodium glycocholate, Amersham; specific activity 57mCi/mmol) and radiolabelled mannitol (0.5µCi, Sigma; specific activity 19.1Ci/mmol) were added into each apical chamber. Subsequent experiments involved the addition of D-[U-¹⁴C] Glucose (Amersham; specific activity 297mCi/mmol) to apical chambers, as indicated in chapter 4. Where

appropriate, metformin, ouabain, and 20µl of a 10mmol/l solution of unlabelled glycocholic acid (Sigma; final concentration 0.133µmol/ml) were also added to the apical or basolateral chambers, as indicated in the relevant chapter. Plates were incubated in a water bath for 24h at 37°C. Basolateral and apical contents were removed and placed into vials containing 8ml scintillation fluid per 1ml sample. Transwell inserts were cut from their plastic supports and the cell monolayer dissolved in 2ml NaOH (1M) for 60 minutes and scintillant added. Samples were counted for ^{14}C and ^3H using a Packard 1600/1900 TR scintillation counter.

2.8.2g Determination of Monolayer Integrity:

Transwell inserts utilised in transfer experiments were stained to determine the integrity of the cell monolayer. The procedure employed (Manufacturers instructions, Millipore, Hertfordshire, 1989) involved washing the cell insert free of culture medium using sterile phosphate buffered saline (PBS).

The monolayer was fixed using 3% glutaraldehyde (Sigma) in PBS stored at 4°C for 15 minutes. Methanol was then added to the insert and incubated at room temperature for 10 minutes. Haematoxylin solution (Sigma; Gill 1) was used to stain the monolayer for 9 minutes before being washed with purified water (Fisher, HPLC grade) and the stain differentiated in 0.5% hydrochloric acid in 70% ethanol for 45 seconds.

The insert was again washed with purified water before the addition of dilute ammonium hydroxide (10 drops of 1M concentrated solution in 100ml distilled

water). The insert was further washed in purified water and was cut free of its supporting matrix. The insert was placed on a microscope slide and mounted in a compound suitable for 'wet' samples such as 'hydromount' (BDH). The nuclei of the Caco-2 cells stain a deep blue colour and the general coverage of the insert with cells was clearly evident under light microscopy. The polyester insert itself did not stain with the haematoxylin; thus any blue colouration was attributed solely to the Caco-2 cells. The presence of the insert did, however, impair the ability to observe cells under higher magnification. As such, this method is useful to determine cell coverage but is not useful for determining whether the cell layer is specifically a monolayer or whether several cell layers are present.

2.8.3 The A7r5 Smooth Muscle Cell Line:

A growing culture of A7r5 muscle cells was purchased from ECACC (European Cell and Culture Collection). A7r5 cells are derived from the thoracic aorta of the DB1X rat and as such are a smooth muscle cell line (Kimes and Brandt, 1976). The cells were routinely propagated in 75cm³ flasks using DMEM (0.11g/l sodium pyruvate, 1000mg/l glucose) supplemented with L-glutamine (2mmol/l), 1% Penstrep solution (Gibco), and 10% FCS. The cells appear flat and ribbon-like whilst proliferating. Once confluence is reached, however, the cells arrange themselves parallel to one other. They also take on a spindle shape and appear thinner than previously seen (Kimes and Brandt, 1976).

2.8.3a Cell Maintenance and Propagation:

The A7r5 cell line, as with many adherent cell lines, was passaged at 80% confluence. Any growth medium was aspirated and the cell layer washed with

3ml PBS-EDTA (2.5g EDTA per litre in Ca^{2+} - and Mg^{2+} -free PBS) for 30 seconds. This step was repeated using fresh solutions before adding 2.5ml trypsin-EDTA (Gibco, 1 × solution containing 0.5g trypsin, 0.2g EDTA, 4Na/l) for 30 seconds. The majority of the trypsin solution was removed leaving approximately 0.3ml, and flasks incubated at 37°C for 3 minutes to facilitate enzyme action. The adhered cells were dislodged with sharp tapping of the flask, and a cell suspension obtained by adding 10ml fresh DMEM. New 75cm³ flasks containing 36ml prewarmed DMEM were seeded by adding 4ml of the cell suspension. Flasks were incubated at 37°C under 5% CO₂ and 95% air. Confluence was usually achieved within 3 days.

2.8.3b Petri Dish Studies:

Cells were passaged, as detailed above. Following trypsinisation, 45ml of fresh DMEM was added to 5ml of the harvested cell suspension. Tissue culture treated petri dishes measuring 22cm in diameter (Corning Costar) were seeded with 12ml of this cell suspension and incubated until confluent.

2.8.3c Uptake of 2-Deoxy-D-[1,2-³H]-Glucose into A7r5 Smooth Muscle Cells:

Confluent monolayers of A7r5 smooth muscle cells cultured on petri dishes (as described above) were incubated with the radiolabelled glucose analogue 2-Deoxy-D-[1,2-³H]-Glucose, as described in section 2.8.1d. The protocol used was identical to that described in section 2.8.1d, with the exception that the volume of all solutions used to wash, incubate, and lyse the A7r5 cells was increased to 8ml

for each petri dish in all cases. Samples were collected and counted for the presence of ^3H using a Packard 1600/1900 TR scintillation counter.

2.S.4 Intracellular Calcium Image Analysis:

Evidence exists indicating metformin may influence calcium-regulated events. Metformin treatment at high concentrations (1-30mmol/l) induced rat-tail artery relaxation (Chen *et al.*, 1997). Additionally, cultured vascular smooth muscle cells from rats treated with therapeutic doses of metformin (1-2 $\mu\text{g}/\text{ml}$ for 1-24 hours) responded by a reduced increase in intracellular calcium, following agonist stimulation (Sharma and Bhalla, 1995). To determine whether metformin could acutely influence the intracellular calcium concentration in cultured cells, preliminary experiments were performed utilising the previously detailed A7r5 smooth muscle cell line. The L6 skeletal muscle cell line was also studied for comparison.

A7r5 smooth muscles cells were cultured onto 22cm tissue culture treated petri dishes until confluent, as described in section 2.8.3b. A small region of cells was isolated using a circular plastic mould approximately 5cm in diameter. Silicone grease was used to seal the mould to the plastic petri dish. Fura-2-AM was used as a fluorescent indicator of intracellular calcium movement. The final working concentration of fura-2-AM was 5×10^{-6} M and was prepared in a 1ml solution using DMEM medium containing 5% FCS, 1% PenStrep and 1% L-glutamine. Cells were incubated for 60 minutes with 500 μl of the fura-2-AM solution under 5% CO_2 and 95% air. Following incubation, cells were perfused for several

minutes with a physiological salt solution (appendix II) buffered to pH7.4 in order to remove any dye not taken up into the cells.

As a fluorescent dye, fura-2-AM is useful for determining the concentration of intracellular calcium due to its chelating properties. Fura-2-AM becomes modified intracellularly following its initial uptake. Once absorbed, the 2-acetoxymethyl-ester bond becomes hydrolysed by various esterase enzymes generating a highly charged molecule that cannot flux back across the cell membrane. The initial presence of the AM ester group results in a hydrophobic molecule that is free to flux across the membrane due to its lack of charge.

2.8.4a Drug Perifusion:

Fura-loaded cells were observed using a digital-imaging camera. A single cluster of cells within the selected area was randomly chosen and used to represent the general cell population, with the same cluster of cells being studied for the duration of the experiment. Fine tubing from a reservoir of medium was used to continually perfuse the isolated cells with PSS bathing solution (Borin *et al.*, 1994) or specific drugs. All drugs used were dissolved in the same PSS bathing solution and perfused at the same rate for a specified period of time.

2.8.4b Apparatus:

During perifusion, a single field of view of isolated cells was captured using a cooled digital CCD Camera (Hamamatsu C4880). The digital camera was attached to an epifluorescence microscope (Olympus Bx50WI) programmed to

capture the fluorescence emission from the fura-2 loaded cells. The objective used was $\times 40$ water immersion objective with a 0.8 numerical aperture.

2.8.4c Fluorescence λ :

Fura-2 can be excited at two wavelengths, 340nm and 380nm. The fluorescence of fura-2 at the latter wavelength is sensitive to the prevailing calcium concentration. The fluorescence at 340nm is calcium insensitive, giving a measure of the amount of the fluorescent dye in any one region. During the calcium imaging experiments, cells were exposed to light of 360 and 380nm. These exposure wavelengths were used to subsequently determine a ratio to best represent visible and actual changes in intracellular calcium concentrations. The ratio is derived by dividing the image at 360nm by the image at 380nm, and gives a measure of the change in calcium.

The computer software involved in these experiments is complex and was custom-developed at Aston University by Dr N. Hartell, and allows manipulation and analysis of the digital image. The few experiments performed herein did not allow full evaluation of the intricate details of the system, however the system has been characterised previously. All experiments were conducted in collaboration with Dr. Hartell. Thus, the methods listed above describe the fundamentals of the technique and are not designed to provide comprehensive details of the technical computational aspects. Experiments were performed through automations written in 'OpenLab' software (Improvision) and reanalysis achieved using Egor software, using procedures written by Dr Hartell.

Smooth muscle (A7r5), and skeletal muscle cells (L6), were perfused with 1×10^{-6} M NA for approximately 1 minute. This perfusion was repeated on several occasions following an arbitrary washout period, and independently of additional drugs. Metformin (1×10^{-3} M) was also perfused independently onto the cells for a period of 15 minutes, and with the subsequent addition of NA. NA and metformin were co-perfused at the same concentrations as used above and any effect upon intracellular calcium levels recorded. The experiments were concluded by the addition of thapsigargin, a toxin that blocks the resequestration of calcium from the cytosol (Thastrup *et al.*, 1990). The computer software employed allowed for the isolation of specific cells or regions of cells, enabling specific intracellular events to be accurately visualised and recorded in more than one cell.

One drawback of using cultured cells is that not all cells reach the confluent stage simultaneously. Thus, differences in the reactivity of fully matured cells compared with less mature cells may exist. Results are expressed graphically and represent alterations in intracellular calcium levels based on fluorescence. Digital images of calcium fluorescence were captured at varying points of the experiment and are included as a visible means of determining the intensity of the fluorescence. Images are numbered (and can be found at the foot of figures 5.8.1-5.8.3) and correspond to numbers above the calcium image trace. Figure 5.8.2 also displays a colour graded bar representing image intensity and should be applied to figures 5.8.1 and 5.8.3. The green colouration of this bar represents basal levels of intracellular calcium, whilst yellow and red represent increasingly greater levels of this cation. An image of the experimental cell cluster is also

included in the right hand margin and identifies specific areas within these cells from which calcium levels were measured.

2.9 Statistical Analyses:

2.9.1 Student's 't'-Test:

The Student's 't' test was employed for both paired and unpaired data sets, where appropriate. When comparing data sets from two different experimental treatments (control and drug treated), the unpaired data test was employed, if applicable. If treatments were 'paired' i.e. from the same animal or batch of cultured cells, the paired test was implemented. Where more than two paired data sets were compared, and the paired ANOVA test could not be implemented due to dissimilar experimental group sizes, the paired 't'-Test was again implemented. Although this increases the chance of identifying a false positive in terms of statistical 'significance', its use is more powerful than that of the unpaired test in such situations.

2.9.2 Analysis of Variance and post-tests:

Analysis of variance (parametric and non-parametric) was employed to determine any significant difference between more than two groups of mean values. This test identifies that there is a significant difference between the data but fails to identify the significantly different treatment groups. In order to identify statistically significant treatments, post-tests were introduced. Such tests include the Tukey test and Bonferonni's modification of the 't'-Test. Analysis of

variance, along with the post-test performed, are indicated in figure legends where implemented.

Chapter Three:

The Effect of Metformin on Bile Salt Absorption:

***In Vivo* and *In Vitro* Studies**

CHAPTER THREE: The Effect of Metformin on Bile Salt Absorption: *In Vivo* and *In Vitro* Studies

3.1 Introduction: *In vivo*

The biguanide family of anti-diabetic agents has received considerable focus over recent decades with one agent, metformin, emerging as a front line treatment for type 2 diabetes. The mode of action and clinical end points of metformin are discussed in detail in chapter 1 and will not be reiterated here. Nevertheless, metformin has been shown to exert a correctional effect on several parameters disproportionately balanced in type 2 diabetes. Plasma cholesterol and lipoprotein concentrations, both of which are typically elevated in obese type 2 diabetic individuals (Cusi and DeFronzo, 1998), can be modified by such therapy. Metformin can lower total circulating cholesterol concentrations, albeit modestly, and predominantly in hypercholesterolaemic individuals. In addition, LDL cholesterol is marginally lowered following metformin therapy, and is associated with a concomitant elevation in HDL levels (Cusi and DeFronzo, 1998). The improvement in the lipid profile of type 2 patients by metformin is of potential advantage in slowing the progression of diabetic macrovascular disease. However, the manner in which metformin may alter these parameters is an issue of considerable debate.

A recent study performed by Scarpello *et al.* (1998), involved type 2 patients maintained on metformin as a monotherapy in order to examine its effects upon

small bowel transit time and bile salt absorption. The overall findings of this study indicated that metformin imposed no effect upon small bowel motility. However, the study provided evidence that metformin altered the enterohepatic circulation of bile salts, resulting in a modest decreased absorption. One current hypothesis concerning metformin's ability to partially correct altered lipid profiles centres on the possibility that the drug may reduce the absorption of bile salts in the terminal small intestine, resulting in increased bile salt loss in the faeces (Scarpello *et al.*, 1998).

The biliary pathway is the principal site for both the elimination and absorption of cholesterol (Hofmann, 1994a). The bile salt pool is subject to strict regulation, with bile acids returning to the liver regulating their own conversion from cholesterol. This regulation is achieved via the enzymes 7 α -hydroxylase (CYP7A) and 27-hydroxylase (CYP27) (Vlahcevic *et al.*, 1999). This negative feedback mechanism affects not only cholesterol biosynthesis but also circulating concentrations of LDL particles (Björkhem, 1985). In addition, Lillienau *et al.* (1993) reported that substrate load may also function as a feedback pathway for bile salt synthesis at the level of the intestine.

Loss of bile acids in faeces, due to their impaired absorption and subsequent passage into the colon, results in the incorporation of more free cholesterol into the bile acid pool through synthesis of bile acids to replace those lost via the faecal route (Grundy *et al.*, 1971). Vlahcevic *et al.* (1991) suggests that the newly synthesised cholesterol pool may provide the source for this increased bile salt synthesis.

Arguably the most important enzymes regulating the free cholesterol pool within hepatocytes are HMG-CoA reductase, 7 α -hydroxylase, sterol 27-hydroxylase, and ACAT (Vlahcevic *et al.*, 1991). These enzymes form a complex negative feedback loop that presumably has inputs at each level. According to Chiang *et al.* (2000), 7 α -hydroxylase is the rate-limiting enzyme for the biosynthesis of bile acids. This is true for bile acids synthesised via the *neutral pathway*. However, 27-hydroxylase is rate-limiting for those bile acids synthesised via the *acidic pathway* (Vlahcevic *et al.*, 1999). Bile acids returning to the liver are believed to suppress the activities of these two enzymes. This phenomenon was demonstrated following bile acid feeding experiments whereby both HMG-CoA reductase and 7 α -hydroxylase activities were decreased (Duckworth *et al.*, 1991). Conversely, however, a recent publication by Fukushima *et al.* (1995) found no significant correlation between 7 α -hydroxylase activity and bile acid feeding in the rat. Nevertheless, the negative feedback hypothesis remains the most attractive hypothesis to date to explain the regulation of bile acid synthesis. In addition, cholesterol returning to the liver from chylomicron remnants, LDL, and HDL particles, regulates the *de novo* synthesis of cholesterol via HMG-CoA reductase modulation.

Reduced bile acid absorption, either through inherent defect or a consequence of drug treatment, leads to up-regulation of cholesterol synthesising enzymes and those regulating bile acid synthesis. The activity of HMG-CoA reductase is stimulated, resulting in increased synthesis of cholesterol for delivery to the metabolically active intracellular pool (Åkerlund *et al.*, 1991; Rudling *et al.*,

1990; Reihner *et al.*, 1990). More of this cholesterol is then converted to bile acids via the enzymes regulating bile salt synthesis. The overall effect of this increased bile salt synthesis is to reduce levels of free and circulating cholesterol, due to depletion of the free intracellular cholesterol pool and increased cholesterol uptake from the circulation.

Preliminary evidence exists linking metformin with reductions in the active transport of taurocholate and glycocholate in rat (Caspary and Creutzfeldt, 1975), and guinea pig intestine (Tomkin, 1976), as well as in humans (Scarpello *et al.*, 1998). A feasibility study was subsequently undertaken to test the current hypothesis that metformin may influence the enterohepatic circulation of bile salts in the rat. Although not a normal constituent of rat bile, sodium glycocholate was used throughout the study because it is handled in a similar manner to taurocholate by its transporters (Lack and Weiner, 1961). Considerable emphasis has been placed upon the importance of the ileal absorptive system in 'mopping up' bile salts remaining in the intestinal lumen. Little attention has been focused upon metformin's effects in the jejunum, often seen as a functionally less important system lending little effect to the overall enterohepatic circulation of bile salts. Studies were therefore undertaken to investigate the role of both the ileum and jejunum in bile salt absorption, and involved the administration of ^{14}C labelled bile salt to a closed intestinal loop and its subsequent recovery in hepatic bile. Preliminary studies concerning the uptake and recirculation of ^{14}C labelled sodium glycocholate demonstrated independent transfer systems in the ileum and jejunum.

The jejunal transfer system is believed to involve passive diffusion of bile salts across the intestinal epithelium. This passive mechanism is thought to be important in the uptake of the least polar bile acids (Hofmann, 1994b). Bile acids are capable of absorption by diffusion along the total length of the intestine but only actively in the distal intestine (Bahar and Stolz, 1999). Initially, it was believed that the ileum played the major role in bile acid uptake. However, McClintock and Shiau (1983) highlighted the important contribution of the jejunum to the overall uptake of bile salts. These authors suggested that the function of the ileal transport system was to conserve the bile salts remaining after jejunal absorption. The jejunum was shown to be of principal importance in bile salt uptake by McClintock and Shiau (1983), using tritiated taurocholate (^3H TC). These authors observed that in anaesthetised rats approximately 30% of luminal ^3H TC entered the bile with less than 1% reaching the distal regions of the small intestine. The absorption mechanism for bile salts in the jejunum was found to be a non-saturable process dependent upon substrate concentration. More recently, evidence has been presented suggestive of a facilitated transporter in the jejunal region. This transporter was found to demonstrate high capacity and low affinity and could be inhibited by high bile acid concentrations (Bahar and Stolz, 1999).

"Since the passive bile salt transport capacity of the jejunum equals that of the ileum and bile salt volume is higher in the jejunum than in the ileum, the jejunum is exposed to, and will absorb, the major fraction of luminal bile salts" (McClintock and Shiau, 1983).

Bergström and Norman (1953) suggested that active bile transport alone cannot account for total bile salt conservation (since it is a saturable process) and that passive mechanisms must contribute to the enterohepatic circulation. However, preliminary studies presented herein involving sodium glycocholate confined to the mid - distal ileum demonstrated that at 20mmol/l, approximately five-tenfold greater than the prevailing concentration in the terminal ileum of fed rats (Dietschy, 1967), uptake of the bile salt solution was virtually absolute. This indicates that saturation of the uptake process did not occur and illustrates the very high capacity of the ileum towards bile salt retention.

Transport of bile salts in the ileum is an active process involving a bile acid/ Na^+ co-transporter in the brush-border membrane, and a bile acid/anion transporter in the basolateral membrane (Lücke *et al.*, 1978; Weinberg *et al.*, 1986). The uptake mechanism involves the enzyme Na^+ - K^+ -ATPase, which is believed to adapt to changes in the pool size of bile salts (Simon *et al.*, 1988).

Bile acid absorption is termed secondarily active because the basolateral Na^+ - K^+ -ATPase enzyme is localised in the basolateral membrane (Phillips and Giller, 1973; Barnard and Ghishan, 1987). According to Van Tilburg *et al.* (1990), this enzyme sustains a 125mM sodium gradient across the brush-border of ileal enterocytes. Little is known regarding the mechanism by which bile salts leave the enterocyte but it is suspected that a sodium-independent anion exchange system operates at the basolateral membrane (Weinberg *et al.*, 1986). The binding, uptake, intracellular transport, and exclusion of bile salts from ileocytes

is dependent upon the presence of specialised binding polypeptides, discussed below.

Photoaffinity labelling studies have identified several proteins believed to be involved in the uptake and removal of bile salts from intestinal epithelial cells. Such transporters were found in brush-border and basolateral membranes, and in the cytosolic fraction of enterocytes. Studies of the brush-border and basolateral membranes identified a 99-kDa protein, believed to be involved in brush-border membrane transport, and two additional proteins possibly involved in basolateral membrane bile acid transport (Kramer *et al.*, 1983; Lin *et al.*, 1988). Moreover, bile acid binding proteins (BABPs) have been identified from enterocytes subject to fractionation. These BABPs are believed to be involved in the intracellular transport of bile salts, and exhibit molecular weights of 14, 35 and 59-kDa (Lin *et al.*, 1993).

The principal BAPB in the cytosol was found to be a 14-kDa protein (Lin *et al.*, 1990), and was subsequently identified as gastrotropin (Vodenlich *et al.*, 1991). A proposed model for transcellular transport of bile acids is suggested by Lin *et al.* (1993), and is described briefly below.

It is believed that transport of the bile acids across the luminal membrane of rat ileum occurs via a 99-kDa protein involving the uptake of sodium and the extrusion of potassium. The intracellular transport of the bile acid molecule is then governed by one or more proteins; either actin (43-kDa protein), and/or the 14 and 35-kDa cytosolic transport proteins. These cytosolic proteins are believed

to transport the bile acid further through the cell, either to the basolateral membrane directly or to a 20-kDa microsomal protein.

A 59-kDa basolateral membrane associated protein then accepts the bile acid before its extrusion from the cell via the 54-kDa-transport protein found within the basolateral membrane, via anion exchange.

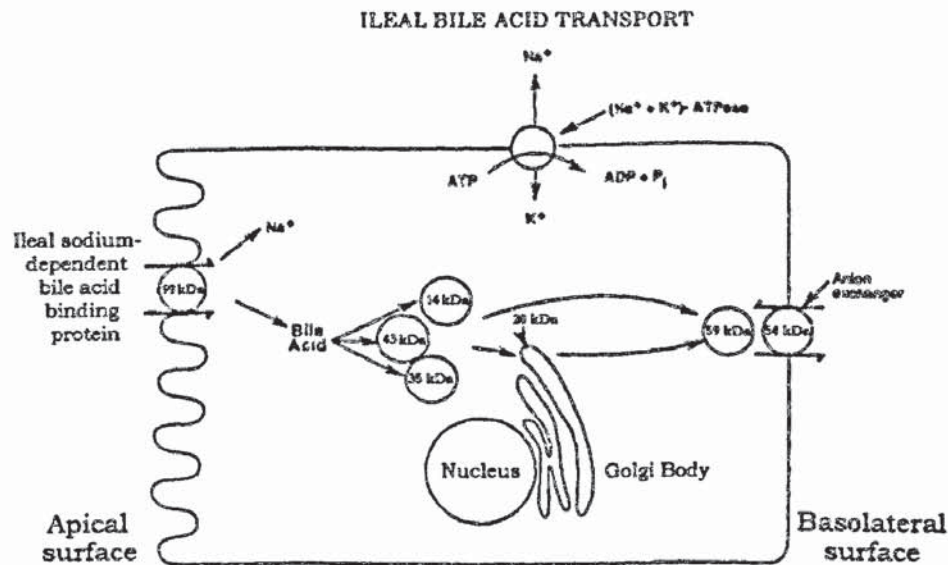


Figure 3.1 Adapted from Lin *et al.*, 1993.
Bile acid transport through Ileal enterocytes.

Recent evidence indicates bile salt nuclear receptors may be important in regulating the activity of enzymes important in bile salt synthesis. Chiang *et al.* (2000) provides evidence that the farsenoid X receptor (FXR, a member of a subfamily of nuclear receptors) may function as a bile acid receptor through which transcription of the gene encoding for the 7 α -hydroxylase enzyme may be modulated. In addition, the activity of the ileal bile acid binding protein may be increased by stimulating the transcription of the gene following activation of the FXR.

Further evidence for this model is provided by Wang *et al.* (1999), who found that extracts of bile acids could specifically activate the FXR receptor. Both chenodeoxycholic acid and deoxycholic acid were found to activate the transcription of the intestinal protein involved in the binding of bile acids. Conversely, the same bile acids were found to decrease the transcription of the 7 α -hydroxylase gene. Wang *et al.* (1999) also implicates a further receptor, the oxysterol receptor (LXR α), in stimulating transcription of 7 α -hydroxylase in response to metabolites of cholesterol; activated FXR may inhibit the transcriptional activity of this receptor. Both FXR and LXR α are expressed in liver, intestine, and kidney, and may modulate the transcriptional activity of several genes in these tissues.

Similarly, the transcriptional activity of the enzyme sterol 27-hydroxylase appears to be tightly regulated. Bile acid diversion leads to increased enzyme activity, whereas down-regulation of the enzyme occurs following the addition of bile acids (Vlahcevic *et al.*, 1996). Thus, regulation of bile acid biosynthesis may occur at the hepatic and intestinal level to modulate the synthesis of cholesterol and affinity and expression of bile acid binding proteins. Indeed, Torchia *et al.* (1996) provide evidence that the bile acid transporters and the rate-limiting enzyme(s) responsible for *neutral* bile acid biosynthesis are responsive to circulating levels of bile acids. Any manipulation of the bile acid pool size by bile acid feeding or sequestration results in modulated enzyme and transporter activity. Interestingly, cholesterol feeding was found to increase the levels of 7 α -

hydroxylase mRNA but suppressed the gene expression of the ileal sodium-dependent bile acid transporter.

The hydrophobicity of bile acids may influence the regulation of bile acid synthesising enzymes. According to Vlahcevic *et al.* (1999), hydrophobic bile acids repressed the activity of 7 α -hydroxylase whereas hydrophilic bile acids did not. Such bile acids may induce their inhibitory effects on gene expression as a consequence of their hydrophobicity. Protein kinase C (PKC) is activated by such bile acids and has been implicated in the mediation of gene repression through the generation of transcriptional factors modified by the action of this second messenger (Vlahcevic *et al.*, 1999).

Interestingly, cholesterol feeding may also modulate the transcription of the 7 α -hydroxylase gene. As detailed by Vlahcevic *et al.* (1999), cholesterol feeding in the rat results in 7 α -hydroxylase transcription. This evidence suggests that cholesterol feeding in the rat results in the rapid conversion of cholesterol into bile acids, due to stimulation of the 7 α -hydroxylase gene by cholesterol. This may be a mechanism through which rats fed a high cholesterol diet prevent hypercholesterolaemia. Similar mechanisms may operate in the mouse although there is no evidence to verify this. Similarly, the transcriptional activity of sterol 27-hydroxylase may also be regulated by the hydrophobicity of bile acids. As with 7 α -hydroxylase, feeding of bile acids down-regulates the transcription of the 27-hydroxylase gene, whereas treatment with bile acid binding resins increases its transcription. These results are suggestive of a feedback loop similar to that

operating for 7 α -hydroxylase. However, present understanding of this mechanism is not as advanced as for 7 α -hydroxylase.

3.2a Results: *In vivo*

The ability of the small intestine to transfer bile salts was examined in preliminary experiments. Data from these studies confirmed evidence in the literature that active bile salt transport occurs in the ileum, whereas passive/facilitated transfer prevails in the jejunum. Subsequent studies concentrated specifically upon the distal and proximal regions of the small intestine utilising ¹⁴C labelled sodium glycocholate as an indicator of bile salt transfer, together with unlabelled glycocholic acid, at concentrations reflecting physiological normality.

3.2b The Effects of Metformin on Glycocholate Transfer in the Ileum and Jejunum:

The effects of metformin treatment on the transfer of ¹⁴C sodium glycocholate into bile, plasma, and peripheral tissues when delivered to a closed ileal loop are shown in figures 3.2.1-3.2.3, respectively. The results clearly illustrate that metformin is associated with an overall inhibitory effect upon glycocholate transfer in the ileum. Metformin treatment resulted in a 61% reduction in the transfer of glycocholate into bile between 10-100 minutes following administration to the ileum. This is consistent with the recent clinical observations made by Scarpello *et al.* (1998). The appearance of glycocholate in hepatic bile was rapid, with maximal incorporation occurring at 20 minutes in both metformin treated and control rats. There followed a gradual decline in bile

salt transfer in both groups with a more prolonged decline associated with metformin. These data suggest that metformin has a highly specific effect upon the active bile salt transporter present in the ileum.

Concentrations of sodium glycocholate in tail vein plasma samples were extremely low (2.79×10^{-7} μCi metformin treatment, 3.28×10^{-7} μCi control, comparisons between peak ^{14}C glycocholate levels) with no significant difference discernible between the groups (3.2.2). These data confirm observations that the peripheral circulation plays little part in the enterohepatic circulation of bile salts. Although differences were evident in the mean values of glycocholate accumulation in tissues, these were not statistically significant (3.2.3). Nevertheless, concentrations of glycocholate were reduced in all the tissues from metformin treated rats.

An intriguing observation which may be indicative of metformin's site of action was the significant difference between the control and metformin groups in the recovery of labelled bile salt from tissues, illustrated in figure 3.3.4. The glycocholate concentration was greater in the ileal wall of rats treated with metformin. Once again this is consistent with the observation that metformin reduced bile salt transfer, suggesting that metformin may slow the passage of the bile salt across the enterocyte brush-border membrane. This is further consistent with data from figure 3.4.2, since reduced uptake of glycocholate through the ileal brush-border would lead to reduced presence in the liver.

Bile salt transfer in the jejunum is proposed to occur by passive or facilitated diffusion (McClintock and Shiau, 1983). This hypothesis was investigated to

elucidate the effect of metformin upon bile salt transfer in this region. Data from these studies (figures 3.3.1-3.3.3) demonstrated a stimulatory effect of metformin upon glycocholate transfer in bile, plasma, and tissue samples following metformin treatment. The passive bile salt uptake mechanism believed to occur under physiological conditions in the jejunum was clearly evident and the data appears to represent a steady-state diffusional process (3.3.1).

Metformin treatment resulted in a marked increase in glycocholate transfer within the jejunal region (threefold enhancement between 20-180 minutes). Despite the increase in glycocholate transfer in the presence of metformin, peak uptake was not achieved until 60 minutes, much later than in control animals. Clearly the ability of the jejunum to transfer bile salts is markedly less than the ileum. This is illustrated when comparing peak uptake data of the control groups from both intestinal regions; the ileum transferred approximately 25 times the concentration of glycocholate compared to the jejunum, presumably reflecting the relative physiological importance of these areas in relation to bile salt reabsorption. These results undoubtedly reflect the relative rate of transport activity in these areas, which is probably linked to the length of the intestinal region and intestinal transit time.

Interestingly, the stimulatory effect of metformin upon glycocholate transfer in the jejunum gave rise to higher glycocholate concentrations in the peripheral venous circulation (3.3.2). Although concentrations of glycocholate in plasma were low (1.3×10^{-7} μCi metformin treated, 5.4×10^{-8} μCi control, comparisons between peak ^{14}C glycocholate levels), significant increments were evident

following metformin treatment. Peak glycocholate concentrations in plasma were recorded at 70 minutes, corresponding roughly with peak glycocholate uptake in bile samples. No statistically significant differences were discernible between tissues harvested following jejunal experimentation. Nevertheless, mean tissue glycocholate concentrations were higher in samples of all tissues from metformin treated rats, with the exception of liver (3.3.3).

Figure 3.3.4 illustrates the effect of metformin on glycocholate transfer into the intestinal wall and the absorption of the intraluminal load from ileum and jejunum. Metformin significantly increased the concentration of glycocholate retained within the intestinal wall of the ileum, supporting the hypothesis of reduced bile salt transfer. Conversely, in the jejunum the concentration of glycocholate was reduced in the presence of metformin. Interestingly, the luminal contents from both regions were only recoverable when metformin was administered, suggesting a slightly reduced net absorption of fluid from the intact lumen in the presence of the drug. Marginal amounts of fluid were recoverable from the lumen of ileum and jejunum from control treated rats. However, they were not sufficient for accurate quantitation.

Observations from the preceding experiments identified a time point when maximal glycocholate transfer was achieved, which was about one hour. Subsequent studies involved repetition of the ileal and jejunal experiments up to and including this time point. Modifications to the protocol involved sample collection from the carotid artery (CA) and hepatic portal vein (HPV).

Metformin, when administered to the ileum, significantly decreased the glycocholate concentration in CA samples (3.4.1). The glycocholate concentration recorded in the HPV was also markedly reduced in the presence of metformin, with significant differences apparent between CA and HPV samples at comparable time points (3.4.3). However, the effects of metformin upon tissues tended to be variable (3.4.2). This result is seen as atypical of the other tissues examined and may be artefactual and due to the limited number of experiments performed in this study. Nevertheless, liver was seen to concentrate the highest levels of glycocholate, a reflection of its role in bile salt extraction and modification, and was particularly evident in control samples.

In direct contrast to its ileal effect, metformin was associated with increased concentrations of glycocholate in the majority of jejunal samples tested. The results of this sub-study do not fully reflect the effect of the drug on bile salt absorption in this region, evident in the earlier experiments. Nevertheless, metformin treatment in the jejunum resulted in a higher mean concentration of glycocholate in CA samples, although the difference was not statistically significant (3.5.1). The effect on the HPV was more marked, with substantially higher glycocholate levels following metformin treatment.

These data, specifically those from the HPV, illustrate convincingly the significant role the HPV plays in transporting significantly greater amounts of bile salts from the intestine to the liver, compared with the arterial system (3.5.2). The fact that glycocholate levels were markedly reduced in HPV samples from the jejunum, compared with those from the ileum, reflects the nature of the residual transport system in these two regions of the intestine. Indeed, the

concentration of labelled bile salt found in the HPV following metformin treatment in the ileum, compared with jejunum, ranged from twofold greater at 30 minutes, to sixfold the concentration at 60 minutes. All tissues studied demonstrated increased levels of glycocholate following metformin administration to the jejunum (3.5.3). The liver, as expected, retained substantially more glycocholate than other tissues.

HPV plasma samples collected during the above studies were compared with plasma from an untreated animal using thin layer chromatography. A small volume of ^{14}C sodium glycocholate was added to the untreated sample prior to analysis. The circulating ^{14}C bile salt (present in the HPV sample) separated on the chromatography plate almost identically to the standard sample. This confirms that the bile salts measured by their radioactive tracers in the circulation reflect the true compounds initially introduced into the intestine prior to hepatic extraction.

Although luminal contents were not recoverable from control animals in the initial studies, the restricted experimental time period of the sub-studies resulted in luminal contents remaining *in situ* in control and drug treated animals. In the jejunum, luminal content ^{14}C glycocholate levels were decreased in the presence of metformin when compared with control. In the ileum however, glycocholate levels were higher in the presence of metformin, than in corresponding controls (3.5.4). These results support the hypothesis of enhanced bile salt transfer in the jejunum and reduced transport in the ileum. When considered collectively, these

data suggest metformin may potentiate opposing actions upon the fluid transport systems resident in the ileum and jejunum by unknown means.

Table 1: Effect of Metformin upon the incorporation of ^{14}C glycocholate into hepatic bile.

Intestinal region	Treatment	% ^{14}C sodium glycocholate recovered in hepatic bile of that initially injected ($1\mu\text{Ci} / 0.0175\mu\text{mol}$)
Ileum	Control	82.3245% \pm 7.255
Ileum	Metformin	35.8762% \pm 7.354
Jejunum	Control	8.1137% \pm 1.167
Jejunum	Metformin	18.5109% \pm 4.034

3.3 Introduction: *In vitro*

Following the *in vivo* observation that bile salt transport could be influenced differentially in the ileum and jejunum as a consequence of metformin treatment, an *in vitro* model was established to examine the effects of this agent upon bile salt transport in isolated everted intestinal sacs.

Everted intestinal sacs have previously been used to study the transport characteristics of sugars (Czyzyk *et al.*, 1968), amino acids (Caspary, 1971; Caspary and Creutzfeldt, 1973), and bile salts (Holt, 1964; Lack and Weiner, 1961; Caspary and Creutzfeldt, 1975). The model for bile salt transport was based on that of Lack and Weiner (1961), with additional methodology derived from Wilson and Wiseman (1954).

The *in vitro* model imposes certain limitations and disadvantages compared with the initial *in vivo* model in that the conditions are less physiological. Importantly, the everted intestinal sac system suffers from the lack of a drainage pathway and thus the active transporter can only proceed up to the point of saturation. The results herein clearly illustrate the loss of 'sensitivity' of the *in vitro* technique and raise the question of whether the everted sac technique is a viable *in vitro* model for the study of bile salt absorption. The major advantage over *in vivo* preparations is that the effects of hormonal and nervous influences upon absorption are eliminated, and adjustments to the culture conditions can be more tightly controlled. Furthermore, it is possible to directly compare control against several different concentrations of the drug on bile salt transport using tissue from the same animal, thereby reducing inter-animal variability.

Sections of proximal and distal small intestine were everted using a glass rod. Ligatures were used to create a closed sac containing unlabelled bile salt in Krebs-Henseleit buffer (appendix II). Sacs were then placed in conical flasks containing 15ml of the same buffer solution. In addition, metformin and labelled bile salt (^{14}C sodium glycocholate) were also added into the solution bathing the everted sac (mucosal fluid). Sacs were incubated for 90 minutes and the transfer of labelled bile salt determined, fluid transfer between the serosal and mucosal surfaces was also calculated (expressed as percentage transfer of control).

3.4 Results: *In vitro*

Ileal everted intestinal sacs were used to determine the influence of several factors upon bile salt absorption. Experiments were performed using unlabelled

bile salt, (glycocholic acid) at both 10 and 20mmol/l in the ileum and 5mmol/l in jejunal sacs. In addition, the effects of incubating intestinal tissue in cold, room temperature, and body temperature buffer were also investigated. Although data pertaining to temperature are not included, it was discovered that incubating buffer at room temperature provided optimum survival conditions for the tissue prior to experimentation. Cold buffer was found to impair the transport capabilities of intestinal tissue.

Figure 3.6.1 represents experiments where the concentration of unlabelled bile salt was 20mmol/l. In the interests of standardisation, this was the concentration used initially in the *in vitro* experiments. These data clearly show that metformin had no significant effect upon bile salt transport. Despite these findings, metformin at 10^{-2} M was seen to reduce the transport of labelled glycocholate into the sac by 6% compared with control. In addition, a small percentage of radiolabelled bile salt was retained in the gut sac wall compared with controls. Whilst these experiments highlighted no effect of metformin, they confirmed that bile salt transport was occurring against a concentration gradient.

Following the initial observations that bile salt transport was not being influenced by metformin, the concentration of unlabelled bile salt was reduced. As noted in the introduction to this section, the *in vitro* model suffers from certain limitations compared with the *in vivo* model. Thus, the concentration of unlabelled bile salt may have resulted in near-saturation of the transport mechanism.

Figure 3.6.2 represents data from experiments where intestinal sacs were incubated in unlabelled bile salt at a concentration of 10mmol/l. Metformin treatment resulted in a near-significant reduction in the accumulation of labelled bile salt into the serosal compartment. At a concentration of 10^{-2} M the ^{14}C glycocholate levels were reduced by 9%, and approximately 7% at 10^{-3} M. Although statistically significant results were not obtained for the remaining data, metformin (10^{-2} M) resulted in a 5% reduction in the transfer of labelled bile salt from the mucosal solution incubating the intestinal sac.

The relatively positive results from the above experiments prompted the use of an increased concentration of metformin. The results of these experiments are represented in figure 3.6.3. Metformin, when administered to the mucosal surface of everted ileal tissue, resulted in no significant inhibitory effect on bile salt transport. These data, whilst unexpected, do confirm preliminary observations that an active transport mechanism is operating in this intestinal region since transfer of labelled glycocholate occurred against a concentration gradient.

The net fluid transfer between the mucosal and serosal environments was determined in the ileum (3.6.4), and represents the same experimental group as in figure 3.6.3. Metformin treatment (5×10^{-2} M) resulted in a significant diminution in the volume of fluid from the mucosal side being transported into the intestinal sac (mucosal fluid transfer). The serosal fluid loss, defined as the increase or decrease in volume inside the sac, was positive. Thus, metformin was associated with net loss of fluid from the serosal compartment in most instances, at high concentrations. In addition, gut fluid uptake, defined as the difference

between the mucosal and serosal transfer, was reduced with metformin treatment. This represents the volume of fluid retained within the intestinal wall and may emanate from serosal loss or mucosal uptake. Fluid uptake per mg tissue was also significantly reduced in the presence of metformin (5×10^{-2} M). These data suggest that whilst bile salt transport was unaffected by metformin, significant effects upon fluid transfer were evident in the presence of the drug.

The high bile salt concentration in conjunction with metformin may have imposed an osmotic burden or an acute toxic effect, and this may be a possible explanation for the fluid transfer data. However, rat small intestine has been shown to induce fluid movement against an osmotic gradient (Parsons and Wingate, 1961). Data from ileal studies proved variable and may be attributed to the effect of metformin upon the dynamics of fluid transfer in this region. Phenethylbiguanide has been linked with reduced bile acid and water absorption *in vivo*, and a similar effect may be induced by metformin (Caspary and Lücke, 1975). The effects observed *in vitro* on fluid transfer may account for some of the clinical side effects observed with metformin at high concentrations.

The effect of metformin upon bile salt transfer in jejunal tissue was also investigated (3.7.1). No significant effect was imposed upon the transfer of bile salt from the mucosal fluid bathing the intestinal sac. Despite this, metformin, when used at higher concentrations (5×10^{-2} M), resulted in increased transfer of ^{14}C glycocholate into the serosal compartment, and increased retention within the intestinal epithelia. All experiments involving jejunum were conducted using unlabelled glycocholate at 5mmol/l since this was deemed an appropriate

concentration for *in vitro* studies. Data concerning the dynamics of fluid transfer into tissue were collated from jejunal experiments (3.7.2). These data involved measuring the volume of fluid lost from the mucosal incubating fluid (mucosal fluid transfer), the increase or decrease in serosal volume (serosal fluid transfer), and the difference between the two (gut fluid uptake). This represents the fraction of fluid retained in the gut wall originating from either serosal or mucosal surfaces.

Transfer data from the jejunum clearly show metformin, at high concentrations, was associated with reduced fluid transfer from the mucosal bathing fluid to the serosal compartment, supporting evidence from initial *in vivo* studies associated with a fluid transfer effect in this region. The fluid uptake in the intestinal wall was also significantly reduced in the presence of metformin, as was overall fluid uptake per mg tissue. Significantly less serosal fluid loss was associated with high metformin concentrations, an effect opposite to that seen in the ileum.

**Appearance of ^{14}C sodium glycocholate
into hepatic bile following ileal
administration.**

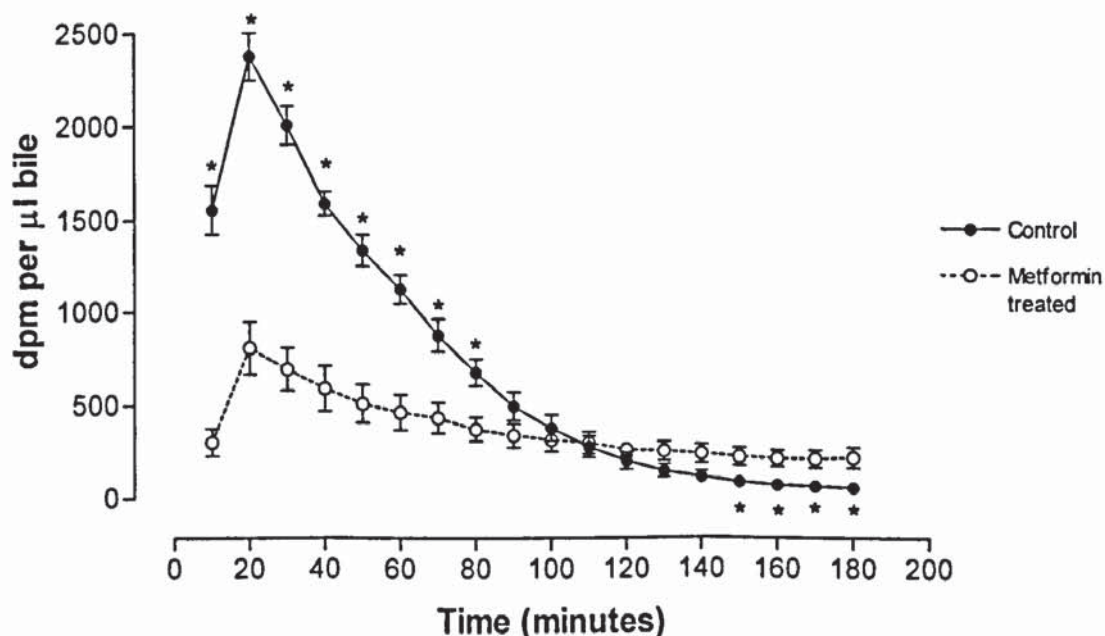


Figure 3.2.1: Effect of metformin (250mg/kg) on the uptake and secretion of ^{14}C sodium glycocholate ($1\mu\text{Ci}$) into hepatic bile in the presence of unlabelled glycocholic acid (1ml of 20mmol/l solution) from a closed loop of ileum of rat. Metformin significantly inhibited bile salt uptake and appearance into bile ($p < 0.05$) by up to 60% between 10-100 minutes. Data are expressed as dpm/ μl bile. Values are mean \pm SEM, $n=6$, * $p < 0.05$ versus control (unpaired Student's 't'-Test).

**^{14}C content of plasma following ileal
administration of sodium glycocholate.**

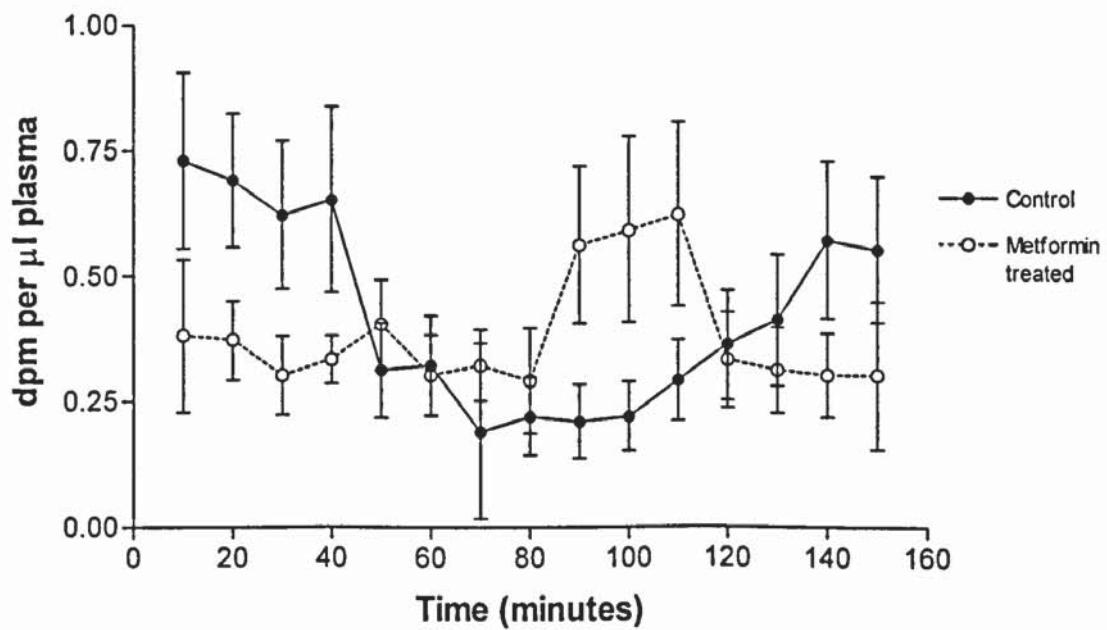


Figure 3.2.2: Plasma ^{14}C content following the introduction of a 1ml bolus containing ^{14}C sodium glycocholate ($1\mu\text{Ci}$), unlabelled glycocholic acid (1ml of 20mmol/l solution), with or without metformin (250mg/kg) into a closed loop of ileum of rat. Data are expressed as dpm/ μl plasma. Values are mean \pm SEM, n=4-7.

^{14}C content of tissues following ileal absorption of sodium glycocholate.

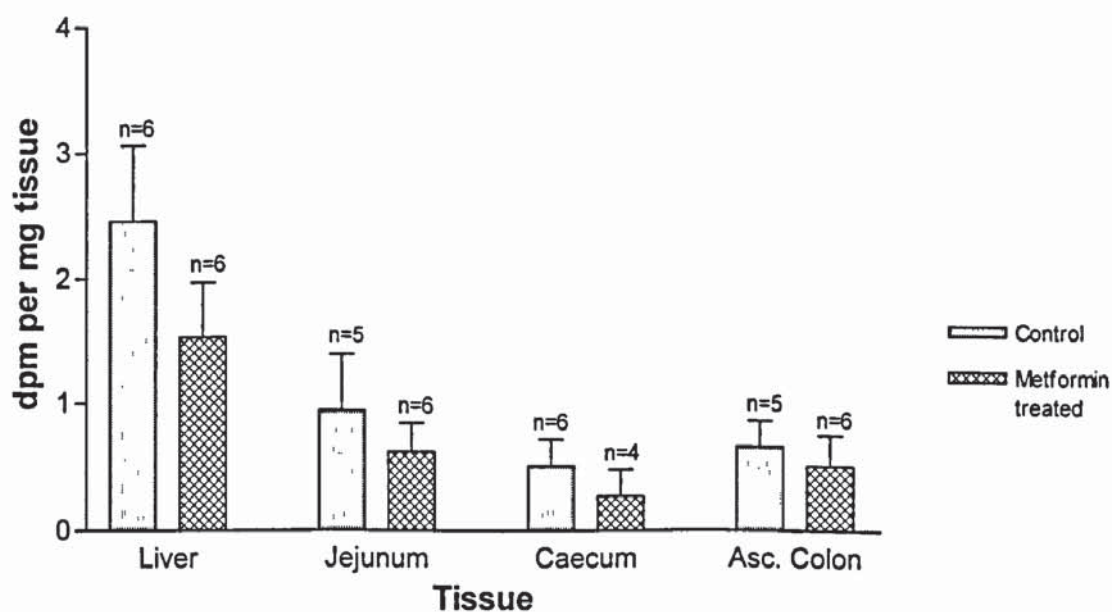


Figure 3.2.3: Tissue ^{14}C content at 180 minutes following the introduction of a 1ml bolus containing ^{14}C sodium glycocholate ($1\mu\text{Ci}$), unlabelled glycocholic acid (1ml of 20mmol/l solution), with or without metformin (250mg/kg) into a closed loop of ileum of rat. Metformin was associated with reduced levels of radiolabel in all tissues. Data are expressed as dpm/mg tissue. Values are mean \pm SEM.

Appearance of ^{14}C sodium glycocholate into hepatic bile following Jejunal administration.

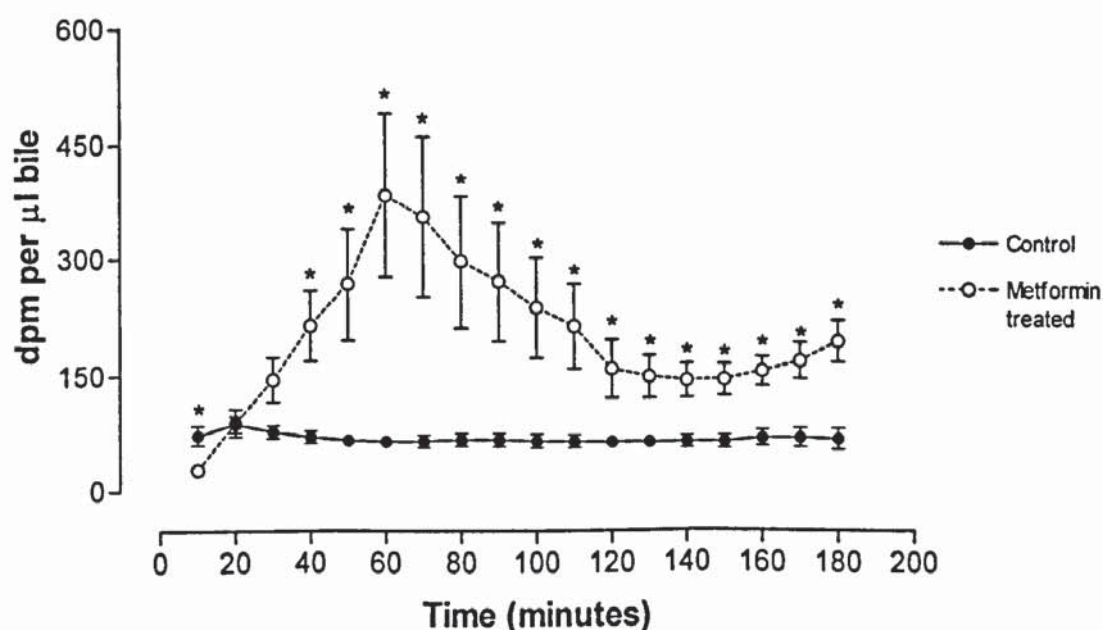


Figure 3.3.1: Effect of metformin (250mg/kg) on the uptake and secretion of ^{14}C sodium glycocholate ($1\mu\text{Ci}$) into hepatic bile in the presence of unlabelled glycocholic acid (1ml of a 8mmol/l solution) from a closed loop of jejunum of rat. Metformin significantly enhanced bile salt uptake and appearance into bile ($p<0.05$) threefold between 20-180 minutes. Data are expressed as dpm/ μl bile. Values are mean \pm SEM, $n=8-10$, * $p<0.05$ versus control (Student's unpaired 't'-Test).

¹⁴C content of plasma following Jejunal administration of sodium glycocholate.

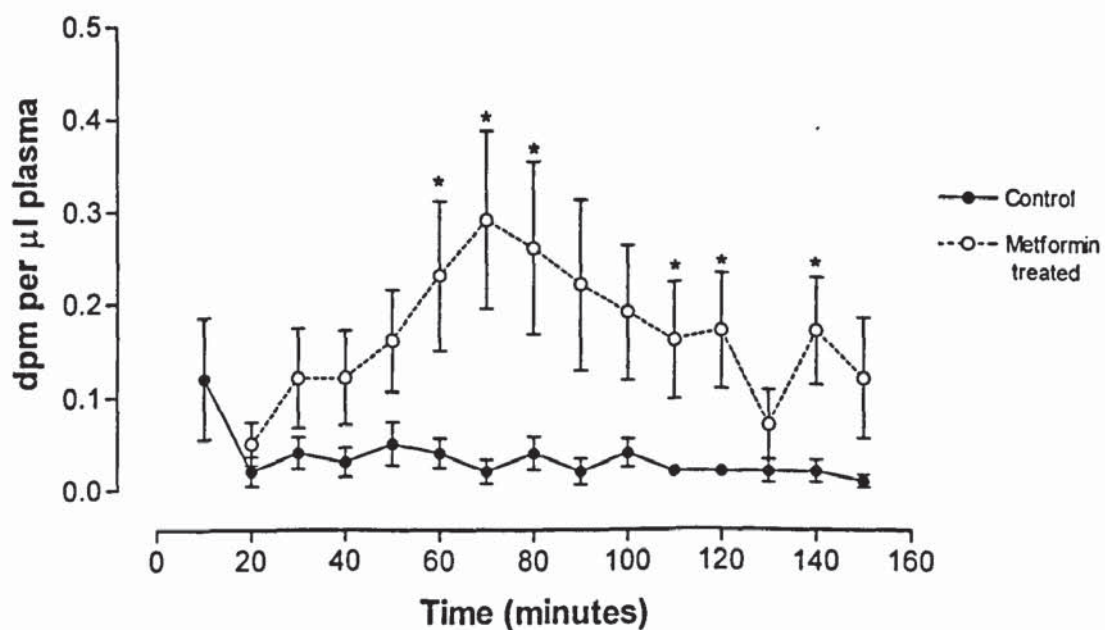


Figure 3.3.2: Plasma ¹⁴C content following the introduction of a 1ml bolus containing ¹⁴C sodium glycocholate (1µCi), unlabelled glycocholic acid (1ml of 8mmol/l solution), with or without metformin (250mg/kg) into a closed loop of jejunum of rat. Metformin significantly ($p < 0.05$) increased ¹⁴C content of plasma at 60-80, 110, 120, and 140 minutes. Data are expressed as dpm/µl plasma. Values are mean \pm SEM, $n=7-12$, * $p < 0.05$ versus control (Student's unpaired 't'-Test).

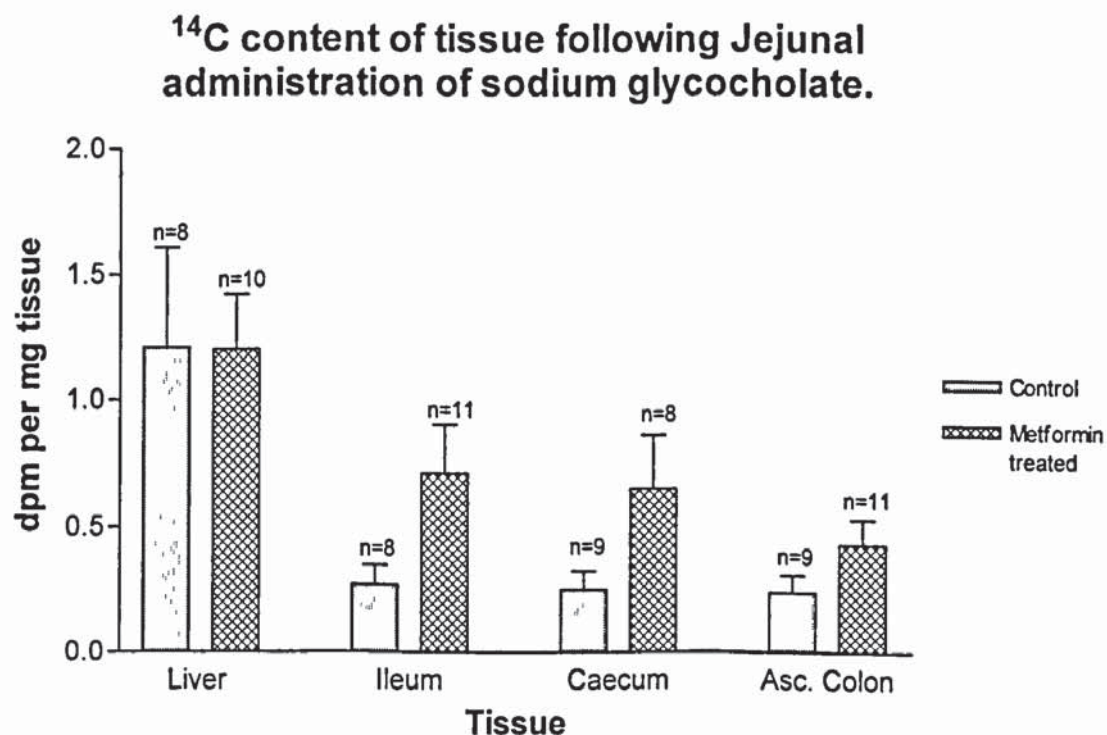


Figure 3.3.3: Tissue ^{14}C content at 180 minutes following the introduction of a 1ml bolus containing ^{14}C sodium glycocholate ($1\mu\text{Ci}$), unlabelled glycocholic acid (1ml of 8mmol/l solution), with or without metformin (250mg/kg) into a closed loop of jejunum of rat. Metformin was associated with increased levels of radiolabel in most tissues. Data are expressed as dpm/mg tissue. Values are mean \pm SEM.

^{14}C content of intestinal wall and luminal contents following administration of sodium glycocholate into ileum or Jejunum.

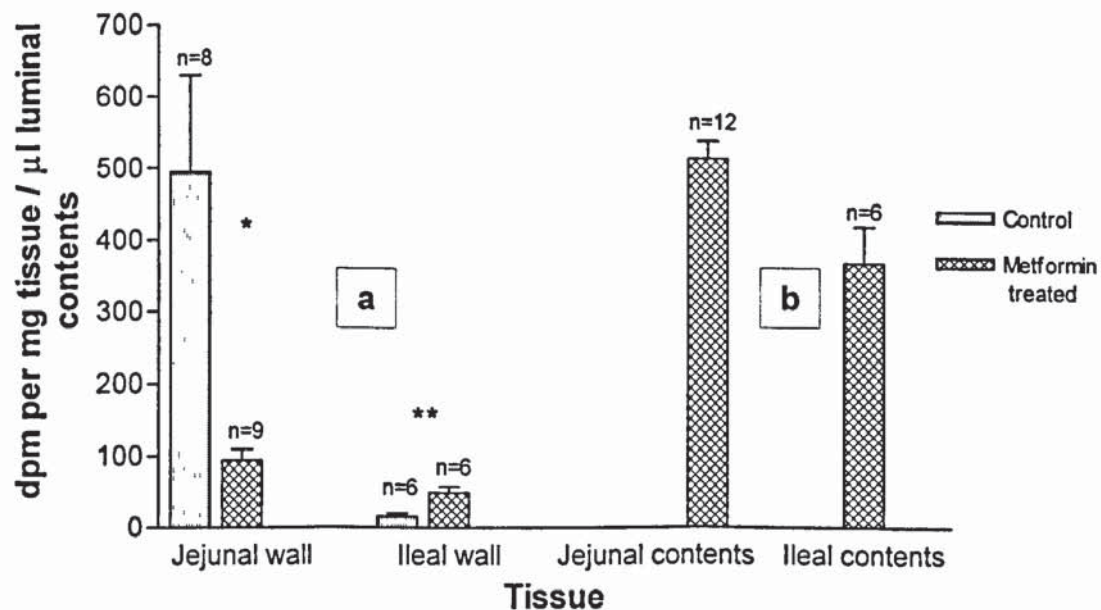


Figure 3.3.4: a) Tissue ^{14}C content following the introduction of a 1ml bolus containing ^{14}C sodium glycocholate (1 μCi), unlabelled glycocholic acid (1ml of 20mmol/l or 8mmol/l solution for ileum and jejunum respectively), with or without metformin (250mg/kg) into a closed loop of ileum or jejunum of rat. b) Intestinal bolus ^{14}C content (described above) from ileum and jejunum collected at the end point of experimentation. Metformin was associated with a significant ($p < 0.05$) increase in ^{14}C content in tissue from the ileum and a significant decrease in ^{14}C levels in tissue from the jejunum. Data are expressed as a) dpm/mg tissue b) dpm/ μl luminal contents. Values are mean \pm SEM, * $p < 0.009$ versus control, ** $p < 0.007$ versus control (Student's unpaired 't'-Test).

^{14}C content of plasma following ileal administration of sodium glycocholate.

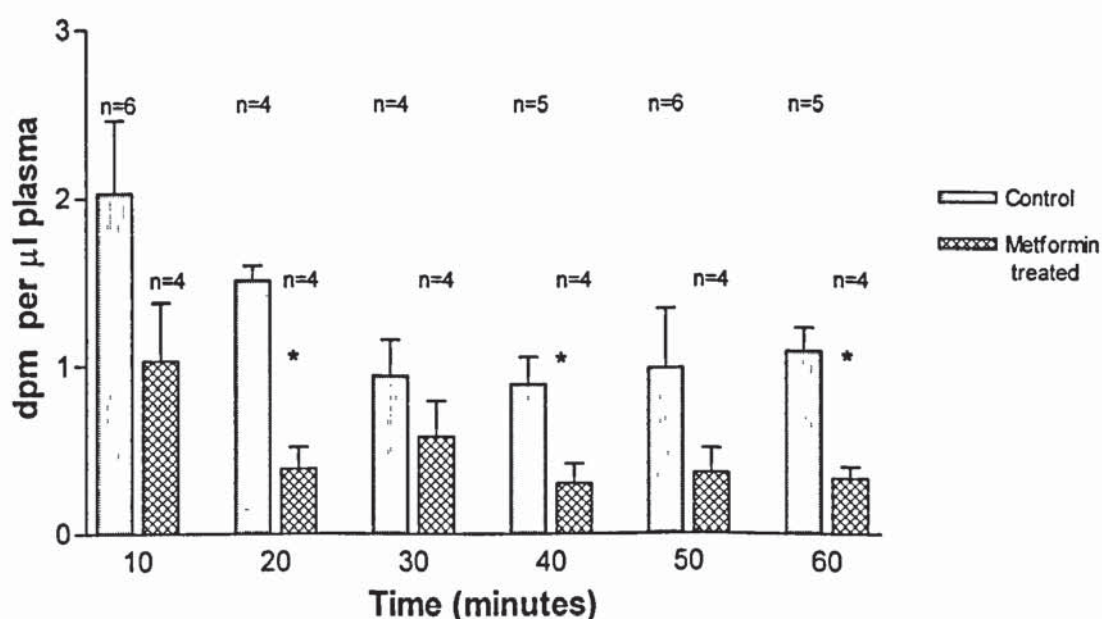


Figure 3.4.1: Carotid artery plasma ^{14}C content following the introduction of a 1ml bolus containing ^{14}C sodium glycocholate ($1\mu\text{Ci}$), unlabelled glycocholic acid (1ml of a 20mmol/l solution), with and without metformin (250mg/kg) into a closed loop of ileum of rat. Metformin significantly ($p < 0.05$) decreased ^{14}C incorporation at 20, 40, and 60 minutes. Data are expressed as dpm/ μl plasma. Values are mean \pm SEM, * $p < 0.05$ versus control (Student's unpaired 't'-Test).

¹⁴C content of tissues following ileal administration of sodium glycocholate.

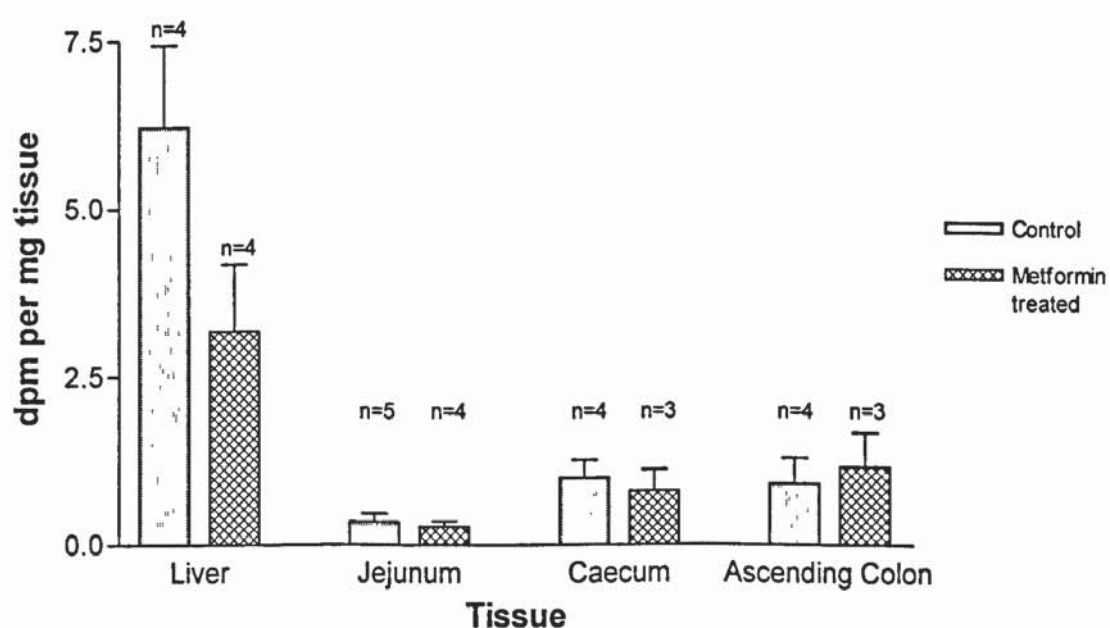


Figure 3.4.2: Tissue ¹⁴C content at 60 minutes following the introduction of a 1ml bolus containing ¹⁴C sodium glycocholate (1μCi), unlabelled glycocholic acid (1ml of 20mmol/l solution), with and without metformin (250mg/kg) into a closed loop of ileum of rat. Data are expressed as dpm/mg tissue. Values are mean ± SEM.

¹⁴C content of plasma following ileal administration of sodium glycocholate.

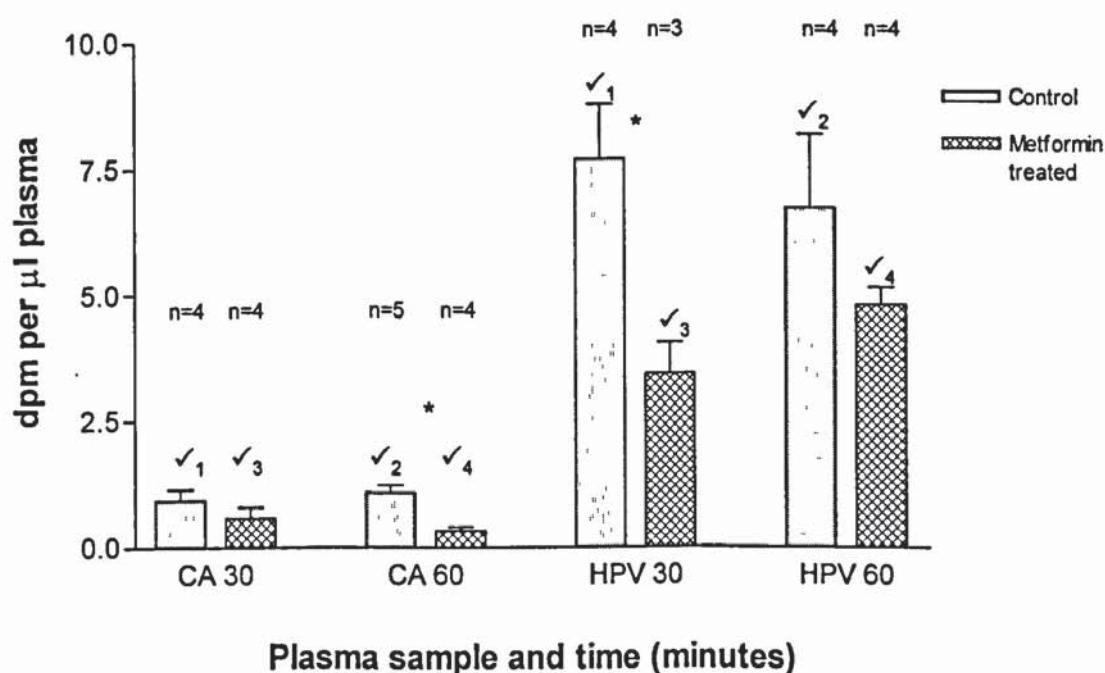


Figure 3.4.3: Carotid artery and hepatic portal vein plasma ¹⁴C content following the introduction of a 1ml bolus containing sodium glycocholate (1µCi), unlabelled glycocholic acid (1ml of 20mmol/l solution), with and without metformin (250mg/kg) into a closed loop of ileum of rat. Metformin significantly ($p < 0.05$) reduced ¹⁴C incorporation into carotid artery and hepatic portal vein plasma (CA versus CA, HPV versus HPV). Significant differences were also observed between CA and HPV samples at comparable time points regardless of treatment. Data are expressed as dpm/µl plasma. Values are mean \pm SEM, * $p < 0.03$ HPV 30 (control) versus HPV 30 (metformin), ** $p < 0.003$ CA 60 (control) versus CA 60 (metformin), ✓₁ $p < 0.009$ CA 30 (control) versus HPV 30 (control), ✓₂ $p < 0.04$ CA 60 (control) versus HPV 60 (control), ✓₃ $p < 0.005$ CA 30 (metformin) versus HPV 30 (metformin), ✓₄ $p = 0.0011$ CA 60 (metformin) versus HPV 60 (metformin) (all tests are Student's unpaired 't'-Test with Welch correction).

^{14}C content of plasma following Jejunal administration of sodium glycocholate.

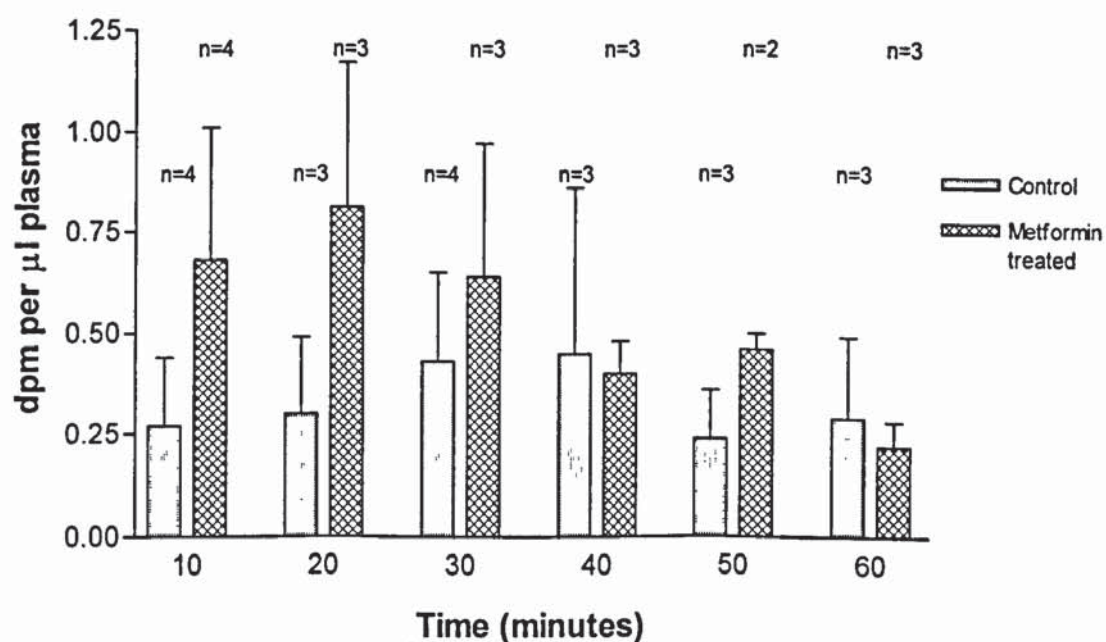


Figure 3.5.1: Carotid artery plasma ^{14}C content following the introduction of a 1ml bolus containing ^{14}C sodium glycocholate ($1\mu\text{Ci}$), unlabelled glycocholic acid (1ml of 8mmol/l solution), with and without metformin (250mg/kg) into a closed loop of jejunum of rat. Data are expressed as dpm/ μl plasma. Values are mean \pm SEM.

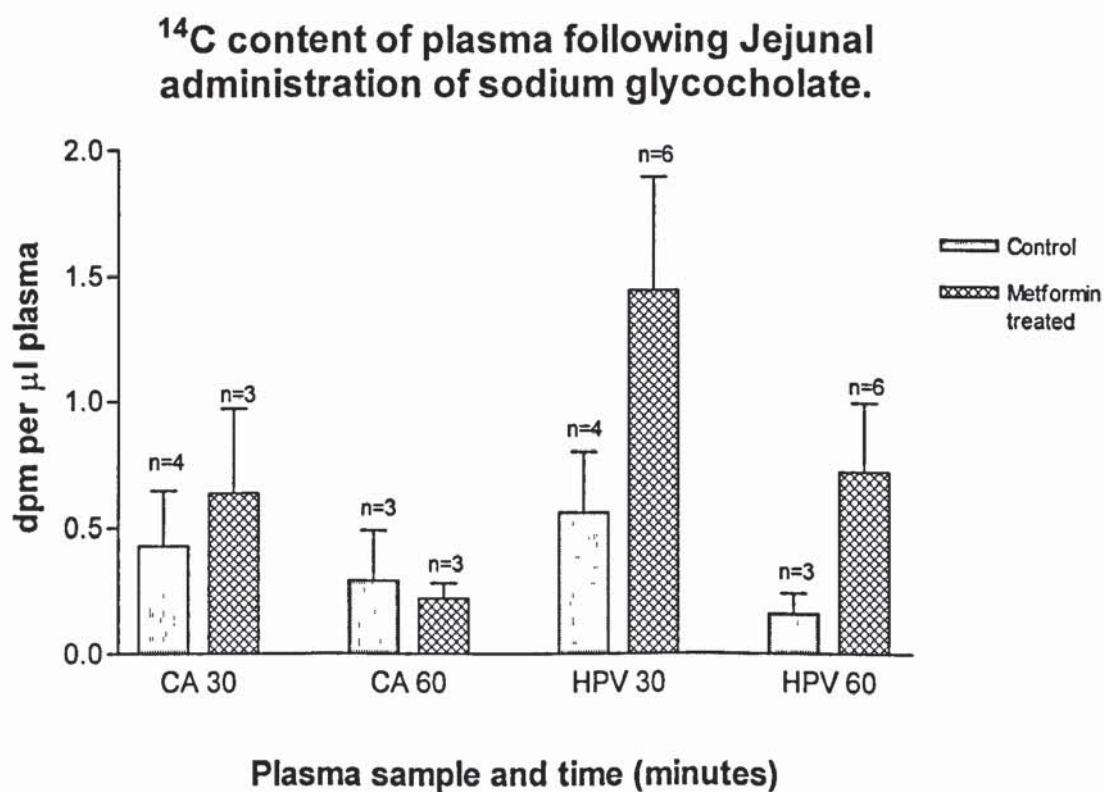


Figure 3.5.2: Carotid artery and hepatic portal vein plasma ^{14}C content following the introduction of a 1ml bolus containing ^{14}C sodium glycocholate ($1\mu\text{Ci}$), unlabelled glycocholic acid (1ml of 8mmol/l solution), with and without metformin (250mg/kg) into a closed loop of jejunum of rat. Data are expressed as dpm/ μl plasma. Values are mean \pm SEM.

^{14}C content of tissues following Jejunal administration of sodium glycocholate.

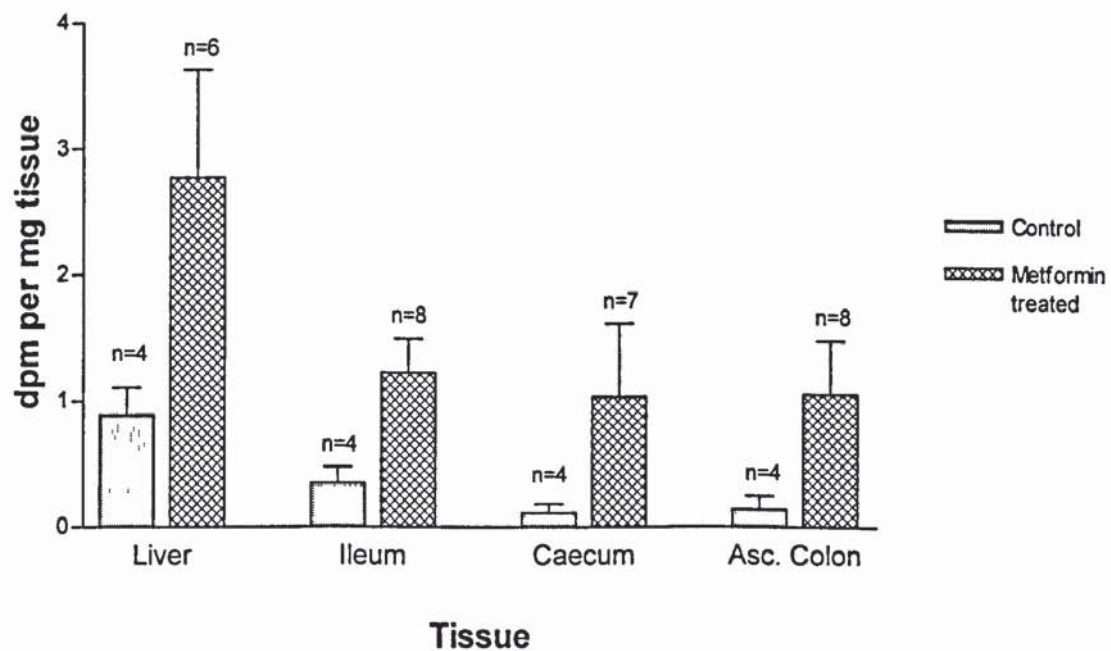
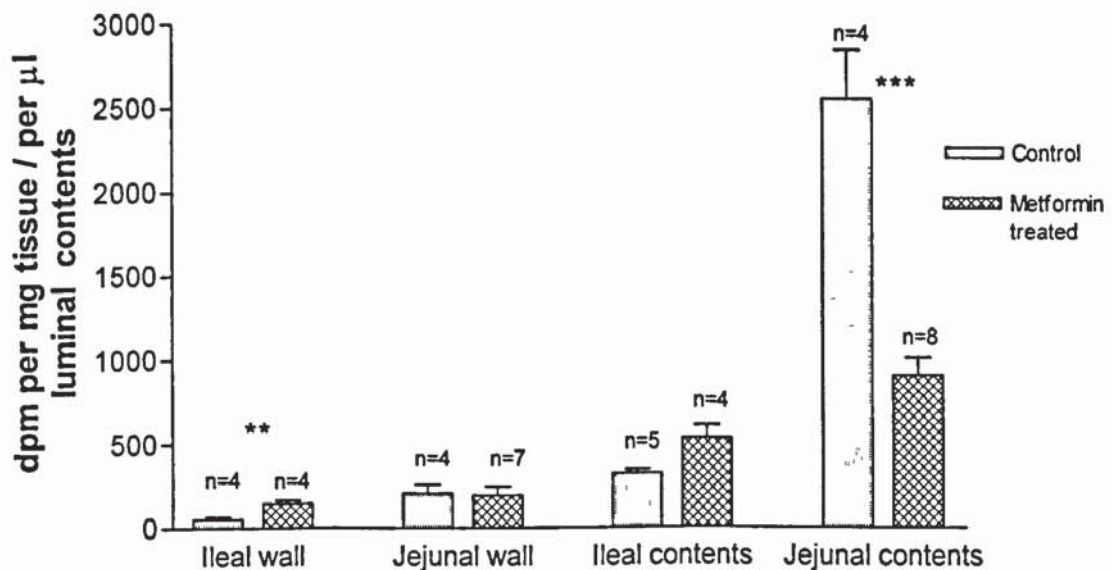


Figure 3.5.3: Tissue ^{14}C content at 60 minutes following the introduction of a 1ml bolus containing ^{14}C sodium glycocholate ($1\mu\text{Ci}$), unlabelled glycocholic acid (1ml of 8mmol/l solution), with and without metformin (250mg/kg) into a closed loop of jejunum of rat. Metformin was associated with increased ^{14}C levels in all tissues analysed. Data are expressed as dpm/mg tissue. Values are mean \pm SEM.

^{14}C content of tissue and luminal contents following administration of sodium glycocholate to ileum and Jejunum.



Tissue

Figure 3.5.4: Concentration of ^{14}C in tissue and luminal contents at 60 minutes following the introduction of a 1ml bolus containing ^{14}C sodium glycocholate (1 μCi), unlabelled glycocholic acid (1ml of 20mmol/l solution for ileum, 1ml of 8mmol/l solution for jejunum), with and without metformin (250mg/kg) into a closed loop of ileum or jejunum of rat. Metformin was associated with a significant ($p < 0.05$) increase in the ^{14}C content of ileal tissue and a significant decrease in ^{14}C levels of luminal contents from the jejunum. Data are expressed as dpm/mg tissue or dpm/ μl luminal contents. Values are mean \pm SEM, ** $p < 0.01$ versus control, *** $p < 0.0001$ versus control (Student's unpaired 't'-Test).

Percentage transfer of ^{14}C sodium glycocholate by everted intestinal sacs of the ileum.

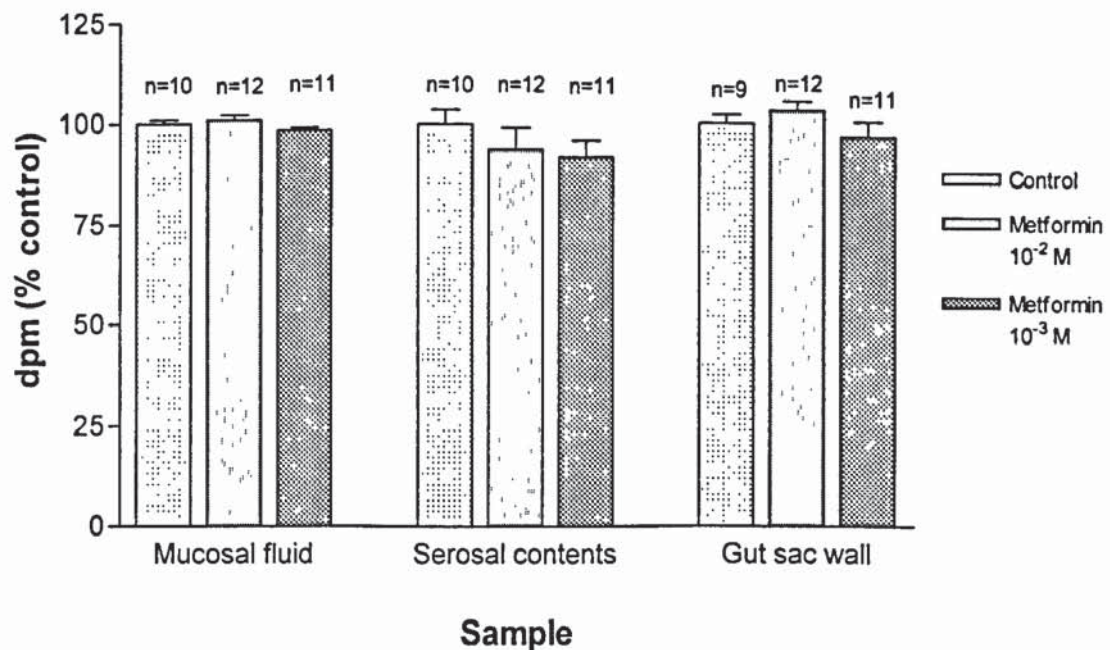


Figure 3.6.1: Fluid ^{14}C content after 90 minutes following the introduction of a 0.5ml bolus of unlabelled glycocholic acid (20mmol/l) into an everted ileal intestinal sac (serosal surface). Intestinal sacs were incubated (mucosal surface) in a buffer solution containing the same concentration of unlabelled sodium glycocholate as described above, ^{14}C sodium glycocholate (1 μCi), with and without metformin (10^{-3} , 10^{-2} M). Data are expressed as percentage control dpm/ μl fluid or dpm/mg tissue. Values are mean \pm SEM.

**Percentage transfer of ^{14}C sodium
glycocholate by everted intestinal sacs of
the ileum.**

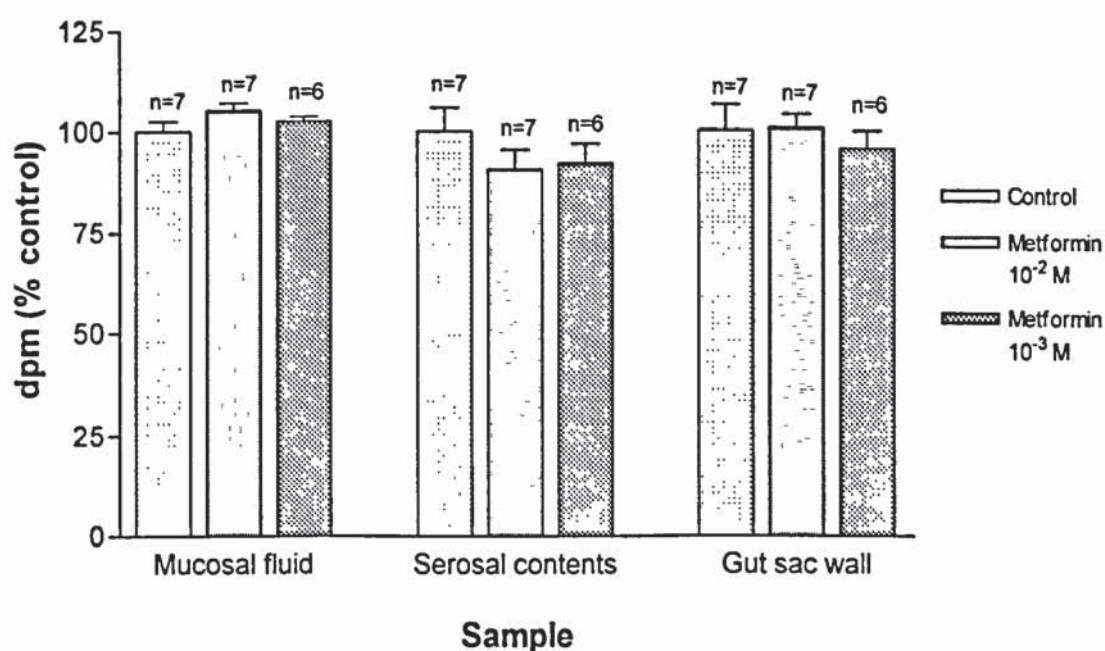


Figure 3.6.2: Fluid ^{14}C content after 90 minutes following the introduction of a 0.5ml bolus of unlabelled glycocholic acid (10mmol/l) into an everted ileal intestinal sac (serosal surface). Intestinal sacs were incubated (mucosal surface) in a buffer solution containing the same concentration of unlabelled sodium glycocholate as described above, ^{14}C sodium glycocholate (1 μCi), with and without metformin (10^{-3} , 10^{-2} M). Data are expressed as percentage control dpm/ μl fluid or dpm/mg tissue. Values are mean \pm SEM.

Percentage transfer of ^{14}C sodium glycocholate by everted intestinal sacs of the ileum.

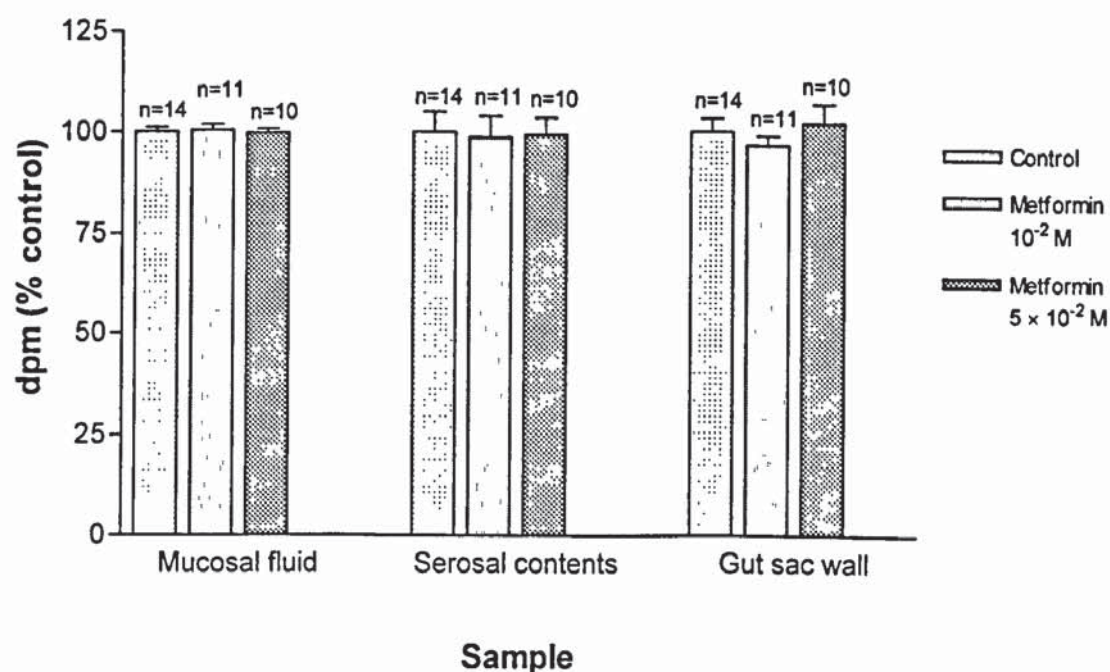


Figure 3.6.3: Fluid ^{14}C content after 90 minutes following the introduction of a 0.5ml bolus of unlabelled glycocholic acid (10mmol/l) into an everted ileal intestinal sac (serosal surface). Intestinal sacs were incubated (mucosal surface) in a buffer solution containing the same concentration of unlabelled sodium glycocholate as described above, ^{14}C sodium glycocholate (1 μCi), with and without metformin (10^{-2} , 5×10^{-2} M). Data are expressed as percentage control dpm/ μl fluid or dpm/mg tissue. Values are mean \pm SEM.

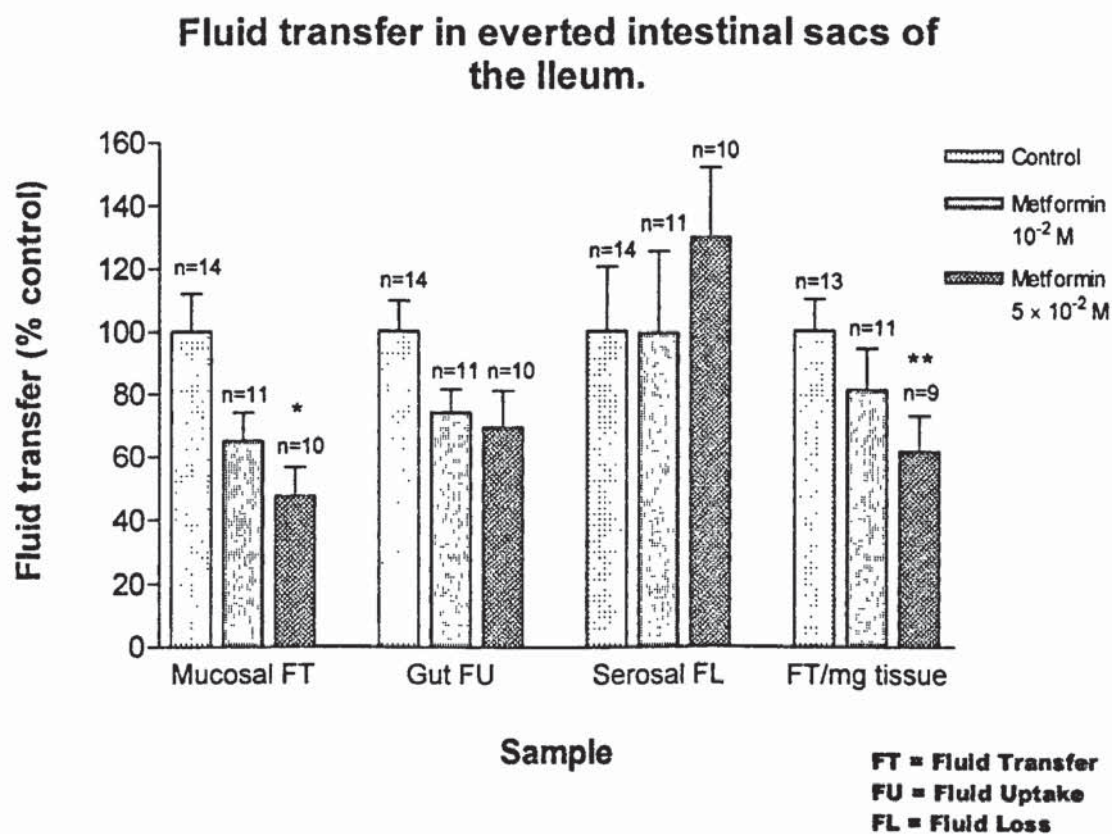


Figure 3.6.4: Volume fluid transfer, uptake, and loss after 90 minutes from serosal and mucosal surfaces of everted intestinal sacs of ileum. Intestinal sacs were incubated with unlabelled glycocholic acid (10mmol/l solution) on serosal and mucosal surfaces, ^{14}C sodium glycocholate (1 μCi) on the mucosal surface, and metformin (10^{-2} , 5×10^{-2} M) on the mucosal surface. Metformin significantly ($p < 0.05$) reduced mucosal fluid transfer and fluid transfer per mg tissue in the ileum. Data are expressed as percentage control fluid transfer (μl). Values are mean \pm SEM, * $p < 0.05$ versus control, ** $p < 0.008$ versus control (Student's paired 't'-Test).

Percentage transfer of ^{14}C sodium glycocholate by inverted intestinal sacs of the Jejunum.

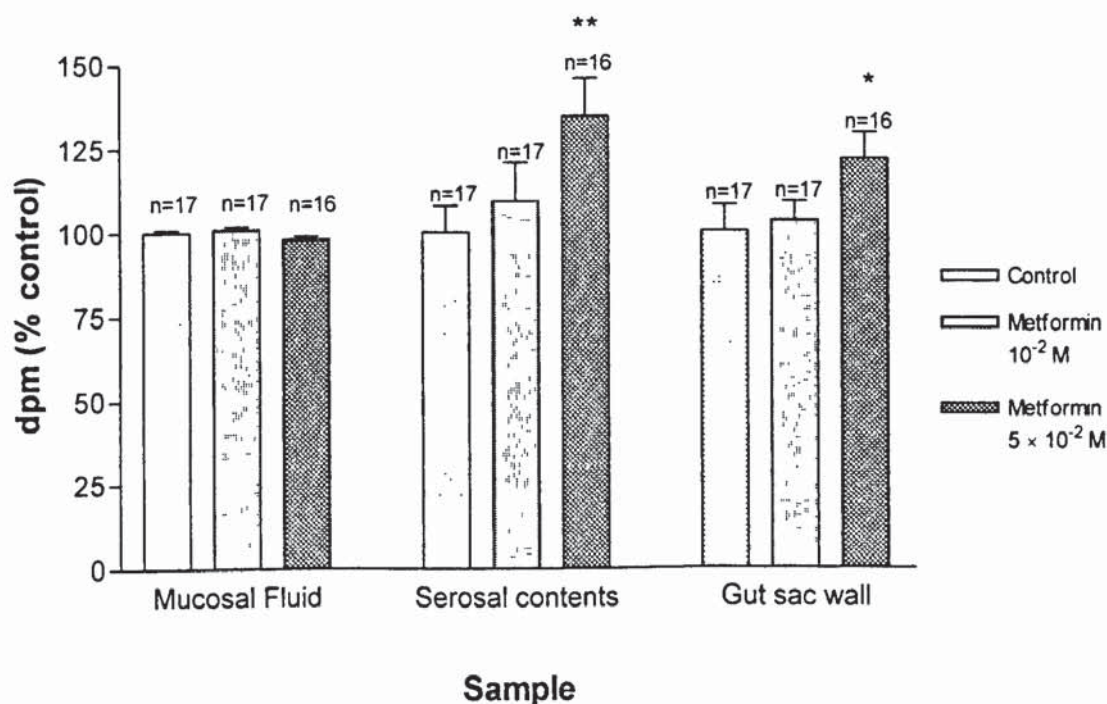


Figure 3.7.1: Fluid ^{14}C content after 90 minutes following the introduction of a 0.5ml bolus of unlabelled glycocholic acid (5mmol/l) into an everted jejunal intestinal sac (serosal surface). Intestinal sacs were incubated (mucosal surface) in a buffer solution containing the same concentration of unlabelled sodium glycocholate as described above, ^{14}C sodium glycocholate (1 μCi), with and without metformin (10^{-2} , 5×10^{-2} M). Metformin significantly ($p < 0.05$) increased radiolabel transfer from the mucosal to serosal surface. Data are expressed as percentage control dpm/ μl fluid or dpm/mg tissue. Values are mean \pm SEM, * $p < 0.02$ versus control, ** $p < 0.003$ versus control (Student's paired 't'-Test).

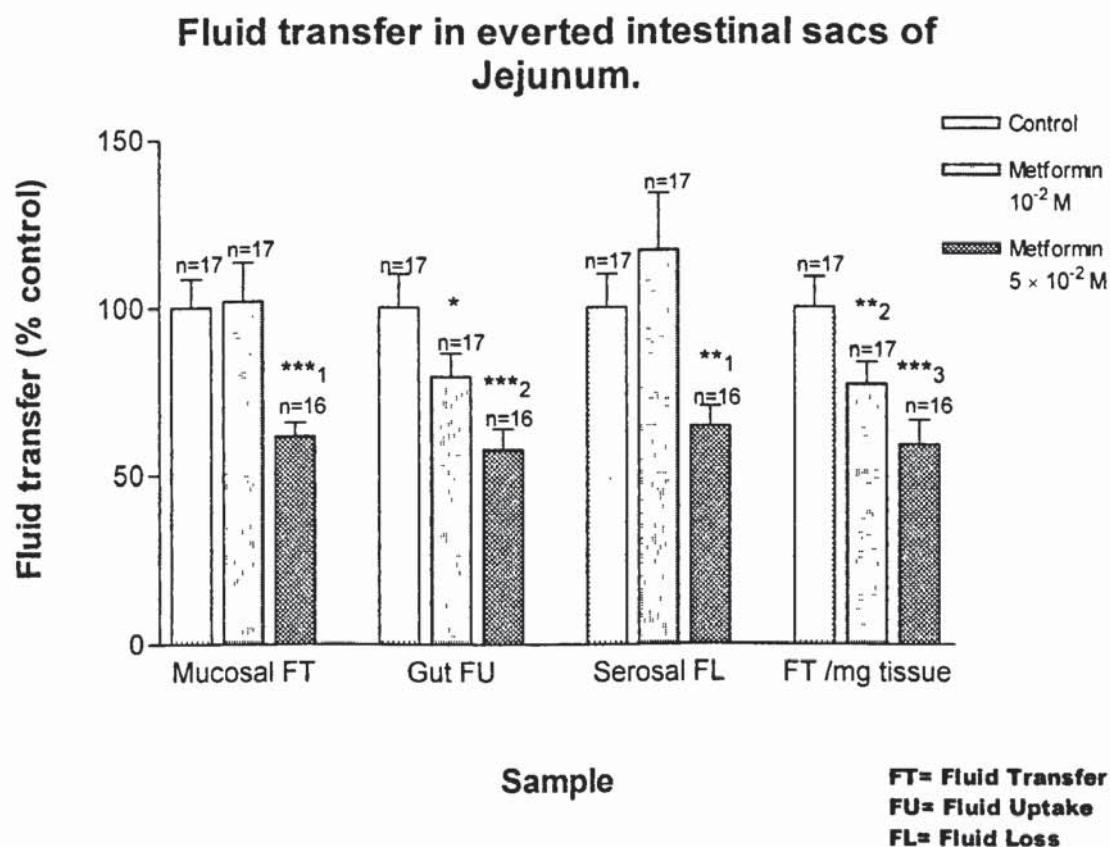


Figure 3.7.2: Volume fluid transfer, uptake, and loss after 90 minutes from serosal and mucosal surfaces of everted intestinal sacs of jejunum. Intestinal sacs were incubated with unlabelled glycocholic acid (5mmol/l solution) on serosal and mucosal surfaces, ^{14}C sodium glycocholate (1 μCi) on the mucosal surface, and metformin (10^{-2} , 5×10^{-2} M) on the mucosal surface. Metformin (5×10^{-2} M) significantly ($p < 0.05$) reduced fluid transfer from the mucosal surface and significantly reduced fluid loss from the serosal surface. Data are expressed as percentage control fluid transfer (μl). Values are mean \pm SEM, * $p < 0.02$ versus control, **₁ $p < 0.003$ versus control, **₂ $p < 0.008$ versus control, ***₁₋₃ $p < 0.0002$ versus control (Student's paired 't'-Test).

3.5 Discussion:

Metformin is presently the most prescribed proprietary agent for the treatment of type 2 diabetes. Conclusions drawn from the United Kingdom Prospective Diabetes Study (UKPDS, 1998) suggest that metformin monotherapy is the most effective initial treatment regimen for the prevention of mortality from macrovascular complications. The ability of metformin to apparently reduce the onset of macrovascular disease may stem from its correctional effect upon cholesterol and lipoprotein levels in obese type 2 patients. A reduction in active absorption of bile salts in the terminal ileum has been demonstrated in type 2 patients receiving metformin as a monotherapy (Scarpello *et al.*, 1998). As a consequence, the present study examined metformin's effect on bile salt absorption (active and passive) in the small intestine, concentrating specifically upon the terminal ileum as a possible mechanism through which the drug could reduce circulating cholesterol concentrations.

Under physiological conditions, metformin exists predominantly in a protonated form (Cusi and DeFronzo, 1998). Whilst the specific uptake mechanism is uncertain (Khan *et al.*, 1992), it becomes heavily concentrated within the cytosol (Wilcock *et al.*, 1991). Experiments performed at Aston University concerned with the effect of metformin upon glucose absorption indicated a decrease in glucose absorption in the presence of metformin. This was subsequently found to be due to increased glucose metabolism by the intestinal wall, resulting in reduced glucose appearance in the serosal compartment (Wilcock and Bailey, 1994).

Absorption of vitamin B₁₂ (also an energy-dependent mechanism) was decreased in patients receiving long-term metformin therapy (Tomkin *et al.*, 1971). Uptake of vitamin B₁₂ occurs by an active process, largely in the distal ileum involving calcium ions. A possible mechanism by which metformin may affect active transporters is provided by Schafer (1976b), and involves the displacement of divalent cations by the induction of a positive membrane charge. Further opinion regarding the mechanism of action of metformin upon intestinal cells is related to mitochondrial function and manipulation of the enzyme systems involved in active transport. Therapeutic concentrations of phenformin have been shown to reduce ATP production through impaired electron conductance along the respiratory chain, by suppressing NADH-linked dehydrogenases found in mitochondrial membranes (Schafer, 1976a). This results, ultimately, in increased conversion of glucose to lactate.

Despite the evidence provided above, metformin used at therapeutic concentrations does not seem to affect ATP production through the electron transport chain or the Krebs cycle (Cusi and DeFronzo, 1998). Only in intestine is there a significant increase in lactate production (Bailey, 1992). Metformin is known to concentrate heavily in the intestinal wall. This site of accumulation may account for its gastrointestinal effects since the drug only achieves modest concentrations in other tissues (Cusi and DeFronzo, 1998).

Bile salts are actively absorbed in the ileum (Bahar and Stolz, 1999) and glycocholate absorption was significantly reduced in this region in the presence of metformin (3.2.1). Initially, it was believed that the ileum played the major

role in bile salt uptake, but McClintock and Shiau (1983) questioned the physiological significance afforded this system. Indeed, the above authors suggested the function of the ileal transport system was to conserve bile salts remaining following jejunal absorption. Bergström and Norman (1953) also suggested that passive mechanisms must contribute to the enterohepatic circulation.

There is little argument that the jejunum plays an important role in bile salt absorption. Nevertheless, the concentration of sodium glycocholate used in the ileal experiments (20mmol/l) was greater than the concentration of bile salts suggested to exist in the terminal ileum of fed rats *in vivo* (Dietschy, 1967; Dietschy, 1968). When considering the concentrations used herein, over 80% of the administered radiolabelled bile salt was recovered in hepatic bile, and reflects the powerful capacity for active absorption that resides in the ileal region (table 1 p119).

Metformin has been shown to traverse the enterocyte layer paracellularly (Nicklin *et al.*, 1996), and influence proteins at the apical and basolateral surfaces (Wiernsperger, 1999). There is convincing evidence from the present study that metformin alters the rate of bile salt transport, particularly in the ileum. Significant reductions were seen in total bile salt uptake in the ileum (table 1), and in plasma samples obtained from CA and HPV (3.4.3) following metformin treatment. Metformin also reduced incorporation of radiolabel into tissues (3.2.3, 3.4.2). These results support the hypothesis that metformin attenuates transfer rates of glycocholate in the ileum.

Absorption of amino acids and glucose across the intestinal brush-border membrane occurs, as with bile salts, via a sodium gradient maintained by a laterally located $\text{Na}^+\text{-K}^+\text{-ATPase}$ pump. Despite these different transporters being highly substrate specific, similarities exist amongst them. However, there is no evidence to imply they are all affected by metformin in a similar manner. Since metformin decreases bile salt transport without any apparent significant effect upon transport of additional actively transported substances, then its effects might be limited to regions concerned solely with bile salt transport at the mucosal/apical surface. Alternatively, metformin may have a highly specific effect on the bile salt transport system independently of a measurable effect on related transport processes in the same cell.

Metformin may questionably penetrate the enterocyte to become concentrated within the cytosol, where it may influence certain cytosolic enzymes. Alternatively, metformin can accumulate within the paracellular space (Nicklin *et al.*, 1996). In this location it may affect ATP/Na^+ transporters which are important in removing sodium ions from the cell, to maintain the active sodium pump mechanism. Other possibilities regarding the target sites for metformin include the tight junctions themselves. Any effect upon these structures could produce alterations in the enterocyte-enterocyte connections and modify the cell cytoskeleton.

Tight junctions are known to be sensitive to nutrients such as glucose, altering their permeability. Exposure of the mammalian small intestinal epithelium to glucose or amino acids, such as would occur during a meal, brings about dilations

in tight junctions between enterocytes (Madara *et al.*, 1987; Madara, 1990). At concentrations of 125mM glucose, at least one-third of glucose absorption in rat intestine *in vitro* occurs via paracellular solvent drag (Fine *et al.*, 1993). Indeed, several additional studies have reported that high glucose concentrations induce significantly greater rates of absorption via solvent drag (Pappenheimer, 1993; Pappenheimer and Reiss, 1987). Alternatively, by binding to membrane proteins, metformin may induce membrane fluidity changes, resulting in translocation of transporters to alternative regions of the cell (Wiernsperger, 1999).

Reduced bile salt uptake in the ileum, associated with increased bile salt excretion in faeces, is a mechanism by which metformin might achieve a reduction in cholesterol levels in hypercholesterolaemic subjects (Scarpello *et al.*, 1998). This has been noted in some experimental animals but remains difficult to quantify in humans due to deconjugation of the unabsorbed bile salts by colonic bacteria (Tomkin, 1976). Since bile contains considerable amounts of cholesterol, and the cholesterol pool within the body is tightly regulated, it is logical that increased bile salt excretion would lead to a net reduction of cholesterol levels. Increased synthesis by the liver and/or intestine may in time correct any imbalance in the cholesterol pool; this would, however, take some time to achieve, allowing a period of time where cholesterol levels were reduced.

There is some evidence to support this hypothesis, at least in theory. Reduced bile salt transport in the ileum, as a consequence of metformin, would lead to bile salts being retained in the distal ileum. Under physiological conditions an osmotic gradient would be created due to the polarity of the salts and acids

concerned. Sodium would also be present in the lumen and this may draw water with it along osmotic gradients into the lumen, resulting in diarrhoea, a common side effect of metformin therapy. Although this hypothesis is rather simplistic in real terms, results from studies presented in chapter 4 imply that membrane integrity may become disrupted by metformin, at least *in vitro*, whilst bile salt transport was simultaneously inhibited. Since chronic metformin administration was not performed in the experimental rats, it is not known whether the colon may counter any increase in fluid retained osmotically from the ileal lumen.

Chronic therapy was undertaken upon mice maintained for the purpose of aortic compliance studies (chapter 5) with no apparent incidence of diarrhoea. In the rat, however, a rapid adaptive mechanism has been described following ileal resection, so that any consequence of chronic metformin therapy may be quickly countered by the small intestine and colon (Vazquez *et al.*, 1989). It is feasible that chronic metformin therapy causes side effects that may be masked by adaptational responses to the drug, possibly at the site of the intestine or colon. Indeed, results from *in vivo* experiments indicated a reduced absorption of fluid from the intestinal lumen in the presence of metformin (3.3.4). This effect may be due to the high concentration of the drug known to accumulate in this region or the concentration of drug used in these studies. The high accumulation of metformin may alter the osmotic properties of the paracellular channels through which both metformin and water flux. The importance of paracellular channels is covered in more detail in the following chapter.

In direct contrast to its effect on the ileum, metformin produced a significant enhancement of bile salt uptake and total bile salt recovery in hepatic bile (10%) when administered to jejunum (table 1 p119). Bile salt uptake was increased threefold compared to controls between 20-180 minutes (3.3.1). Nevertheless, the capacity of the jejunum to transfer bile salts is significantly lower than the ileum. The gross difference between the two regions of the small intestine is illustrated by the fact that ileum incorporated nearly 25 times the amount of glycocholate (control samples) compared with jejunum (control samples) at peak uptake points. Taken overall, the percentage of ^{14}C sodium glycocholate recovered in hepatic bile, compared to the concentration injected ($1\mu\text{Ci}$ or $0.0175\text{ }\mu\text{mol}$), stands at approximately 8% in jejunum (control) compared with over 80% in the ileum (control). This clearly demonstrates the functional and anatomical differences that exist amongst these two regions of small intestine. Despite this, direct comparisons between the ileal and jejunal preparations remain limited due to the different concentrations of unlabelled bile salt used in the two regions.

Plasma samples obtained from tail vein contained trace amounts of radiolabel when metformin was delivered to the jejunum (3.3.2). The concentration of glycocholate present in plasma may reflect ^{14}C sodium glycocholate bound to plasma proteins and the fraction of labelled bile salt not extracted by the liver. However, the modest levels in plasma (when compared to levels in bile) were significantly increased following metformin treatment. This suggests that metformin significantly enhances bile salt uptake in the jejunum, resulting in increased glycocholate levels in bile and the peripheral circulation. The enhancement of bile salt absorption and recirculation in the jejunum implies

either an effect of metformin upon the permeability of this intestinal region, or that metformin in some way augments the diffusional process.

It may be plausible that metformin is involved in allowing increased sodium availability through increased cellular permeability/tight junction permeability, thereby providing these co-factors. There is evidence to suggest that cellular integrity may be diminished at high concentrations of metformin, as seen experimentally in chapter 4. If this effect occurs *in vivo*, then water flux would be expected to increase as cell integrity is attenuated. However, metformin was associated with reduced fluid transfer from the intestinal lumen suggesting that this mechanism may not operate *in vivo*. Nevertheless, the paracellular flux of metformin may influence the distribution of $\text{Na}^+\text{-K}^+\text{-ATPase}$ transporters along the paracellular channel, which may affect the sodium gradient required for bile salt absorption.

The two different absorption processes in the proximal and distal small intestine and the two different effects of metformin upon these transport mechanisms poses a baffling contradiction. There is little documentation regarding the effect of metformin upon jejunal bile salt transport since the ileum was always considered the principle target for the drug, being an energy-dependent system. It is evident that the role of the jejunum may have been greatly underestimated and that it plays a more significant role than initially believed.

It should be stated that the experiments performed herein must be interpreted with due caution since they do not reflect precisely the conditions seen

physiologically. For example, the bile salt mixture was isolated to a region of intestine for a period of three hours. This would not occur under normal circumstances and thus the effect of metformin seen in these experiments upon jejunal tissue may exaggerate the local effect of metformin in that region without taking account of the normal rate of passage of bile salts along the small intestinal tract. The concentration of bile salt absorbed in the jejunum in the presence of metformin would depend upon gut transit time and the ability of the drug to become proportionally concentrated along the length of the intestine. One can postulate that the drug would not become so heavily concentrated in the intestinal wall under conditions of unrestricted transit along the intestinal lumen, if given orally at the same concentration.

Concentrations of metformin used experimentally are typically greater than those likely to be achieved during clinical use of the drug, although higher concentrations are customarily required in animals to induce similar effects. The question remains as to whether metformin imposes a transient toxic effect upon the gut or a more prolonged toxic effect, which could account for the drugs side effects relating to reduced fluid transfer. The question may be answered by testing the functionality of the tissue following drug treatment. This would be best achieved by repeating the *in vivo* bile salt transfer experiments. Under such circumstances, and following peak bile salt transfer, the drug and control treatments would be reversed following a flush out period to demonstrate that drug treated ileum could revert to normal transfer rates of bile salts.

Thus, the present studies have shown that metformin is associated with both significant suppression and enhancement of bile salt absorption, in the ileum and jejunum respectively, *in vivo*. This effect was highly reproducible in the intact animal. Similar effects were not reproducible in the everted intestinal sac technique of Wilson and Wiseman (1954) and Caspary and Creutzfeldt (1975). The reasons for this may be several-fold. Intestinal tissue is highly sensitive to fluctuations in temperature and to physical damage. The process of everting the intestine could result in some damage to the mucosal absorptive surface. In addition, the concentration of bile salt used herein was significantly greater than that used by Caspary and Creutzfeldt (1975) (10 μ mol/ml compared to 0.2 μ mol/ml). Thus, saturation of the active transporter may have occurred since the serosal and mucosal incubation fluids contained the same high concentration of unlabelled bile salt.

Recently, Barthe *et al.* (1998) detailed a method whereby tissue viability and activity is improved considerably in comparison to the technique used herein, and involves the use of tissue culture medium in place of salt solutions. According to Barthe *et al.* (1998), the use of simple salt buffers results in significant loss of tissue viability within 30 minutes of incubation, with over 50% of the epithelium having disappeared. These findings are significant and may partially account for the loss of sensitivity of this technique compared with earlier *in vivo* techniques. A clear effect of metformin has been demonstrated in the ileal and jejunal regions of the small intestine. The key question remains: How does metformin induce its effects in these regions and what processes are involved? The active transport mechanism involved in bile salt transport in the ileum remains an attractive target

for the action of metformin and will be addressed in more detail in the next chapter.

Chapter Four:

Bile Salt Transport in the Caco-2 Epithelial Cell Line

CHAPTER FOUR: Bile Salt Transport in the Caco-2 Epithelial Cell Line

4.1 Introduction:

Observations by Scarpello *et al.* (1998), that metformin induced a modest decrease in bile salt absorption, led to experimental analyses in whole animals and isolated tissues from rat (chapter 3). The nature of these experiments was to elucidate whether metformin significantly influences bile salt absorption.

Metformin was seen to significantly decrease bile salt (^{14}C sodium glycocholate) absorption when delivered to a segment of ileum *in situ*. Conversely, metformin significantly enhanced the absorption of bile salt when administered to the jejunum in the intact animal.

Experiments were then performed in isolated tissue segments according to the methods of Lack and Weiner (1961) and Wilson and Wiseman (1954). Metformin failed to significantly influence bile salt transport in the ileal segments. However, in jejunal preparations, bile salt transport was significantly increased following incubation with metformin. Analysis of fluid transfer data suggests metformin may influence the dynamics of fluid transfer within the small intestine. Interestingly, the volume of fluid transported per milligram tissue was significantly less in the presence of metformin compared with control tissue in both ileal and jejunal intestinal preparations. These experiments supported

evidence for an active transport system operating in ileal enterocytes concentrating bile salts against a concentration gradient, whereas a different transfer mechanism seems to operate in the jejunum.

The purpose of the studies performed herein was to determine whether metformin could also influence bile salt transport in the human Caco-2 cell line. In addition, to specifically manipulate one or more transport systems in order to identify a possible mechanism through which metformin may influence bile salt transfer.

Caco-2 cells are derived from a human colon adenocarcinoma (Fogh *et al.*, 1977). They are commonly utilised as a model for transport studies since they are of colonic origin, and undergo spontaneous differentiation into cells expressing enterocyte-like characteristics, including cell polarisation and the presence of tight junctions and microvilli (Pinto *et al.*, 1983).

As an epithelial cell layer model, Caco-2 cells have been utilised in the study of bile acid, vitamin B₁₂, and sugar transport (Hidalgo and Borchardt, 1990; Dix *et al.*, 1990; Blais *et al.*, 1987). The aforementioned molecules all share a common characteristic in that they are actively transported. Hidalgo and Borchardt (1990) provide evidence for the transport of taurocholate from apical to basolateral surfaces of Caco-2 monolayers being temperature-, energy-, and sodium-dependent. Studies involving vitamin B₁₂, performed by Dix *et al.* (1990), confirmed that absorption and internalisation of this molecule was restricted to the apical membrane. Sugar transport in Caco-2 cells was also shown to be sodium-dependent, as detailed by Blais *et al.* (1987). Caco-2 monolayers have

also been shown to express GTP-binding proteins, and these have been implicated in intracellular vesicular transport (Opdam *et al.*, 2000).

Specific details pertaining to the origins of bile salt synthesis, excretion, function, and absorption are provided in chapter 3 and will not be reiterated here. Nevertheless, Caco-2 cells express many characteristics of functional enterocytes and as such are an ideal model for experimental bile salt transport studies.

In a study by Kanda *et al.* (1998), specific constituents from human bile were found to induce expression of the intestinal bile acid binding protein (I-BABP), a bile acid binding protein found in the cytosol of ileocytes (Grober *et al.*, 1999). Several important conclusions were drawn from this study. Specifically, Caco-2 cells expressed the I-BABP gene in response to bile acids but not fatty acids or phospholipids, with the expression being concentration-dependent. In addition, the bile acid chenodeoxycholic acid was the most potent inducer of I-BABP gene expression at micromolar concentrations. The potency of bile acids for inducing such expression was dependent upon their physiochemical state, with unconjugated dihydroxy acids being the most potent. The induction of I-BABP expression was found to be generally transcriptional and represents a pathway of protein receptor generation capable of being up-regulated in Caco-2 cells (Grober *et al.*, 1999).

Similarly, and according to Grober *et al.* (1999), the expression of the I-BABP gene along with corresponding mRNA levels were shown to be influenced by bile acid feeding and retention. Grober *et al.* (1999) also provide evidence that I-BABP expression is stimulated through the interaction of a specific nuclear

receptor by its ligand. Additional information on this receptor and its possible role in bile salt transport is provided in chapter 3.

The feeding of mice with taurocholate increased I-BABP mRNA levels, whilst the sequestration of bile acids with the binding resin cholestyramine caused a significant reduction in I-BABP mRNA levels (Grober *et al.*, 1999). These data suggest a role for bile acids in regulating the expression of I-BABP. Interestingly, comparable effects were not seen in rats following similar treatments (Arrese *et al.*, 1998), presumably reflecting physiological and anatomical differences between these species such as the absence of a gall bladder in the rat. These studies support earlier evidence for bile acids inducing expression of I-BABP in the ileum (Kanda *et al.*, 1996).

Root *et al.* (1995) provide further evidence for the presence of a specific bile acid transporter in the apical membrane of Caco-2 cells. In this study a specific inhibitor of the ileal bile acid transporter (2164U90) was used to block active uptake of bile acids in Caco-2 cells and everted ileal intestinal sacs. Decreased taurocholate transfer from the mucosal to basolateral surfaces of Caco-2 monolayers was recorded following treatment with the hypocholesterolaemic compound. In addition, an effect of the bile salt transporter inhibitor on glucose transport was also investigated to determine the specificity of the compound. Results from experiments utilising jejunal brush-border membrane vesicles confirmed glucose transport was not inhibited by this compound.

These results suggest that inhibitors of a specific transporter or transport process do not affect collectively sodium-dependent transporters and their substrates. Indeed, results from studies presented herein further suggest that the inhibition of

bile salt transfer by metformin appears selective towards the bile salt transporter since glucose transport remained unaffected. However, the question as to whether metformin demonstrates a specific affinity towards the ileal bile salt transporter remains open to debate.

Hidalgo and Borchardt (1990), also using Caco-2 cell monolayers, found taurocholate was transported transcellularly. This transport was only partially inhibited by ouabain, leading to suggestions of both a sodium-dependent and independent pathway for taurocholate transport in Caco-2 cells. Conversely, this model was re-examined by Chandler *et al.* (1993), who determined that taurocholate transport by differentiated Caco-2 cells was predominantly sodium-dependent, with Caco-2 cells expressing many of the features characteristic of ileocytes, including temperature-dependence, unidirectional transport, and sensitivity to inhibitors. Hidalgo and Burchardt (1990) remark that differences in the transport characteristics of Caco-2 cells are evident between low and high passage number cells. Therefore, in addition to preferentially selecting low passage numbers, cells were split prior to reaching confluence.

Circumstances such as these may account for the conflicting results evident between the two studies detailed above. However, in rebuke of this, the experiments performed herein utilised cells from passage 40 up to approximately passage 80 with little loss of reproducibility. These experiments were based on transport studies performed at Aston University by Nicklin *et al.* (1996), in which cells between passages 95-115 were used. Several different batches of Caco-2 cells were in fact utilised in the present studies, and may account for the minor

discrepancies in reproducibility evident in early studies. Thus, batch variations may well account for differences in transport characteristics between low and high passage numbers. Alternatively, subtle differences in culture conditions may also influence cell functionality. In support of this argument, Woodcock *et al.* (1991) reported that different clones of Caco-2 cells displayed significant differences not only in their ability to transport taurocholic acid, but also in the membrane resistance generated by these different monolayers, as determined by transepithelial resistance measurements. Nevertheless, studies performed herein found that little variation was evident over the range of passage numbers utilised in terms of Caco-2 cells actively transporting bile salts.

The studies briefly detailed in this introduction further substantiate the use of Caco-2 cells as a model for epithelial transport. Indeed, this cell line may reflect the most realistic model for intestinal transport studies available to date, and may prove important in providing an insight into the effect of metformin on bile salt transfer in the terminal ileum.

Taurocholic acid is the predominant primary bile acid in rat (Elliot, 1985). Many studies utilising Caco-2 cells preferentially use this bile acid. Studies herein utilised sodium glycocholate, a major bile acid of human bile. Glycocholate has previously been shown to be transported similarly to taurocholate in rat (Lack and Weiner, 1961), and hence was used in transport studies herein, maintaining consistency with previous studies in intact animals and isolated tissues.

4.2 Results:

Observations made in previous *in vivo* and *in vitro* experiments (chapter 3) support evidence from the published literature relating to bile salt uptake. These studies confirmed that in the ileum an active transport mechanism is responsible for the vast majority of bile salt absorption. Conversely, a passive or facilitated mechanism appears to be responsible for bile salt absorption in the jejunum. The use of a dedicated intestinal cell line, such as the Caco-2 cell model, allows further exploration into the mechanisms involved in bile salt transfer. The Caco-2 cell line can only realistically be utilised to study the transport characteristics of the terminal small intestine, since they undergo spontaneous differentiation into cells with similar features to ileal enterocytes. This point represents a juncture in that the effect of metformin in the jejunum, whilst interesting, will not be researched further in the present project.

The experiments performed herein utilised Caco-2 cells to study the transport of radiolabelled ^{14}C sodium glycocholate. Evidence will be provided for an active mechanism for bile salt transport. Ouabain, a specific $\text{Na}^+\text{-K}^+\text{-ATPase}$ inhibitor, and metformin were both found to inhibit this active transport mechanism. Preliminary experiments suggest that metformin may be specific for the bile salt transporter and may confer a protective effect on membrane integrity.

Caco-2 monolayers cultured on polyester inserts for 21 days were used to study the transport of radiolabelled (^{14}C) sodium glycocholate. In addition to this synthetic bile salt, tritiated mannitol (^3H) was used as a marker for cell monolayer integrity. Mannitol is a compound not actively transported and is of a sufficient

molecular size not to cross the cell layer paracellularly. Incubating solutions were analysed following a 24 hour incubation at 37°C. The volume of the apical chamber was 1.5ml, whilst the basolateral chambers held 2.6ml of balanced salt solution. The incubating solutions of the apical and basolateral compartments were analysed for determination of bile salt and mannitol transfer. Inserts were cut from their supports and counted also. Results are expressed as percentage of the total radioactive counts for each individual chamber and represent the percentage of the counts remaining in the relative chambers.

The effect of metformin upon ^3H mannitol transfer from the apical chamber of transwell inserts is illustrated in figures 4.1.1-4.1.3. Mannitol transfer into the basolateral chamber of control wells accounted for 8.5% of the total added to the apical chamber and suggests that a high degree of membrane integrity was achieved (4.1.2). Metformin treatment at 10^{-3} , 10^{-4} , and 10^{-5} M resulted in between 7-10% mannitol transfer after 24 hours. However, metformin at 10^{-2} M resulted in a significant (40%) transfer of mannitol into the basolateral chamber. Transfer into the basolateral chamber was over 31% greater at the highest metformin concentration (10^{-2} M), compared with controls. No significant differences were evident between the cell monolayer samples. Nevertheless, least radioactivity was detected in the cell monolayer after treatment with 10^{-2} M metformin (4.1.3). The fact that significantly more mannitol traversed the cell monolayer following a high concentration of metformin suggests that disruption of the membrane or the tight junctions may have occurred. Whilst the amount of radiolabel (^3H) recovered in the cell monolayer was not statistically significant, it

was less than control values and may support the notion of reduced monolayer integrity.

The transport of glycocholate was significantly influenced by the presence of metformin. In apical samples taken from control wells, 49% of labelled bile salt was transported into the basolateral chamber (4.1.5). Statistically significant effects were not evident at the lower metformin concentrations. However, high concentrations of metformin (10^{-2} M) resulted in a significant inhibition of bile salt transport (59% apical ^{14}C content; 4.1.4). Significantly less of the bile salt was transported into the basolateral chamber with significantly more of the label being retained within the cell monolayer (4.1.6).

Ouabain, an ATPase inhibitor, was utilised to inhibit bile salt transfer via inhibition of the $\text{Na}^+\text{-K}^+\text{-ATPase}$ pump. In addition, studies were undertaken to determine if the inhibitory effect of metformin on bile salt transfer could be attributed to a synergistic effect of the two compounds.

Transfer of labelled mannitol from the apical to basolateral chambers was, on average, 5% in control wells (4.2.2). This compared to 8% in ouabain treated monolayers (10^{-4} M) and 14% in metformin treated wells (10^{-2} M). In combination, metformin (10^{-2} M) and ouabain at all concentrations resulted in significantly greater flux of the non-transportable marker. These results suggest that metformin and ouabain, when administered in combination, alter the membrane integrity allowing the transfer of mannitol across the membrane to occur. Significantly less radiolabel was recovered in the cell monolayer of wells

treated with metformin and ouabain in combination (4.2.3). This supports the hypothesis that a disruption of the membrane integrity is a consequence of drug treatment.

Glycocholate transfer was significantly influenced by the presence of both metformin and ouabain. Transfer of bile salt from apical to basolateral chambers was, on average, 85% in control wells (4.2.5). In the presence of ouabain (10^{-4} M) this was reduced to 58%, and with metformin (10^{-2} M) to 63%. Thus, both ouabain and metformin, as individual treatments, significantly reduced transport of the synthetic bile salt to a similar degree. Metformin, when administered with ouabain (10^{-2} and 10^{-5} M respectively), did not produce a greater inhibition than either metformin or ouabain alone. However, when the same concentration of metformin (10^{-2} M) was added to ouabain at 10^{-3} and 10^{-4} M, the inhibitory effect on apical to basolateral transport became additive, with basolateral glycocholate levels falling to 39% and 45% respectively. These results suggest that metformin and ouabain may inhibit bile salt transfer through the same or similar routes, i.e. the active bile salt transporter.

The amount of radiolabel detected in the cell monolayer was significantly greater in the combined metformin and ouabain treatments, and in the metformin treatment alone, compared with control values (4.2.6). This suggests that whilst the mannitol data imply some loss of membrane integrity, this had little effect upon bile salt transfer. Indeed, the greater radioactive content of the monolayer samples supports the hypothesis of inhibited transport. Results from figures 4.1.1 and 4.2.1 clearly demonstrate some form of membrane disruption with metformin

alone, and in combination with ouabain (at high concentrations). Interestingly, ouabain as an individual treatment did not appear to significantly affect membrane integrity. Thus, while one might conclude that both metformin and ouabain could inhibit bile salt transfer through similar mechanisms, it is clear that metformin imposes an effect upon membrane integrity that is different to that of ouabain.

Preliminary experiments were performed to determine the effect of unlabelled glycocholic acid ($0.133\mu\text{mol/ml}$) on the transfer of radiolabelled glycocholate. Data from these experiments are represented in figures 4.3.1-4.3.3. These data, however, are combined with control data from previous experiments (4.2.1-4.2.3, and 4.2.4-4.2.6) to provide a visual comparison between the two treatments. Statistical comparisons have been determined between the treatment groups for individual samples, i.e. apical versus apical comparison.

The presence of unlabelled bile salt increased the transfer of mannitol from the apical into the basolateral chamber. Over twice the amount of ^3H mannitol was detected in the basolateral chamber following the addition of $0.133\mu\text{mol/ml}$ unlabelled glycocholic acid (4.3.2). However, this was not statistically significant and implies that the concentration of unlabelled glycocholic acid added, whilst increasing mannitol flux basolaterally, does not significantly impair membrane viability. Significantly less of the labelled bile salt was transported into the basolateral chamber in the presence of unlabelled bile salt (4.3.3). In addition, significantly more radioactive marker was present in the cell monolayer following treatment with unlabelled glycocholic acid.

These results provide convincing evidence that unlabelled glycocholic acid actively competes with the apical bile salt transporter thereby reducing the net transfer of labelled bile salt. The observation of increased mannitol flux from the apical to basolateral chambers may reflect a mild toxic effect of bile salts. Such molecules are known to be toxic at high concentrations (Rafter and Branting, 1991). These authors provide evidence that at bile salt concentrations of 5mmol/l, the mucosal permeability of colonic cells increases significantly. In addition, decreasing the pH from around 8 to 5.5 in the colon prevented cellular damage normally induced by 5mmol/l deoxycholate. According to Rafter and Branting (1991), lowering the pH may lower the solubility of the bile acid. In the studies presented herein, pH levels fell in all samples with the exception of controls.

The concentration of unlabelled bile salt added to the apical chamber was significantly lower than the concentration estimated to be normally present in the terminal small intestine of fed rats (Dietschy, 1967). However, it is important to note that even at this relatively low bile salt concentration, ^{14}C labelled glycocholate transfer was significantly reduced whilst mannitol transfer was not significantly affected. This highlights the sensitivity and specificity of the Caco-2 cell model for the active transport of bile salt molecules. Furthermore, it confirms the presence of a saturable transport system in this cell line.

In order to demonstrate conclusively that bile salt transfer in the Caco-2 culture model is unidirectional, experiments were performed with ^3H mannitol and ^{14}C labelled glycocholate added to the basolateral chambers. Results of these experiments (4.4.2-4.4.3) are combined with control data from previous experiments, allowing visual comparisons to be made between the normal apical

to basolateral transfer and the basolateral to apical route. Statistical comparisons were computed for ^{14}C sodium glycocholate data; similar tests were not computed for ^3H mannitol data, as differences are clearly evident. Under normal conditions of apical to basolateral transfer, the percentage of mannitol remaining in apical chambers averaged 92%. When mannitol was added to the basolateral chamber, approximately 5% flux occurred into the apical chamber. This figure compares almost identically with the value found in basolateral chambers following the addition of ^3H mannitol to the apical compartment. In addition, significantly less ($p < 0.001$) mannitol was retained within the cell monolayer following its addition to the basolateral chamber (4.4.2).

Significant differences were also evident in the transfer of labelled bile salt. Basolateral to apical flux accounted for 3% of the labelled bile salt and represented a significantly lower value than the 13% remaining in the apical chamber during standard apical to basolateral flux experiments (4.4.3). From these results it can be concluded that transport of labelled bile salt is unidirectional occurring along the apical to basolateral route.

Preliminary experiments were performed to determine if the inhibitory effect of metformin and ouabain on bile salt transfer is related to a specific effect upon bile salt transporters, or a more general effect on energy-dependent transport systems (figures 4.5.1-4.5.6). Radiolabelled D-glucose (^{14}C D-glucose) was added, along with ^3H mannitol, to the apical chamber of test wells. Experimental design was identical to previous experiments. Mannitol transfer from apical to basolateral chambers accounted for 5% of the total in control wells. This figure increased to

between 9 and 13% when metformin and ouabain were incubated simultaneously at varying concentrations. A little more mannitol fluxed into the basolateral chamber in wells treated with ouabain at 10^{-4} M (8%), and metformin at 10^{-2} M (19%), implying that at such concentrations these drugs may interfere moderately with membrane integrity. Despite this effect, the transfer of labelled glucose was not significantly influenced by any treatment (4.5.4 – 4.5.6). It is possible to conclude from these preliminary data that the ATPase inhibitor ouabain does not significantly inhibit the sodium-coupled transport of glucose from the apical surface. Similarly, metformin does not appear to influence glucose transfer. However, from the data pertaining to mannitol flux, it is clear that metformin may have a mild toxic effect upon the cells when present at high concentrations. Interestingly, metformin, when incubated with ouabain (10^{-5} – 10^{-3} M) resulted in slightly less mannitol flux occurring into the basolateral chamber, suggesting that metformin may impose a protective effect on the integrity of the cell layer.

Although conclusions have been drawn from these data, it is important to stress that these studies are only preliminary and represent an initial series of experimental observations. Metformin was seen to allow greater mannitol flux in early experiments than those performed subsequently. This may be accounted for by improvements in experimental conduct in later studies, with improvements being gained over time. However, since control wells were included in each series of experiments, comparisons within each study remain fully validated. In addition, it is noteworthy that the Caco-2 cell line may be subject to variance within individual batches of cells, e.g. passage number and growth on the membrane. More than one batch of cells was utilised during these experiments,

and spanning several passages. This may have contributed to the spread of data evident between different experiments.

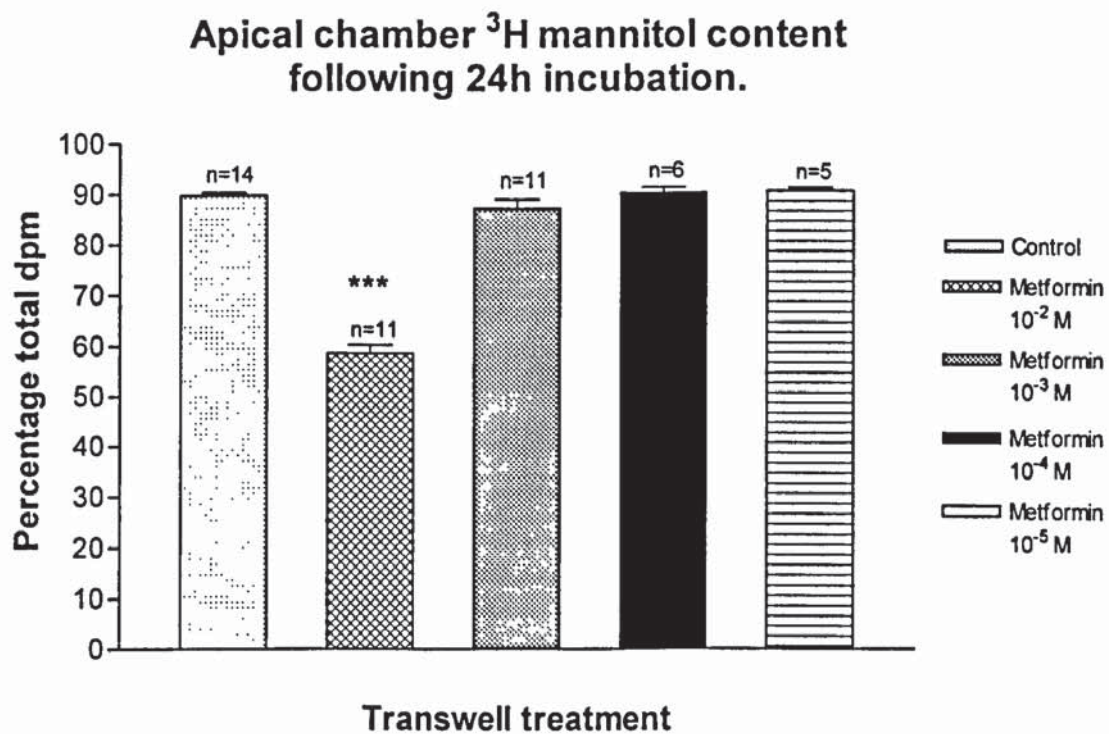


Figure 4.1.1: Effect of metformin (10^{-5} – 10^{-2} M) at 24h on the percentage flux of ^3H mannitol from the apical chamber across Caco-2 monolayers cultured on polyester membranes of transwell culture plates. Metformin, at high concentrations, significantly ($p < 0.05$) enhanced mannitol flux from the apical compartment. Data are expressed as percentage total dpm and represent the percentage dpm remaining in the apical compartment. Values are mean \pm SEM, *** $p < 0.0001$ versus control (Student's paired 't'-Test).

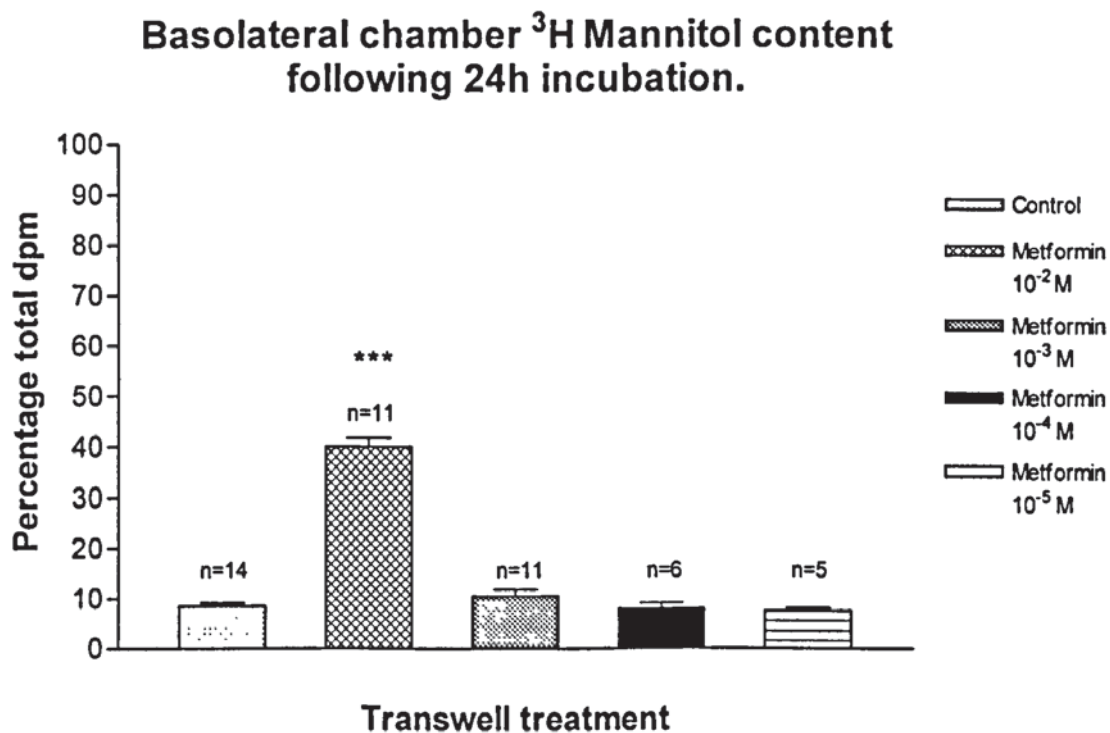


Figure 4.1.2: Effect of metformin (10^{-5} – 10^{-2} M) at 24h on the percentage flux of ^3H mannitol into the basolateral chamber across Caco-2 monolayers cultured on polyester membranes of transwell culture plates. Metformin, at high concentrations, significantly ($p < 0.05$) enhanced mannitol flux into the basolateral compartment. Data are expressed as percentage total dpm and represent the percentage dpm in the basolateral compartment. Values are mean \pm SEM, *** $p < 0.0001$ versus control (Student's paired 't'-Test).

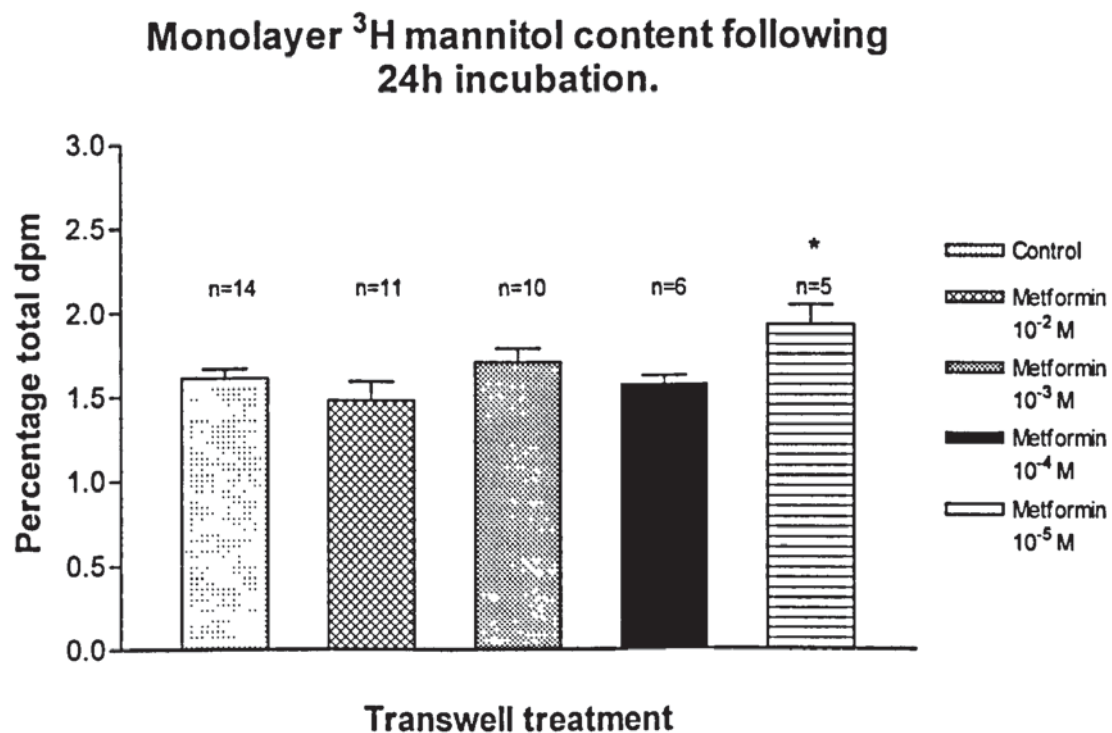


Figure 4.1.3: Effect of metformin (10^{-5} – 10^{-2} M) at 24h on the percentage ^3H mannitol within the cell monolayer of Caco-2 cells cultured on polyester membranes of transwell culture plates. Data are expressed as percentage total dpm. Values are mean \pm SEM, * $p < 0.03$ versus control (Student's paired 't'-Test).

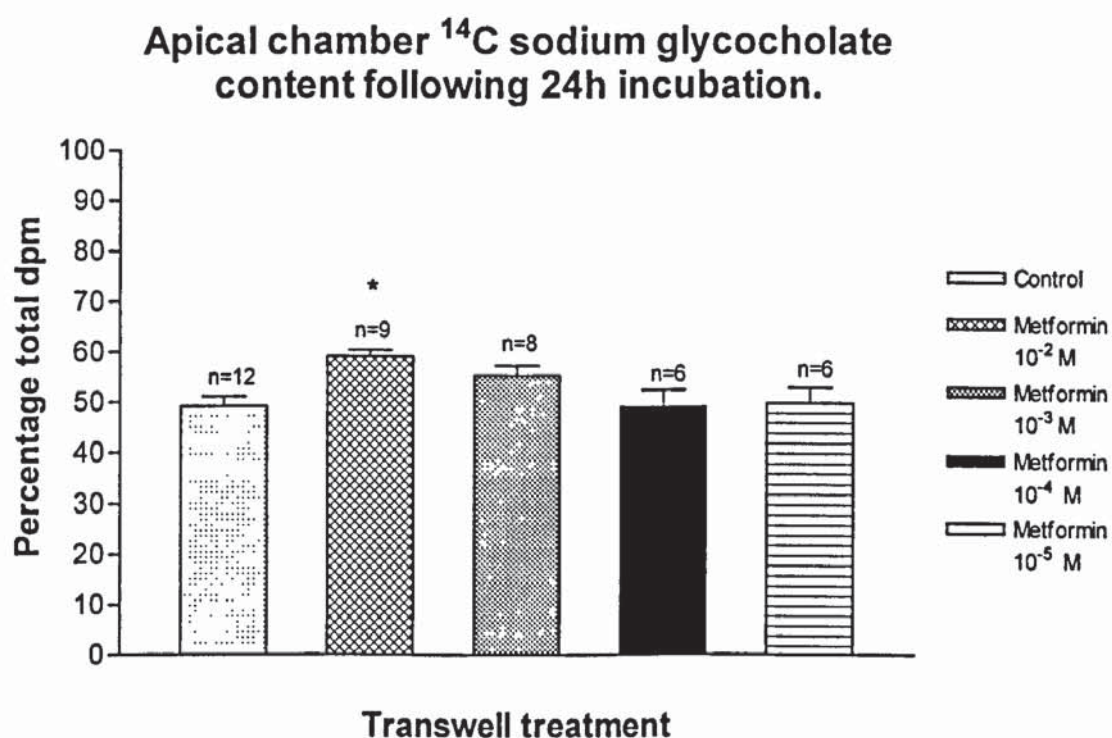


Figure 4.1.4: Effect of metformin (10^{-5} – 10^{-2} M) at 24h on the percentage transfer of ^{14}C sodium glycocholate from the apical chamber across Caco-2 monolayers cultured on polyester membranes of transwell culture plates. Metformin, at high concentrations, significantly ($p < 0.05$) inhibited bile salt transfer from the apical compartment. Data are expressed as percentage total dpm and represent the percentage dpm remaining in the apical compartment. Values are mean \pm SEM, * $p < 0.03$ versus control (Student's paired 't'-Test).

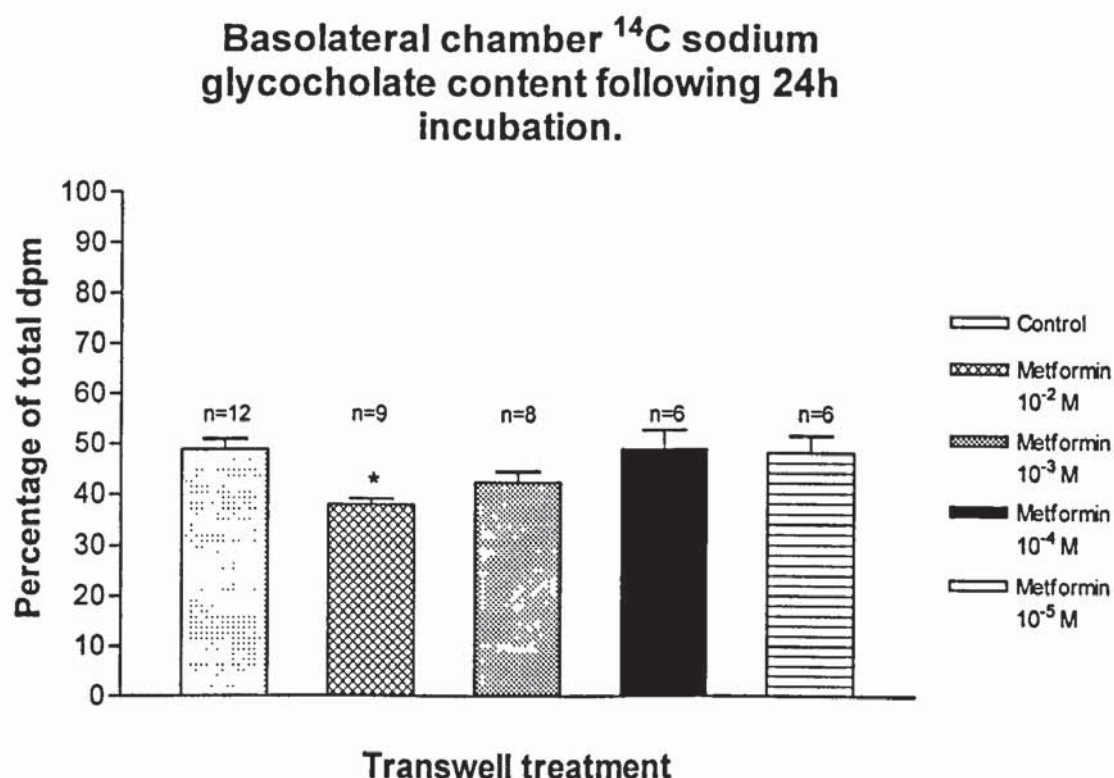


Figure 4.1.5: Effect of metformin (10^{-5} – 10^{-2} M) at 24h on the percentage transfer of ^{14}C sodium glycocholate into the basolateral chamber across Caco-2 monolayers cultured on polyester membranes of transwell culture plates. Metformin, at high concentrations, significantly ($p < 0.05$) inhibited bile salt transfer into the basolateral compartment. Data are expressed as percentage total dpm and represent the percentage dpm remaining in the basolateral compartment. Values are mean \pm SEM, * $p < 0.03$ versus control (Student's paired 't'-Test).

**Monolayer ^{14}C sodium glycocholate
content following 24h incubation.**

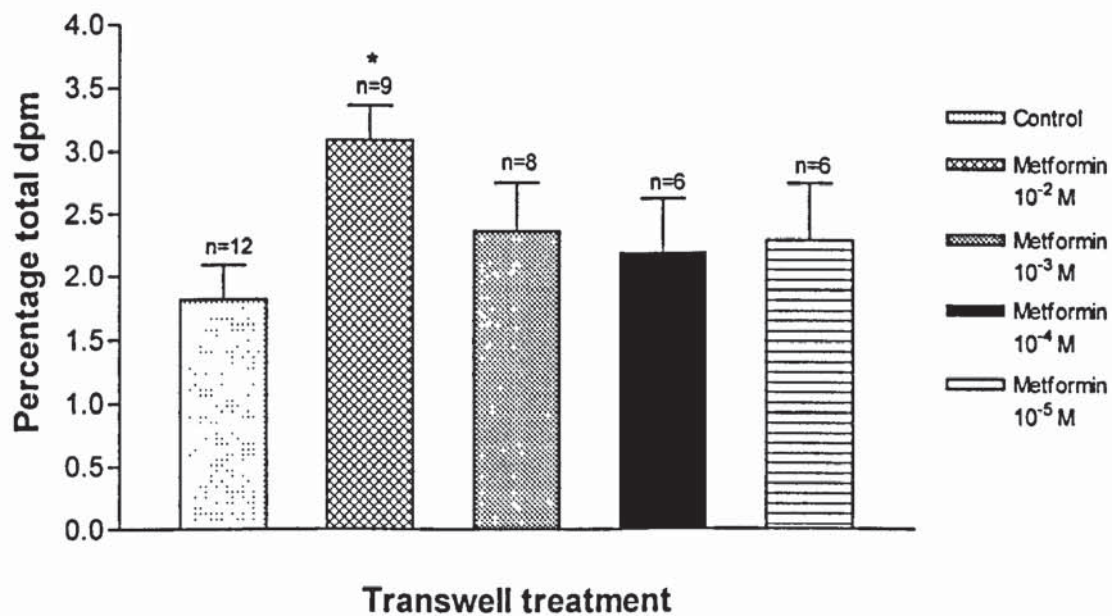


Figure 4.1.6: Effect of metformin (10^{-5} – 10^{-2} M) at 24h on the percentage ^{14}C sodium glycocholate within the cell monolayer of Caco-2 cells cultured on polyester membranes of transwell culture plates. Metformin, at high concentrations, was associated with significantly ($p < 0.05$) greater amounts of radiolabel within the cell monolayer. Data are expressed as percentage total dpm. Values are mean \pm SEM, * $p < 0.02$ versus control (Student's paired 't'-Test).

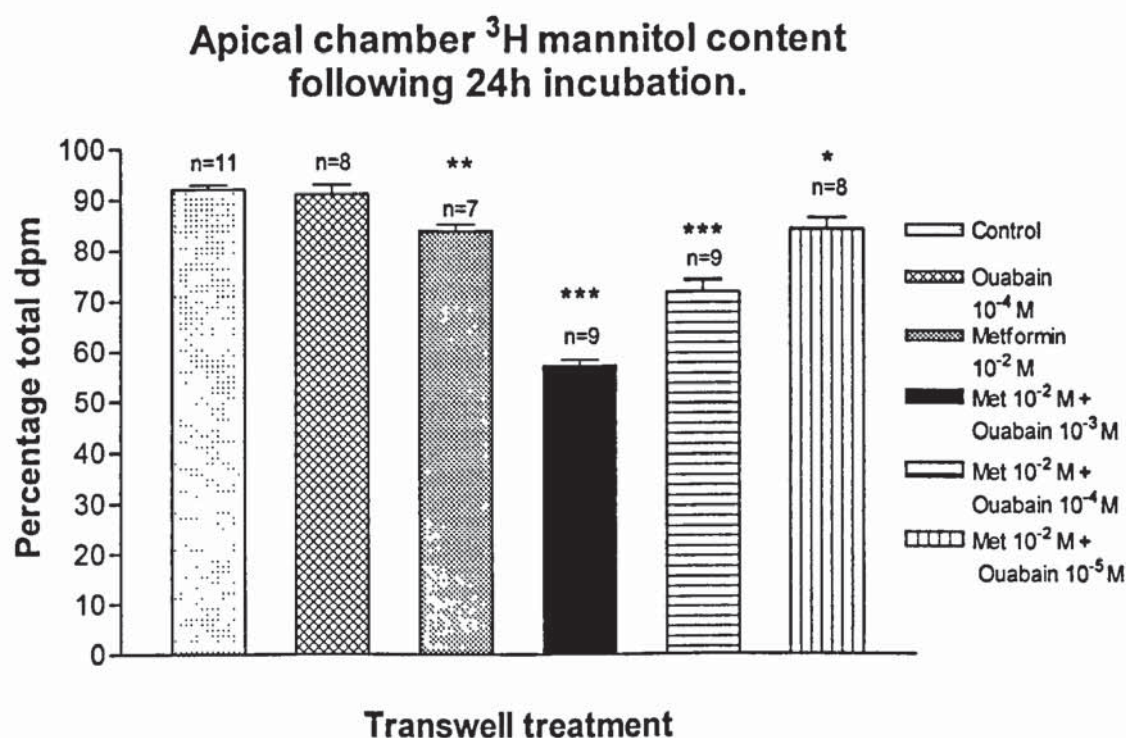


Figure 4.2.1: Effect of metformin (10^{-2} M) and ouabain (10^{-5} – 10^{-3} M), alone and in combination, at 24h on the flux of ^3H mannitol from the apical chamber across Caco-2 monolayers cultured on polyester membranes of transwell culture plates. Metformin, alone at high concentrations, and metformin, in combination with ouabain at all concentrations, significantly ($p < 0.05$) increased mannitol flux. Data are expressed as percentage total dpm and represent the percentage dpm remaining in the apical compartment. Values are mean \pm SEM, * $p < 0.02$ versus control, ** $p < 0.003$ versus control, *** $p < 0.0001$ versus control (Student's paired 't'-Test).

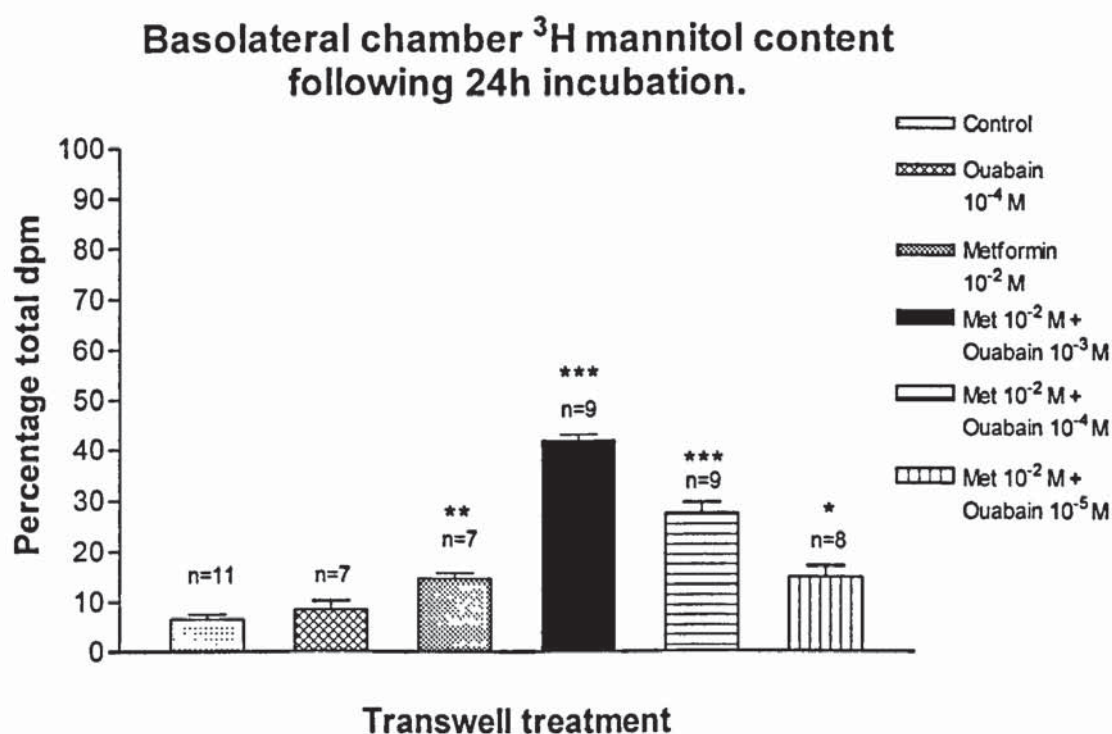


Figure 4.2.2: Effect of metformin (10^{-2} M) and ouabain (10^{-5} – 10^{-3} M), alone and in combination, at 24h on the flux of ^3H mannitol into the basolateral chamber across Caco-2 monolayers cultured on polyester membranes of transwell culture plates. Metformin, alone at high concentrations, and metformin, in combination with ouabain at all concentrations, significantly ($p < 0.05$) increased mannitol flux into the basolateral compartment. Data are expressed as percentage total dpm and represent the percentage dpm remaining in the basolateral compartment. Values are mean \pm SEM, * $p < 0.009$ versus control, ** $p < 0.003$ versus control, *** $p < 0.0001$ versus control (Student's paired 't'-Test).

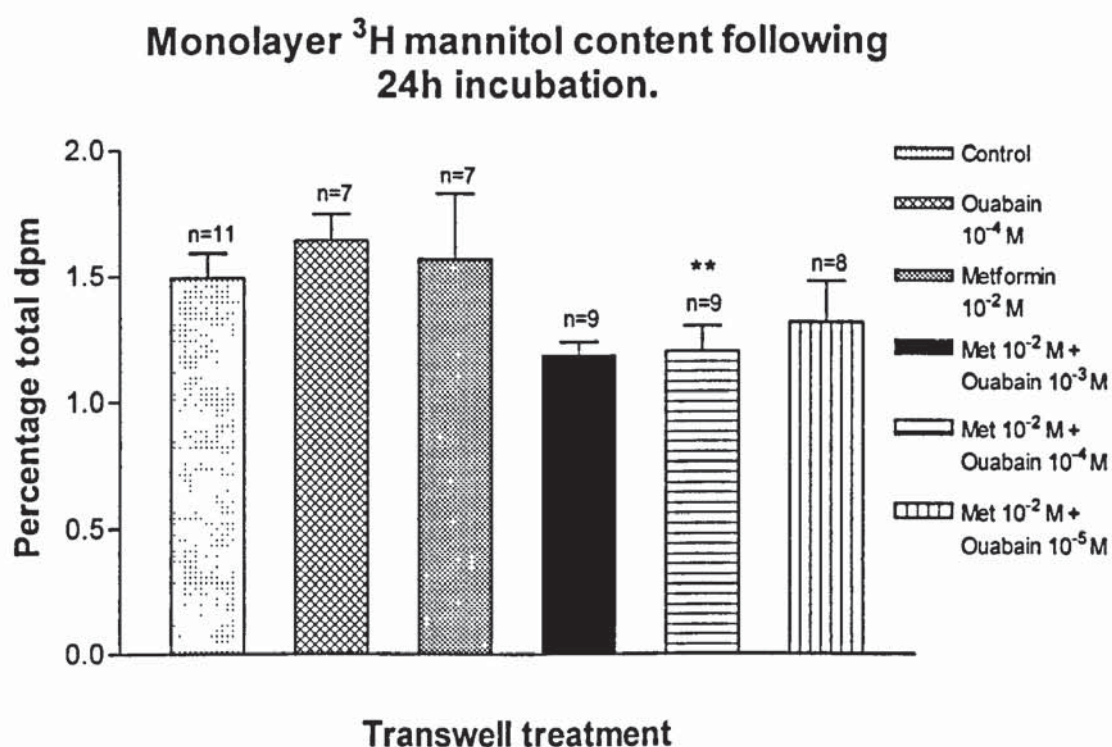


Figure 4.2.3: Effect of metformin (10^{-2} M) and ouabain (10^{-5} – 10^{-3} M), alone and in combination, at 24h on the percentage ^3H mannitol within the cell monolayer of Caco-2 cells cultured on polyester membranes of transwell culture plates. Metformin and ouabain, in combination, were associated with significantly ($p < 0.05$) less radiolabel within the cell monolayer. Data are expressed as percentage total dpm. Values are mean \pm SEM, ** $p < 0.009$ versus control, (Student's paired 't'-Test).

**Apical chamber ^{14}C sodium glycocholate
content following 24h incubation.**

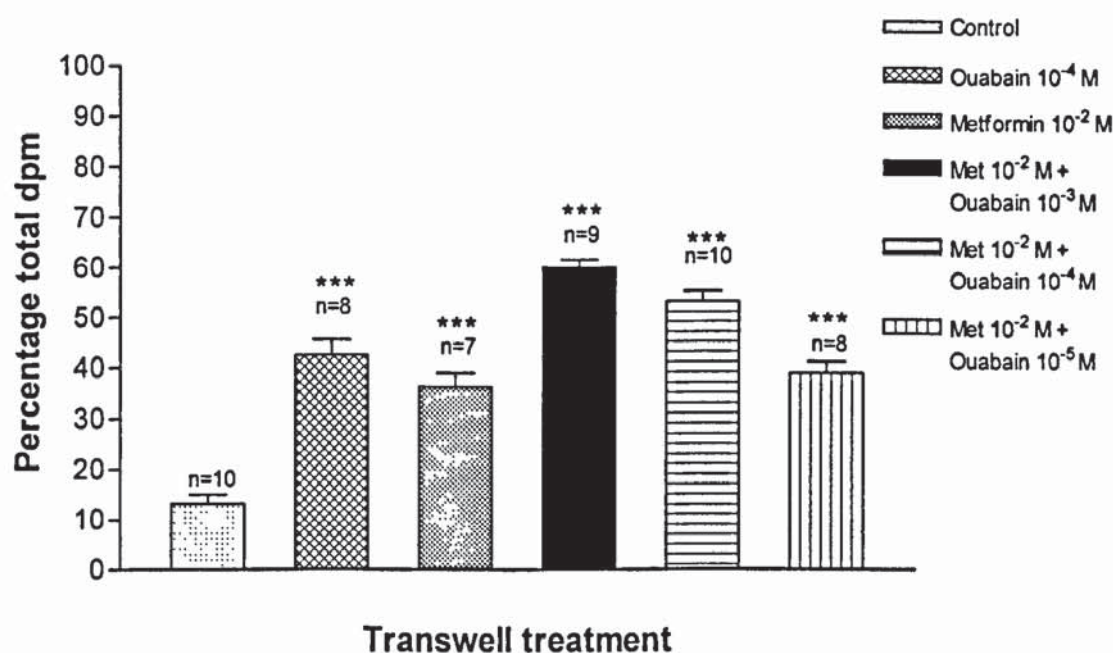


Figure 4.2.4: Effect of metformin (10^{-2} M) and ouabain (10^{-5} – 10^{-3} M), alone and in combination, at 24h on the transfer of ^{14}C sodium glycocholate from the apical chamber across Caco-2 monolayers cultured on polyester membranes of transwell culture plates. Both metformin and ouabain, alone and in combination, significantly ($p < 0.05$) reduced bile salt transfer. Data are expressed as percentage total dpm and represent the percentage dpm remaining in the apical compartment. Values are mean \pm SEM, *** $p < 0.0001$ versus control, (Student's paired 't'-Test).

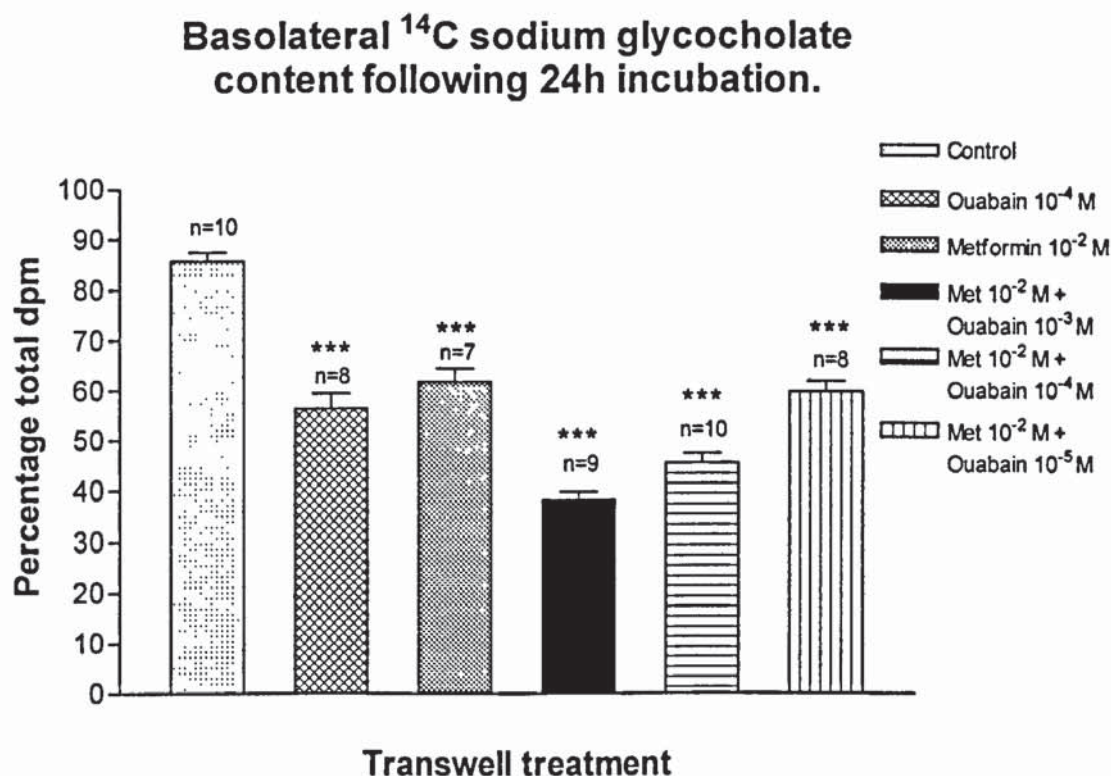


Figure 4.2.5: Effect of metformin (10^{-2} M) and ouabain (10^{-5} – 10^{-3} M), alone and in combination, at 24h on the transfer of ^{14}C sodium glycocholate into the basolateral chamber across Caco-2 monolayers cultured on polyester membranes of transwell culture plates. Metformin and ouabain, alone and in combination, significantly ($p < 0.05$) reduced bile salt transfer into the basolateral compartment. Data are expressed as percentage total dpm and represent the percentage dpm remaining in the basolateral compartment. Values are mean \pm SEM, *** $p < 0.0001$ versus control (Student's paired 't'-Test).

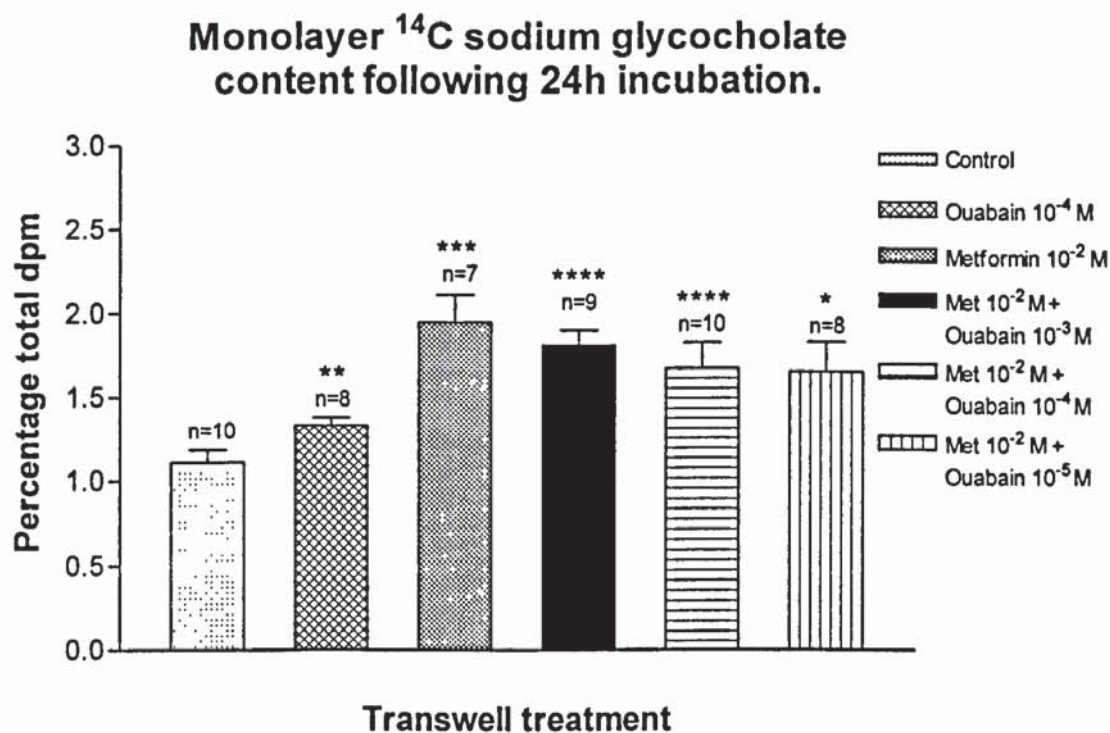


Figure 4.2.6: Effect of metformin (10^{-2} M) and ouabain (10^{-5} – 10^{-3} M), alone and in combination, at 24h on the percentage ^{14}C sodium glycocholate within the cell monolayer of Caco-2 cells cultured on polyester membranes of transwell culture plates. Metformin and ouabain, alone and in combination, were associated with significantly ($p < 0.05$) greater levels of radiolabel within the cell monolayer. Data are expressed as percentage total dpm. Values are mean \pm SEM, * $p < 0.01$ versus control, ** $p < 0.008$ versus control, *** $p < 0.005$ versus control, **** $p < 0.0001$ versus control (Student's paired 't'-Test).

Transfer of ^3H mannitol and ^{14}C sodium glycocholate following 24h incubation in presence of unlabelled bile salt.

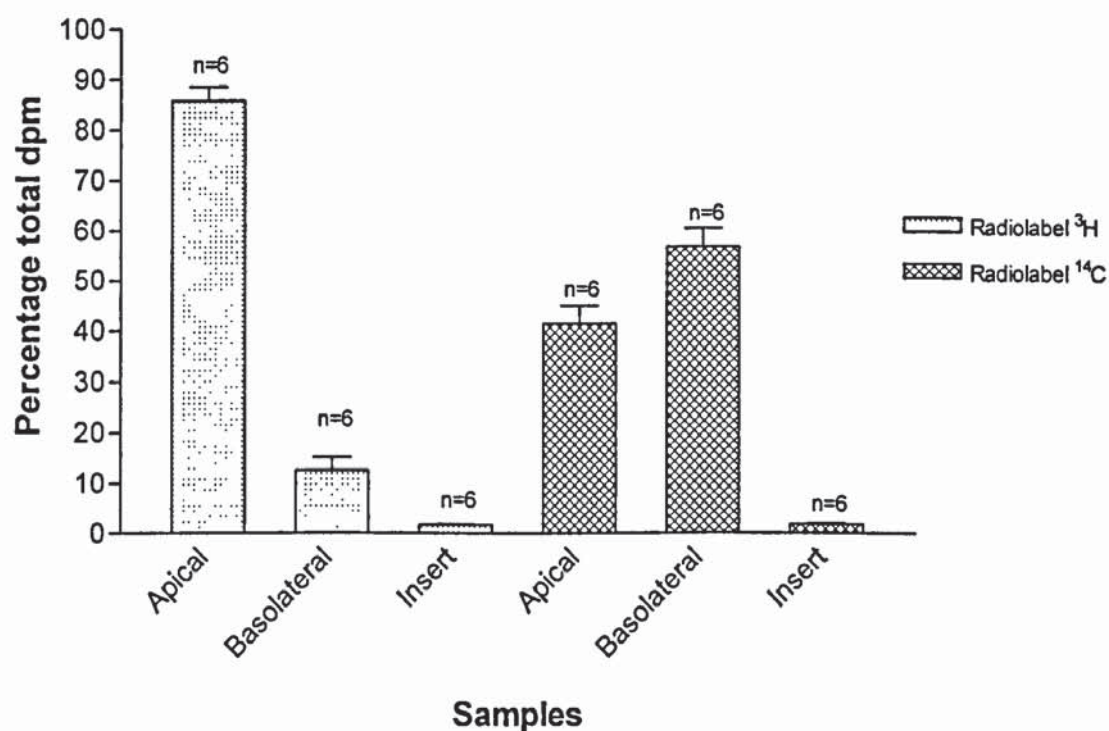


Figure 4.3.1: Effect of unlabelled glycocholic acid ($0.133\mu\text{mol/ml}$ added to the apical chamber) on the transfer of ^3H mannitol and ^{14}C sodium glycocholate at 24h from the apical chamber across Caco-2 monolayers cultured on polyester membranes of transwell culture plates. Data are expressed as percentage total dpm and represent the percentage dpm in the apical, basolateral, and monolayer samples. Values are mean \pm SEM.

Effect of of unlabelled glycocholic acid on the transfer of ^3H mannitol.

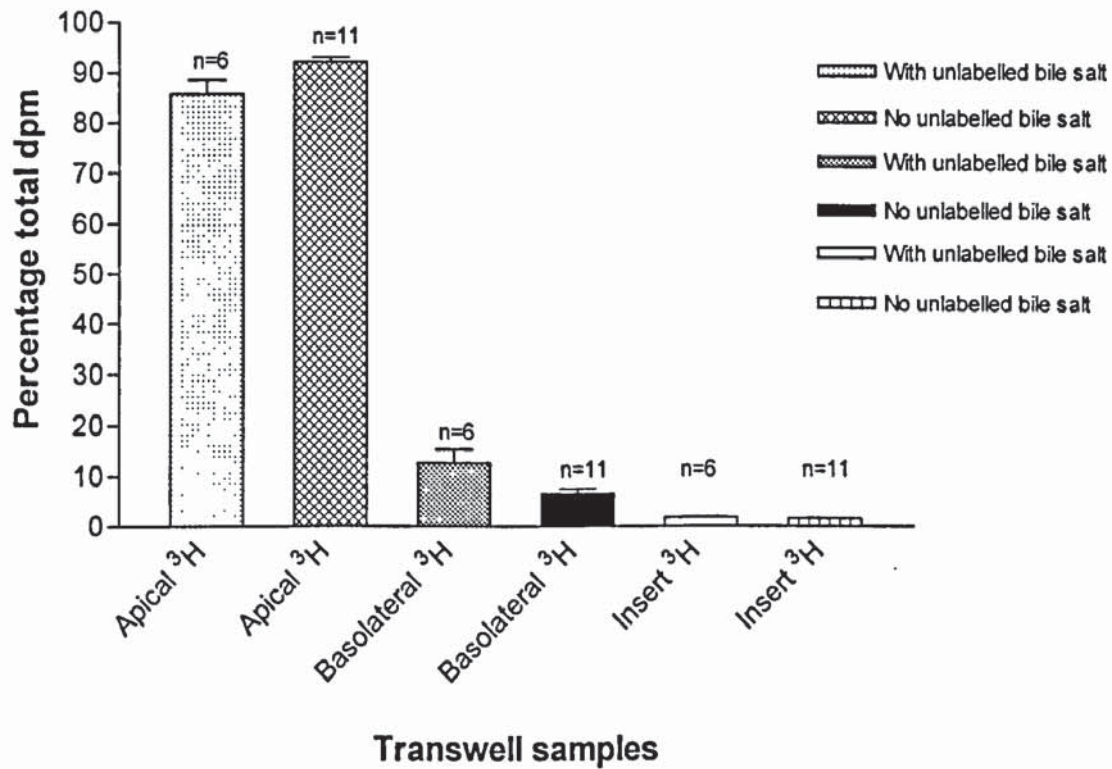


Figure 4.3.2: Effect of unlabelled glycocholic acid ($0.133\mu\text{mol/ml}$ added to the apical chamber) on the transfer of ^3H mannitol at 24h from the apical chamber across Caco-2 monolayers cultured on polyester membranes of transwell culture plates. Data are expressed as percentage total dpm and represent the percentage dpm in the apical, basolateral, and monolayer samples. Values are mean \pm SEM.

Effect of unlabelled glycocholic acid on the transfer of ^{14}C sodium glycocholate.

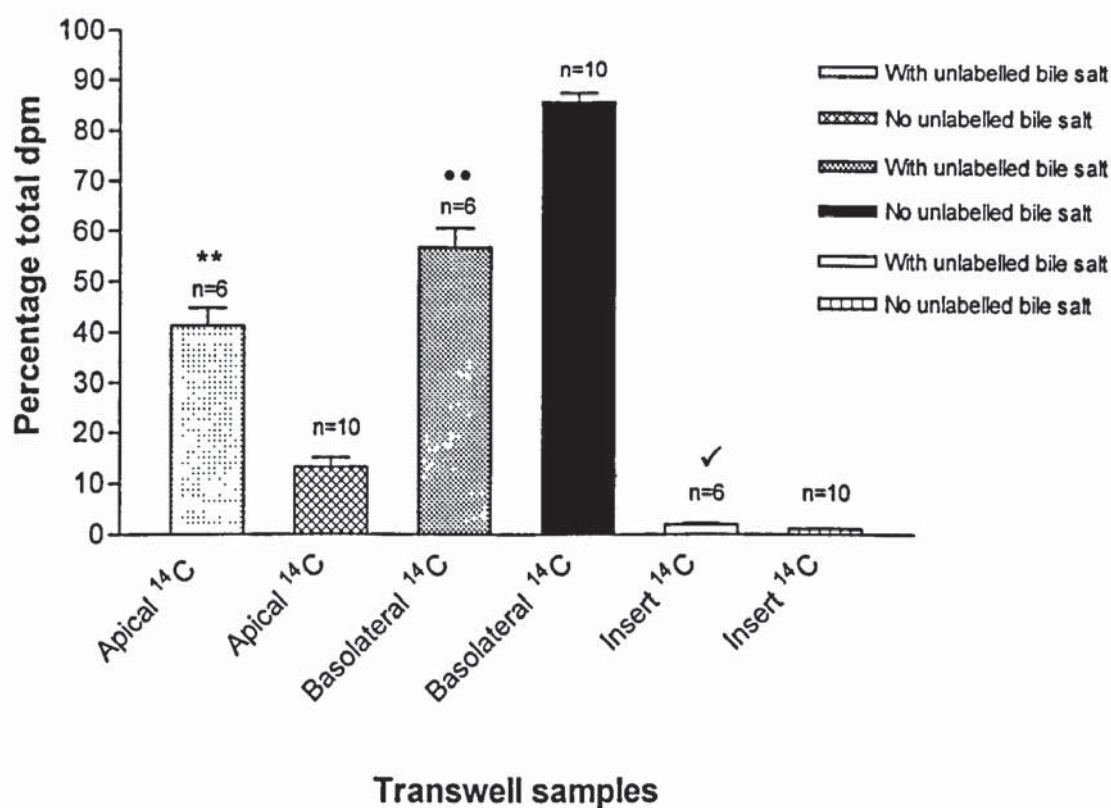


Figure 4.3.3: Effect of unlabelled glycocholic acid ($0.133\mu\text{mol/ml}$ added to the apical chamber) on the transfer of ^{14}C sodium glycocholate at 24h from the apical chamber across Caco-2 monolayers cultured on polyester membranes of transwell culture plates. Unlabelled glycocholic acid significantly ($p<0.05$) reduced the transfer of ^{14}C labelled bile salt. Data are expressed as percentage total dpm and represent the percentage dpm in the apical, basolateral, and monolayer samples. Values are mean \pm SEM, ** $p<0.0001$ apical versus apical comparison, •• $p<0.0001$ basolateral versus basolateral comparison, ✓ $p<0.04$ insert versus insert comparison (Student's paired 't'-Test).

Reverse transfer of ^3H mannitol and ^{14}C sodium glycocholate following 24h incubation.

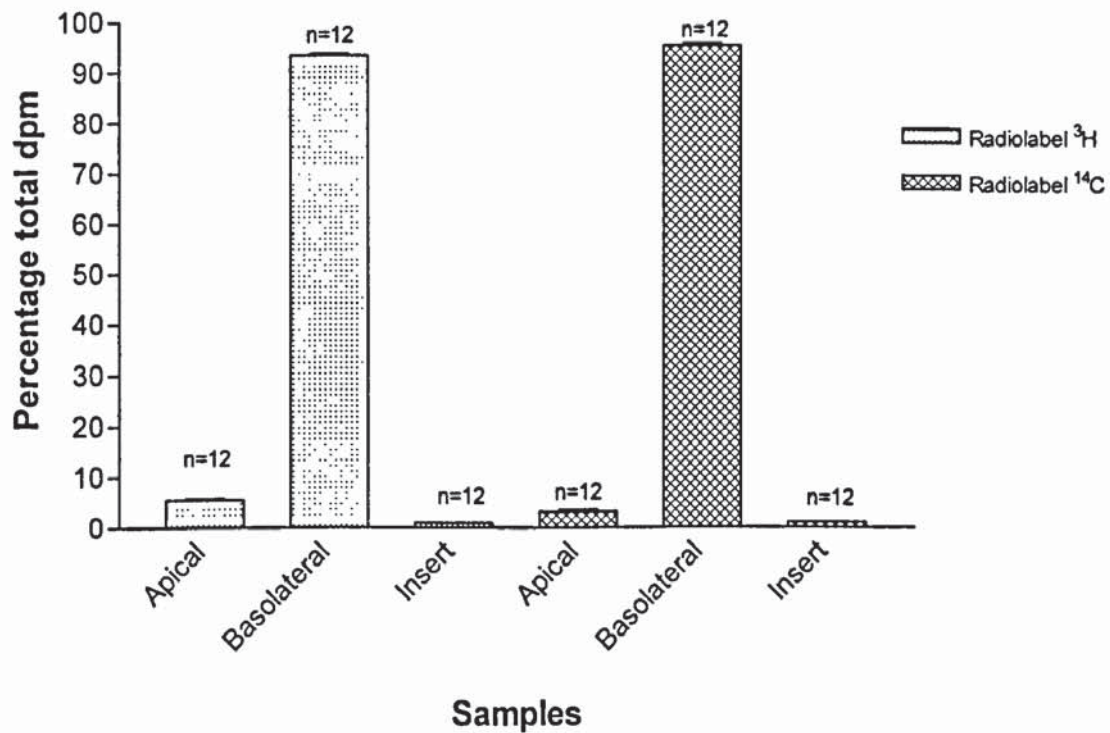


Figure 4.4.1: Reverse transfer of ^3H mannitol and ^{14}C sodium glycocholate at 24h from the basolateral chamber across Caco-2 monolayers cultured on polyester membranes of transwell culture plates. Data are expressed as percentage total dpm and represent the percentage dpm in the apical, basolateral, and monolayer samples. Values are mean \pm SEM.

Reverse flux of ^3H mannitol compared with normal apical to basolateral flux.

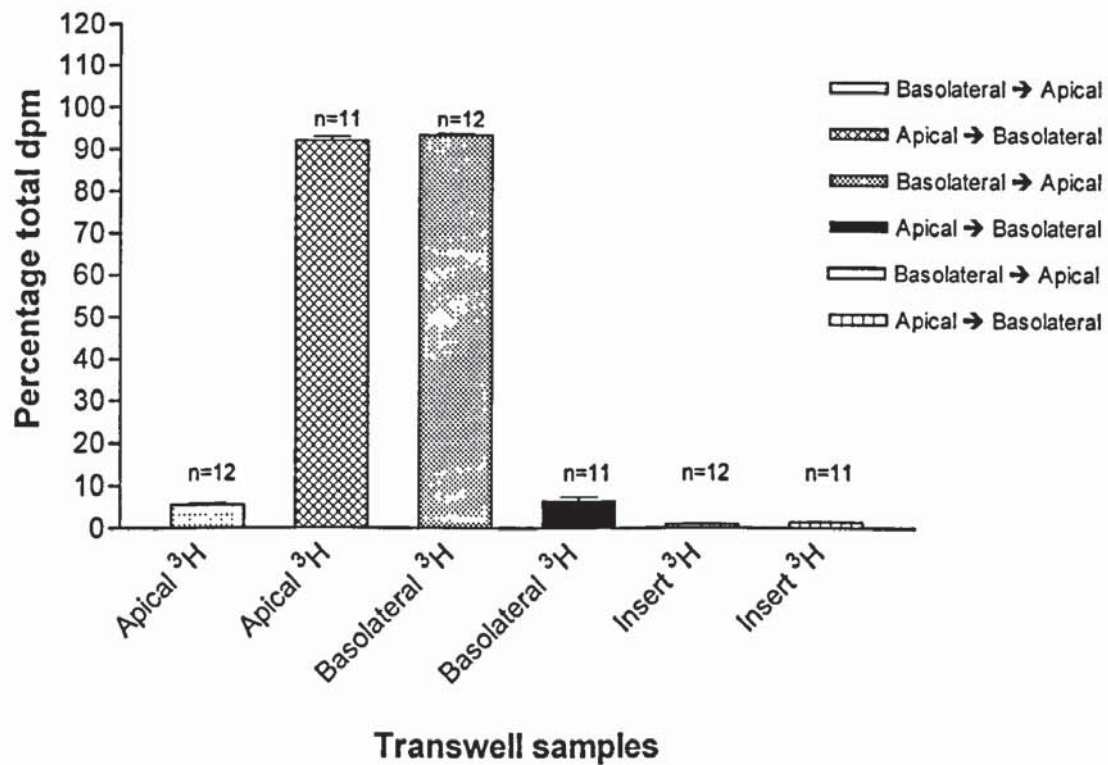


Figure 4.4.2: Comparison of the basolateral to apical flux of ^3H mannitol at 24h compared with the normal apical to basolateral route across Caco-2 monolayers cultured on polyester membrane supports of transwell culture plates. Data are expressed as percentage total dpm and represent the percentage dpm in the apical, basolateral, and monolayer samples. Values are mean \pm SEM (significant differences were evident between all corresponding samples $p < 0.001$, Student's unpaired 't'-Test).

Reverse transport of ^{14}C sodium glycocholate compared with normal apical to basolateral transport.

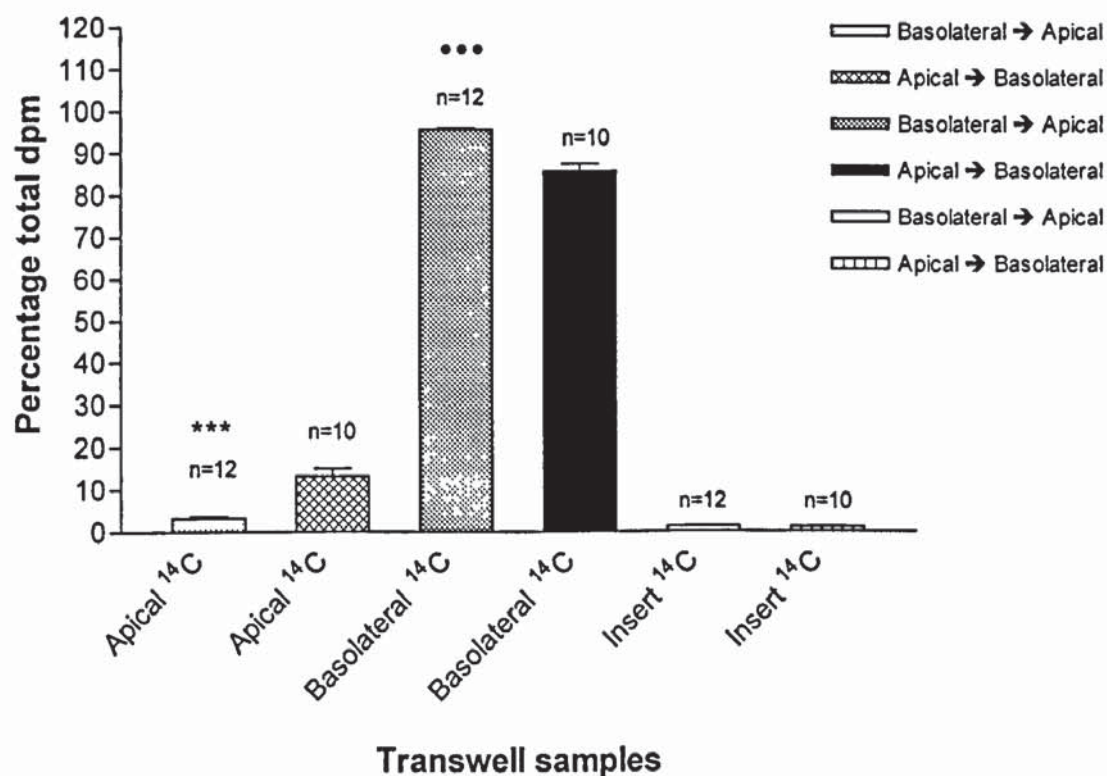


Figure 4.4.3: Comparison of the basolateral to apical flux of ^{14}C sodium glycocholate at 24h compared with the normal apical to basolateral route across Caco-2 monolayers cultured on polyester membrane supports of transwell culture plates. Data are expressed as percentage total dpm and represent the percentage dpm in the apical, basolateral, and monolayer samples. Values are mean \pm SEM, ***p=0.0002 apical versus apical comparison, ***p=0.0002 basolateral versus basolateral comparison (Student's unpaired 't'-Test).

Apical chamber ^3H mannitol content following 24h incubation.

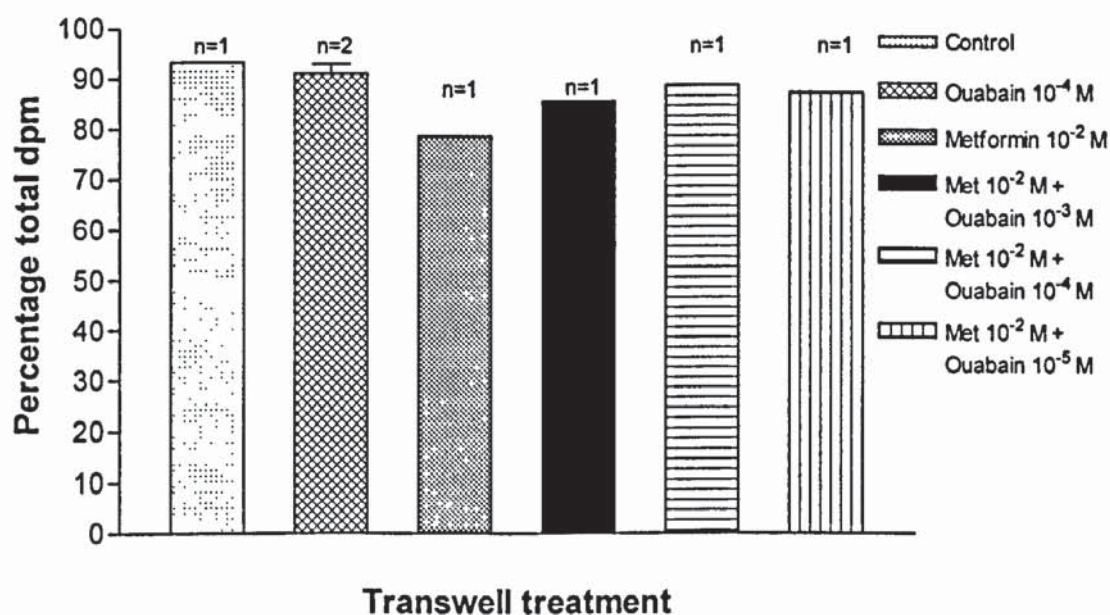


Figure 4.5.1: Effect of metformin (10^{-2} M) and ouabain (10^{-5} – 10^{-3} M), alone and in combination, at 24h on the flux of ^3H mannitol from the apical chamber across Caco-2 monolayers cultured on polyester membranes of transwell culture plates. Data are expressed as percentage total dpm and represent the percentage dpm remaining in the apical compartment. Values where appropriate are means \pm SEM.

**Basolateral chamber ^3H mannitol content
following 24h incubation.**

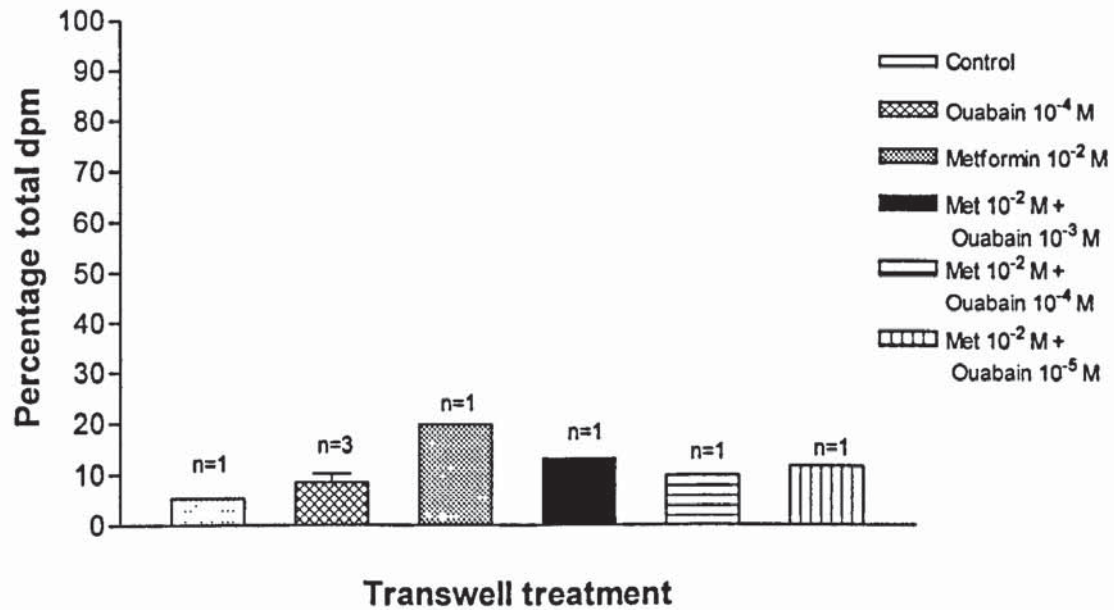


Figure 4.5.2: Effect of metformin (10^{-2} M) and ouabain (10^{-5} – 10^{-3} M), alone and in combination, at 24h on the flux of ^3H mannitol into the basolateral chamber across Caco-2 monolayers cultured on polyester membranes of transwell culture plates. Data are expressed as percentage total dpm and represent the percentage dpm remaining in the basolateral compartment. Values where appropriate are means \pm SEM.

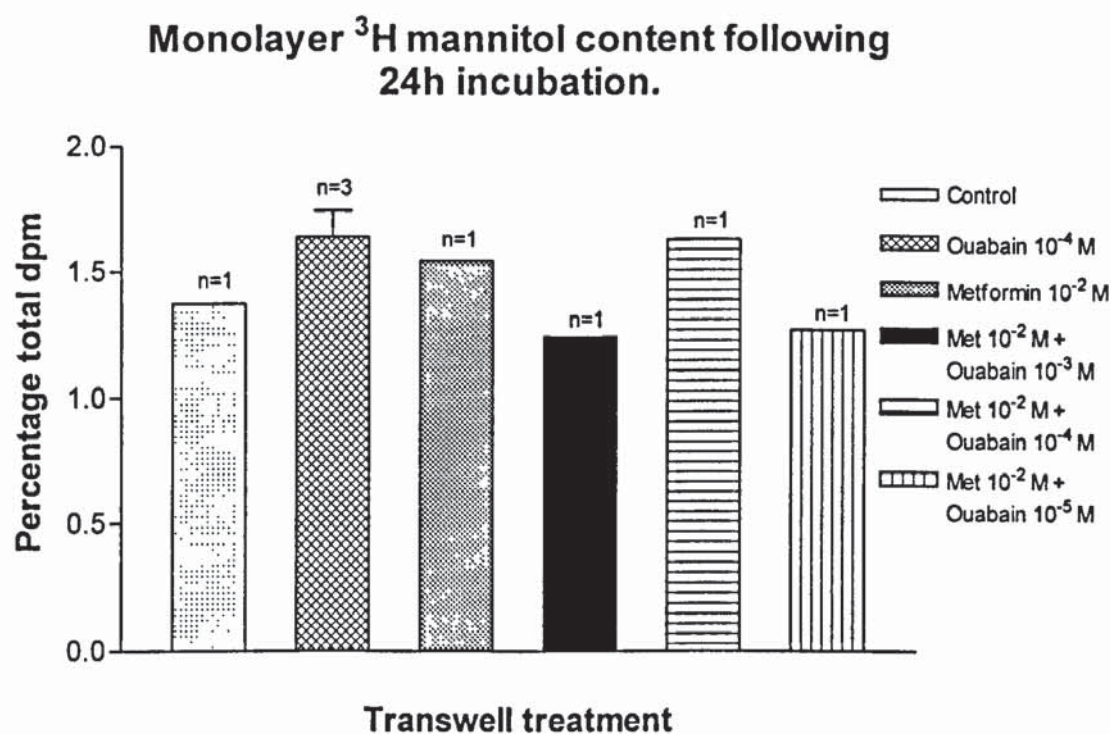


Figure 4.5.3: Effect of metformin (10^{-2} M) and ouabain (10^{-5} – 10^{-3} M), alone and in combination, at 24h on the percentage ^3H mannitol within the cell monolayer of Caco-2 cells cultured on polyester membranes of transwell culture plates. Data are expressed as percentage total dpm. Values where appropriate are means \pm SEM.

**Apical chamber ^{14}C D-glucose content
following 24h incubation.**

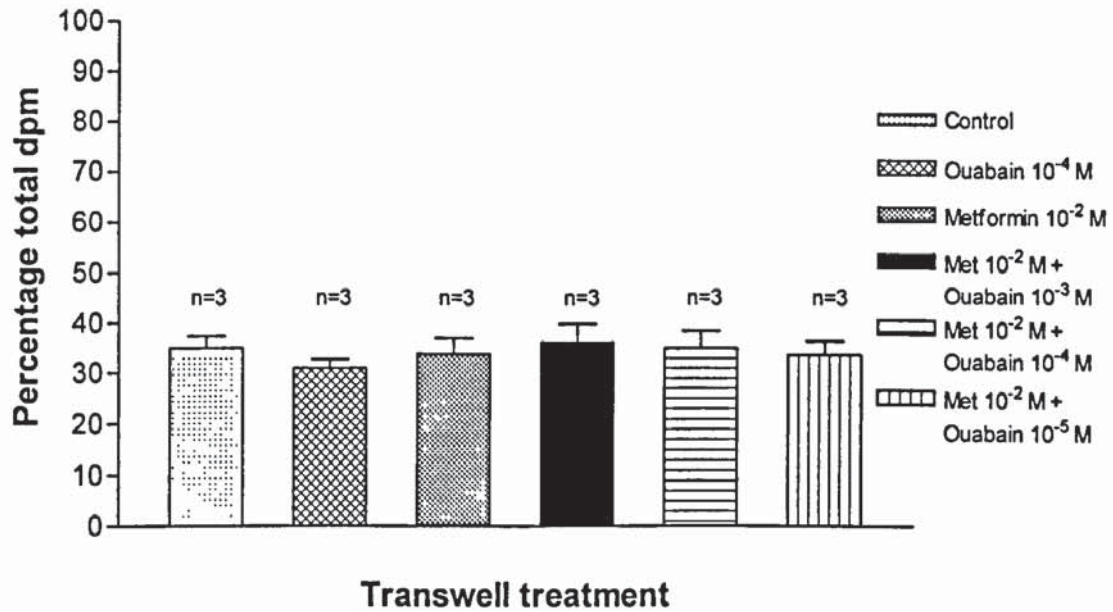


Figure 4.5.4: Effect of metformin (10^{-2} M) and ouabain ($10^{-5} - 10^{-3}$ M), alone and in combination, at 24h on the transfer of ^{14}C D-glucose from the apical chamber across Caco-2 monolayers cultured on polyester membranes of transwell culture plates. Data are expressed as percentage total dpm and represent the percentage dpm remaining in the apical compartment. Values are means \pm SEM.

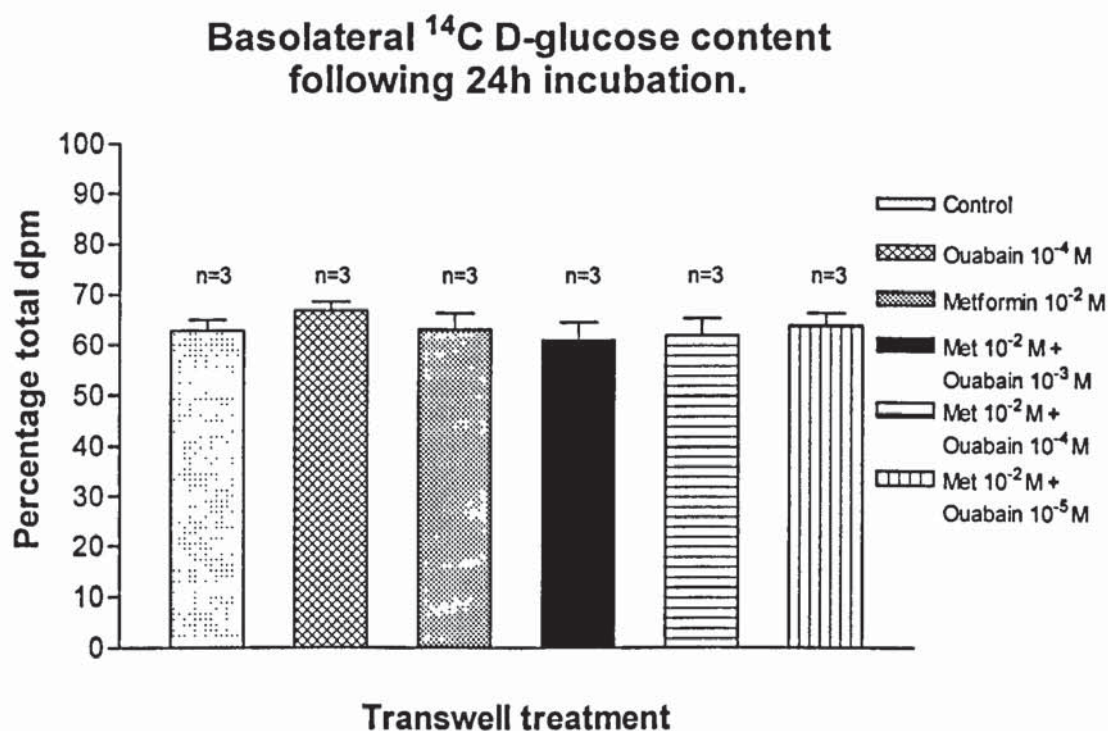


Figure 4.5.5: Effect of metformin (10^{-2} M) and ouabain (10^{-5} – 10^{-3} M), alone and in combination, at 24h on the transfer of ^{14}C D-glucose into the basolateral chamber across Caco-2 monolayers cultured on polyester membranes of transwell culture plates. Data are expressed as percentage total dpm and represent the percentage dpm remaining in the basolateral compartment. Values are means \pm SEM.

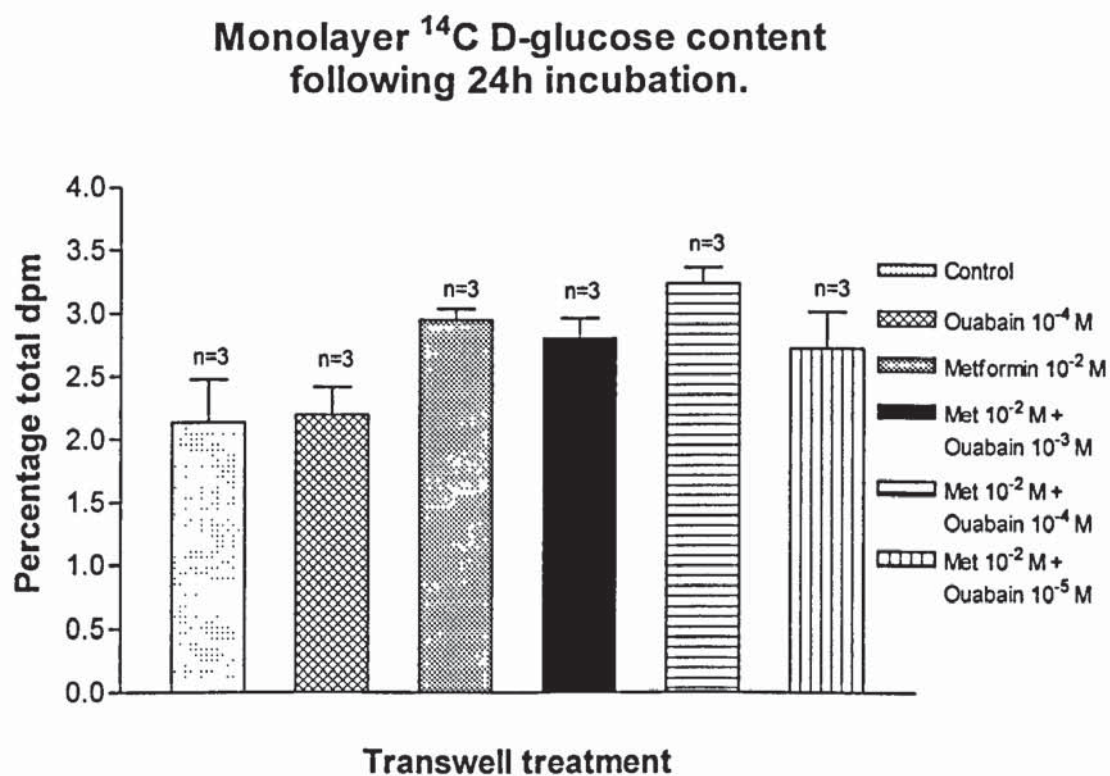


Figure 4.5.6: Effect of metformin (10^{-2} M) and ouabain (10^{-5} – 10^{-3} M), alone and in combination, at 24h on the percentage ^{14}C D-glucose within the cell monolayer of Caco-2 cells cultured on polyester membranes of transwell culture plates. Data are expressed as percentage total dpm. Values are means \pm SEM.

4.3 Discussion:

The experiments performed herein conclusively demonstrate that bile salt transport is energy-dependent, unidirectional, and sodium-dependent. It is also apparent that metformin and ouabain significantly reduce bile salt transport, supporting the *in vivo* observations in chapter 3. When metformin and ouabain were simultaneously incubated, an additive inhibitory effect was seen. Glucose transport, also an energy-dependent transport system, was not inhibited by either metformin or ouabain at the concentrations tested. It is important to note the inhibitory effect of metformin upon bile salt transport, confirming the functional similarities of the Caco-2 model to ileal enterocytes. The presence of mannitol as a non-transportable marker, and its high rate of flux following drug treatment, draws attention to the possibility that such drugs may have influenced membrane integrity. This may be the consequence of a toxic drug effect, alternatively, an effect on the tight junctions of Caco-2 cells.

Metformin at 10^{-2} M resulted in a substantial diminution in the ability of the Caco-2 membrane preparation to prevent mannitol flux (figure 4.2.2). However, metformin in the same instance significantly inhibited bile salt transfer (figure 4.2.5). When metformin and ouabain (10^{-3} M) were incubated simultaneously (4.2.2 and 4.2.5), a comparable effect was evident upon mannitol and bile salt transport, as seen in earlier experiments (4.1.2 and 4.1.5). These results imply that a membrane effect is a consequence of both metformin and ouabain treatment; the origin of this effect is presently unknown.

An attractive hypothesis relating to increased mannitol flux across membrane preparations lies with cellular tight junctions. It is possible that metformin could affect these structures, since metformin is absorbed via the paracellular route, as indicated by its site of accumulation (Nicklin *et al.*, 1996). The extent of metformin's effects in this region might permit mannitol flux. Metformin's effects do not appear, however, to permit the transfer of bile salts. Nevertheless, if this effect were reproducible *in vivo* and if the untransported bile salts were to impose a sufficient osmotic gradient, water flux into the distal intestinal lumen could result, possibly contributing to the diarrhoea that is often associated with higher doses of metformin. Indeed, results from the everted intestinal sac studies (chapter 3), whilst not proving an ideal model for studying metformin's effects on bile salt transport, clearly demonstrated an osmotic effect in the presence of this drug. This was characterised by reduced fluid uptake from the mucosal surface into the serosal compartment of the ileum.

The question of whether metformin influences tight junction resistance may be approached by transepithelial resistance measurements. This approach offers a means of determining the state of cell monolayers in terms of their membrane resistance. In a study by Gan *et al.* (1998), apical to basolateral mannitol transfer in Caco-2 cell monolayers was inhibited threefold by the presence of a compound known to increase transepithelial resistance in such cells (ranitidine). This compound also inhibited its own absorption as a consequence of its membrane resistance effects. These results are in direct opposition to those obtained for mannitol transfer in our studies, and as such imply that increased transepithelial resistance via tight junction modulation did not occur. An effect of bile salts

themselves upon membrane integrity can be ruled out, since approximately 85% of mannitol remained in the apical chamber of monolayers incubated with both labelled and unlabelled bile salts. In the absence of unlabelled bile salt, mannitol retention in the apical compartment increased to over 90% (4.3.2).

Tight junctions function to prevent the diffusion or back-diffusion of substances through the intercellular space (Cereijido *et al.*, 1998). Such structures connect adjacent cells at the apical surface and function as semi-permeable diffusion barriers (Balda and Matter, 1998). It is not my intention to describe in detail the assembly and components of these tight junctions, since further experimentation would need to be performed to identify whether such proteins are subject to modulation by metformin. Nevertheless, the primary function of tight junctions will be discussed briefly along with their modulation by nutritional factors.

The pore size of tight junctions has not been fully established, possibly because the size of such structures may vary during different physiological states, such as during digestion and peristaltic movements. Indeed, pore size has been reported to vary over a wide range. Intestinal epithelia are reported to exhibit a pore radius of between 30-40 Å (Wild *et al.*, 1997). These pores permit the transfer of small solutes and water via the paracellular route and may account for 85% of ion flow in the small intestine. They are also a route for the transfer of certain low molecular weight substances. However, as detailed by Hofmann and Mysels (1988), bile salt molecules possess a diameter of 20 and 7 Å whereas paracellular channels in the proximal small intestine possess pores with a size of 4-8Å, thereby preventing the passive absorption of bile salts.

Tight junctions are connected to the cell cytoskeleton and it is via this network of proteins that tight junction resistance may be influenced. Modulation of the cell cytoskeleton may be achieved by intracellular signals such as PKC, calmodulin, G-proteins and phospholipase C (PLC). Calcium is believed to be important in the formation and maintenance of these structures (Wild *et al.*, 1997). As stated, modulation of tight junctions can be achieved by nutrients such as glucose. The concentration of glucose encountered during a meal can alter the permeability of tight junctions, inducing dilation (Wild *et al.*, 1997). Following activation of sodium-linked nutrient transporters, such as for glucose, dilations of tight junctions occur allowing increased flux of solutes along the paracellular pathway (Turner and Madara, 1995).

Under normal circumstances, the presence of tight junctions limits the flux of D-mannitol across epithelial cells via the paracellular route. In the presence of sodium and glucose, such markers are apparently cleared from the lumen more rapidly possibly via a solvent drag pathway (Turner and Madara, 1995). However, the concentrations of glucose required to permit substantial solvent drag are unphysiological. Nevertheless, as detailed by the above authors, permeability changes in tight junctions are associated with alterations in the cell cytoskeleton and may be linked to the phosphorylated state of myosin light chain (MLC). The phosphorylation of MLC is modulated by the actions of myosin light chain kinase (MLCK) and myosin light chain phosphatase (MLCP). Intracellular calcium levels may regulate the actions of these enzymes; this is discussed in more detail in chapter 5.

A hypothesis proposed by Turner and Madara (1995) involves the activation of MLCK by calcium following sodium-linked nutrient transport, leading to an increase in tight junction permeability. Studies in vascular smooth muscle cells presented herein (chapter 5), demonstrate that metformin is associated with enhanced contractile and relaxant responses to noradrenaline (NA) and acetylcholine (Ach), respectively. These metabolic processes are highly sensitive to the levels of intracellular calcium. Metformin may influence smooth muscle contractility through intracellular calcium levels or second messenger systems (see chapter 5); a similar drug-dependent effect may function to modulate tight junctions. Evidence exists indicating increased calcium levels in the intestinal epithelium may be due to stretch-activated calcium channels (Chrisyensen, 1987). If this effect occurs *in vivo* then increased calcium levels may result in increased tight junction permeability. This may be linked to the extent of nutrient cell swelling as a consequence of nutrient-induced osmotic load.

Tight junctions may be sensitive to changes in pressure and volume in the intercellular space, as detailed by Wild *et al.* (1997). Increased intercellular pressure and volume may result from increased permeability of tight junctions. According to Wild *et al.* (1997), this would lead to increased backflux of salt and water if the driving forces were favourable, leading to net loss of sodium chloride, and water transport across the epithelium. Thus, tentatively, one possible mechanism through which metformin could influence bile salt transport in the ileum is by influencing the permeability of tight junctions. Evidence exists demonstrating these structures can be modulated by luminally absorbed nutrients

such as glucose. It seems feasible that metformin's reported effects on membrane fluidity, active transport systems, or its vasoprotective effects (the origins of which are currently unknown but may be achieved through second messengers), may influence tight junction permeability. Equally, metformin may inhibit bile salt transport through specific effects upon the bile salt transporter or the enzyme systems regulating its activity.

If metformin is shown to increase membrane permeability to nutrient flux, this may have implications clinically in the absorption of nutrients such as fat-soluble vitamins and other drugs absorbed via the paracellular route. However, it is unlikely that metformin's effects upon intestinal permeability would be sufficient to significantly impair fat-soluble vitamin absorption, partly due to their site of absorption (across brush-border membranes) and partly due to the jejunal uptake mechanism. Indeed, a significant proportion of bile salt uptake may occur in the jejunal region together with the absorption of fat digestion products and fat-soluble vitamins. Hypotheses relating to metformin's sites and mode(s) of action are presented in more detail in chapter 6.

Caco-2 cells thus provide an excellent model for studying active intestinal transport systems since they are structurally and functionally similar to intestinal ileocytes. However, the Caco-2 model does not provide information relevant to the jejunal effect of metformin (to enhance transfer of bile salts) since passive transport systems in Caco-2 cells appear to be lacking. To date a characterised jejunal cell line is not currently available for such study.

Chapter Five:

The Effect of Metformin and Cholesterol on the Compliance of Aortic Smooth Muscle

CHAPTER FIVE: The Effect of Metformin and Cholesterol on the Compliance of Aortic Smooth Muscle

5.1 Introduction:

Type 2 diabetes is strongly associated with premature vascular mortality; deaths related to coronary heart disease (CHD) are as much as four times higher amongst the diabetic population than in non-diabetics (Standl, 1999). It is believed diabetic dyslipidaemia plays a crucial role in the progression of this complication. Hyperglycaemia, hyperinsulinaemia, and insulin resistance are also believed to contribute (Standl, 1999). Risk factors for atherosclerosis, such as high blood pressure and smoking, have also been identified for non-diabetic individuals. It is, however, the cumulative effect of these factors together with susceptibility of individuals towards the diabetic metabolic profile, which renders the individual at high risk of vascular morbidity and mortality.

5.1.1 Smooth Muscle:

Vascular smooth muscle together with the endothelial cell layer is involved in maintaining the delicate balance of tonicity within the vascular system. Under normal conditions, these two systems operate effectively in the maintenance of blood pressure and flow. In the diabetic individual it is now generally accepted that the normal function of vascular smooth muscle and/or the endothelium becomes severely impaired, particularly during atherosclerosis (Drouet, 1999). Vascular smooth muscle is autonomically controlled by sympathetic inputs. In

order to understand the possible functional defects of this tissue in diabetes, it is important to understand how the tissue is structurally composed, and, additionally, how the vascular smooth muscle contributes to the overall function of the vessel.

Major arteries, such as thoracic aorta used in the studies herein, must by nature be compliant to the demands of the cardiovascular system. Such vessels achieve this through the presence of elastin and collagen fibres. The ability of the tissue to contract or relax in response to stimuli is essential in the maintenance of arterial tone. Endothelial cells line the lumen of the artery and are continuous with this structure. Separating the endothelium and the smooth muscle are several layers termed the media and adventitia. The smooth muscle forms the outermost layer and is controlled by sympathetic innervation (although innervation may be poor for the thoracic aorta), leading to the release of noradrenaline (NA), and thus contraction (Hirst and Edwards, 1989). The endothelium also promotes relaxation and/or contraction. Thus, there exists a state of constant innervation from both tissues resulting in the precise control of vascular tone (Cocks, 1996).

In a review by Chen *et al.* (1988), both haemoglobin and methylene blue were found to increase the resting tension of smooth muscle in rat aorta. This effect was more pronounced during contractions induced by NA, and suggests that NA stimulated the release of endothelium-derived relaxing factor (EDRF) and that this factor was spontaneously released during resting conditions (Chen *et al.*, 1988).

5.1.2 Endothelium:

The continuous endothelial monolayer lining the vascular lumen is functionally very diverse, contributing to the maintenance of vascular tonicity and to the fluidity of blood (Baron and Quon, 1999). In addition, it is believed the endothelium plays important roles in the secretion of hormones, which in turn influence vascular tone and endothelial regeneration and modification. (Moncada and Higgs, 1993; Baron and Quon, 1999). Endothelial cells release a variety of substances that modulate vascular function. The most renowned is EDRF, endothelium-derived hyperpolarising factor (EDHF), and endothelin itself. These substances make significant contributions to the long-term viability of the vasculature and will now be briefly discussed.

The relaxation response of isolated arteries *in vitro* can be demonstrated by a number of agents. One agent in particular is used repeatedly to demonstrate this effect, and was indeed the agent of choice in the current studies. Acetylcholine (Ach) acts via its muscarinic receptor to bring about a relaxation of vascular smooth muscle. Muscarinic Ach receptors exist on both smooth muscle and the endothelium (Goyal, 1989; Furchgott, 1984), enabling the generation of either a contractile or relaxant response. This is dependent most probably upon the affinity of the agent for its receptor, receptor number, and possibly the local concentration of the drug. Thus, once the organ has been dissected from the animal and prepared experimentally in an organ bath containing a suitable salt solution, Ach can be used to elicit a relaxation of the vessel following contraction with an agent such as NA.

It is now widely accepted that the endothelial cell layer must be present and functional in order to bring about relaxation in response to Ach (Chen and Cheung, 1992). Relaxation is believed to result from the generation of a diffusible substance from the endothelial cell layer, believed to be nitric oxide (NO) or another local signal (Ignarro *et al.*, 1987). Moncada and Higgs (1993) suggest the actions of nitric oxide synthase enzymes (NOS) upon the amino acid L-arginine are essential for the formation of this compound. There is some dispute as to whether NO is the only EDRF and whether NO exists exclusively in all vascular beds, since Garland and McPherson (1992) noted in the rat mesenteric artery that NO played no apparent role in the endothelium-dependent relaxation in response to Ach.

The relaxation response to Ach is generated by the endothelial production of NO, which diffuses from the endothelial cell layer and directly activates the soluble form of guanylate cyclase in smooth muscle by interacting with its available haem group (Busse, 1987; Förstermann *et al.*, 1986). Stimulation of guanylate cyclase results in vascular relaxation via increased cyclic GMP (cGMP) activation from GTP (Waldman and Murad, 1988). The concentration of this second messenger (cGMP) has been shown to increase in a time-dependent and concentration-dependent manner. This increment in the levels of cGMP in response to Ach has been observed prior to the relaxation response (reviewed by Ignarro and Kadowitz, 1985).

The precise mechanism by which cGMP relaxes vascular smooth muscle is poorly understood. According to the review by Ignarro and Kadowitz (1985),

cGMP directly relaxes vascular smooth muscle. Indeed, activators of guanylate cyclase have been shown to stimulate cGMP-dependent protein kinase (Rapoport *et al.*, 1982; Lincoln, 1983). Furthermore, cGMP may induce relaxation through its effect on calcium metabolism within the smooth muscle cell. This effect is possibly limited to a lowering of intracellular calcium levels (Ignarro and Kadowitz, 1985) or modulating the activity of calcium sensitive second messengers.

5.1.3 Hyperpolarisation:

Acetylcholine, as well as inducing direct relaxation of vascular smooth muscle, also causes membrane hyperpolarisation, in certain arteries, prior to the onset of relaxation (Chen *et al.*, 1988). This has been demonstrated in isolated arteries of several species, including rat, following contraction with agents such as NA (Taylor *et al.*, 1988).

As with EDRF, believed to be NO, it appears that a functional endothelial cell layer is required for the release of this hyperpolarising factor, suggesting an endothelial-derived factor (Furchgott and Zawadzki, 1980). Controversy surrounded these findings, since Chen *et al.* (1988), provided evidence that certain substances were able to relax vascular smooth muscle without causing membrane hyperpolarisation. This ultimately led to the supposition that several factors may be released from the endothelial cell layer influencing vascular smooth muscle reactivity. Further evidence supported the theory of distinct factors mediating relaxation and hyperpolarisation. According to Chen and Cheung (1992), cGMP production and vasodilation itself can be blocked using

haemoglobin and methylene blue. However, these same agents had no effect upon membrane hyperpolarisation.

Methylene blue is known to block the endothelium-dependent relaxation response (Furchgott, 1984) and haemoglobin also abolishes Ach-induced endothelium-dependent vasodilations. Both of these agents may achieve this through specific interaction with NO (Martin *et al.*, 1985). The presence of these blocking agents in rat aorta and pulmonary artery inhibited relaxation whilst the hyperpolarisation induced by Ach remained unaffected (Chen *et al.*, 1988).

Furthermore, it was determined that the hyperpolarisation induced by Ach reflects alterations in potassium conductance across the cell membrane of smooth muscle (Chen *et al.*, 1988). This hyperpolarisation is short-lived compared to the response to NO and the two factors appear to be released following stimulation of different receptors. According to Chen *et al.* (1988), M₁ receptors appear to mediate the release of EDHF in response to Ach, whereas M₂ receptors are involved in the release of EDRF. The sulphonylurea glibenclamide is capable, in certain mesenteric arteries, of blocking NO-induced hyperpolarisation, but not the hyperpolarisation induced by Ach (Garland and McPherson, 1992). Thus the hyperpolarisation response in some arteries may involve K⁺ channels (Parkington *et al.*, 1995; Plane *et al.*, 1995).

Current evidence indicates that NO may play a significant role in the maintenance of vascular tone in large arteries such as thoracic aorta, whereas EDHF may play a significant role in tonicity in smaller resistance arteries.

Indeed, Hwa *et al.* (1994) reported a NO-dependent effect during Ach-induced relaxation of rat superior mesenteric artery, whereas the relaxation response in mesenteric resistance arteries was resistant to inhibitors of NO. Thus, it would appear from these studies that the role of NO in large vessel relaxation is well established. However, the method by which relaxation occurs in resistance arteries is still open to some debate. It may be that a mechanism requiring heavy involvement of EDHF persists in these smaller arteries.

As stated at the beginning of this chapter, sympathetic inputs at the level of smooth muscle leads to persistent release of NA, promoting continual basal contraction (Hirst and Edwards, 1989). In response, it seems the endothelium also releases relaxing factors, striking a balance that moderates vascular tone. Thus, it would logically follow that if EDHF was the predominant pathway for relaxation in smaller arteries, constant innervation from this pathway may exist. Indeed, a parallel pathway controlling relaxation has been hypothesised. In studies supporting this hypothesis, NO played the principal role in relaxation in porcine coronary artery. A second mechanism, potassium-sensitive also appeared to contribute to the relaxation (Nagao and Vanhoutte, 1992). This system, seen as a 'failsafe', could generate over 60% relaxation if the NO pathway failed (Kilpatrick and Cocks, 1994). The question remains as to why would a back-up system for the NO pathway exist. Has evolution adapted specifically a dual-signalling pathway to regulate vascular tone? If EDHF is the predominant or only mechanism to achieve relaxation in resistance arteries, its protracted hyperpolarisation effect could possibly lower resistance in these arteries.

A hypothesis has been suggested for the hyperpolarisation effect specifically in resistance arteries, and may involve relaxation of smooth muscle by reducing the influx of calcium through voltage-gated channels (Garland *et al.*, 1995). The reduced calcium influx, together with increased efflux of intracellular potassium, would lead to lowered intracellular calcium concentrations and movement of the membrane potential away from the contraction threshold respectively. Thus, the concept of dual innervation is certainly plausible and stems from the presence of M₁ and M₂ receptors on functional endothelium (Komori and Suzuki, 1987).

Recently, studies have been performed on blood vessels from endothelial nitric oxide synthase knockout mice (Chataigneau *et al.*, 1999). These authors reported increases in vascular resistance and blood pressure following chronic inhibition of nitric oxide synthase (NOS). If the endothelial isoform of NOS was specifically inhibited (eNOS), an increase in systemic blood pressure also ensued. The above authors reported that the relaxation induced by Ach was abolished in mice expressing the eNOS gene when NOS activity was inhibited, implying that NO is the predominant endothelium-derived relaxing factor. Ach-induced relaxations were found not to occur in eNOS deficient mice, supporting conclusions regarding the role of NO in large vessel relaxation. Interestingly, an EDHF response was not identified in murine coronary arteries (Félétou and Vanhoutte, 1996).

5.1.4 Endothelin:

Endothelin is a peptide, and one of several factors released by endothelial cells. There are three forms of endothelin, ET-1, ET-2, and ET-3 (known as rat

endothelin) (Inoue *et al.*, 1989; Yanagisawa *et al.*, 1988a). As reviewed by Hopfner and Gopalakrishnan (1999), endothelial cells are known to release ET-1, mainly towards the luminal surface which influences vasodilation via the ET_B receptor.

Endothelin receptors are G-protein linked and are termed ET_A and ET_B. Hopfner and Gopalakrishnan (1999) consider the primary effect of ET-1 is to cause dilation of the vessel followed by a slower and more protracted contraction. However, as in the case of NO, different vascular beds may express either of the endothelin receptors preferentially. Thus, endothelin released by the endothelium can oppose the actions of factors such as EDRF, contributing to the maintenance of vascular tone. Yanagisawa *et al.* (1988b) demonstrated a calcium-dependence for the contractile response induced by endothelin. The contractile response is long lasting and in isolated vessels is difficult to attenuate, even with repeated washings.

Endothelin is mentioned here since, in the present studies, following contraction with NA and subsequent relaxation with Ach, a marked contractile response occurred often above the initial levels induced by NA alone. This effect is believed to be the consequence of endothelin release and is a 'natural' response to the rapid change in the mitogenic activity of the smooth muscle.

The normal circulating concentration of endothelin is typically low (1-5pmol and rarely surpasses 25pmol) even in disease states (Hopfner and Gopalakrishnan, 1999). In type 2 diabetes, conflicting data are available regarding circulating levels of endothelin. However, in states where levels are raised, good metabolic

control imposes a correctional effect (Hopfner *et al.*, 1998). Kita *et al.* (1998) reported that a dose of ET-1, below that normally associated with an effect (3×10^{-10} M), significantly increased the contractile response in normotensive rat mesenteric arteries contracted with NA. This effect was attributed solely to the ET_B subunit. Thus, when we consider the potency of endothelin, the fact that in certain disease states, such as diabetes, circulating levels may be raised, and that different vascular beds may have a differing affinity for the peptide. The suggestion by Kita *et al.* (1998) that endothelin may play a significant role in various disease states encountered in syndrome X, including hypertension and vasospasm, seem plausible.

Endothelin has been found to activate phospholipase C (PLC) in cultured vascular smooth muscle, which ultimately leads to the activation of the phosphoinositol pathway (Resink *et al.*, 1988; Sugiura *et al.*, 1989; Van Renterghem *et al.*, 1989). The inositol pathway and its role in vascular smooth muscle contraction will be discussed in more detail later in this chapter.

It is apparent that the endothelium plays a significant role in maintenance of vascular tone. The endothelium not only influences its own functioning but that also of neighbouring vascular smooth muscle, through its various secreted factors. We have concentrated in some detail on the factors released by the endothelium, since in diseases such as diabetes the balance of these factors may become disrupted. In states of diabetes there are commonly many conditions, such as hypertension, the aetiology of which may be attributed to disturbances in

the vasculature. The impact of insulin and diabetes on the normal functioning of the vascular system will now be briefly discussed.

5.2 How Diabetes and its Associated Conditions Affect Vascular Function.

Hyperinsulinaemia and insulin resistance are commonly expressed in the pathogenesis of type 2 diabetes. Insulin, under normal conditions, is involved in many metabolic functions. In lipoprotein metabolism, it is essential in the normal functioning of LPL (Bagdade, 1997). In addition, it is important in normal LDL metabolism (Chait *et al.*, 1979). The frequently encountered conditions of hyperinsulinaemia and insulin resistance in the diabetic profile may impose themselves as major risk factors for cardiovascular disease (Stout, 1990).

Insulin contributes, via the production of NO, to vasodilation (Scherrer *et al.*, 1994). Insulin has been shown to increase leg blood flow in non-insulin resistant subjects (Baron, 1994). However, the ability of insulin to increase blood flow in muscle in conditions such as NIDDM was severely impaired (Baron, 1994).

Vasodilation in response to insulin is severely attenuated in NIDDM patients (Laakso *et al.*, 1992), and appears also to be linked with the degree of obesity. Since obesity is strongly associated with type 2 diabetes, then diabetes and/or obesity may lead to the predisposition of impaired vascular reactivity to insulin. In support of this hypothesis, Westerbacka *et al.* (1999) reported that insulin decreased arterial stiffness in non-obese individuals, whereas in obesity the ability of insulin to induce the same effect was severely reduced.

Baron and Brechtel (1993) conclude that since the vasodilation response to insulin is impaired in insulin resistant subjects, this may reflect a defect in endothelial function, possibly at the level of NO synthesis or release. In a separate study, subjects with insulin resistance exhibited a lower level of NO production than in insulin-sensitive subjects (Steinberg *et al.*, 1997).

Endothelial cells express receptors for insulin (Baron and Quon, 1999). According to King and Johnson (1985), such receptors function to transport insulin to target tissues via the endothelial cell layer. Although not principally involved in glucose transport, since they do not express GLUT 4 transporters, endothelial cells may take up insulin to regulate NO synthesis in some way.

Studies by Zeng and Quon (1996) determined that insulin could stimulate an increase in NO production in a dose-dependent manner, and significantly quicker than insulin could impose its vasodilatory actions (Laakso *et al.*, 1990; Baron, 1994). As suggested by Baron and Quon (1999), this time difference in insulin's actions between *in vivo* and *in vitro* preparations may reflect additional effects of this hormone on vascular tissue. The ability of insulin to stimulate glucose uptake occurs over a period of hours, and according to the above authors is linked with vasodilation, possibly accounting for its protracted effects *in vivo*.

A potential mechanism for vasodilation induced by insulin was proposed by Baron (1994), whereby insulin may induce relaxation via hyperpolarisation and by reducing calcium influx. Alternatively, insulin may influence the functioning of Ca^{2+} -ATPase transporters, since this transporter plays a significant role in

intracellular calcium efflux. The expression of such transporters may be reduced in animal models of obesity (Baron, 1994). The obvious end point of a defect in this transporter would be heightened intracellular concentrations of calcium, and presumably contractility.

As discussed in chapter 1, dyslipidaemia plays a significant role in the development of vascular disease. Hypertriglyceridaemia is the most common form of dyslipidaemia and is associated with increased levels of IDL, VLDL, and LDL particles (Standl, 1999). The altered lipid profile frequently evident in type 2 diabetes has important implications in vascular function. Dyslipidaemia is a positive risk factor for CHD, predisposing the diabetic individual to a significantly greater risk of mortality. Andrews *et al.* (1987) demonstrated an effect of LDL on reducing EDRF-induced relaxations. In addition, native LDL, at high concentrations, and modified LDL, may repress endothelium-dependent relaxation (Jacobs *et al.*, 1990). NO-induced relaxation was also inhibited by LDL at concentrations comparable to hypercholesterolaemia.

Various proposals have been suggested as to how oxidised LDL may inhibit these NO-dependent relaxations; including, interaction of oxidised LDL directly with NO leading to its inactivation (Galle *et al.*, 1991; Chin *et al.*, 1992). Alternative proposals include an alteration in the activity of the NO released (Myers *et al.*, 1994). Liao *et al.* (1995) also demonstrated an effect of oxidised LDL in reducing the expression of NOS mRNA levels. Despite these numerous hypotheses, the precise mode of action of oxidised LDL upon vascular reactivity is presently not yet known.

As well as influencing relaxation responses, oxidised LDL molecules have been shown to increase the responsiveness of blood vessels to various agonists, demonstrated by an increased contractile response (Galle *et al.*, 1990). Unlike previous reports (Jacobs *et al.*, 1990), Galle *et al.* (1990) found no such effect with native LDL. Furthermore, ET-1 release may be increased in endothelial cells exposed to oxidised LDL (Boulanger *et al.*, 1992). This provides evidence of an additional mechanism whereby vascular tissue may be preferentially 'primed' to respond to contractile stimuli.

Hypercholesterolaemia is a major risk factor for atherosclerotic vascular disease. According to Steinberg *et al.* (1989), the genesis of atherosclerotic disease is positively associated with elevated levels of LDL. The artificially elevated levels of this lipoprotein and others in diabetes may lead to the accumulation of cholesterol in the arterial wall, as detailed in chapter 1.

As reviewed by Cox and Cohen (1996), major constituents of the vascular wall, including endothelial cells, have been shown to induce LDL modification to such an extent that uptake via the scavenger receptor can occur. Smooth muscle cells have also demonstrated an ability to modify LDL (Cox and Cohen, 1996), thereby contributing to the process of atherogenesis. This process is covered in more detail in the introductory chapter of this thesis.

Oxidised LDL has been found to influence several metabolic pathways and may indicate a role in its ability to modify vascular function. Kugiyama *et al.* (1992) reported activation of PKC in human endothelial cells. In addition, inhibition of

endothelium-dependent relaxation and the mobilisation of calcium by oxidised LDL were blocked by PKC inhibitors (Ohgushi *et al.*, 1993). Oxidised LDL may, alternatively, influence the activity of G-proteins. Indeed, down-regulation of the G_I subunit and a reduction in the activity of GTPase enzyme by oxidised LDL has been reported (Liao and Clark, 1995). In addition, the generation of reactive oxygen species is well known to result in damage to cellular processes (Rubanyi, 1988). NO has previously been shown to be directly inactivated by superoxide anion (Gryglewski *et al.*, 1986), as has Ach-induced relaxation (Seccombe *et al.*, 1994).

Substantial evidence exists linking oxidised LDL with vascular dysfunction independently of diabetes. Endothelial cells are known to express the receptor that recognises acetylated LDL and thus may play an active role in the uptake of the modified lipoprotein (Stein and Stein, 1980; Voyta *et al.*, 1984). Although LDL oxidation is a serious issue independent of diabetes, it is often evident in overt type 2 diabetes. This lipoprotein fraction plays a role in dyslipidaemia and hypercholesterolaemia contributing to accelerated atheroma formation.

Type 2 diabetics often exhibit a range of abnormalities in parameters such as lipids. Whatever the aetiology of the condition, it makes a major contribution to the elevated mortality levels of diabetes. Although the following paragraphs are related to diabetes specifically, this is the term attributed to the overall condition and in no way attempts to explain the origins of the vascular dysfunction evident in this condition.

Altan *et al.* (1989) reported that in type 2 diabetic rats' relaxation to Ach was significantly reduced. In addition, the vascular response to agonists, such as NA, is reportedly heightened in diabetic patients (Hogikyan *et al.*, 1999). Indeed, Hogikyan *et al.* (1999) provides evidence for increased constriction of forearm arteries in response to NA in type 2 diabetics. Results from these studies suggested an overall enhancement in arterial tone in these subjects, and may have implications in hypertension in diabetes.

Vascular dysfunction is evident in additional studies, and endothelial cells have been implicated in this phenomenon (Cohen, 1993). Endothelial cell dysfunction may be a consequence of hyperglycaemia due to diversion of metabolism of glucose via alternative pathways (Gonzalez *et al.*, 1986; Gonzalez *et al.*, 1984). The rampant hyperglycaemia characteristically present in diabetes may also influence vascular function via the formation of advanced glycosylation end products (AGE). Such end products have been shown to influence the activity of NO, as detailed by Cohen (1993), and thus may subsequently alter responses from vascular tissue. In response to such hypotheses, Soulis *et al.* (1999) reported vascular hypertrophy in diabetes could be reduced by inhibiting the formation of these AGEs. Since blood glucose concentrations were not monitored in the present studies, the effect of glycaemia upon vascular reactivity cannot be quantified and will not be discussed further.

As mentioned in the context of oxidised lipoproteins, reactive oxidative species have been found to profoundly influence the activity of the vasculature. Pieper *et al.* (1997) provide evidence for such reactive species in endothelial cell

dysfunction. As stated previously, and according to Pieper *et al.* (1997), NO may become inactivated in the presence of $\cdot\text{O}_2^-$; this in turn caused the contraction of vascular smooth muscle. Hydroxyl radicals are also believed to potentiate this effect; several authors have reported increased production of these reactive species in some diabetic animal models, as reviewed by Pieper *et al.* (1997).

5.3 Atherosclerosis:

Mortality rates linked to CHD increase dramatically in the diabetic population (Jarrett, 1989). In a recent review, evidence is provided for up to 80% of diabetic-related deaths being attributed to CHD (Laakso and Lehto, 1997). CHD is by nature a progressive disease whose roots may be traced to adolescence. However, diabetes is positively correlated with such disease and the diabetic profile certainly exacerbates the condition. Those risk factors associated with diabetes and positively correlated with CHD were covered previously in chapter 1.

Gross macroscopic changes can occur in the wall of vascular tissue in CHD, leading to occlusion of the luminal space. However, subtle changes also occur within vascular tissue and may include increased vessel calcification or the formation of AGEs (Laakso and Lehto, 1997). Such changes may occur prior to gross changes in vessel morphology, and include calcification of the medial layer of arterial tissue leading to a loss of vessel elasticity. Occlusion of the vessel lumen does not occur under these circumstances, and may represent an early stage in the degenerative vascular process.

The glycation of proteins, such as collagen, is believed to play an important role in exacerbating the progression of atherosclerosis, as discussed in chapter 1

(Brownlee *et al.*, 1985). In addition, prolonged hyperglycaemia may adversely affect a variety of haemostatic factors, rendering individuals susceptible to CHD. In particular, increased levels of PAI-1 and von Willebrand factor have been identified in NIDDM patients (Laakso and Lehto, 1997). A recent review by Jokl and Colwell (1997) suggests there exists an imbalance in the thrombotic state in diabetes, which may play a crucial role in exacerbating vascular disease. I have already discussed in detail one form of vascular abnormality, namely endothelial dysfunction. The endothelium also plays important roles in haemostasis, via the production of NO, which as discussed earlier is important in vascular tone. In addition, the endothelium itself acts to prevent thrombogenic formation via preventing the aggregation of platelets. The formation of a blood clot, or thrombus, requires the participation of platelets, and the fibrinolytic system. In diabetes, it is suggested that alterations in the activity of platelets, as well as other factors, may increase the risk of vascular events (Drouet, 1999). Any damage to the endothelial cell layer would also lead to exposure of the vascular wall to various proteins normally prevented from such interaction, promoting platelet aggregation.

An alteration in the expression of various receptors on the surface of platelets is known to occur in diabetes. In a recent review by Jokl and Colwell (1997), fibrinogen receptors were reported to be over-expressed in diabetes, which may lead to enhanced fibrinogen binding to platelets and their subsequent aggregation. Levels of fibrinogen in type 2 diabetes are reported to be elevated, and is seen as a positive risk factor for cardiovascular disease (Jokl and Colwell, 1997). In addition, hyperglycaemia may lead to generation of glycosylated fibrinogen, a

structure much more resistant to breakdown by the fibrinolytic system (Jörneskog *et al.*, 1996). Furthermore, the effect of insulin on increasing platelet cGMP levels accounts for the anti-aggregatory effect of the hormone; this is suggested to be altered in diabetes (Trovati *et al.*, 1994). Platelets, when exposed to damaged vessels, become attached to collagen in particular (Mustard and Packham, 1970). The exposed collagen may also initiate the activation of factor XII, thereby stimulating the coagulation cascade (Niewiarowski *et al.*, 1966).

Final steps in the clotting cascade result in the formation of a clot or thrombus; this involves the conversion of soluble fibrinogen to insoluble fibrin. This conversion is stimulated by thrombin which is stimulated by an activated factor X. This factor is in turn activated by additional factors which will not be discussed in this context. The fibrin clot structure is initially maintained by electrostatic interactions. Factor XIII covalently cross-links the fibrin α and γ -chains and thus functions to stabilise clot formation (Ariëns *et al.*, 1999). Factor XIII consists of four subunits, two A-subunits and two B-subunits. The activity of the enzyme resides within the A-subunits (Muszbek *et al.*, 1996). In the study of Ariëns *et al.* (1999), the levels of subunit-A were found to be elevated with age and smoking, one of the major independent risk factors for vascular disease. However, the authors are keen to emphasise that the links between factor XIII levels and vascular disease could not be confirmed in their study.

Furthermore, Ariëns *et al.* (1999) provide evidence for increased levels of this factor in NIDDM patients suffering from macrovascular disease (micro- and macroangiopathy and obliterative atherosclerosis). This study suggests that factor XIII may correlate positively with atherothrombotic disorders.

The levels or activity of several factors involved in the fibrinolytic system may be altered in diabetes. Elevations in PAI-1 levels have been linked with atherosclerosis (Salomaa *et al.*, 1995). PAI-1 plays an important role in inhibiting the fibrinolytic system (Drouet, 1999) and prevents the breakdown of the thrombus by tPA by interacting with fibrin, thus maintaining the structure of the clot (Jokl and Colwell, 1997). Studies utilising atherosclerotic lesions from diabetic patients determined PAI-1 levels were increased within these lesions compared to non-diabetics (as detailed by Drouet, 1999). Tissue plasminogen activator (tPA) functions to activate plasmin, which subsequently dissolves fibrin within the blood clot. Under normal circumstances, a delicate balance exists between these two parameters (Jokl and Colwell, 1997). According to these authors, type 2 diabetes specifically is associated with increases in PAI-1 levels and a decrease in tPA levels, leading to impaired fibrinolysis. Platelets are themselves a rich source of PAI-1; a hypersensitive platelet profile may therefore contribute to the development of thrombosis.

In a recent publication by Jörneskog *et al.* (1996), fibrinogen levels were elevated in diabetic patients who did not display signs of vascular disease. This study indicated that in a group of type 1 diabetic patients alterations in the fibrin gel structure were evident. According to the above authors, hyperglycaemia may be responsible for altering the properties of the fibrin clot. Those diabetics who suffer from advanced atherosclerosis also display increased viscosity of their blood, which indeed may be due to a combination of factors including elevated fibrinogen levels (Jokl and Colwell, 1997).

The general process of atherogenesis and current hypotheses as to its aetiology has been covered in chapter 1. However, detail will now be directed to the importance of atherosclerosis in diabetes. Lipoproteins such as LDL exhibiting abnormalities such as glycation play a profound role in atherogenesis. Initially, the consensus of many attributed atherogenesis and foam cell formation to LDL modified by acetylation or glycation (Steinberg *et al.*, 1989). However, recent evidence suggests that the immune system may also play a role in antibody formation against such molecules, leading to the formation of immune complexes. It is not my intention to detail the immunogenic process leading to the progression of this disorder; the reader is instead directed to the recent review by Lopes-Virella *et al.* (1997) for further information.

Lopes-Virella *et al.* (1997) also provide evidence for glycated LDL molecules being potentially atherogenic, leading to foam cell formation. Uptake of these modified lipoproteins into macrophages was, according to the above authors, proportional to the extent of glycation and independent of the oxidised LDL receptor pathway. In addition, a study by Bellomo *et al.* (1995) reported high levels of antibodies against glycated and glyco-oxidised LDL in diabetic patients. These authors suggest that autoantibody generation against such molecules may be involved in the progression of atherosclerosis via uptake by macrophages. The antibodies generated are believed to come into contact with modified LDL in the vessel wall, forming immune complexes. These immune complexes are then avidly taken up by macrophages and metabolised unconventionally, as detailed previously (Lopes-Virella *et al.*, 1997).

The complexity of the atherogenic process is discussed briefly in chapter 1 and involves numerous cell types. Growth factors are released at various stages during atherogenesis, 'recruiting' additional cells into the process. These growth factors not only stimulate the growth and development of the vascular smooth muscle but also incorporate immune cells into the proliferative process. Reactive oxygen species are also liberated from macrophages and may have implications in localised effects upon the endothelium or oxidation of lipoproteins.

Activated monocytes release a myriad of factors influencing cell proliferation and receptor expression; these may play a role in the promotion of atherogenesis. Cytokines involved in atherogenesis are released predominantly from endothelial cells and macrophages. The overall effect of cytokine release is to promote smooth muscle cell proliferation and recruitment of further immune cells into the affected area. The growth factors involved in atherogenesis will not be covered comprehensively since our interest lies in improved vascular responsiveness that may be seen in the presence of atherosclerotic disease. Nevertheless, diabetes is associated with alterations in the release of various growth factors (Clemmons, 1997).

This summary of literature pertaining to atherosclerosis and vascular function was designed to give the reader an overview of the multitude of factors involved in vascular disease. The complexity of the issue, and sheer volume of contributory factors make it impossible to assign appreciable credit to all influences. The aim of the studies herein was to determine if hypercholesterolaemia could be induced in a murine model and whether this

would in turn lead to atherogenesis in the major arteries. It was also investigated whether metformin could provide a so-called 'vasoprotective' influence, possibly attenuating the deposition of cholesterol within the arteries and thereby preventing a loss of vessel compliance and responsiveness. In order to investigate the role of lipids and cholesterol in the progression of atherosclerotic disease, and the possible 'protective' effect supplied by metformin, the following experimental model was used.

Initial experiments involved animals sustained on a high cholesterol (5%) diet for a period of eight-nine months. In addition, a further experimental group received the same diet in the presence of metformin in their drinking water at a concentration of 250mg/kg. These studies were subsequently repeated using a myograph system, a more sensitive method for determining small vessel responsiveness. Animals involved in the study were maintained on the same diet as those in the previous set of experiments for a period of nine months, and included an overall control group maintained on a standard laboratory rodent diet.

5.4 Results:

5.4.1 Vascular Compliance Study #1:

The contraction of murine thoracic aorta in response to NA, following cholesterol feeding and metformin treatment, is represented in figures 5.1.1-5.1.3. Two experimental groups were studied: one sustained on a high cholesterol diet and one on a high cholesterol diet plus metformin. NA (concentration range 3×10^{-9} – 1×10^{-6} M) resulted in concentration-dependent contractions, using standard

organ bath and vessel compliance apparatus. Figure 5.1.3 clearly illustrates that metformin treatment resulted in significantly greater contractions at submaximal and maximal concentrations of NA, with significance reached across a range of concentrations when compared with cholesterol only values. Metformin treatment resulted in a 22% increase in contraction compared with maximal contractile values in the cholesterol fed group. The EC_{50} values for the two groups were computed and were not found to differ significantly between treatments.

Figures 5.2.1-5.2.4 represent data of food ingested and weight gained over the duration of study #1. The mean of food consumed in g per mouse per month (5.2.1) showed very little fluctuation between groups. Likewise, no significant difference was evident between treatments when the overall means of food consumed per day were compared (5.2.2). However, when the mean body weight of the relative groups at week 1 and week 33 (near to the experimental end point) were compared, significant differences were observed (5.2.3). No significant difference was evident for the combined cholesterol and metformin group between weeks 1 or 33. However, the cholesterol fed group showed a significant ($p<0.01$) weight gain between the two time points as one might expect. It is concluded from the data presented herein that metformin may offset any increase in body weight in animals eating a cholesterol-enriched diet. This result is consistent with the current literature with regard to metformin's ability to stabilise bodyweight in patients receiving the drug (UKPDS, 1998).

At the time of killing, animals were anaesthetised with halothane whilst blood was collected via cardiac puncture for the determination of factor XIII activity.

The animals were then killed under terminal anaesthesia. Halothane, a known vasorelaxant, produces a progressive diminution in blood pressure, which is proportional to the depth of anaesthesia (Green, 1982). The vasodilatory effect of this anaesthetic may influence the functioning of aortic vessels. Several preliminary studies were conducted to determine the effect of cervical dislocation and anaesthesia on vessel damage, whilst allowing sufficient time for maximal blood withdrawal.

Anaesthesia under halothane resulted in a greater contractile response than a vessel dissected following cervical dislocation (data not presented). There is a high probability that the vasodilation induced by halothane in some way influences the functioning of the NO pathway which, as stated at the beginning of this chapter, is involved in the continued maintenance of arterial tone via sympathetic nerve inputs. The loss of this relaxant influence has the effect of allowing the contractile process to proceed unchecked; hence a more powerful contraction than seen in vessels from animals killed by cervical dislocation. In the interests of allowing reasonable amounts of blood to be collected, all animals were killed under halothane anaesthesia by cervical dislocation in study #1. Since the same anaesthetic was used at the same concentration for both groups of animals, this should not interfere with the comparison of aortic contractility between the two groups. However, it is possible that the effect of the anaesthetic might be altered by metformin, which might influence the results. Therefore, in a subsequent study (study #2) the gaseous anaesthetic was omitted and animals were killed by cervical dislocation.

5.4.2 Vascular Compliance Study #2:

Data from the initial vascular compliance study proved interesting, and this study was subsequently repeated using more sensitive apparatus. The apparatus used was based on the Mulvany and Halpern design whereby the tissue segment is held between two wire supports and stretched to a desired resting tension (1g in the present studies). These wire supports are attached to a sensitive force transducer, which by way of a pen chart (BBC Goerz) records changes in the contractile properties of the tissue. The apparatus used allowed for improvements in the sensitivity of the experimental technique. Specifically, incubating buffer was maintained more precisely at 37°C throughout the experiment by way of individual heating elements to each bath. All baths were covered throughout the experiment whilst allowing drug administration, aeration, and washing of the tissue to proceed unhindered. The transducer was more sensitive, the apparatus inherently more stable, and calibration could be performed when desired. In addition, the volume of buffer delivered to each tissue bath could be more accurately measured, which has obvious implications in the concentration of drug administered.

In study #2, an additional control group (standard rodent diet, untreated) was included. As with study #1, metformin treatment resulted in a significant increase in the contractile capacity of the tissue. Metformin treatment resulted in an approximate 20% additive contractile response compared with controls and a 7% additive response when compared with cholesterol fed animals (5.3.4). At the lowest NA concentration (5×10^{-9} M) heightened tissue sensitivity to NA in the metformin treated group was clearly evident, resulting in a contraction of 45%

when expressed as a percentage of control (5.3.3). When this is compared to the control group and cholesterol fed group, contraction was 27% and 32%, respectively (5.3.4). Thus, chronic metformin therapy resulted in increased maximal and submaximal tissue sensitivity to NA.

Cholesterol feeding slightly increased the sensitivity of aorta to NA (above 1×10^{-7} M) when expressed as a percentage of control. As with study #1, EC_{50} values were similar for NA-stimulated contraction in the control and cholesterol fed groups (5.3.1, 5.3.2). However, metformin treatment resulted in a marginally lower EC_{50} value and demonstrated the greatest increase in sensitivity in the concentration required to elicit 50% of the maximal contractile response (5.3.3). The fact that both studies produced essentially identical data implies that the initial study was entirely valid and that metformin can improve the compliance of aortic vessels, and may indeed be one mechanism whereby metformin reduces cardiovascular risk in type 2 diabetes.

True vascular compliance is determined by the ability of the tissue to stretch to meet the requirements of the cardiovascular system and to accommodate blood flow to tissues and organs. With respect to this, the ability of aorta to relax was investigated in this study by the addition of Ach following maximal NA-stimulated contraction.

Figure 5.3.5 demonstrates the effect of Ach on the relaxation of aortic tissue. Metformin treatment resulted in a significantly greater vasodilatory response at Ach concentrations 10^{-7} and 10^{-6} M, when compared with controls. In addition, when compared with values for cholesterol fed animals, metformin was

associated with increased relaxation at 10^{-9} , 10^{-7} , and 10^{-6} M. Cholesterol feeding resulted in no significant increase in relaxation when compared with controls. In fact, relaxations in the control group were generally greater than those observed in the cholesterol fed group at the Ach concentrations of 10^{-9} - 10^{-7} M.

The data presented herein suggest that metformin therapy improved the compliance of aortic vessels both in terms of contraction and relaxation. Of similar interest, and perhaps importance, is the effect of cholesterol feeding both increasing the contractility of the tissue to NA and reducing the vasodilatory response to Ach. The implications are that a reduced relaxational response to Ach would allow the contractile inputs responsible for maintaining tonicity to proceed without its equal and opposite effect. Indeed, the increased contractile response following cholesterol feeding (evident herein) would greatly exacerbate this effect *in vivo*, and may lead to increases in blood pressure and, ultimately, hypertension, a major risk factor for CHD. Despite significant differences in the percentage relaxation of pre-contracted vessels, only marginal differences were seen in EC_{50} values between the treatment groups. Nevertheless, sensitivity to Ach in metformin treated mice clearly increased at the higher concentration range used experimentally herein. The lack of a significant effect at the lower concentration range of Ach implies that overall tissue compliance cannot be assumed to have increased. Nevertheless, there exists an increased propensity for vascular tissue from metformin treated animals to relax more so than tissue from untreated or cholesterol fed animals, at these higher drug concentrations.

The amount of food ingested and bodyweight values for animals from study #2 are shown in figures 5.4.1-5.4.4. No significant difference was observed in relation to the average value for food consumed per month between the cholesterol fed and metformin treated groups. Similarly, the mean of food consumed on a daily basis demonstrates no significance between the treatment groups. Significant differences were observed, however, relating to increases in body weight (5.4.3). Significant increases in weight were observed between week 1 and week 36 in cholesterol fed, and cholesterol fed and metformin treated groups; the greatest weight gain being observed in the cholesterol fed group. No significant difference was observed in the body weight of the control group between the beginning and end point of the study.

At week 36, the cholesterol fed group demonstrated the greatest weight gain, significantly higher than both control and metformin treated groups at the same time point. This progressive increment in body weight is clearly illustrated in figure 5.4.4. Cholesterol fed animals increased in weight from 45.4g to 55.6g by week 36, an increase of 10.2g. In contrast, those animals receiving metformin increased in body weight by 7.15g compared with the 1.6g increase in weight in the control group. Significant differences in weight exist at various weekly intervals; however, these values were not included due to limitations in the available plot size of the relevant graph (5.4.4). The significance of weight gain between groups is represented, instead, using one way ANOVA and post-tests.

5.4.3 Factor XIII Activity Assay:

Blood samples were removed from experimental mice whilst either under anaesthesia, or immediately following cervical dislocation. Samples were collected into eppendorf tubes as nine parts blood with one part anticoagulant (0.1M tri-sodium citrate). Eppendorfs were placed immediately on ice; samples were later centrifuged at 4°C for 30 minutes at 2560rpm. The plasma supernatant was separated from the red cell pellet and stored at -20°C until required. The assay was performed at Leeds General Infirmary under the direction of Dr R. Ariëns in the Unit of Molecular Vascular Medicine. Plasma samples were transported in a frozen state under dry ice.

Factor XIII is a coagulation factor present in blood. This factor is converted into its active form in the presence of calcium and the enzyme thrombin. The function of factor XIII is to stabilise the fibrin clot. Factor XIII activity in samples from study #1 was significantly reduced in the metformin treated group (5.5.1). The results are expressed as percentage of a pooled plasma group. The cholesterol fed group demonstrated a factor XIII activity value of 107%, whilst in the metformin treated group 90% activity was recorded compared to the control value of 100% (derived from plasma pooled from untreated mice of the same sex and strain). This effect, whilst small, is significant and supports the hypothesis that metformin treatment may improve the coagulation state in some way by altering the balance of fibrin clot formation and fibrinolysis.

Results from the second study support this conclusion (5.5.2). Factor XIII activity was significantly decreased in both the cholesterol and metformin treated groups

compared with controls. Metformin treatment resulted in a lower mean factor XIII clotting activity, but on this occasion no significant difference was evident between metformin and cholesterol treatments. Overall, factor XIII activity of both cholesterol fed and metformin treated groups was lower in the plasma samples of study #2. This anomaly between the two studies remains unexplained. Nevertheless, the significant difference between the experimental groups remains fully validated due to the use of internal controls in the latter study. In conclusion, results from this study suggest that metformin therapy reduces the activity of factor XIII when administered in conjunction with a cholesterol rich diet. Cholesterol feeding alone, whilst appearing to produce lower factor XIII levels, does not reduce levels to the same extent as metformin treatment. There may be several reasons why results from the two studies may be somewhat variable; these are discussed briefly in section 5.5.3.

5.4.4 Total Plasma Cholesterol Assay:

Table 2: Total Plasma Cholesterol levels following Cholesterol and Metformin feeding.

STUDY #1	CHOLESTEROL LEVEL MMOL/L (MONTH 1)	CHOLESTEROL LEVEL MMOL/L (MONTH 5)	CHOLESTEROL LEVEL MMOL/L (MONTH 9)
Cholesterol fed	< 3.88	4.13	2.97
Cholesterol fed & Metformin treated	< 3.88	3.28	2.66

Cholesterol levels were determined upon commencement of the chronic cholesterol feeding studies using a hand-held *Accutrend GC* plasma cholesterol analyser (Boehringer Mannheim). All total plasma cholesterol levels failed to register above the minimum level required for the assay (3.88mmol/l). Cholesterol levels were further recorded midway through, and at the experimental end point of study #1, by the CHOD-PAP assay method described in chapter 2 (section 2.5), and generally show a reduction in total cholesterol levels. The reduced plasma cholesterol levels were unexpected due to the nature of the diet the animals were receiving.

The fact that a 5% cholesterol-enriched diet induced no overall increase in total plasma cholesterol levels suggests that these animals can clearly adapt to such elevations in cholesterol intake. Although no clear conclusions can be drawn relating to the effect of cholesterol feeding upon *de novo* cholesterol synthesis, one hypothesis is that the liver must extract or utilise a significant proportion of the cholesterol from the circulation. If this cholesterol is not utilised metabolically, then it must be excreted. The results clearly indicate that hypercholesterolaemia is extremely difficult to induce in a lean murine model, which may account for the lack of studies with diet-induced hypercholesterolaemic mice in the literature. Recently, it has been claimed that cholesterol feeding alone in an attempt to induce hypercholesterolaemia in mice is insufficient. Cholesterol feeding merely results in the up-regulation of the enzyme systems involved in bile acid biosynthesis and the synthesis of greater volumes of bile acids from this cholesterol source (Vlahcevic *et al.*, 1999). Thus,

cholesterol over and above the physiological level may merely be excreted via the biliary route.

In regard to this statement, any possible 'modification' in the function of aortic vessels in animals undergoing cholesterol feeding is not attributable to increased cholesterol deposition within the vessel wall, since this would only occur under conditions where circulating cholesterol levels were significantly elevated.

Cholesterol levels recorded from animals receiving metformin tended to show a small overall decline over the entire study, as did those for the cholesterol fed group. Cholesterol levels recorded at month five of the study clearly show cholesterol feeding had raised circulating cholesterol levels in the cholesterol fed group above the levels recorded at the beginning of the experiment. The group receiving metformin showed no increase above basal levels. By month nine, circulating cholesterol levels had fallen significantly from their month five values ($p < 0.002$ cholesterol month nine versus cholesterol month five, Student's paired 't'-Test). The greatest reduction was evident in the cholesterol fed group; however, metformin treatment resulted in the lowest total plasma cholesterol levels between the two groups.

If these data are assumed to represent the true nature of the effect of cholesterol feeding, it appears that acute feeding of cholesterol initially results in increased circulating total cholesterol levels. Long-term feeding, however, resulted in lower overall circulating cholesterol levels than those recorded at month five, and may be partially explained by observations made in the previous paragraphs. Care must be taken when interpreting these results since repeated freeze thawing of samples may influence sample viability, as might prolonged periods of storage.

5.4.5 Uptake of 2-Deoxy-D-[1,2-³H]-Glucose by L6 Skeletal Muscle and A7r5

Smooth Muscle Cells:

2-Deoxy-D-Glucose uptake studies were performed to elucidate the effects of metformin and insulin upon basal glucose uptake in muscle cells (figures 5.6.1, 5.6.2). In L6 muscle cells, metformin (10^{-3} M) significantly enhanced glucose uptake in skeletal muscle following 24h incubations. Similarly, insulin (10^{-8} M), when administered alone, also significantly stimulated glucose uptake above controls ($p < 0.0001$). Metformin and insulin, when incubated simultaneously, induced an additive effect upon glucose uptake, supporting data previously generated at Aston University (Bates, 1999). The aim of this study was to compare the glucose uptake capabilities of the L6 skeletal muscle cell line with that of the A7r5 smooth muscle cell line.

Smooth muscle A7r5 cells proved unresponsive to both metformin and insulin at concentrations proven to stimulate glucose uptake in L6 cells (5.7.1-5.7.6). However, at high metformin concentrations (10^{-2} M) a significant increase in 2-DG uptake was achieved (5.7.2). The lack of appreciable effect to stimulate 2-DG uptake at the lower concentration range may reflect the growth state of the cells, or, alternatively, relative expression of insulin receptors. In rat L6 skeletal muscle, metformin has been shown to stimulate glucose uptake both dependently and independently of the insulin receptor binding status. This is discussed in more detail in section 5.5.

5.4.6 Calcium Imaging in Skeletal and Smooth Muscle Cells:

Recent studies have suggested that metformin may influence ion fluxes across aortic plasma membranes (Chen *et al.*, 1997; Sharma and Bhalla, 1995). In order to elucidate the acute effect of metformin upon calcium flux, preliminary experiments were performed with the A7r5 smooth muscle cell line and L6 skeletal muscle cell line. Cells were “loaded” with the fluorescent indicator Fura-2-AM by pre-incubation with this agent (5×10^{-6} M for 60 minutes).

Smooth muscle cells (A7r5), when challenged with NA (10^{-6} M for 60 seconds), demonstrated rapid intracellular calcium peaks (figure 5.8.1). These peaks were, on average, twice as large in relation to basal calcium levels and occurred within 60 seconds; intracellular calcium decline was equally as rapid. Not all cells from the experimental cluster responded with the same intensity, however. The increase in intracellular calcium levels appears to be independent of whether cells were isolated or in contact with neighbouring cells.

Following a washout period (5 minutes), metformin (10^{-3} M for 15 minutes) was perfused onto the cells and resulted in a steady rise in intracellular calcium levels over a period of 11 minutes. These levels of intracellular calcium were equivalent to, and in some cases above, the levels achieved following NA challenge. Prior to further NA challenge, calcium levels began to slowly decline. When cells were subsequently challenged with NA in the presence of metformin, intracellular calcium levels failed to peak as previously observed under noradrenergic stimulation. Intracellular calcium levels then declined to their original levels over

a period of minutes. In some cases, levels of intracellular calcium substantially diminished below basal values and may represent a toxic drug effect.

The effect of acute exposure to metformin was also elucidated. Figure 5.8.2 represents the effect of exposure to metformin (10^{-3} M) on intracellular calcium levels in A7r5 smooth muscle cells. Metformin perfusion over a period of approximately 20 minutes resulted in no significant effect upon intracellular calcium levels. The addition of thapsigargin increased intracellular calcium levels twofold. This is primarily due to blockage of intracellular calcium sequestering pumps, causing a significant increase in intracellular calcium levels when added to the cells, as one might expect. This demonstrates that the cells were viable, that calcium was present intracellularly, and that calcium channels were still operational.

Since the A7r5 smooth muscle cell line proved unresponsive to insulin and metformin treatment as a stimulus for glucose uptake at levels known to stimulate glucose uptake in L6 cells, and since metformin treatment had only a marginal effect on calcium levels, L6 cells were challenged with NA and metformin to elucidate any effects upon intracellular calcium. NA perfusion onto fura-2 loaded cells resulted in a substantial but transient increase in intracellular calcium levels on more than one occasion (5.8.3). A delayed effect was evident in some isolated cells and may reflect their growth status since not all cells reach confluence at the same rate. Fully matured cells may express more sensitive receptors and signalling pathways than those that are less mature. Nevertheless, the increment in intracellular calcium was greater in the L6 cells than following a

similar challenge in the A7r5 cells, and may reflect the relative size and extent of intracellular calcium stores between these cells.

The calcium peaks seen following NA challenge in L6 cells are characterised by rapid increases in calcium levels followed by an equally rapid fall in intracellular calcium, and presumably reflects the phenotype of the cells and their role in short-lived contractions. These calcium increments, when compared with those observed in A7r5 cells, are distinctly different. Calcium increments in the A7r5 cells were considerably smaller and took considerably longer to achieve. The blunted peak response in the smooth muscle cells represents a short period of sustained calcium influx or release, and thus response, an inherent function of vascular smooth muscle cells. Similarly, a reduction in the intracellular calcium level was more protracted than in the L6 cells.

Metformin perfusion onto L6 cells had no incremental effect upon intracellular calcium levels when administered alone. Simultaneous administration of metformin (10^{-3} M) and NA (10^{-6} M) resulted in intracellular calcium peaks but at a lower level than those seen for NA alone, suggesting that metformin may block calcium-induced calcium release.

These data do not provide irrefutable evidence in relation to the action of metformin on intracellular calcium levels in either cell line studied. However, transient effects are clearly seen following metformin perfusion on vascular smooth muscle cells. How metformin might achieve these effects will be considered in the discussion of this chapter.

The acute administration of metformin in these experiments allows a period of minutes for any noticeable drug effect. The study by Sharma and Bhalla (1995) utilised smooth muscle cells pre-treated with metformin for 1-24 hours. Thus, the window of opportunity for any drug effect may have been too small for accurate quantitation in the present studies. Although metformin only has a marginal effect on the intracellular calcium concentration in a proportion of cells when administered acutely, its effects may be more potent in more mature vascular smooth muscle cells isolated from a mature adult mouse, or following chronic metformin treatment. Sufficient time was not available to test newly harvested cells from thoracic aorta. This method would require the extensive characterisation of the cells and their culture time in order for their recovery from isolation to occur. The isolation procedure could not be achieved under aseptic conditions, and the culture time required to allow cell recovery, adherence, and subsequent growth was considered too great to exclude the possibility of culture infection.

5.4.7 Histology of Aortic Vessels:

Figures e-1 (appendix I) show representative cryostat sections of murine thoracic aorta collected, embedded, and frozen at the time of killing from animals fed a normal or cholesterol-enriched diet (chapter 2 sections 2.3.1b and 2.4.1). Sections were stained with haematoxylin and eosin (appendix II) as an indicator of vessel structure. Additional stains were employed to determine whether cholesterol deposition within the vessel wall and/or vessel lumen had occurred. Several variations of the standard cholesterol-specific staining technique were attempted. However, only one proved applicable to the mouse aorta, details of which are

given in chapter 2 section 2.4.2. In addition, thoracic aorta was embedded, stained, and sectioned for electron microscopy. Figures m and n (appendix I) show micrographs taken under transmission electron microscopy and detail the luminal and endothelial region of the aortic vessel. These photographs function to confirm the integrity of the constituent layers of the vessel and show no structural abnormalities. No cholesterol was detected in the sub-intima either extracellularly or intracellularly following cholesterol staining. There was no accumulation of macrophages and no evidence of foam cell formation. In addition, the endothelial layer and general morphology of the smooth muscle cells appeared normal in tissues from most mice, if not slightly disrupted. Any disruption presumably reflects vessel damage incurred during the dissection process.

**Effect of cholesterol feeding upon the
contraction of thoracic aorta in response
to noradrenaline.**

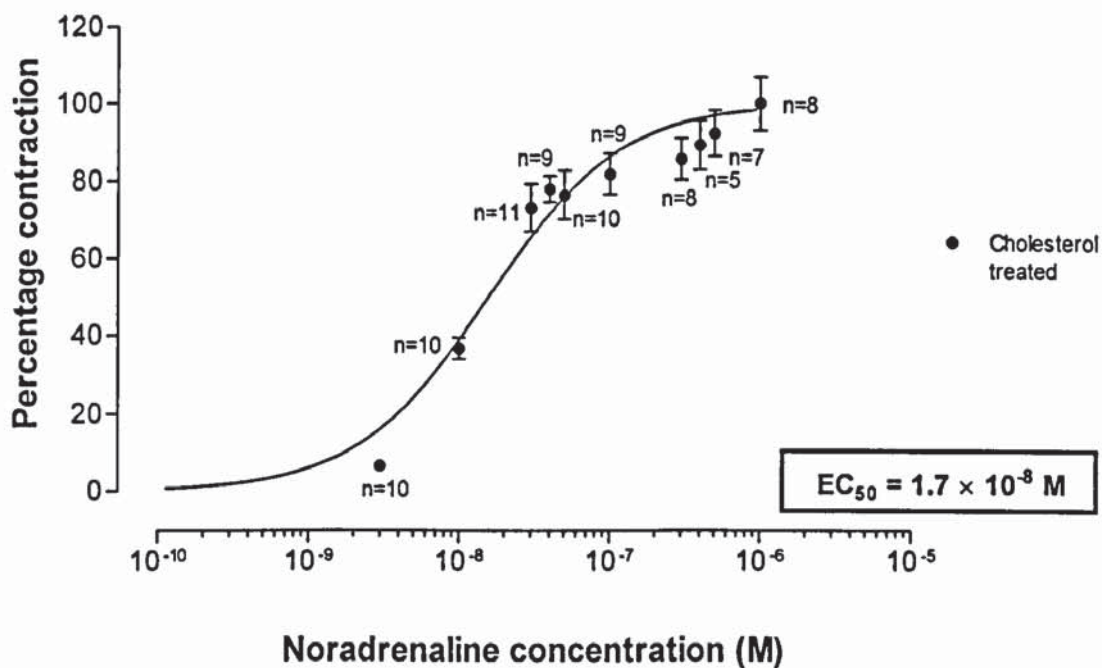


Figure 5.1.1: The effect of chronic cholesterol feeding for a period of eight-nine months on the percentage contractile response of murine thoracic aorta under a resting tension of 1g in response to noradrenaline ($3 \times 10^{-9} - 1 \times 10^{-6}$ M). High cholesterol diet consisted of 5% cholesterol and 4% fat. Data are expressed as percentage contractions (cm). Values are mean \pm SEM. The lowest contractile value corresponding to 3×10^{-9} M noradrenaline represents a contraction of 0.49cm, whereas the highest contractile value corresponding to 1×10^{-6} M noradrenaline represents a contraction of 7.45cm.

Effect of metformin and cholesterol feeding upon the contraction of thoracic aorta in response to noradrenaline.

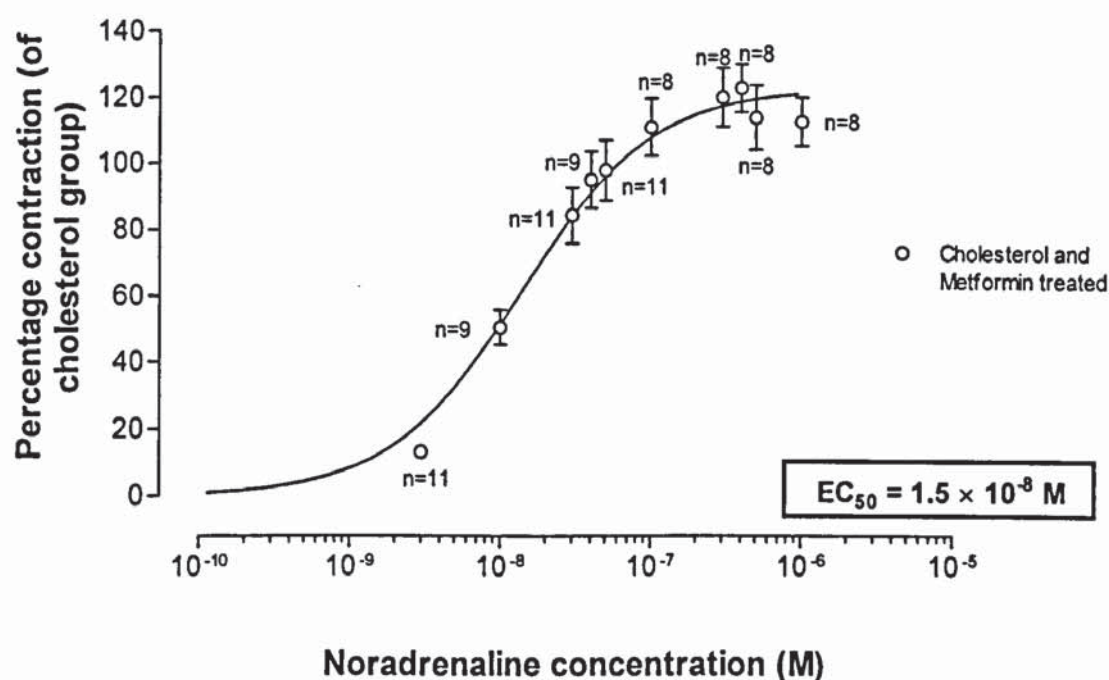


Figure 5.1.2: The effect of chronic cholesterol feeding and chronic metformin treatment (250mg/kg), for a period of eight-nine months, on the percentage contractile response of murine thoracic aorta under a resting tension of 1g in response to noradrenaline ($3 \times 10^{-9} - 1 \times 10^{-6} \text{ M}$). High cholesterol diet consisted of 5% cholesterol and 4% fat. Data are expressed as percentage contractions of the cholesterol fed group. Values are mean \pm SEM. The lowest contractile value corresponding to $3 \times 10^{-9} \text{ M}$ noradrenaline represents a contraction of 0.99cm, whereas the highest contractile value corresponding to $4 \times 10^{-7} \text{ M}$ noradrenaline represents a contraction of 9.15cm.

Effect of metformin and cholesterol feeding upon contraction of thoracic aorta in response to noradrenaline.

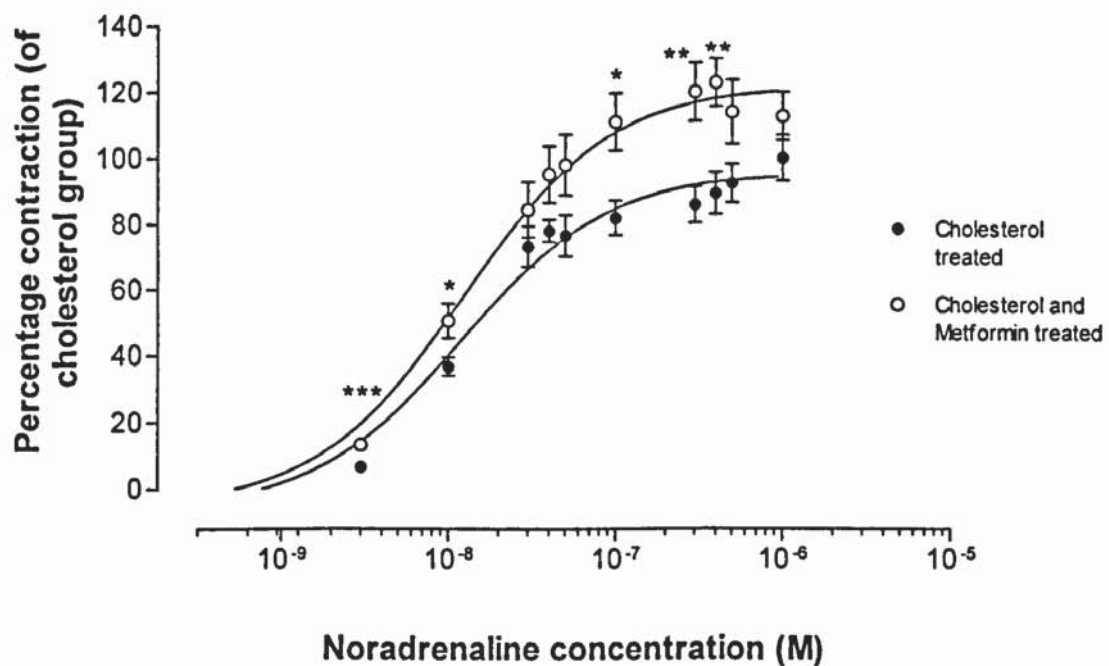


Figure 5.1.3: The effect of chronic cholesterol feeding \pm metformin treatment (250mg/kg in drinking water), for a period of eight-nine months, on the percentage contractile response of murine thoracic aorta under a resting tension of 1g in response to noradrenaline ($3 \times 10^{-9} - 1 \times 10^{-6}$ M). High cholesterol diet consisted of 5% cholesterol and 4% fat. Metformin significantly ($p < 0.05$) increased percentage contraction of thoracic aorta compared with controls (cholesterol fed group). Data are expressed as percentage contractions of the cholesterol fed group. Values are mean \pm SEM, * $p < 0.04$ versus control, ** $p < 0.006$ versus control, *** $p < 0.0001$ versus control (Student's unpaired 't'-Test).

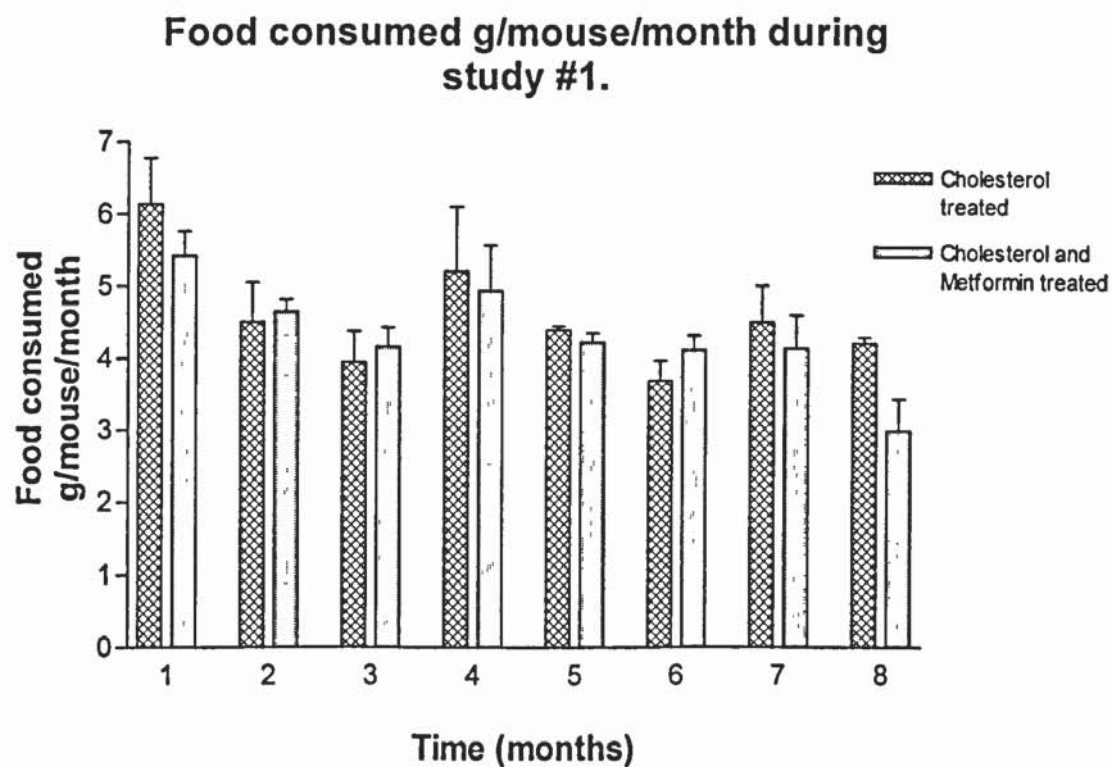


Figure 5.2.1: Average food consumption in g/mouse/month over the experimental period in mice fed a high cholesterol (5%) diet containing 4% fat, with and without metformin (250mg/kg in drinking water). Data are expressed as weight of food consumed (g). Values are mean \pm SEM, n=8.

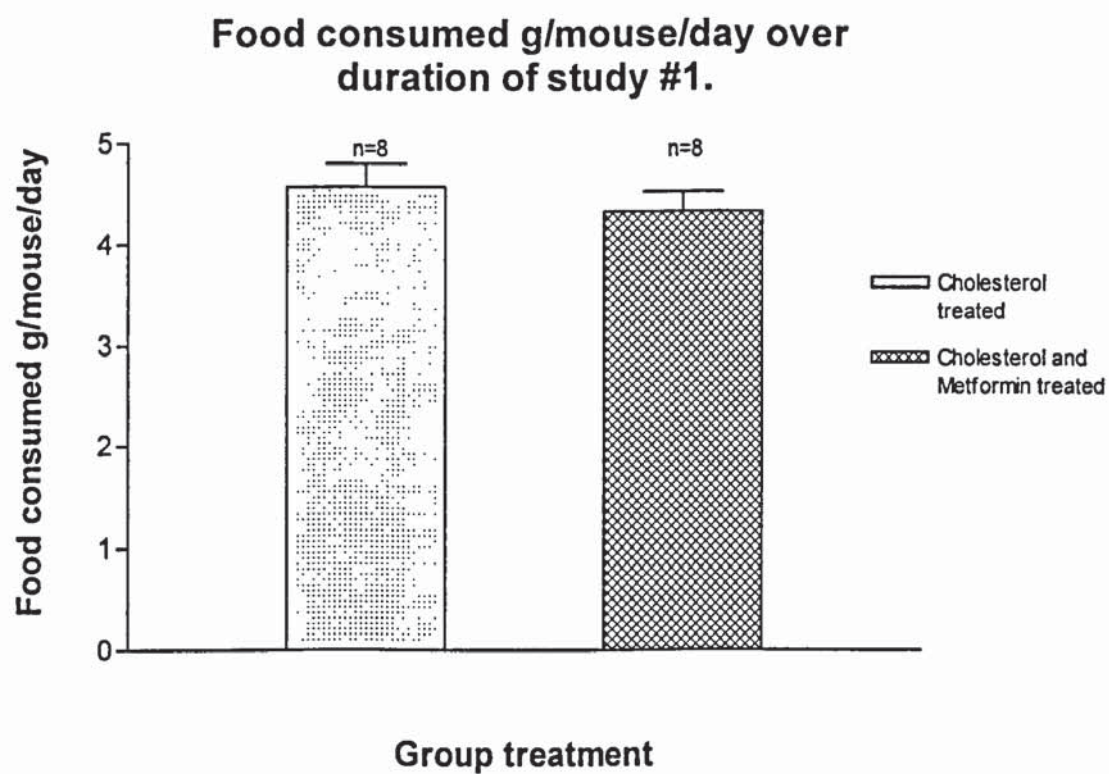


Figure 5.2.2: Average food consumption in g/mouse/day over the experimental period in mice fed a high cholesterol (5%) diet containing 4% fat, with and without metformin (250mg/kg in drinking water). Data are expressed as weight of food consumed (g). Values are mean \pm SEM.

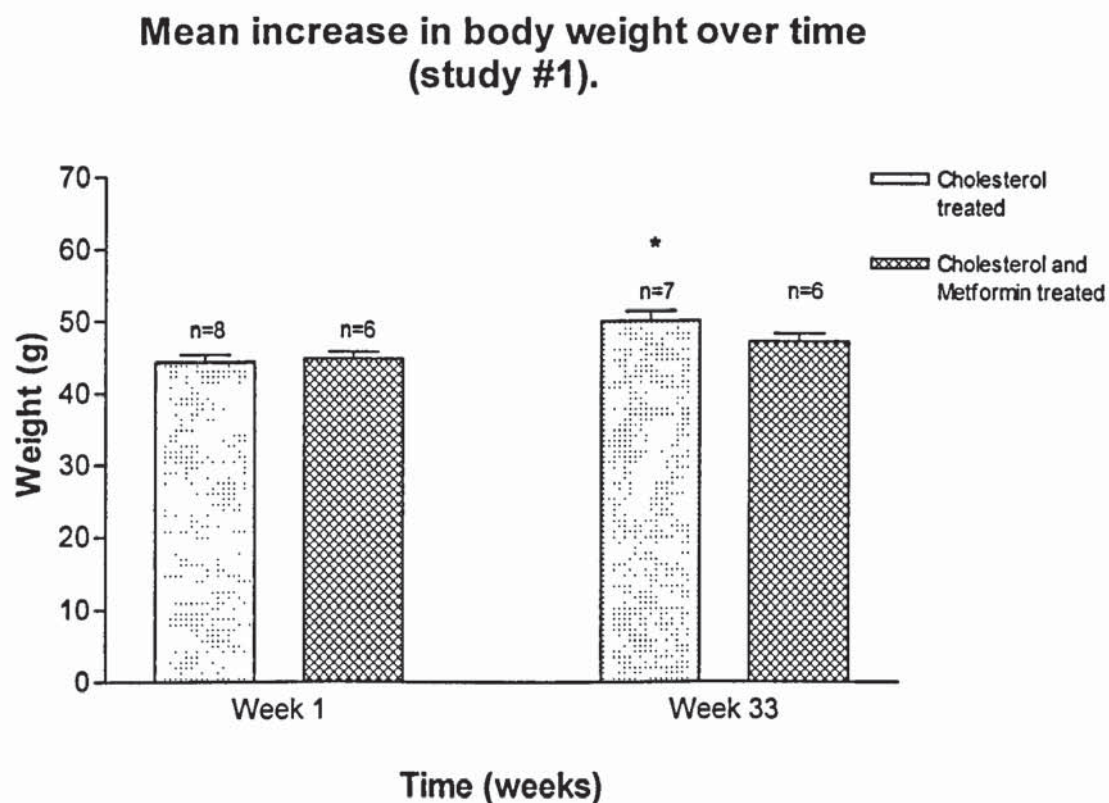


Figure 5.2.3: Mean increase in body weight between weeks 1 and 33 in mice fed a high cholesterol (5%) diet containing 4% fat, with and without metformin (250mg/kg in drinking water). Cholesterol feeding in the absence of metformin resulted in significant ($p<0.05$) weight gain. Data are expressed as body weight values (g). Values are mean \pm SEM, * $p<0.01$ cholesterol week 1 versus cholesterol week 33 (Student's paired 't'-Test).

Mean increase in body weight over time (study #1).

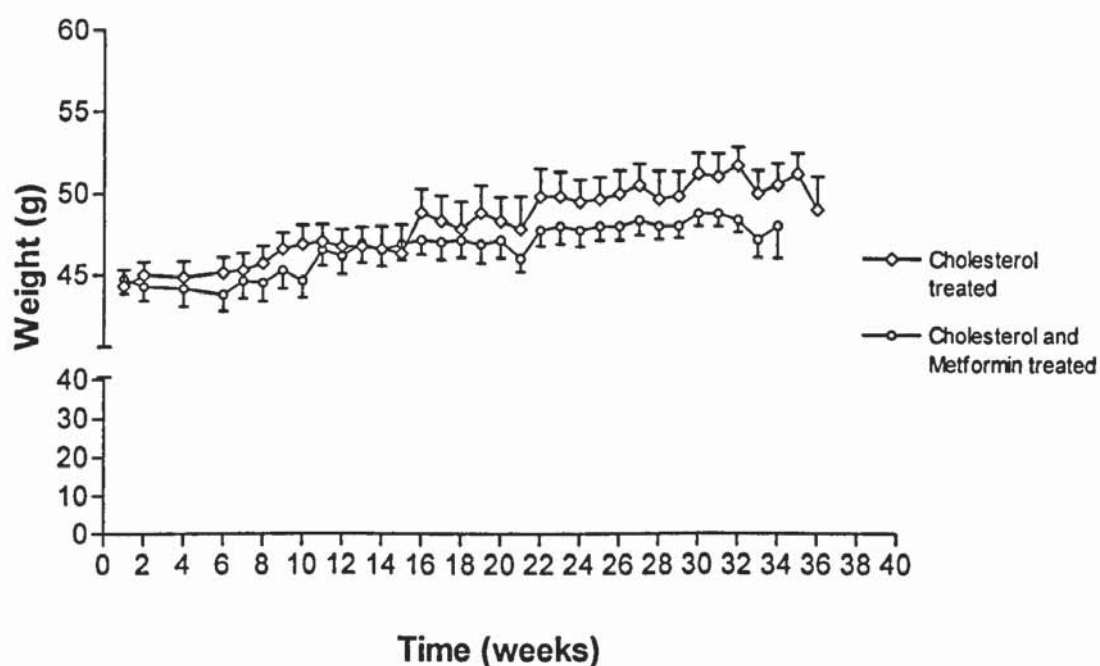


Figure 5.2.4: Illustration of the mean weekly body weight values between weeks 1 and 36 of study #1 in mice fed a high cholesterol (5%) diet containing 4% fat, with and without metformin (250mg/kg in drinking water). Data are expressed as weekly body weight values (g). Values are mean \pm SEM.

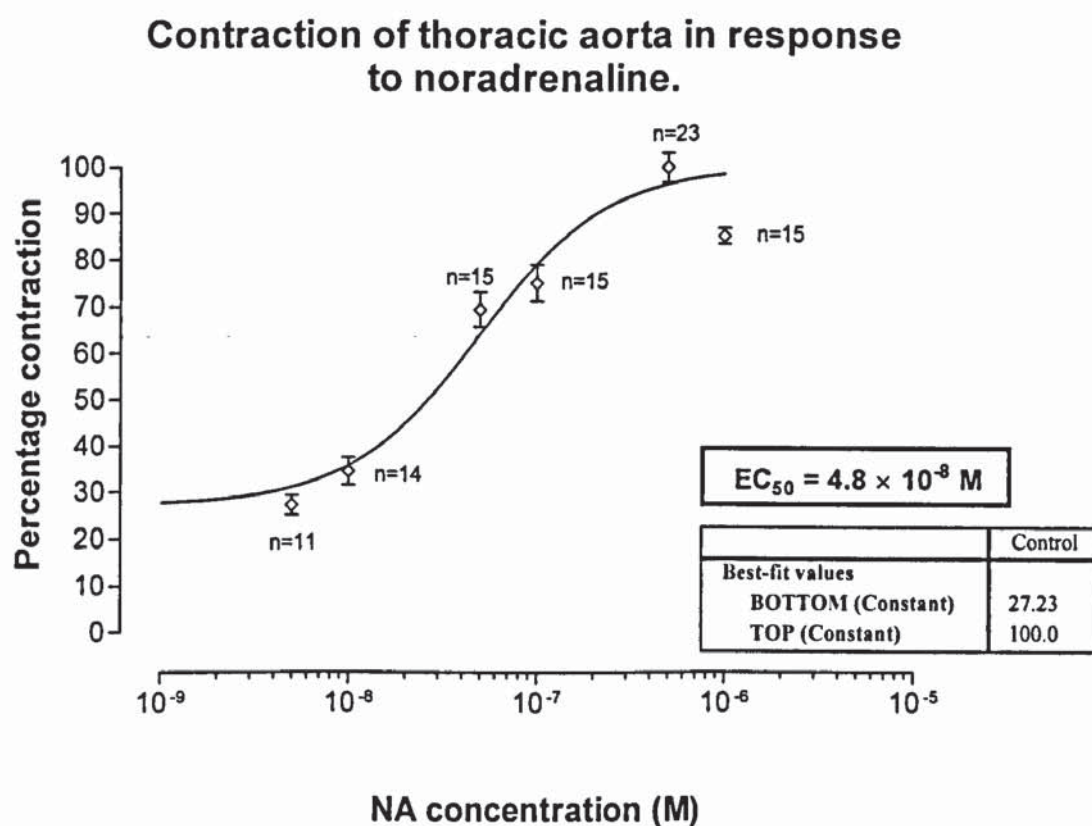


Figure 5.3.1: Percentage contractile response of murine thoracic aorta under a resting tension of 1g in response to noradrenaline ($5 \times 10^{-9} - 1 \times 10^{-6}$ M) in mice fed a standard rodent diet for a period of nine months. Data are expressed as percentage contractions (cm). Values are mean \pm SEM. The lowest contractile value corresponding to 5×10^{-9} M noradrenaline represents a contraction of 1.873cm, whereas the highest contractile value corresponding to 5×10^{-7} M noradrenaline represents a contraction of 6.878cm.

Effect of cholesterol feeding upon the contraction of thoracic aorta in response to noradrenaline.

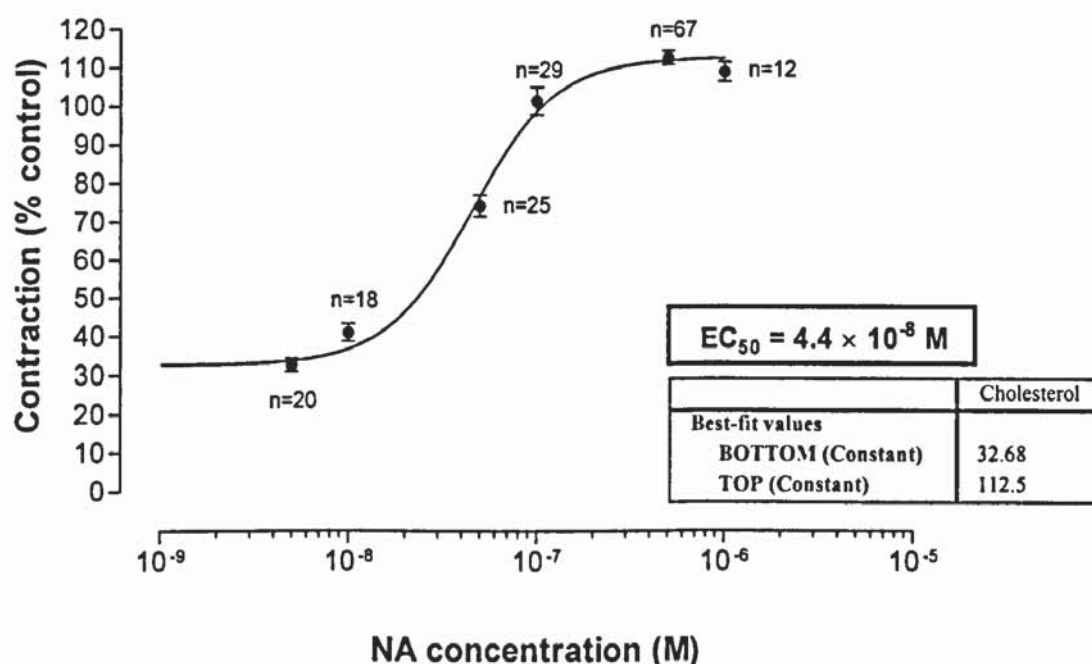


Figure 5.3.2: Percentage contractile response of murine thoracic aorta under a resting tension of 1g in response to noradrenaline ($5 \times 10^{-9} - 1 \times 10^{-6} \text{ M}$) following chronic cholesterol feeding for a period of nine months. High cholesterol diet consisted of 5% cholesterol and 4% fat. Data are expressed as percentage contractions of the control group. Values are mean \pm SEM. The lowest contractile value corresponding to $5 \times 10^{-9} \text{ M}$ noradrenaline represents a contraction of 2.248cm, whereas the highest contractile value corresponding to $5 \times 10^{-7} \text{ M}$ noradrenaline represents a contraction of 7.736cm.

Effect of metformin and cholesterol feeding upon the contraction of thoracic aorta in response to noradrenaline.

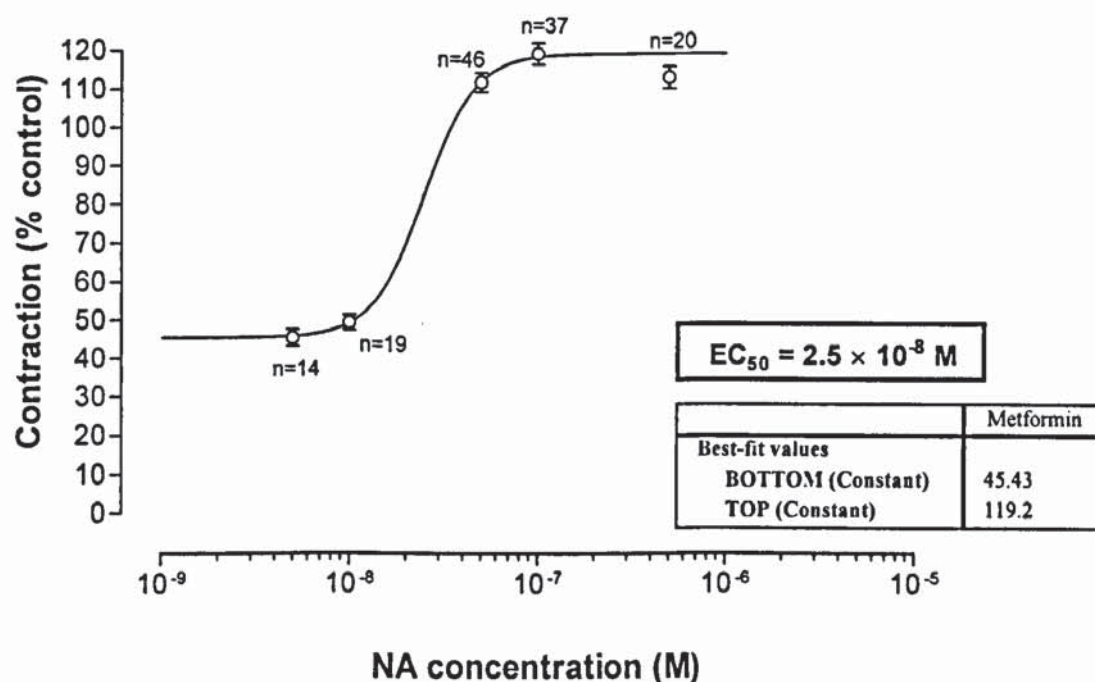


Figure 5.3.3: Percentage contractile response of murine thoracic aorta under a resting tension of 1g in response to noradrenaline ($5 \times 10^{-9} - 1 \times 10^{-6}$ M) following chronic cholesterol feeding and chronic metformin treatment (250mg/kg in drinking water) for a period of nine months. High cholesterol diet consisted of 5% cholesterol and 4% fat. Data are expressed as percentage contractions of the control group. Values are mean \pm SEM. The lowest contractile value corresponding to 5×10^{-9} M noradrenaline represents a contraction of 3.125cm, whereas the highest contractile value corresponding to 1×10^{-7} M noradrenaline represents a contraction of 8.202cm.

Effect of cholesterol feeding \pm metformin treatment upon the contraction of thoracic aorta in response to noradrenaline.

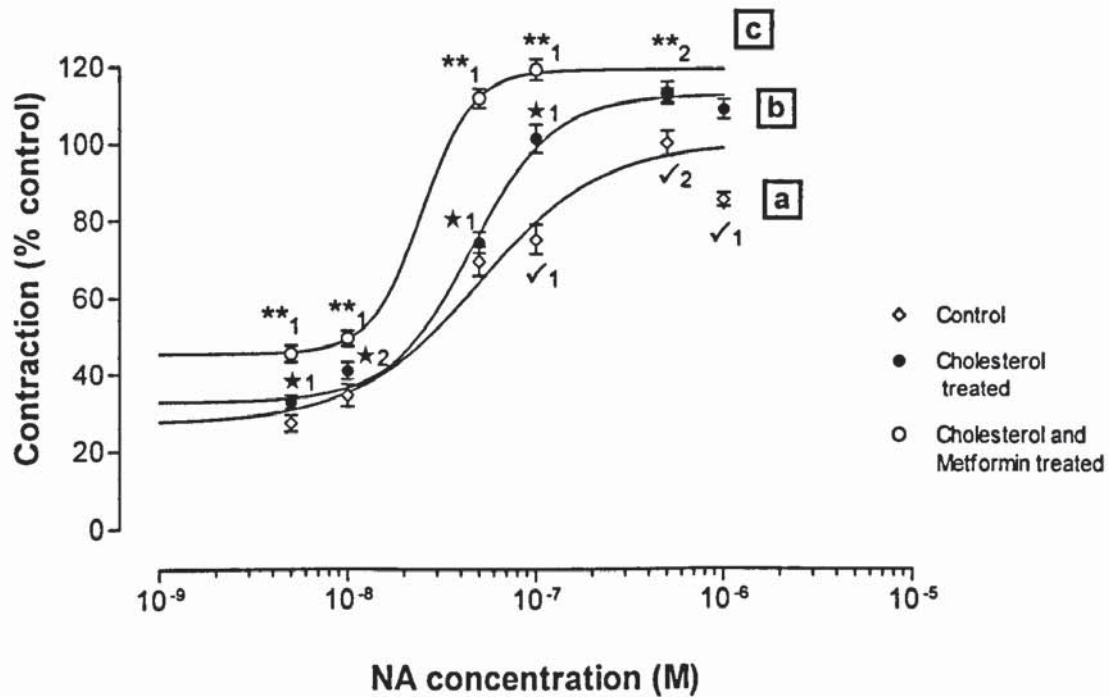


Figure 5.3.4: Percentage contractile response of murine thoracic aorta under a resting tension of 1g in response to noradrenaline ($5 \times 10^{-9} - 1 \times 10^{-6}$ M) following feeding of, a) standard rodent diet, b) high cholesterol (5%) diet containing 4% fat, c) high cholesterol (5%) diet containing 4% fat, with metformin (250mg/kg in drinking water) for a period of nine months. Metformin treatment and cholesterol feeding significantly ($p < 0.05$) increased contractions of mouse aorta above control values. Data are expressed as percentage contractions of the control group. Values are mean \pm SEM, **₁ $p < 0.001$ metformin versus control, **₂ $p < 0.01$ metformin versus control, $\sqrt{1}$ $p < 0.001$ control versus cholesterol fed group, $\sqrt{2}$ $p < 0.01$ control versus cholesterol fed group, *₁ $p < 0.001$ metformin versus cholesterol fed group, *₂ $p < 0.05$ metformin versus cholesterol fed group (one way ANOVA with Bonferroni post-test).

**Effect of cholesterol feeding \pm metformin
on the relaxation of thoracic aorta in
response to acetylcholine.**

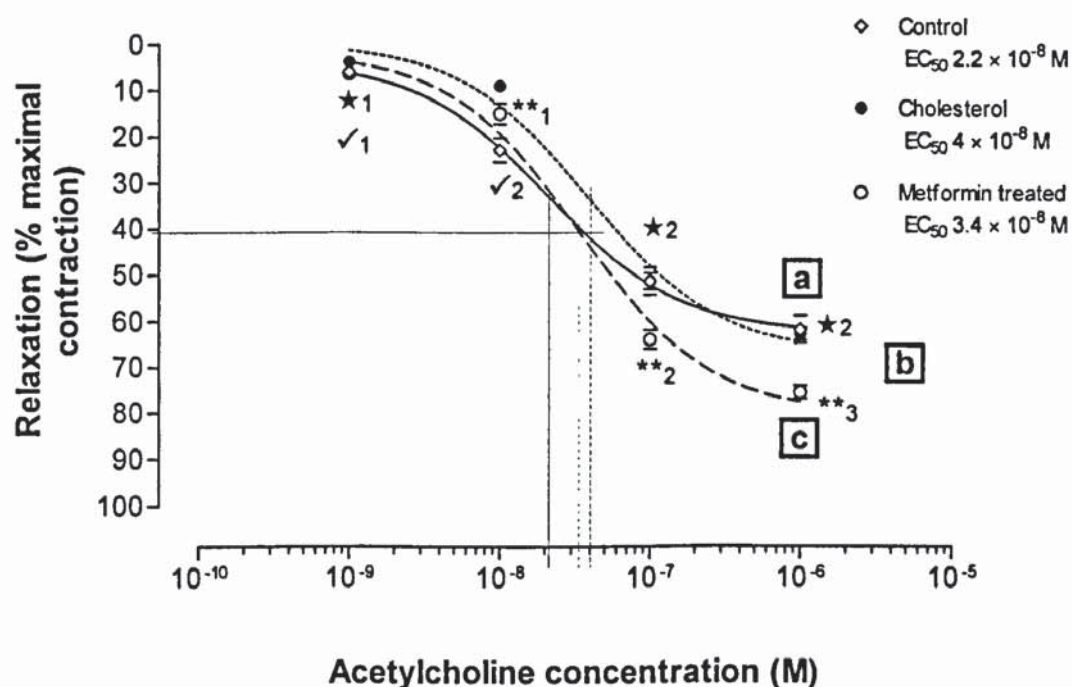


Figure 5.3.5: Percentage relaxation of murine thoracic aorta (pre-contracted with noradrenaline) in response to acetylcholine ($1 \times 10^{-9} - 1 \times 10^{-6}$ M) following the feeding of, **a)** standard rodent diet, **b)** high cholesterol (5%) diet containing 4% fat, **c)** high cholesterol (5%) diet containing 4% fat with metformin (250mg/kg in drinking water) for a period of nine months. Metformin significantly ($p < 0.05$) increased relaxation of thoracic aorta at high concentrations of acetylcholine. Data are expressed as percentage relaxation of the maximal contractile response (cm). Values are mean \pm SEM, $\star_1 p < 0.05$ metformin versus control, $\star_2 p < 0.01$ metformin versus control, $\star_3 p < 0.001$ metformin versus control, $\checkmark_1 p < 0.05$ control versus cholesterol fed, $\checkmark_2 p < 0.001$ control versus cholesterol fed, $\star_1 p < 0.01$ metformin versus cholesterol fed, $\star_2 p < 0.001$ metformin versus cholesterol fed (Nonparametric ANOVA with Dunn's post-test).

Food consumed g/mouse/month during study #2.

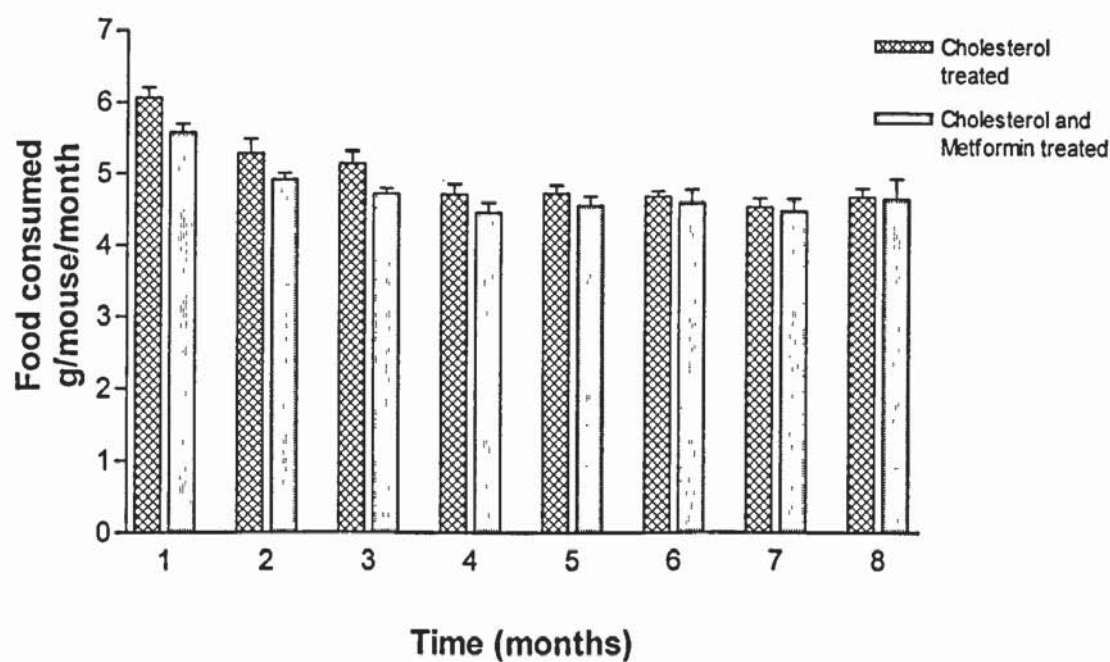


Figure 5.4.1: Average food consumption in g/mouse/month over the experimental period in mice fed a high cholesterol (5%) diet containing 4% fat, with and without metformin (250mg/kg in drinking water). Data are expressed as weight of food consumed (g). Values are mean \pm SEM, n=10.



Figure 5.4.2: Average food consumption in g/mouse/day over the experimental period in mice fed a high cholesterol (5%) diet containing 4% fat, with and without metformin (250mg/kg in drinking water). Data are expressed as weight of food consumed (g). Values are mean \pm SEM.

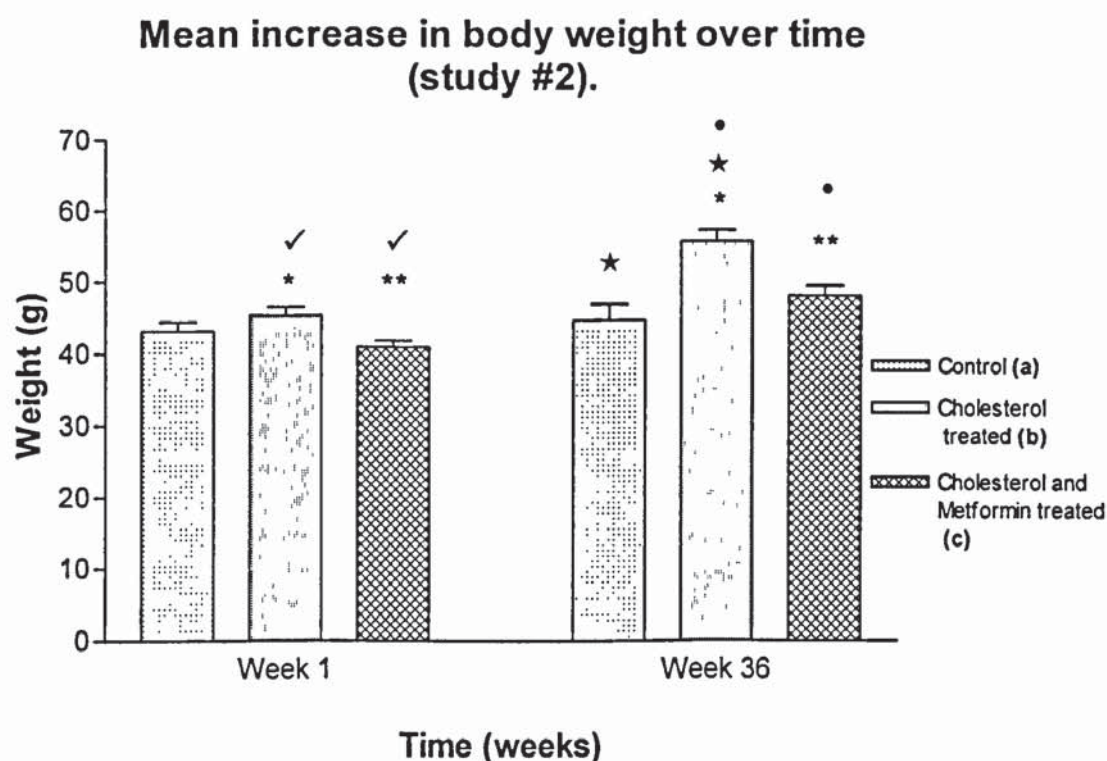


Figure 5.4.3: Mean increase in body weight between weeks 1 and 36 in mice fed a, a) standard rodent diet, b) high cholesterol (5%) diet containing 4% fat, c) high cholesterol (5%) diet containing 4% fat with metformin (250mg/kg in drinking water). Cholesterol feeding resulted in significant ($p < 0.05$) weight gain with and without metformin. No significant weight gain was observed in the control group. At week 36, weight gain in the cholesterol fed group was greater than in control and metformin groups. Data are expressed as body weight values (g). Values are mean \pm SEM, $n=10$ * $p < 0.0001$ cholesterol week 1 versus cholesterol week 36 (Student's paired 't'-Test), ** $p < 0.0001$ metformin week 1 versus metformin week 36 (Student's paired 't'-Test), $\checkmark p < 0.009$ cholesterol week 1 versus metformin week 1 (Student's unpaired 't'-Test), * $p < 0.001$ control week 36 versus cholesterol week 36 (Student's unpaired 't'-Test), • $p = 0.0021$ metformin week 36 versus cholesterol week 36 (Student's unpaired 't'-Test).

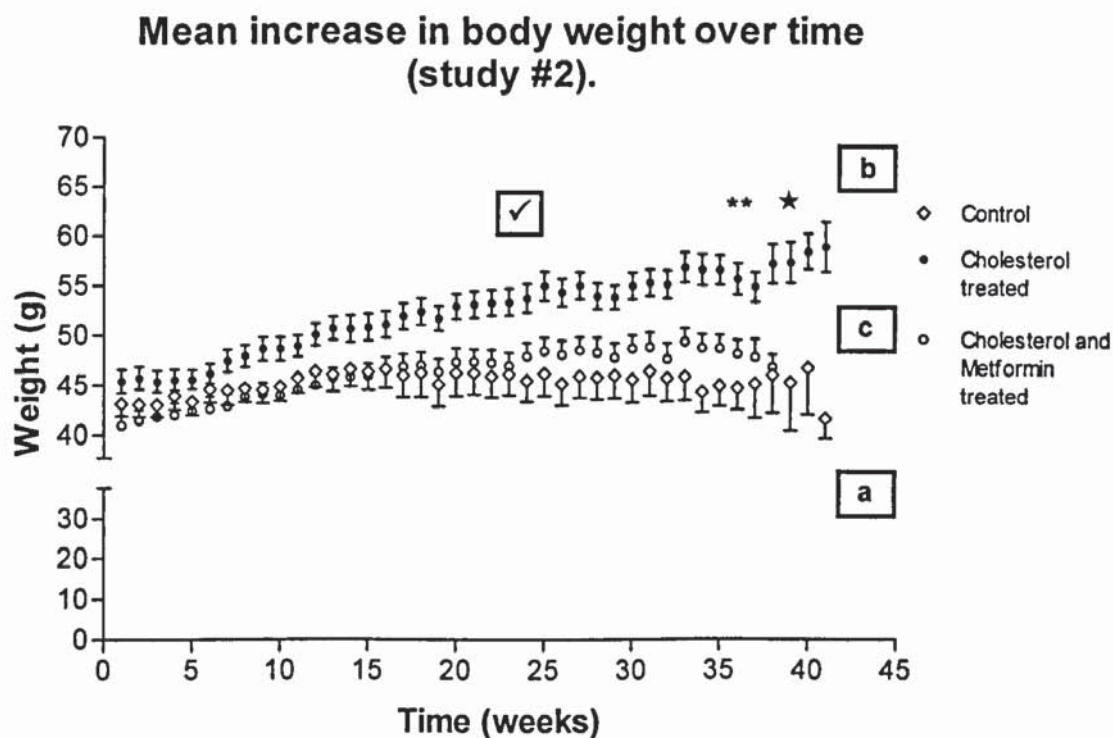


Figure 5.4.4: Illustration of the mean weekly body weight values between weeks 1 and 41 of study #2 in mice fed a, a) standard rodent diet, b) high cholesterol (5%) diet containing 4% fat, c) high cholesterol (5%) diet containing 4% fat, with metformin (250mg/kg in drinking water). Cholesterol feeding resulted in significant ($p < 0.05$) increases in weight gain. Data are expressed as weekly body weight values (g). Values are mean \pm SEM, $\checkmark p < 0.0001$ (one way ANOVA), $**p < 0.001$ cholesterol versus metformin (Bonferroni post-test), $\star p < 0.001$ cholesterol versus control (Bonferroni post-test).

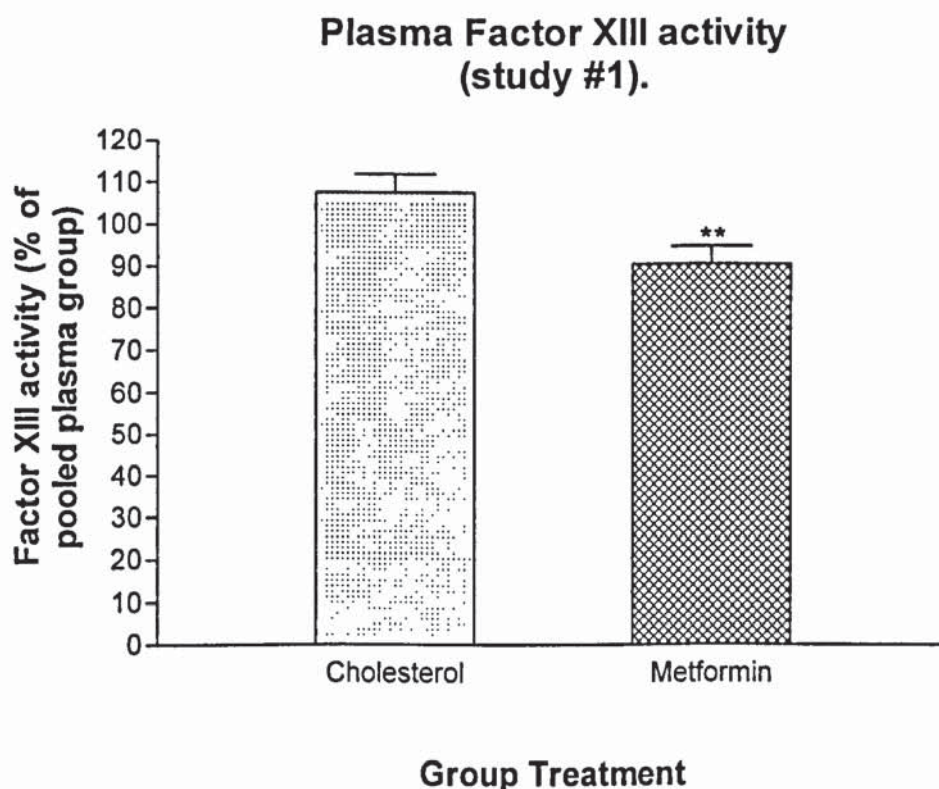


Figure 5.5.1: Activity of blood coagulation factor XIII in plasma from mice fed a high cholesterol (5%) diet containing 4% fat, with and without metformin (250mg/kg in drinking water) for a period of eight-nine months. Factor XIII activity was measured through cross-linking reactions using fibrinogen coated microtiter plates and a chromogen-induced colour reaction. A pooled plasma sample from untreated mice was used as a measure of normal 100% factor XIII activity. Metformin was associated with significantly ($p < 0.05$) lower factor XIII levels than in cholesterol fed animals alone. Data are expressed as percentage activity of the pooled plasma group. Values are mean \pm SEM, $n=10$, ** $p < 0.02$ versus cholesterol fed group (Student's unpaired 't'-Test).

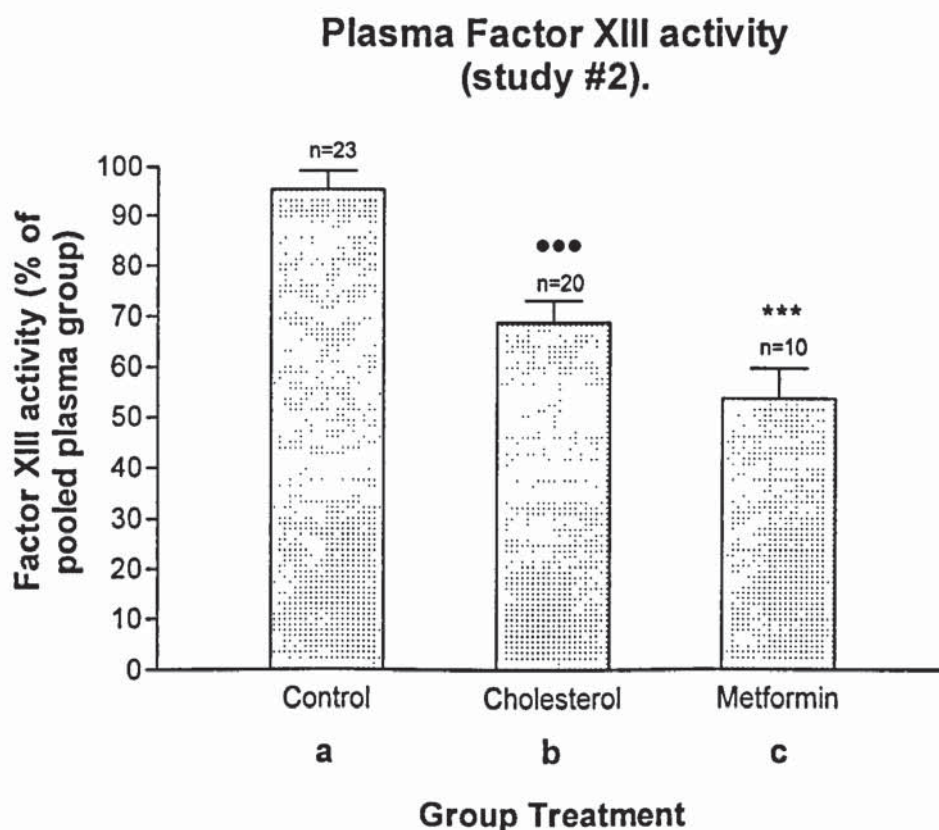


Figure 5.5.2: Activity of blood coagulation factor XIII in plasma from mice fed a, a) standard rodent diet, b) high cholesterol (5%) diet containing 4% fat, c) high cholesterol (5%) diet containing 4% fat with metformin (250mg/kg in drinking water) for a period of nine months. Factor XIII activity was measured through cross-linking reactions using fibrinogen coated microtiter plates and a chromogen-induced colour reaction. A pooled plasma sample from untreated mice was used as a measure of normal 100% factor XIII activity. Cholesterol feeding, and cholesterol feeding in the presence of metformin, was associated with significant ($p < 0.05$) reductions in the activity of factor XIII compared with controls. Data are expressed as percentage activity of the pooled plasma group. Values are mean \pm SEM, $n=10$, *** $p < 0.001$ metformin versus control, *** $p < 0.001$ cholesterol fed group versus control (one way ANOVA with Bonferroni post-test).

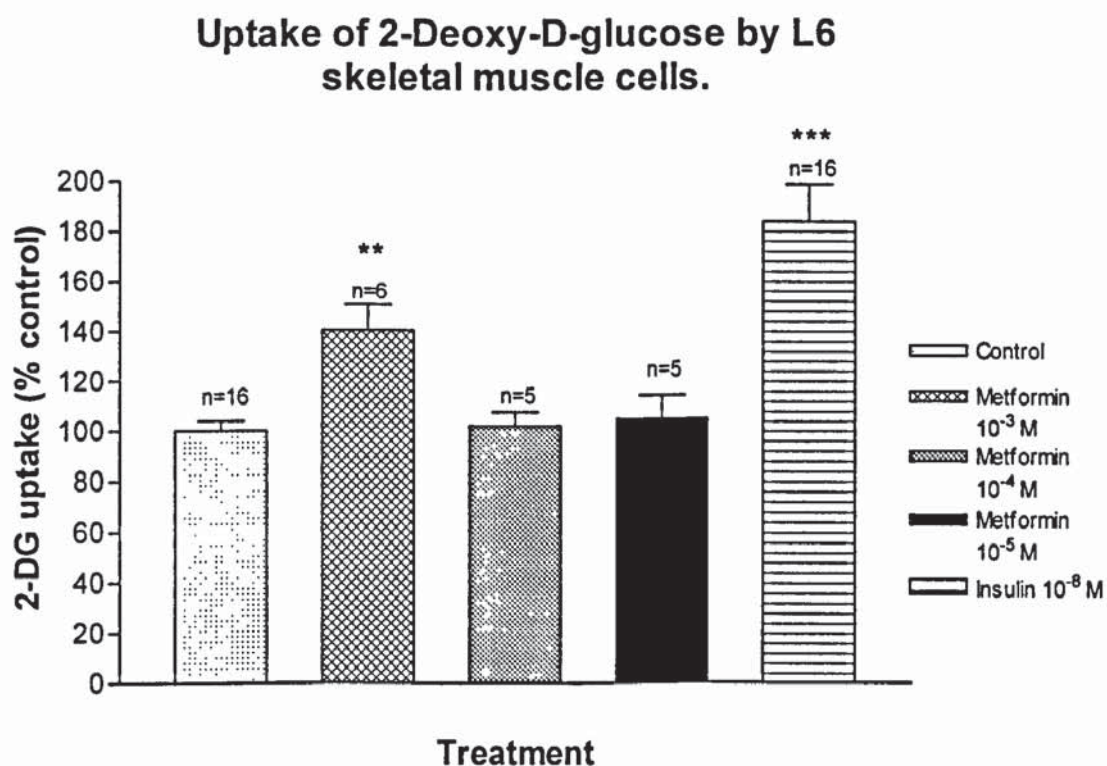


Figure 5.6.1: Effect of metformin (10^{-3} – 10^{-5} M) and insulin (10^{-8} M) at 24h, on the uptake of 2-Deoxy-D-glucose by L6 skeletal muscle cells. Metformin, at high concentrations, and insulin, significantly ($p < 0.05$) enhanced glucose uptake. Data are expressed as percentage of control. Values are mean \pm SEM, ** $p < 0.002$ versus control, *** $p < 0.0001$ versus control (Student's paired 't'-Test).

Uptake of 2-Deoxy-D-glucose by L6 skeletal muscle cells.

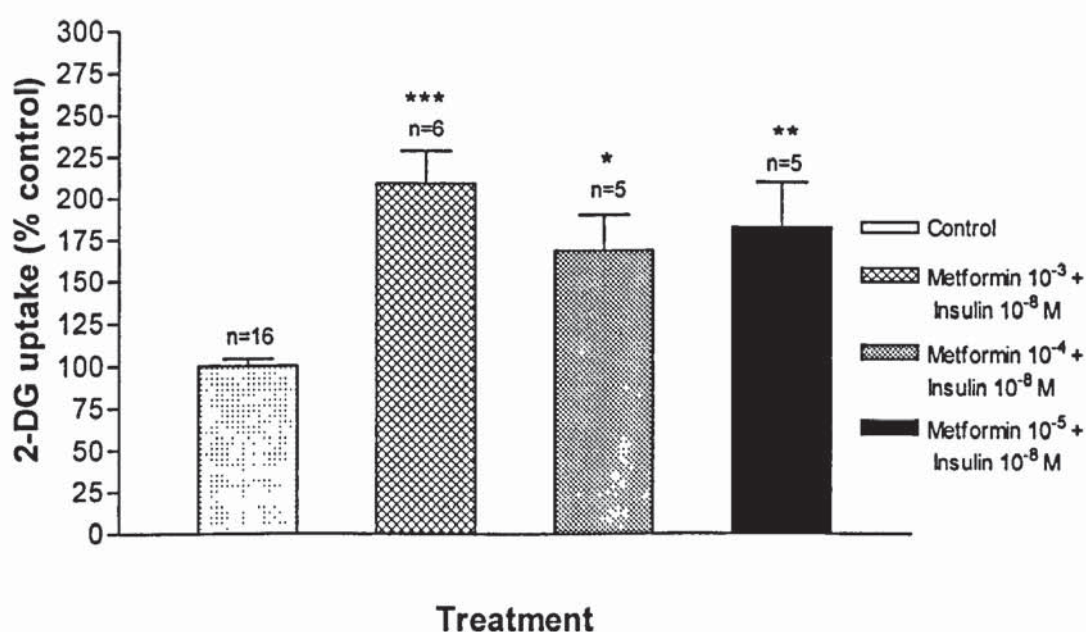


Figure 5.6.2: Combined effect of metformin (10^{-5} – 10^{-3} M) and insulin (10^{-8} M) at 24h, on the uptake of 2-Deoxy-D-glucose by L6 skeletal muscle cells. Metformin, and insulin, significantly ($p < 0.05$) enhanced glucose uptake above controls, at all concentrations. Data are expressed as percentage of control. Values are mean \pm SEM, *** $p < 0.002$ versus control, * $p < 0.03$ versus control, ** $p < 0.02$ versus control (Student's paired 't'-Test).

Uptake of 2-Deoxy-D-glucose by A7r5 vascular smooth muscle cells.

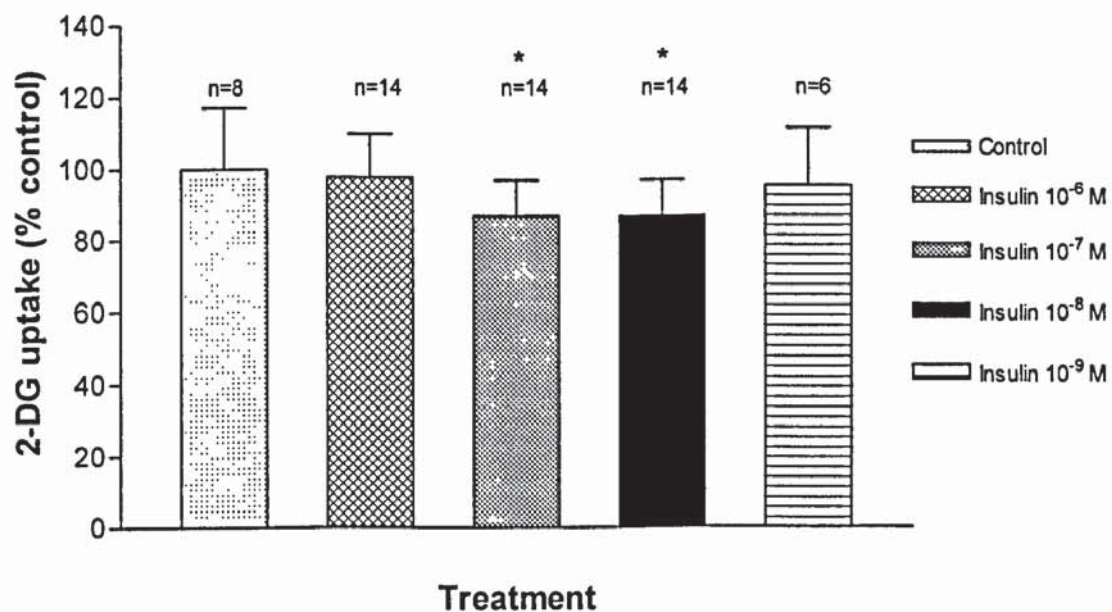


Figure 5.7.1: Effect of insulin (10^{-9} – 10^{-6} M) at 24h, on the uptake of 2-Deoxy-D-glucose by A7r5 vascular smooth muscle cells. Insulin significantly diminished glucose uptake at 10^{-8} and 10^{-7} M. Data are expressed as percentage of control. Values are mean \pm SEM, * p <0.05 versus control (Student's paired 't'-Test).

Uptake of 2-Deoxy-D-glucose by A7r5 vascular smooth muscle cells.

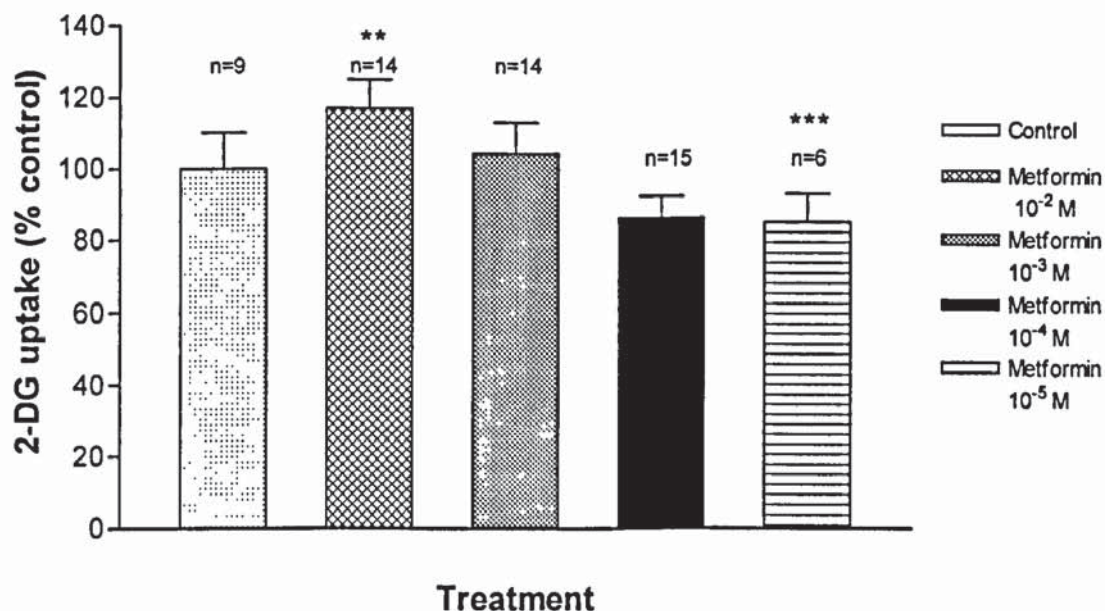


Figure 5.7.2: Effect of metformin (10^{-5} – 10^{-2} M) at 24h, on the uptake of 2-Deoxy-D-glucose by A7r5 vascular smooth muscle cells. Metformin significantly ($p < 0.05$) enhanced glucose uptake at high concentrations and significantly diminished glucose uptake at lower concentrations. Data are expressed as percentage of control. Values are mean \pm SEM, ** $p < 0.004$ versus control, *** $p < 0.002$ versus control (Student's paired 't'-Test).

Uptake of 2-Deoxy-D-glucose by A7r5 vascular smooth muscle cells.

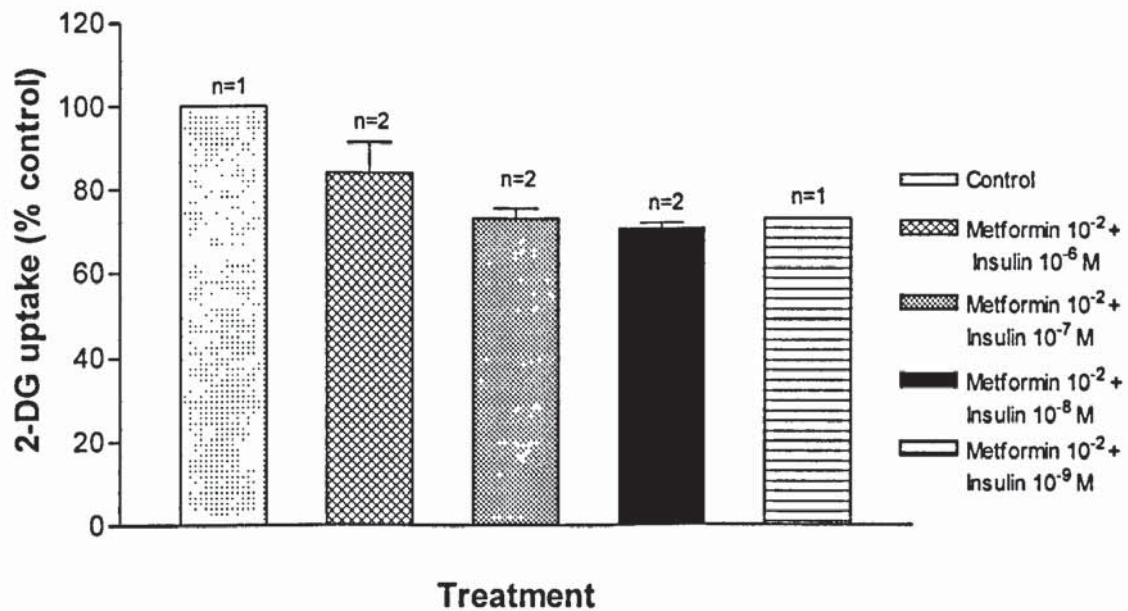


Figure 5.7.3: Combined effect of metformin (10^{-2} M) and insulin ($10^{-9} - 10^{-6}$ M) at 24h, on the uptake of 2-Deoxy-D-glucose by A7r5 vascular smooth muscle cells. Insulin and metformin were associated with reduced glucose uptake at all concentrations. Data are expressed as percentage of control. Values where appropriate are mean \pm SEM.

Uptake of 2-Deoxy-D-glucose by A7r5 vascular smooth muscle cells.

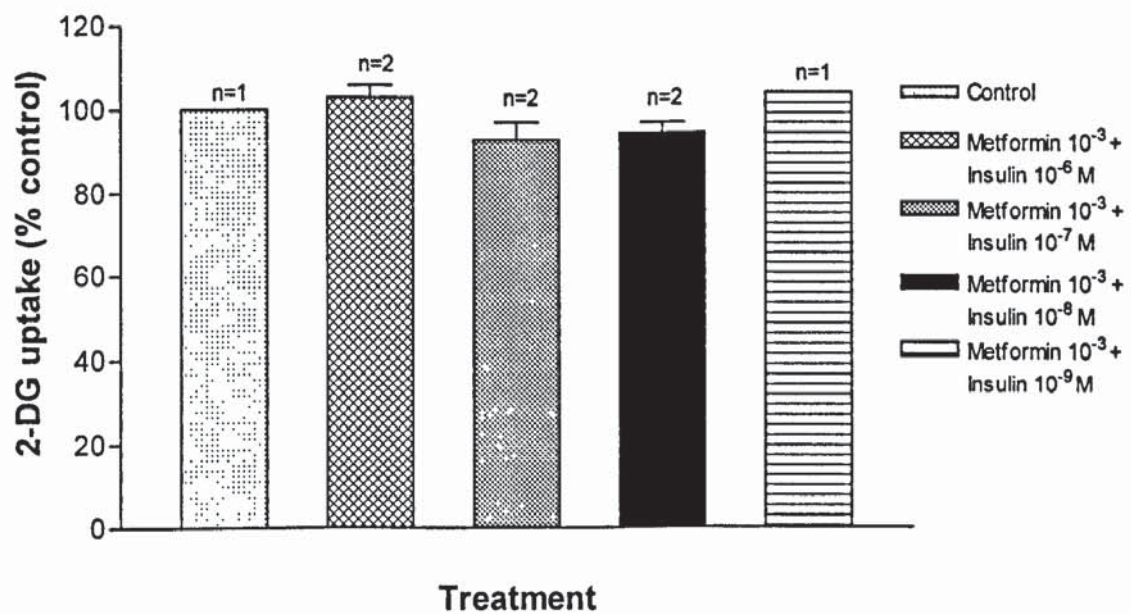


Figure 5.7.4: Combined effect of metformin (10^{-3} M) and insulin (10^{-9} – 10^{-6} M) at 24h, on the uptake of 2-Deoxy-D-glucose by A7r5 vascular smooth muscle cells. Data are expressed as percentage of control. Values where appropriate are mean \pm SEM.

Uptake of 2-Deoxy-D-glucose by A7r5 vascular smooth muscle cells.

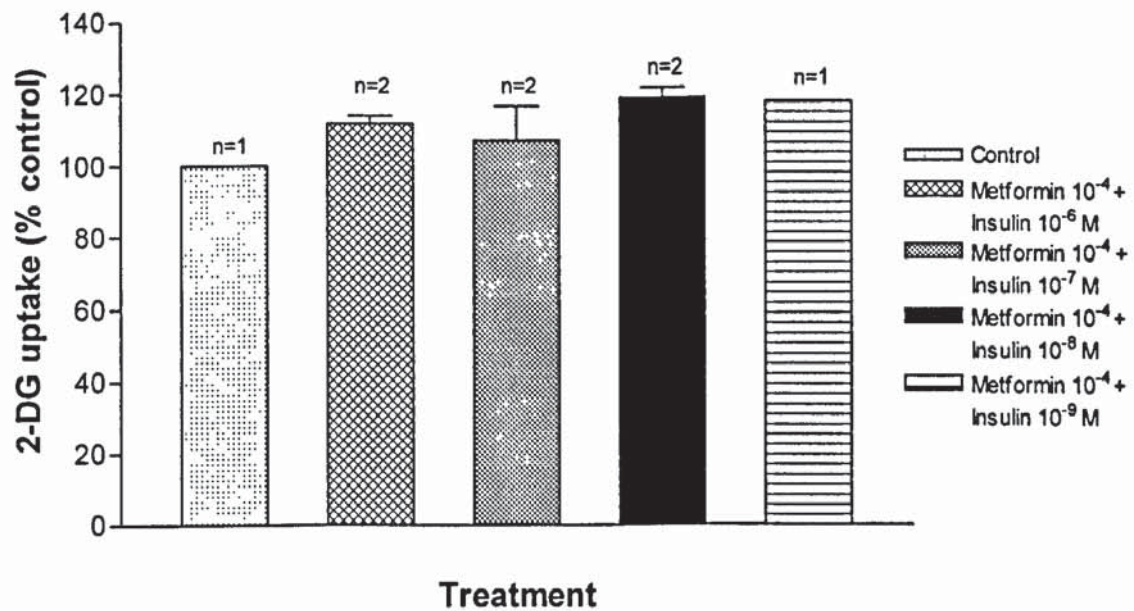


Figure 5.7.5: Combined effect of metformin (10^{-4} M) and insulin (10^{-9} – 10^{-6} M) at 24h, on the uptake of 2-Deoxy-D-glucose by A7r5 vascular smooth muscle cells. Data are expressed as percentage of control. Values where appropriate are mean \pm SEM.

Uptake of 2-Deoxy-D-glucose by A7r5 vascular smooth muscle cells.

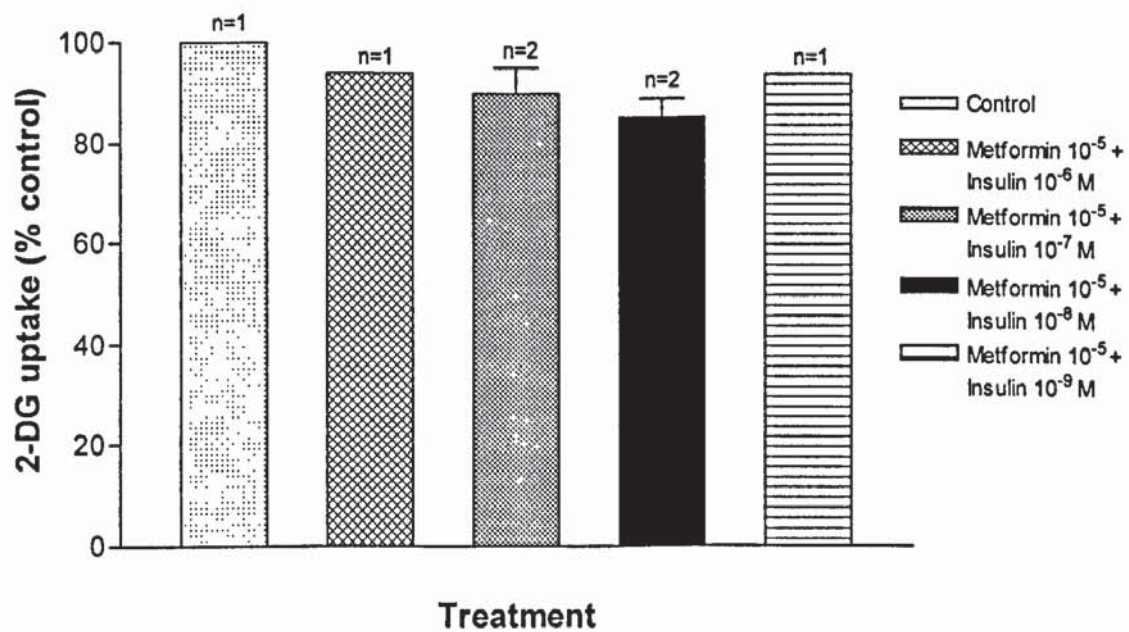


Figure 5.7.6: Combined effect of metformin (10^{-5} M) and insulin (10^{-9} – 10^{-6} M) at 24h, on the uptake of 2-Deoxy-D-glucose by A7r5 vascular smooth muscle cells. Data are expressed as percentage of control. Values where appropriate are mean \pm SEM.

Figures 5.8.1 and 5.8.2: Effect of noradrenaline (10^{-6} M) and metformin (10^{-3} M) alone and in combination on intracellular calcium levels in A7r5 smooth muscle cells incubated with Fura-2 (5×10^{-6} M) and excited using the fluorescence wavelength 360:380nm. Noradrenaline perfusion (1 minute) resulted in clearly defined intracellular calcium peaks whereas metformin perfusion (15 minutes) resulted in a transient rise in intracellular calcium levels (5.8.1). Metformin, when perfused alone for approximately 20 minutes, resulted in no obvious effect upon intracellular calcium levels (5.8.2). Numbers above the trace indicators of intracellular calcium fluorescence relate to the colour plates situated at the foot of figures 5.8.1 and 5.8.2. Metformin administration is represented by the blue trace on the fluorescence indicator graph; thapsigargin perfusion is represented by the red trace. A colour bar (figure 5.8.2) represents changes in the intensity of the intracellular calcium fluorescence, with green representing basal levels and red representing stimulated levels. This colour range should be related to the colour plates situated at the foot of each figure as a visual estimation of fluorescence intensity. The colour lines on the trace indicator graph represent regions of cells selected for analysis.

Figure 5.8.3: Effect of noradrenaline (10^{-6} M) and metformin (10^{-3} M) alone and in combination on intracellular calcium levels in L6 skeletal muscle cells incubated with Fura-2 (5×10^{-6} M) and excited using the fluorescence wavelength of 360:380nm. Noradrenaline perfusion (1 minute) clearly stimulated intracellular calcium levels in several cells on more than one occasion. Metformin (10^{-3} M), when perfused onto L6 cells, had no obvious effect upon intracellular calcium levels. Simultaneous perfusion of noradrenaline (10^{-6} M) and metformin (10^{-3} M) caused intracellular calcium peaks to occur; such peaks were, however, less pronounced than observed following noradrenaline perfusion alone. As with previous figures, colour plates at the foot of figure 5.8.3 represent numbers above the trace indicators of calcium fluorescence and represent different stages during the experimental period. The colour bar in figure 5.8.2 should be related to the colour plates as a measure of fluorescence intensity.

Figure 5.8.1 Applications of 1 μ M Noradrenaline in the absence and presence of 1mM Metformin
A7r5 cells incubated with 5 μ M Fura2-AM

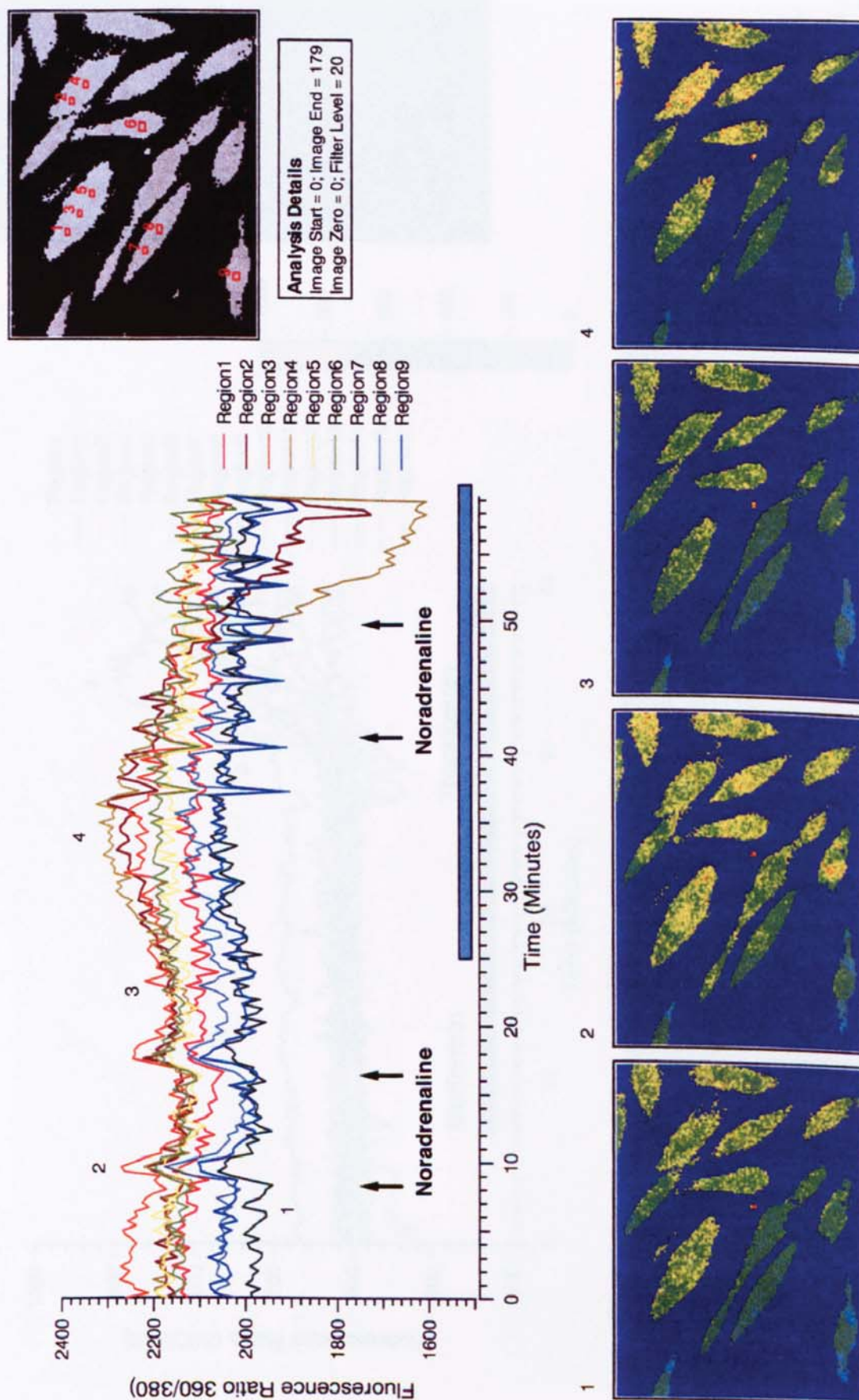
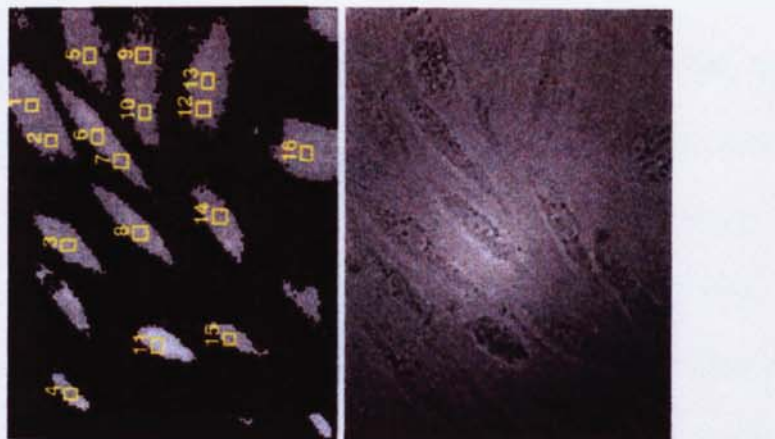
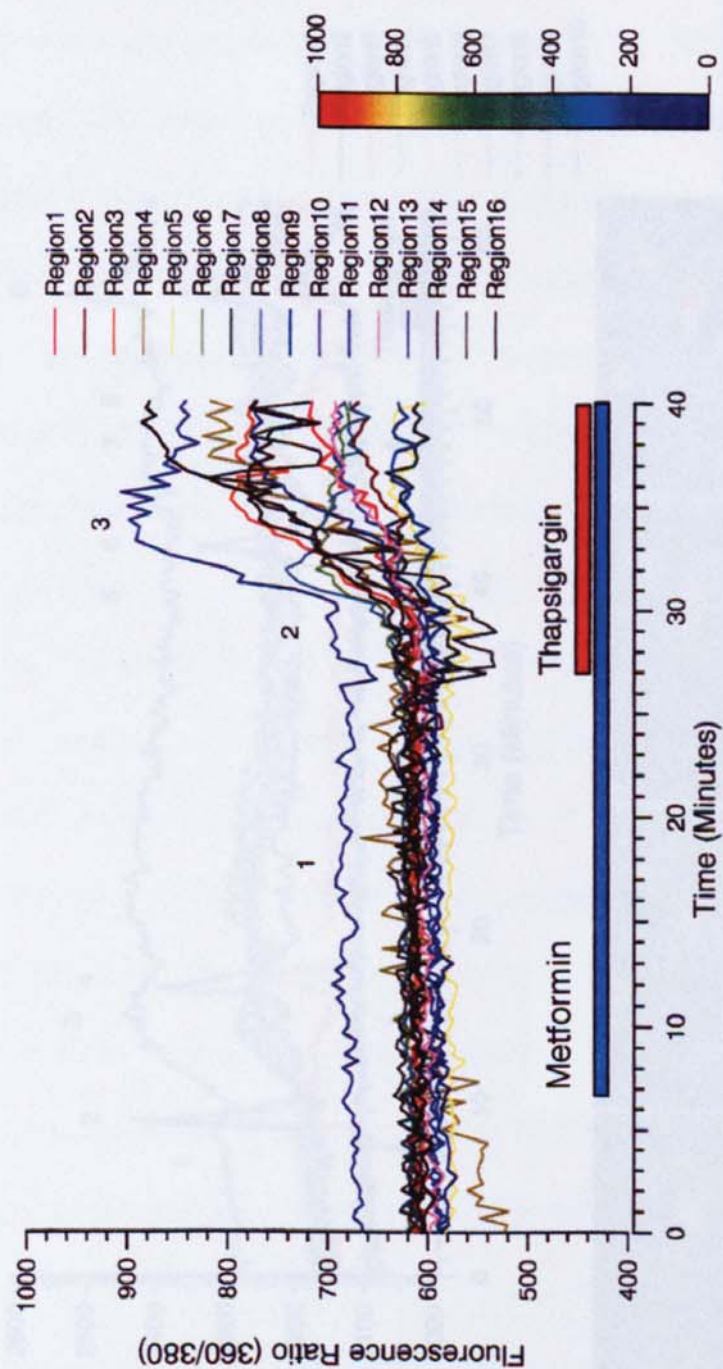


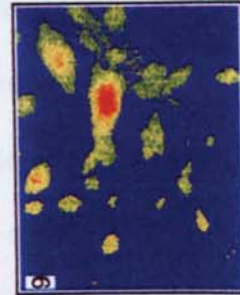
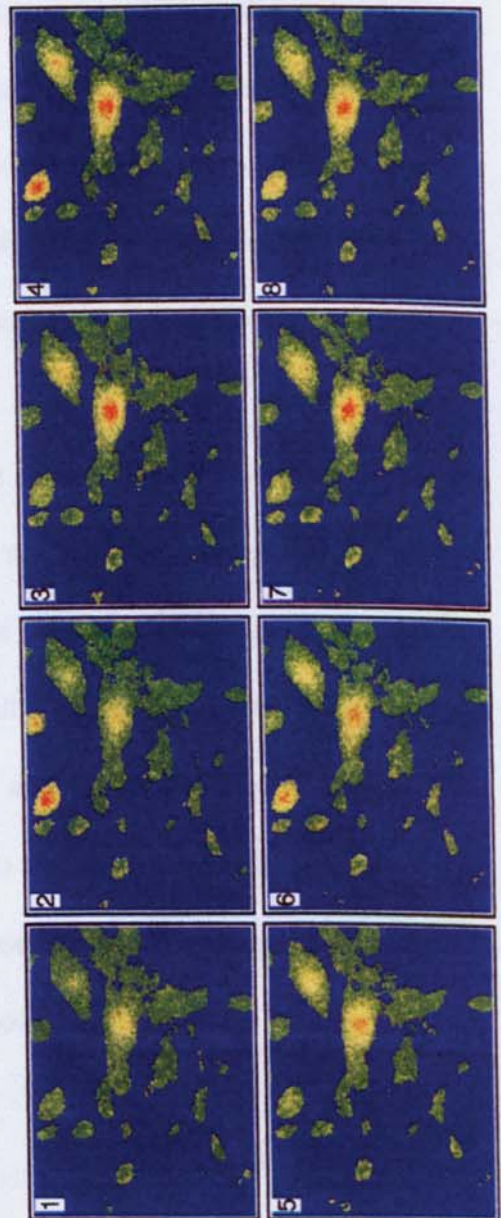
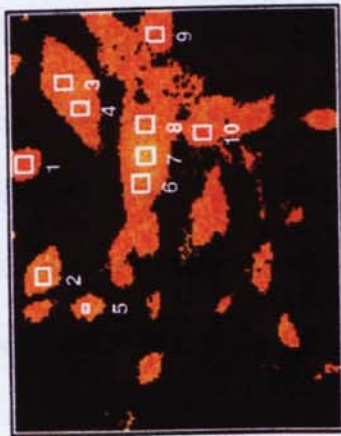
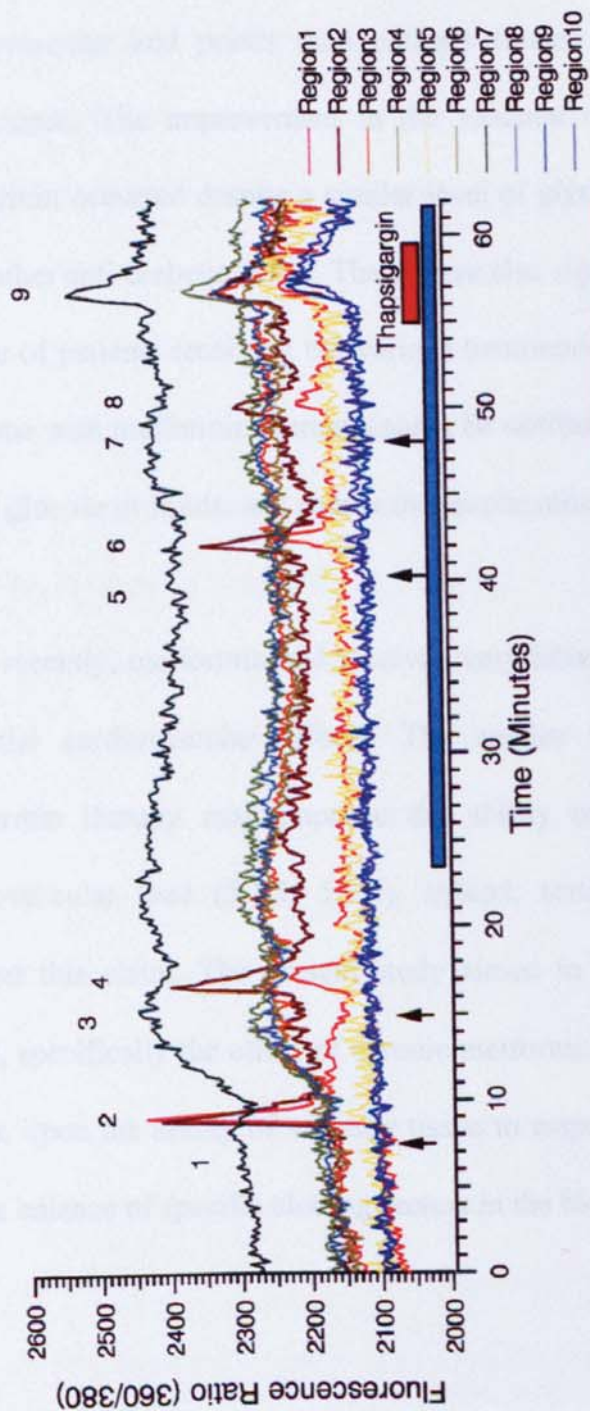
Figure 5.8.2 A7r5 cells incubated with 5 μ M Fura2-AM
Application of Metformin and Thapsigargin



Analysis Details
Image Start = 0; Image End = 121
Image Zero = 0; Filter Level = 20

Figure 5.8.3

Applications of 1 μ m Noradrenaline in the absence and presence of 1mM Metformin
L6 cells incubated with 5 μ M Fura2-AM



Analysis Details

Image Start = 0; Image End = 375
Image Zero = 0; Filter Level = 20

5.5 Discussion:

Greater than 80% of mortality rates in diabetics can be attributed to cardiovascular complications. Any intensive drug treatment regimens that improve glycaemic control are usually associated with reduced cardiovascular morbidity and mortality. According to the UKPDS (1998), metformin therapy in type 2 diabetic patients, treated throughout with the drug for an average of over 10 years, showed a greater reduction in the incidence of micro- and macrovascular end points than patients treated with alternative anti-diabetic compounds. The improvement in the vascular outcome of patients receiving metformin occurred despite a similar level of glycaemic control as that achieved with other anti-diabetic drugs. There were also significant differences in the lipid profile of patients receiving the various treatments. Thus, the improved vascular outcome with metformin therapy cannot be attributed only to improved control of blood glucose or lipids; and some other explanation must be sought.

Until recently, metformin had received very little attention with reference to its potential cardiovascular effects. The studies reported herein suggest that metformin therapy may improve the ability of vascular tissue to adapt to cardiovascular load (5.1.3, 5.3.4). Indeed, results from the UKPDS (1998) support this claim. The present study aimed to address these effects in some detail, specifically the effect of chronic metformin therapy upon total cholesterol levels, upon the ability of vascular tissue to respond to agonist stimulation, and on the balance of specific clotting factors in the blood.

In order to understand the effect of metformin upon vascular responsiveness, it is important to understand how the activity of vascular smooth muscle is maintained at a membrane and cellular level. Smooth muscle cell membranes are excitable membranes, they contain ion channels sensitive to changes in membrane potential and agonist stimulation. In arteries such as the thoracic aorta, rapid contractions brought about via changes in membrane potential play little part in the maintenance of arterial tone. Conduit arteries, like thoracic aorta, require maintenance of tone rather than rapid contraction and relaxation (Hirst and Edwards, 1989). Arterial tone is maintained by slow contractions and relaxations, and may occur independently of alterations in membrane potential.

In small resistance arteries, smooth muscle cell membranes exist in a state of polarisation of approximately -70mv in the intracellular compartment. If the cell membrane becomes depolarised in any way, a threshold may be reached to generate an action potential. This threshold exists at around -40mv , and movement of the membrane potential above this generates an action potential resulting in vessel contraction. Conduit arteries also demonstrate a resting membrane potential of between -60 to -70mv but do not generate large action potentials. They are instead regulated to maintain tone via slower more controlled responses (Hirst and Edwards, 1989).

Contractility of vascular smooth muscle is under the overall control of calcium ions. Conduit arteries contain substantial amounts of intracellular calcium, stored within an extensive network of sarcoplasmic reticulum (Somlyo, 1980). This has been verified using rat thoracic aorta (Ashida *et al.*, 1988). This allows conduit

arteries to generate contractile responses independently of the influx of extracellular calcium, although sustained contractions may utilise extracellular calcium sources.

The mechanisms involved in the binding of NA to its receptor and the generation of a contractile response are complex. Vascular smooth muscle has poor innervation, and sympathetic inputs generally impinge on the adventitial surface of arteries rather than penetrate the smooth muscle itself (Hirst and Edwards, 1989). Thus, contraction of vascular smooth muscle achieved via NA may depend on the concentration of the transmitter released, the density of α_1 receptors, and the distance the transmitter must diffuse to bind to its receptor. Accordingly, the excitability of smooth muscle cells is linked to the depth of innervation (Bülbring and Tomita, 1987).

The noradrenergic receptors are G-protein linked. Interaction of NA with its receptor initiates a transmembrane signal that allows interaction of the GDP-bound G-protein with the agonist and receptor complex (Shaw and McGrath, 1996). This interaction allows for GDP (guanosine diphosphate) to be replaced by GTP (guanosine triphosphate) which becomes tightly bound to the α subunit of the G-protein. Binding of GTP in turn initiates a conformational change in the inactive α subunit allowing the β and γ subunits to dissociate, leaving the active α subunit with GTP tightly bound (Northup *et al.*, 1983). In vascular smooth muscle it is the activated α subunit of the G_p family/form of G-protein that brings about muscular contraction via second messenger generation.

5.5.1 Second Messenger Systems:

Activation of the noradrenergic G_p -protein linked receptor leads to activation of PLC via PLC and $G_{p\alpha}$ interaction. PLC in turn mediates the formation of myo-inositol-1,4,5-trisphosphate (IP_3) and diacylglycerol (DAG) from the hydrolysis of phosphatidylinositol-4,5-bisphosphate (PIP_2) (Bülbring and Tomita, 1987). IP_3 is known to stimulate the release of calcium from intracellular stores via specific receptor interactions, which ultimately results in calcium and calmodulin association and subsequent actin-myosin interactions (Berridge, 1993).

According to Kamm and Stull (1985), the fundamental apparatus for muscular contraction, namely actin and myosin, are present in all smooth muscle cells. Briefly, contraction is achieved by interaction between thick myosin heads and thin actin filaments operating in a sliding pattern. This process is cyclical in nature, with the myosin heads undergoing a conformational change once attached to allow attachment further along the actin filaments. This process is energy-dependent, and derived from ATP hydrolysis. In addition to actin and myosin, there are a number of additional proteins thought to play a role in smooth muscle contraction, particularly in tonic contractions. Since this thesis fails to focus on the mechanistic aspect of vascular contractility, these proteins will not be discussed further.

The development of force in vascular smooth muscle is dependent ultimately upon phosphorylation of myosin's regulatory light chain (MLC_{20}) by myosin light chain kinase (MLCK) (Gailly *et al.*, 1997). According to Adelstein and Eisenberg (1980) and Stull (1980), MLCK requires interaction between active

calmodulin and the catalytic subunit of MLCK. When activated by the binding of calmodulin, MLCK then phosphorylates myosin P-light chain. Phosphorylation results in actin-myosin ATPase activity, actin-myosin interaction, and subsequent muscular contraction (Somlyo and Himpens, 1989).

It is generally agreed that contraction in vascular smooth muscle involves two distinct phases, a fast and a slow component (Bohr, 1963). Indeed, according to Rinaldi and Cingolani (1992), these phases can be defined according to the source of calcium initiating the response. The fast component of the response is generated by release of intracellular calcium from organelles such as the sarcoplasmic reticulum (SR). The slow response, however, may depend upon the influx of extracellular calcium (Bohr, 1963). Thus, a slower, more sustained contractile response may require calcium supplied from extracellular sources, or additional pathways operating at lower intracellular calcium concentrations.

Current literary publications relating to this sustained contraction in vascular smooth muscle imply a role of additional proteins in regulating this effect. Such pathways may or may not be intimately linked to the PKC pathway. Numerous signalling pathways have been implicated in the calcium-sensitising effect, thereby allowing sustained contractions; these include PKC, and Rho-kinase (Kitazawa *et al.*, 2000).

Myosin II is believed to be the only known substrate for MLCK (Horowitz *et al.*, 1996). The activity of myosin II, the most important protein in smooth muscle contractility, may be influenced by a variety of pathways. As briefly mentioned,

calcium sensitisation is believed to play an important role in sustained smooth muscle contractions. Somlyo and Somlyo (2000) suggest such calcium sensitisation is achieved through Rho-kinase. Rho-A is a monomeric G-protein that cycles between inactive (GDP-bound) and active (GTP-bound) forms (Kawano *et al.*, 1999). The activated form of the Rho-A in turn activates a Rho-kinase which phosphorylates the myosin binding subunit (MBS) of myosin phosphatase, leading to inhibition of myosin light chain phosphatase (MLCP) activity (Kimura *et al.*, 1996). Inhibition of phosphatase activity permits phosphorylation of myosin light chain (MLC) to proceed, and therefore contraction. The protracted tonic contraction in vascular smooth muscle may be a consequence of extracellular calcium influx, and can be attenuated by inhibitors of Rho-kinase. Specific inhibitors of Rho-kinase have been shown to correct blood pressure in some rat models of hypertension (reviewed by Kawano *et al.*, 1999).

The second messenger pathways involved in the contraction of smooth muscle are reviewed by Bülbring and Tomita (1987). DAG is the second product generated by the hydrolysis of PIP₂, and is believed to cause activation of PKC. According to Malarkey *et al.* (1996), a variety of intracellular proteins have been identified as targets for activated PKC; these include, amongst others, MLCK. As such, both the rapid and sustained phases of the contractile response are believed to involve PKC in some manner. Ikebe and Brozovich (1996) suggest that PKC activated via agonist and G-protein interaction inhibits the enzyme MLCP, resulting in force enhancement.

Regulation of MLC and its role in smooth muscle contraction may be achieved by two mechanisms. One such mechanism involves an increase in the activity of the phosphorylating enzyme. The second mechanism involves decreasing the activity of the same enzyme through G-proteins and second messengers (Kitazawa *et al.*, 1991; Kubota *et al.*, 1992). Indeed, as detailed by Kitazawa *et al.* (1999), increased sensitivity towards calcium (i.e. calcium sensitisation) is achieved through a net increase in MLC phosphorylation induced by decreased MLCP activity. No effect is seen on MLCK activity. In recent years, a specific inhibitor of MLCP has been identified and is expressed in smooth muscle (Kitazawa *et al.*, 2000). According to these authors, the inhibitory effect of CPI-17 upon MLCP activity can be increased substantially by PKC-mediated phosphorylation. This increases the calcium sensitivity of MLC phosphorylation and therefore contraction.

The studies undertaken by the above authors highlighted that increased intracellular calcium was not required to modulate MLCP activity. In conclusion, the authors suggest that isoforms of PKC that are calcium-independent and/or Rho-kinases may be involved in this sensitisation pathway. The complex regulatory functions of the many different isoforms of PKC remain to be fully appreciated (Way *et al.*, 2000). However, the structure and function of those currently known to exist is comprehensively reviewed by Webb *et al.* (2000) and will not be discussed any further in this context.

Evidence conveyed by Way *et al.* (2000) and Malarkey *et al.* (1996) certainly support a theory for sustained contraction via calcium- and DAG-independent forms of PKC; this would enable contraction to proceed in conditions of low

intracellular calcium. Support for this hypothesis stems from Khalil *et al.* (1992), who noted that in ferret aorta, when stimulated with NA, PKC_ε (calcium-independent form) is translocated to the plasma membrane following inducement of calcium-independent contractions. Further support stems from Rasmussen *et al.* (1987), whose hypothesis involves a role for PKC in the maintenance of contraction, even at low intracellular calcium concentrations. However, despite this and other lines of evidence, the role PKC plays in the maintenance of contraction remains open to wide debate.

In addition to the pathway outlined above, DAG may be derived from an additional route. During agonist-induced contractions, DAG may be derived from phosphatidylcholine hydrolysis, mediated by phospholipase D (PLD) (Horowitz *et al.*, 1996). DAG derived via this route is ultimately dependent upon the force generating agonist. In contrast to the PIP₂ hydrolysis pathway, DAG generated via PLD does not result in IP₃ generation. As such, mobilisation and release of intracellular calcium would not occur.

Thus, from the pathways outlined above, it is evident that regulation of vascular smooth muscle contraction is a complex process involving numerous pathways that may operate independently or in synergy. This subject is complicated further by the possibility that if these pathways do indeed act synergistically, at what point do they synergise, and what is the factor(s) responsible for this convergence. Nevertheless, it is clear that in order for contraction to initially occur, calcium plays a fundamental role.

5.5.2 Smooth Muscle Relaxation:

Relaxation of vascular smooth muscle, as with contraction, is fundamentally controlled by the prevailing intracellular calcium levels. The NO pathway, detailed in the introduction to this chapter, accounts for endothelium-dependent vasodilation in arteries such as thoracic aorta (Mieyal *et al.*, 1998). The pathways regulating smooth muscle contraction were covered extensively in the previous section. However, the relaxation response in vascular smooth muscle involves modulation of this regulation.

Lee *et al.* (1997) provide evidence for cGMP activating the enzyme MLCP resulting ultimately in calcium desensitisation and is supported by reports from Wu *et al.* (1996). Additional mechanisms may also function, possibly synergistically, and involve increased sequestration of intracellular calcium, and reducing intracellular calcium levels by attenuating extracellular influx, stimulating efflux, and promoting hyperpolarisation (Lincoln and Cornwell, 1993).

Evidence that soluble guanylate cyclase mediates the relaxation response is supported by experimental evidence utilising a specific activator of soluble guanylate cyclase (Wegener *et al.*, 1997). One particular form of cGMP-dependent protein kinase is distributed extensively in vascular smooth muscle; cGMP-dependent kinase I α . As reviewed by Lohmann *et al.* (1997), activation of this kinase results in decreased intracellular calcium levels through phosphorylation of the IP₃ receptor. Furthermore, Lincoln *et al.* (1995) provides evidence for protein kinase G (PKG) phosphorylating IP₃ receptors. It is believed

that PKG is almost exclusively associated with proteins in the SR, such as the IP₃ receptor, and may influence their function via phosphorylation.

In addition, other mechanisms have been proposed and may account for reducing intracellular calcium levels. These include inhibition of voltage-dependent calcium channels, inhibition of IP₃ formation, stimulation of Na⁺-Ca²⁺ exchange, and stimulation of Ca²⁺-activated K⁺-channels. However, the exact mechanisms by which cGMPIα induces relaxation are unknown. According to Surks *et al.* (1999), the relaxant response in vascular smooth muscle is characterised by reduced intracellular calcium levels and by calcium desensitisation, a consequence of MLCP stimulation. This pathway may play a fundamental role in vascular smooth muscle relaxation in response to NO and cGMP.

The sustained generation of NO in response to stimulation by agonists is dependent upon the influx of extracellular calcium (Demirel *et al.*, 1994). Indeed, activation of the enzyme responsible for synthesising NO (nitric oxide synthase, NOS) requires increased intracellular levels of calcium via external sources and internal stores (Demirel *et al.*, 1994). A calcium-dependent form of NOS has recently been confirmed to exist in bovine vascular smooth muscle cells, and may act to regulate smooth muscle contraction via NO generation (Brophy *et al.*, 2000).

The increase of intracellular calcium in endothelial cells, following agonist stimulation, is achieved initially by the release of calcium from intracellular stores, followed by sustained extracellular calcium influx. Ca²⁺-sensitive K⁺-

channels play an important role in potentiating this calcium influx, inducing hyperpolarisation (Chen and Cheung, 1992). As detailed by Demirel *et al.* (1994), opening of Ca^{2+} -sensitive K^{+} -channels, following initial intracellular calcium release, causes membrane hyperpolarisation and permits prolonged calcium entry which may function to allow sustained NO synthesis. NO in turn may induce smooth muscle relaxation via activation of smooth muscle guanylate cyclase and cGMP. It appears that potassium channels may play a significant role in smooth muscle relaxation in smaller arteries following stimulation by EDHF (Cocks, 1996), with NO and stimulation of soluble guanylate cyclase predominating in larger arteries.

Increases in intracellular calcium through the opening of voltage- or receptor-operated channels are regarded as the classical mechanisms by which sustained muscular contraction of vascular smooth muscle is achieved. Depletion of intracellular calcium stores following initial contractions allows extracellular calcium to enter the cell to replenish these stores. Calcium replenishment is induced by emptying of IP_3 sensitive stores and is responsible for sustaining contraction (Putney, 1986). Although the precise mechanism regulating this effect is unknown, it is invoked by alterations in the smooth muscle membrane potential, which are linked to the noradrenergic G-protein receptor. More recently, and as described previously, sensitisation of the contractile 'apparatus' by PKC isoforms may permit sustained contraction in the presence of low intracellular calcium levels (Malarkey *et al.*, 1996). Indeed, SR contain IP_3 channels and ryanodine channels, sequestering pumps, and proteins to store calcium (Berridge, 1993). IP_3 receptors on the SR influence the influx of

extracellular calcium at sites where the SR lies close to the plasma membrane. When intracellular stores are emptied, influx of calcium may be stimulated. When they are full, influx is inhibited. In addition, inositol phosphates can influence calcium channel activity. Thus, regulation of intracellular calcium levels is a highly complex process involving numerous pathways that may function independently or with partial interdependence.

As detailed by Aaronson and Smirnov (1996), NA, following agonist-receptor interaction, opens a receptor-operated channel. This channel is non-specific in nature and allows various cations to enter the cell, including calcium. In addition, the release of calcium from the SR (detailed above) activates a calcium-dependent chloride channel. The subsequent cellular depolarisation generated from the influx of extracellular calcium opens Ca^{2+} -sensitive K^{+} -channels (voltage-sensitive), allowing potassium to leave the cell and may represent a mechanism whereby the depolarisation of smooth muscle is regulated by potassium-induced hyperpolarisation. Several additional types of calcium channels also exist in vascular smooth muscle, including L-type and T-type channels (Bean, 1989; Tsien *et al.*, 1991). However, their contribution to calcium homeostasis in vascular smooth muscle remains debatable.

Evidently, calcium plays a significant role in the potentiation and protraction of muscular contraction, be it through receptor or voltage-sensitive channels. The voltage-sensitive pathway is seen as the most important pathway for catecholamine action (Bülbring and Tomita, 1987). As such, the efficient

regulation of membrane potential is crucial in maintaining functionality; this is undoubtedly reflected in potassium conductance.

Smooth muscle cell membranes, as with the majority of membranes, are readily permeable to potassium. Significant concentration and electrochemical gradients exist between intracellular (130-140mM) and extracellular (5mM) compartments (Hirst and Edwards, 1989). The resting membrane potential is in the large part dependent upon the potassium gradient across the plasma membrane. The various types of potassium channels believed to be present in vascular smooth muscle will be briefly discussed. It is not within the scope of this thesis to comprehensively categorise such ion channels. Evidence exists suggesting metformin may influence events linked with calcium flux. As such, I shall concentrate specifically on these ion channels, with brief references to those potassium channels involved in calcium homeostasis.

Ambiguity exists relating classification of potassium channels and their relative distribution in smooth muscle. It is largely assumed that the vascular smooth muscles express Ca^{2+} -sensitive, and ATP-dependent K^{+} -channels, in addition to delayed rectifier channels (K_{DR}) (Aaronson and Smirnov, 1996). According to Longmore and Weston (1990), the Ca^{2+} -sensitive K^{+} -channels are rarely open at the resting membrane potential. The role of these channels becomes apparent when intracellular calcium levels increase; potassium efflux is then stimulated, limiting the depolarising effect. Such channels are believed to attenuate the depolarising action of NA that occasionally occurs in response to high NA concentrations, as evidenced in rabbit pulmonary artery (Aaronson and Smirnov,

1996). Such channels may be closely related to a receptor-operated channel whose function is also to extrude calcium, limiting the depolarising actions of NA.

Voltage-dependent potassium channels are stimulated and open in situations involving membrane depolarisation (Nelson and Quayle, 1995). It is believed that such channels exist to rectify the depolarisation induced by agonists by permitting potassium extrusion from the cell. Voltage-gated channels may be divided into several families, delayed rectifier channels, inward rectifiers, and transient channels (Adams and Nonner, 1990). Whether each of these channel types exists in vascular smooth muscle is debatable. An inward rectification channel (K_{IR}) has been identified in certain types of smooth muscle but may not be expressed abundantly in thoracic aorta. Such channels become active during membrane hyperpolarisation and may also function to limit the extent of such actions. These channels have been identified in a variety of smooth muscle, and may well be a feature of smaller arteries (Nelson and Quayle, 1995).

ATP-dependent K^+ -channels are believed to exist in vascular smooth muscle. Their function is seen as protective and they will open under hypoxic conditions, causing tissue relaxation and increased blood flow. A review by Nelson *et al.* (1990) suggests such channels exist in aortic smooth muscle. ATP-dependent K^+ -channels are sensitive to the intracellular ATP concentration; high ATP levels result in channel closure. Potassium channels have been identified in rat aorta. These channels were activated by reduced intracellular ATP levels and thus may play a role in the regulation of arterial tone (Longmore and Weston, 1990).

However, the role ATP-dependent K⁺-channels play in regulating vessel tone in large conduit arteries remains unclear.

5.5.3 Mechanisms through which Metformin may influence Vascular Responses:

Chronic metformin therapy in mice, over a eight-nine month period, resulted in significantly greater arterial contraction and relaxation compared to age-matched cholesterol fed and control groups (5.1.3, 5.3.4, 5.3.5). Metformin appears to improve the compliance of vascular tissue independently of any major effect upon circulating total cholesterol or glucose levels (as indicated in the data presented herein). Indeed, Sirtori *et al.* (1984) reported improved vascular blood flow in non-diabetic patients with peripheral vascular disease following metformin therapy. In this study there was minimal effect on lipoprotein levels. However, HDL levels were seen to increase marginally. Similarly, chronic metformin therapy was seen to increase peripheral blood flow by 30%, in a separate study (Montanari *et al.*, 1992).

Metformin has recently been reported to influence the contractile properties of rat tail artery by decreasing levels of intracellular calcium (Chen *et al.*, 1997). In light of this evidence it may be feasible that metformin may influence arterial contraction in other vascular beds in a similar manner. Since regulation of intracellular calcium concentration and extracellular calcium influx are essential in maintaining vascular tone, both of these sources of calcium play fundamental roles in the contractile response, as previously discussed.

Chen *et al.* (1997) suggest a possible mechanism through which metformin may influence smooth muscle excitability. Similar effects have been confirmed in studies involving smooth muscle cells herein. The above authors utilised a significantly higher concentration of metformin (1-30mmol/l) than used in the present studies, and administration was acute whereas the cholesterol feeding studies involved chronic administration. In addition, Chen *et al.* (1997) used rat tail artery from which the endothelium had been removed. Arteries were then contracted using phenylephrine and relaxed using high doses of metformin (1-30mmol/l). Metformin, at high concentrations, resulted in repolarisation of the artery and reduced magnesium influx (Mn^{2+}). According to the above authors, repolarisation was identified as the most likely mechanism by which metformin achieved vessel relaxation since no change was observed in the intracellular sensitivity to calcium. In addition, there were no associated changes in intracellular calcium via voltage-gated channels, or indeed through calcium efflux.

Further evidence in support of a role for metformin in influencing calcium flux is provided by Sharma and Bhalla (1995). These authors noted that metformin, at therapeutic concentrations, significantly reduced the increase in intracellular calcium following agonist stimulation. The mechanism through which metformin achieves this is presently unknown. Nevertheless, the above authors make the point that a variety of anti-diabetic agents have been shown to influence calcium flux. These include the thiazolidinediones, specifically ciglitazone. According to the above authors, metformin can also influence calcium flux across pancreatic β

cells, an area previously thought to be exclusive to sulphonylureas which close ATP-dependent K^+ -channels on β cells.

It is evident from the results detailing the contractile response of thoracic aorta that cholesterol feeding resulted in increased vascular contractions compared with controls (5.3.4). This result is perplexing, since the hypothesis originally envisioned was one of a less responsive vessel to stimulation by agonists. Clearly, no significant cholesterol deposition was evident within the arterial wall (figure j, appendix I). Wong (1996) provides evidence that cholesterol feeding in rabbits leads to increased membrane excitability to depolarising agents compared to control animals. It is hypothesised that cholesterol feeding may disrupt the integrity of the plasma membrane and membrane receptors, rendering the membrane more sensitive to stimulation. Certainly, the results presented here support this hypothesis in terms of consequence, i.e. greater aortic contractility of cholesterol fed animals. However, the present study does not support the hypothesis in terms of cause. As stated, cholesterol accumulation could not be detected by standard histochemical means within the vessel wall. This suggests an alternative mechanism may operate in the murine model, a model notoriously difficult for inducing hypercholesterolaemia. Alternatively, the ability of this model to compensate for the high cholesterol influx may account for a less pronounced effect than that reported in rabbit. Indeed, the results presented herein demonstrate a clear effect of cholesterol feeding on vascular reactivity, although not as large as those reported by Wong (1996).

Aorta was most responsive to NA in animals fed a cholesterol-enriched diet and treated with metformin. The increased sensitivity of aorta from metformin treated animals could in theory be attributed to an improved lipoprotein profile with this drug. Prolonged cholesterol feeding could result in changes in membrane structure and possibly in circulating lipoprotein particle size and distribution. Metformin lowers circulating LDL levels (Rains *et al.*, 1989) and marginally increases HDL levels (Cusi and DeFronzo, 1998). It is conceivable that the mechanism by which metformin increases tissue compliance may act in unison with the effect of high cholesterol feeding, since both findings were evident in the present studies.

Relaxation of isolated aorta was significantly greater in the metformin treated group compared with control (5.3.5). This once again supports the hypothesis that metformin may influence the compliance of vascular tissue. Animals fed a high cholesterol diet were least sensitive to Ach, with control animals achieving greater relaxation. Although these results are not statistically significant, they may be suggestive of a role of lipoproteins in attenuating relaxation in response to certain vasodilators. Chin *et al.* (1992) provide evidence for both native and oxidised LDL in attenuating the vasodilator response by inactivating the relaxing factor from the endothelium. In addition, this lipoprotein effect may also potentiate vasoconstriction by interacting directly with vascular smooth muscle (Galle *et al.*, 1990). Alternatively, oxidised LDL has been shown to inhibit signalling pathways mediated by G_i-proteins (Liao and Clark 1995). Once again, metformin's effect to alter the lipoprotein profile may in part account for the

improved relaxation in response to vasodilators. This seems most likely for the direct action of oxidised lipoproteins upon vascular smooth muscle.

Utilising diabetic models to study vascular reactivity requires careful consideration of the end points to be determined. There are many relevant parameters and variables to consider, of which the lipoprotein fractions and insulin represent only two of many. Diabetes is a progressive disease affecting a multitude of tissues and metabolic functions. Indeed, thoracic aorta has been shown to exhibit increased relaxation following the induction of diabetes, with subsequent impairment of relaxation later in the disease process (Pieper, 1999). The enhanced relaxation in this study was due to an increase in NO release; the reasons for which are currently unknown. What is evident from such a study is that determining the effect of a self-induced disease state upon vascular tissue function is complicated by time-dependent adaptations to disease duration. Although in the present studies attempts to induce hypercholesterolaemia in lean mice failed to show any macroscopic alterations in vessel morphology, this does not necessarily suggest that subtle changes in vessel and membrane structure, and therefore functionality of this tissue were not induced.

Diabetes can affect a variety of pathways intimately involved in modulating vascular tone. For example, rabbit aorta exposed to hyperglycaemia demonstrated impaired relaxation and increased generation of vasoconstrictor substances (Tesfamariam *et al.*, 1991). This impaired relaxation appeared to involve activation of PKC. The above authors suggest that elevated glucose may explain the increased DAG synthesis and subsequent PKC activation. Conversely, in a

study by Okumura *et al.* (1991), the composition of DAG altered during diabetes and was associated with a decrease in its levels and presumably its actions, one of which is activation of PKC. Evidence also exists for increased contractile responses in the aorta of diabetic rats. The enhanced contractions were considered to be a consequence of PKC activity, possibly through enhanced levels of DAG (Adebe and MacLeod, 1990).

The present study provides evidence of a possible role for metformin in influencing calcium flux across plasma membranes (5.8.1). Scarborough and Carrier (1984) performed studies utilising isolated aorta from diabetic rats, and noted a greater contractile force in response to NA compared with controls. There are implications for increased α -adrenoreceptor-mediated contractions in these vessels in diabetes, involving both α -1 and 2 subtypes. The enhanced contractions may be in part related to increased calcium dependency from extracellular routes. The above authors concluded that the α -2 adrenoreceptor subtype was specifically involved in the enhanced contractions seen in thoracic aorta (Scarborough and Carrier, 1984). Similarly, insulin-dependent diabetes may also affect intracellular levels of free calcium in vascular smooth muscle stimulated with NA. Tam *et al.* (1997) noted an alteration in receptor-linked calcium signalling in response to NA, with lower concentrations of NA eliciting a response in diabetic vascular smooth muscle. This relationship was found to create a leftward shift in the dose-response to NA and calcium, and reduce the maximal peak response. The dose-response relationship in the present studies in metformin treated animals also demonstrated a leftward shift, a steeper slope, and a small reduction in the EC_{50} value. This may represent a greater sensitivity in

metformin treated tissues for agonist stimulation and implies that maximal contraction may be achieved at lower drug concentrations.

High concentrations of metformin are known to impose growth-inhibiting effects upon vascular cells (Bünting *et al.*, 1986). Although this effect was seen *in vitro*, it was achieved utilising cells from diabetic and non-diabetic individuals. If this effect is characteristic of metformin then similar effects may be expected *in vivo*. Metformin has been purported to have moderate anti-atherogenic effects, in part, through lowering of plasma VLDL and LDL levels and increased HDL levels (Bailey, 1992). This mechanism may operate in unison with the growth-inhibiting effect to promote the anti-atherogenic properties of metformin. Unfortunately, the diameter of aortic vessels, as a crude indicator of vascular proliferation, could not be accurately determined during the present studies. Although accumulation of cholesterol in the vessel lumen or wall was not detected in control, cholesterol fed, or metformin and cholesterol treated groups, no conclusions (positive or negative) can be drawn relating to differences in the thickness of the aortic wall between these groups.

As detailed at the beginning of this chapter, insulin may act directly upon vascular tissue influencing its tone (Baron, 1994). The normal vasodilatory action of insulin is diminished in diabetes and may lead to reduced glucose delivery to peripheral tissues (Peuler *et al.*, 1997). In addition, insulin-like growth factor-1 (IGF-1) is produced by vascular smooth muscle and may also have important roles in the functionality of this tissue (Dominguez *et al.*, 1996). Metformin has previously been shown to increase insulin sensitivity (Cusi and DeFronzo, 1998)

and is known to increase glucose uptake in a variety of cell types, including adipose tissue (Fantus and Brosseau, 1986), and skeletal muscle (Bates, 1999), through effects upon the insulin receptor. In addition, metformin may increase glucose uptake independently of the action of insulin, via increased translocation of glucose transporters (Klip *et al.*, 1992; Hundal *et al.*, 1992). Results from studies performed by Dominguez *et al.* (1996) indicate that metformin stimulates both insulin and insulin-like growth factor receptors at their tyrosine kinase domains in vascular smooth muscle from rat. Metformin at high doses was also found to stimulate glucose uptake.

The stimulation of glucose uptake by both metformin and insulin was investigated in the present study. Experiments were performed utilising a smooth muscle cell line (A7r5) derived from embryonic DB 1X rat thoracic aorta, and L6 skeletal muscle cells. 2-Deoxy-D-Glucose uptake (2-DG) was determined in the presence of metformin and insulin as individual and combined treatments. Metformin (10^{-3} M) significantly enhanced glucose uptake in L6 cells (5.6.1). Insulin also stimulated glucose uptake significantly above control values at concentrations of 10^{-8} M and above, also in the L6 cell line (5.6.1). Studies performed previously at Aston University (Bates, 1999) comprehensively determined that both metformin and insulin stimulate glucose uptake in the L6 rat skeletal muscle cell line; the results of studies presented herein confirm these earlier observations. A significant additive effect was also evident when both drugs were present at submaximally stimulating concentrations (5.6.2).

Glucose uptake in the A7r5 smooth muscle cell line was, however, clearly not stimulated by metformin or insulin at concentrations proven to enhance uptake in the L6 cell line. Significant glucose uptake was evident, however, at high concentrations of metformin (10^{-2} M; figure 5.7.2). A study by Dominguez *et al.* (1996) reported an approximate 50% additive effect over controls of metformin on 2-DG uptake in cultured vascular smooth muscle cells from rat. In the present studies, the additive effect of metformin on stimulating 2-DG uptake at the approximate concentration used in the Dominguez study was 16%, significantly less than that reported by the above authors. Continued passaging of the A7r5 cell line may have led to an alteration in the number or distribution of undefined receptors for metformin, and may account for the differences between these studies.

Furthermore, the smooth muscle cell line was grown initially in high-glucose medium (25mmol/l) before being serum-starved in low-glucose medium (5mmol/l), prior to the addition of drugs. This step was necessary since significant glucose uptake was not achieved when the cells were maintained in high-glucose medium throughout. Furthermore, glucose uptake is ultimately reflected by cell number, and again significant uptake was not being achieved due to an insufficiently large cell population. Thus, cells were grown in low-glucose and low-serum medium in petri dishes to achieve quantitative uptake data.

Smooth muscle was not expected to demonstrate the same degree of glucose dependency as skeletal muscle since, unlike skeletal muscle, it is not a major site for insulin-stimulated glucose disposal. Nevertheless, the fact that both insulin and metformin could not significantly stimulate glucose flux at non-

supraphysiological concentrations suggests that insulin receptors or post-receptor signalling pathways may be limited in vascular smooth muscle, or alternatively, that as the cell passage number increased the number or sensitivity of receptors diminished. Furthermore, metformin (10^{-2} M) and insulin (10^{-8} M) failed to stimulate 2-DG uptake when incubated simultaneously (5.7.3-5.7.6). Indeed, percentage 2-DG uptake was substantially reduced in A7r5 cells following the above treatments suggesting metformin may stimulate glucose uptake through alternative pathways than those implicated in the L6 cell line.

Receptors for both insulin and IGF exist on many cell types (Pfeifle and Ditschuneit, 1983). Both polypeptides can cross-react with the opposing receptor types with low affinity and may lead to differential effects upon growth status. Pfeifle *et al.* (1982) noted that the metabolic effects of insulin were significantly greater than those of IGF, and that IGF induces greater growth-promoting effects than insulin (Pfeifle and Ditschuneit, 1983). Furthermore, these authors conclude that the expression of both insulin and IGF receptor types is dependent upon the growth state of the cells. Specifically, the transition of cells from the growing to the stationary phase resulted in a reduction in the number of insulin-specific binding sites. This was attributed to down-regulation of the insulin binding sites by serum factors. Results from this study indicated that when confluent cultures of rat aortic smooth muscle cells were transferred into serum-free medium for 1 day prior to experimentation, insulin was able to displace 125 I-labelled insulin from its binding site, a process not seen with cells grown in 10% serum. These results suggest that the high serum content of the growth medium used in the present studies may have influenced insulin binding and/or action.

The A7r5 cells utilised in the studies herein were, as previously stated, grown in high-glucose medium containing 10% serum. This unphysiological glucose concentration may have influenced insulin binding by down-regulating receptors. Although confluent cultures were transferred to low-glucose, low-serum medium (1%) prior to experimentation the medium was not serum-free and any influence the 10% serum concentration imposed on insulin receptors may have been propagated. Indeed, the results presented by Pfeifle and Ditschuneit (1983) indicate that, at a concentration of 10^{-6} M, 60% of the 125 I-labelled insulin remained bound to insulin receptors even in serum-free medium after one day. These results suggest that both insulin and possibly glucose may influence the binding and action of insulin upon propagated arterial smooth muscle cells.

Assays of factor XIII activity in mouse plasma support evidence from the literature that metformin may influence the levels or activity of clotting factors in the blood (Ariëns *et al.*, 2000), many of which are imbalanced in diabetes. Chronic metformin therapy of experimental groups from both studies maintained on a high cholesterol diet, resulted in significant reductions in the activity of this clotting factor, compared with controls (5.5.1, 5.5.2). Similarly, the cholesterol treated group (study #2) also demonstrated lower FXIII activity compared with control animals. Statistical significance was not observed between the cholesterol and metformin treated groups. There may be several reasons for this. First, the same plasma samples were used for both the cholesterol assays and the FXIII assays. As stated previously, the plasma samples were stored for prolonged periods during which time FXIII activity may diminish. In addition, haemolysis occurred in some samples despite the use of an anticoagulant and their immediate

storage on ice. This may result in the formation of small clots, possibly diminishing FXIII activity. Indeed, fibrin clots in plasma are reported to commonly hinder the accurate determination of FXIII activity (Song *et al.*, 1994). In addition, coating of the microtiter plates with mouse fibrinogen may not have been uniform since the assay is routinely used for human FXIII assays. Since the assay has not been routinely applied to murine plasma, the development of the assay described in the methods (2.6.1) represents a novel application of the human assay. Although all standard precautions and appropriate controls were undertaken, it is possible that inter-assay variations could be brought about by factors that as yet remain unidentified. All samples from control, cholesterol, and cholesterol and metformin treated mice were compared against a standard pooled plasma sample from the same strain of mouse used in the compliance experiments.

A further control to compare between assays would ideally utilise the control group from each study as the standard since these animals were not subject to any experimental manipulation. However, within-assay controls showed accuracy and reproducibility of repeats. Despite the possible limits of comparing between assays for study #1 and study #2, the results were similar for the two studies and support the hypothesis that metformin treatment may correct an imbalance in this clotting factor. The fact that cholesterol treatment also led to reduced FXIII activity levels compared with control may be indicative of a more complex relationship between FXIII activity levels and cholesterol and their function *in vivo*.

Through evidence provided in this discussion, it appears that the most appropriate interpretation for the mode of action of metformin on aortic compliance is through calcium fluxes across the plasma membrane of either the smooth muscle itself or the endothelium. The precise mechanisms influencing these events are presently not understood. In light of this view, studies were performed utilising vascular smooth muscle to determine the effect of metformin treatment upon calcium uptake using calcium image analysis.

Intracellular calcium levels in vascular smooth muscle cells (A7r5), determined through intracellular calcium fluorescence, transiently increased in the presence of metformin following noradrenergic stimulation (5.8.1). The transient increase in intracellular calcium levels observed following metformin perfusion continued for a period of approximately 10 minutes before a steady decline in intracellular calcium levels occurred. In a separate study, metformin, when perfused onto smooth muscle cells and in the absence of agonist stimulation, resulted in no quantifiable effect upon intracellular calcium levels (5.8.2).

When the effects of NA and metformin were subsequently investigated on intracellular calcium levels in the L6 skeletal muscle cell line, again no effect was seen following metformin perfusion, despite substantial intracellular calcium peaks after NA challenge (5.8.3). Repeated challenge with NA in the presence of metformin may have led to diminished and delayed calcium peaks in the L6 cells compared to previous stimulations, and may reflect a depletion of intracellular stores or diminished intracellular calcium release. However, the observed increase in intracellular calcium levels following the addition of thapsigargin

would suggest that depletion of intracellular calcium stores had not occurred. Thus, metformin may be associated with a marginally diminished contractile response, at least in L6 skeletal muscle cells. Metformin could realistically induce differing effects in cells of different origins. As such, dissimilar effects may be seen in smooth and skeletal muscle and may be related to receptor expression or second messenger systems regulating contractility.

It is important not to overstate the findings of these studies since they represent a small group of preliminary experiments. Nevertheless, metformin perfusion onto smooth muscle cells induced a visible and transient increase in intracellular calcium levels. This effect was moderately rapid and may imply a role for metformin in increasing intracellular calcium levels prior to noradrenergic stimulation. If I am permitted to extrapolate and hypothesise on these findings, and if this *in vitro* effect was to represent conditions *in vivo*, increased intracellular calcium levels, in conjunction with NA stimulation, might lead to enhanced contraction, particularly in the presence of sensitised contractile apparatus. Similarly, a greater reduction of calcium levels, as could be seen following intracellular calcium peaks, might lead to increased relaxation in the presence of sensitised second messengers and contractile apparatus, as discussed previously.

Despite the data and hypotheses presented herein, irrefutable evidence cannot be presented regarding the acute effects of metformin upon vascular reactivity in isolated cells. It is clear, however, that metformin treatment significantly influences vascular reactivity following chronic therapy independently of

cholesterol. Realistically, the acute effect investigated in these studies may have been too acute to observe a clear drug effect. Since an irrefutable effect was observed in mice treated chronically with metformin, future experiments might involve cells isolated from chronically treated animals. In these circumstances the effects of metformin upon calcium flux may be far more conclusive. Clearly, this path requires considerable investigation in the future.

Many mechanisms may be responsible for the enhanced and attenuated agonist-induced responses of aortic vessels seen experimentally and in diabetes, too many for the scope of this thesis. Nevertheless, metformin unequivocally improves the compliance of vascular tissue, partially rectifying some of the imbalances characteristic of diabetes. More importantly perhaps is the effect of metformin on tissues independent of an obvious diabetic disease state, as seen in the present studies. This indicates that metformin can exert its effects on the vasculature independently of plasma glucose and cholesterol concentrations, and in the absence of advanced vascular disease.

Chapter Six:

General Discussion

z

CHAPTER SIX: General Discussion

6.1 The Hypothesis behind this Study:

The premise of this thesis was based upon the clinical observation that metformin therapy is often associated with modest reductions in circulating cholesterol levels (Cusi and DeFronzo, 1998). Further clinical studies demonstrated that metformin may cause bile salt malabsorption in the terminal small intestine of type 2 diabetic patients (Scarpello *et al.*, 1998). The latter finding by Scarpello *et al.* (1998) prompted the hypothesis that the modest cholesterol reductions evident in hypercholesterolaemic individuals may be a consequence of this reduced bile salt reabsorption. This hypothesis led to three main areas of questioning. First, could metformin alter directly bile salt transport in the small intestine? Second, could metformin therapy reduce circulating cholesterol levels in non-hypercholesterolaemic animals? Third, is the reported beneficial effect of metformin upon macrovascular complications related to its cholesterol lowering effect, or is it independent of circulating cholesterol?

The overall aims and objectives of this study were to assess the effect of metformin upon intestinal bile salt transit *in vivo* and *in vitro*. In addition, to determine any effect upon large vessel compliance as an indicator of susceptibility to macrovascular disease. These approaches were designed to test the above hypotheses and provide insights into the possible mode of action of this drug.

6.2 Summary of Results:

The main findings from the *in vivo* studies relating to bile salt absorption were as follows. Metformin was associated with a marked reduction in the transport of ^{14}C sodium glycocholate in the ileal region of the small intestine. Conversely, metformin significantly enhanced the absorption of radiolabelled glycocholate in the jejunum. The ileal and jejunal areas represent distal and proximal regions of the small intestine, with active and passive/facilitative mechanisms operating, respectively. Metformin's effects in these regions were directly opposing. *In vitro* studies were then performed utilising everted intestinal sacs based on the technique of Wilson and Wiseman (1954) and Caspary and Creutzfeldt (1975). The aim of these studies was to determine if metformin could influence bile salt transport in this model to support the *in vivo* findings.

Metformin did not significantly alter bile salt absorption in everted intestinal sacs of the ileum. As demonstrated previously, however, bile salt transport was stimulated above control values in jejunal preparations. Interestingly, metformin was associated with significant effects on fluid transfer in both intestinal regions. Thus, bile salt absorption appears to occur independently of associated fluid movement, at least *in vitro*. Membrane preparations of the human-derived Caco-2 colonic cell line provided further support for metformin's effects *in vivo*. Metformin and the ATPase inhibitor, ouabain, significantly reduced bile salt transport in this cell model. An additive inhibitory effect was seen at high concentrations when both compounds were incubated simultaneously. Mannitol, an inert marker, was used as a measure of cell membrane integrity. Both

metformin and ouabain treatment resulted in significantly greater flux of this compound across the cell layer whilst simultaneously inhibiting bile salt transfer.

Lean mice, fed a cholesterol-enriched diet and treated chronically with metformin, demonstrated greater large vessel compliance to both contractile and relaxant agonists. Relaxation of pre-contracted tissue using Ach was greater in metformin treated animals than in control or cholesterol fed animals. This effect was, however, only visible at the higher drug concentration range of 10^{-5} and 10^{-6} M Ach. These results imply that there exists a propensity for vascular tissue from metformin treated animals to demonstrate increased contraction and relaxation significantly beyond the capacity of untreated and cholesterol fed animals. Interestingly, the control group, which received a standard chow diet without metformin, showed greater relaxation following Ach stimulation than the group receiving high cholesterol, but a lower contractile response to NA. The leftward shift in the dose-response following metformin therapy was significantly greater than that of the high cholesterol treated group at high concentrations of NA, and implies greater sensitivity towards stimulus.

The main conclusions from the two compliance studies were as follows. The increased sensitivity in the cholesterol fed group was independent of both significant weight gain and cellular cholesterol deposition. In diabetic animal models, increased sensitivity to contractile stimuli has been reported on numerous occasions. Thus, the increased sensitivity in the cholesterol fed group over controls is not unique. Cholesterol deposition was not detected within the intestinal lumen or vessel wall for any experimental group. Interestingly,

hypercholesterolaemia is reported to be particularly difficult to induce in rodents. Recent evidence implicates cholesterol in the control of the activity of bile salt synthetic enzymes such that cholesterol feeding appears to result in the up-regulation of these enzymes and ultimately increased bile salt synthesis, thereby utilising this excess cholesterol (Bahar and Stolz, 1999). This may serve as a possible route of elimination for surplus cholesterol in order to maintain circulating cholesterol levels within the normal range.

The findings of this research may have far reaching implications of clinical significance. Although irrefutable conclusions cannot be drawn from the data presented herein regarding metformin's mode of action, insights have been made into how metformin may influence transepithelial transport of large molecular weight compounds. The present data, together with recent evidence regarding bile salt uptake regulation, considered in context with known sites of accumulation of metformin in the intestine, have led to the following hypotheses regarding the mode of action of this compound.

6.3 Hypotheses for the Cholesterol Lowering Effect of Metformin:

The data presented in this study suggests that metformin may be a specific inhibitor of the ileal bile acid transporter or the enzyme systems regulating its action. This conclusion stems from the similar and additive inhibitory effects of metformin and ouabain treatment in the Caco-2 cell model. The accumulation of metformin along the paracellular channels, and its reported effects upon membrane fluidity, may influence the distribution of these transporter proteins in the apical membrane. Alternatively, as stated previously, within cells metformin

is known to concentrate in the cytosol (Wilcock *et al.*, 1991). If this drug accumulates heavily within cells, it may modify the membrane structure of intracellular organelles that may be uniquely involved in the bile salt transport process, bile salt transporter synthesis, or the activity of organelles providing energy for this system.

Recently, the effect of metformin upon the respiratory chain of mitochondria has been reassessed. This study (by Owen *et al.*, 2000) suggested that metformin accumulates in the mitochondrial membranes within hepatocytes and specifically inhibits mitochondrial respiration. This could reduce ATP production and account for the drug's ability to reduce gluconeogenesis (Owen *et al.*, 2000). What makes this study difficult to interpret is the high level of metformin within the mitochondrial membrane, estimated to be one thousandfold greater than the circulatory concentration. The above authors attribute many effects of metformin to an inhibitory effect upon mitochondrial respiration, including lactate production by the intestine. Since metformin is known to accumulate heavily within the intestine, the inhibition of mitochondrial respiration in this region would be expected to be greater than the effect evident in hepatocytes. Thus, preliminary evidence exists linking metformin with effects on membrane-linked biochemical systems. Its accumulation within these membranes, if proven, could provide a mechanism for metformin to act (at least in part) within intestinal cells to influence energy-dependent enzyme driven reactions. These reactions may be essential to the functioning of a range of actively driven processes, including ileal bile acid transport.

The recently publicised findings regarding feedback regulation of bile acid transporters through nuclear receptors, mentioned previously in chapter 3, may represent one such energy driven process (Chiang *et al.*, 2000; Wang *et al.*, 1999; Makishima *et al.*, 1999; Parks *et al.*, 1999). Little is known regarding the specifics of this process; however, delivery of the bile salt combined with a carrier protein is one model suggested in the literature (Vlahcevic *et al.*, 1999). It is widely accepted that once bile salts are absorbed by their specific ileal carriers they are transported through the cell to the basolateral membrane where they are secreted. This process of intracellular movement may require mitochondrially-derived energy. If metformin does not inhibit bile salt interaction with its nuclear receptors directly, it may inhibit the movement of these salts/acids and their carriers through the cytosol consequent to the mitochondrial effects described above, ultimately, reducing their extrusion from the cell. Increased intracellular levels of bile salts may also regulate the activity of the apical ileal bile acid transporter, regulating bile salt uptake. This would account for the so-called 'specific' effect of the drug upon ileal bile salt absorption. These transporters are reportedly regulated by feedback inhibition, and elevated levels of bile salts within cells may provide this negative stimulus.

Metformin is known to influence the activity of enzyme systems in intestinal cells, specifically those involved in regulating cholesterol biosynthesis. A study by Scott and Tomkin (1983) demonstrated that metformin reduced the activities of both HMG-CoA reductase and ACAT in intestinal cells from diabetic rats. Little effect was evident in control animals. These same authors also postulated that since both of these enzyme systems are membrane-bound, fluidity changes

induced by metformin binding might influence their activity. Similarly, the presence of the energy-dependent $\text{Na}^+\text{-K}^+\text{-ATPase}$ along the lateral membrane channel between ileocytes, which is responsible for maintaining the sodium gradient for active bile salt absorption, may provide a further site of action for metformin, if the drugs ATP-dependent effects in mitochondria are confirmed.

The issues discussed thus far predominantly reflect the active bile salt transporter and enzymes regulating the activity of ileal bile salt transport in the brush-border membrane. However, potentially important data were generated regarding metformin's effects upon the structural integrity of epithelial cells. These experiments (chapter 4) may provide important insights into the side effects of metformin therapy, particularly diarrhoea. Turner *et al.* (1997) provided evidence that regulation of tight junction permeability is linked to MLC phosphorylation and can be induced by sodium-glucose co-transport. In this study, the onset of sodium-coupled glucose transport resulted in a significant attenuation of transepithelial resistance, allowing the increased flux of nutrient-sized molecules such as mannitol. These results support the present findings with regard to increased mannitol flux. However, a direct effect of metformin upon the structure of tight junctions was not investigated in the present studies.

Mannitol has a similar molecular weight to glucose but a significantly smaller molecular weight than sodium glycocholate. The increased mannitol flux evident in experiments discussed in chapter 4, along with diminished bile salt transport, prompts two conclusions. First, if tight junctions become more permeable as a result of metformin and/or ouabain treatment, this effect is limited and only small

molecular weight compounds would benefit from paracellular absorption, or those compounds absorbed via this route. Second, the diminished transport of sodium glycocholate suggests a specificity of metformin toward the ileal bile acid transporter or the enzyme systems regulating its activity. Indeed, the additive inhibitory effect of co-treatment with metformin and ouabain does not clearly point to a single point of action of the two compounds, i.e. the $\text{Na}^+\text{-K}^+\text{-ATPase}$ enzyme located along the paracellular channels. It may be that metformin and ouabain impose similar effects upon different regions with these effects being additive during their simultaneous incubation.

The integrity of the tight junction structure is dependent upon extracellular calcium (Pérez *et al.*, 1997). According to Pérez *et al.* (1997), epithelial cells may regulate tight junction permeability through intracellular messengers such as PKC, G-proteins, IP_3 , and calmodulin. This has been confirmed recently by Turner *et al.* (1999) who identified a link between increased tight junction permeability and increased phosphorylation of MLC by MLCK; this enzyme in turn may be regulated by PKC activity.

Extracellular calcium depletion in the above study resulted in a substantial increase in mannitol transfer (Pérez *et al.*, 1997). Intracellular calcium levels were also identified as being critical in tight junction permeability since increased intracellular calcium flux resulted in enhanced mannitol flux across the epithelial membrane of rat jejunal cells. Decreased intracellular calcium levels, by inhibiting calcium release from intracellular stores, also resulted in increased mannitol flux, as did PKC activation in Caco-2 cells. These differential calcium-induced effects may signify an inherent sensitivity to intracellular levels of this

cation and the importance of calcium in regulating tight junction permeability. It is tempting at this point to draw comparisons with the vascular effects of metformin and postulate that metformin may influence calcium driven events in both tissues. Although a small increase in intracellular calcium levels was evident following acute metformin perfusion of A7r5 smooth muscle cells, the magnitude of effect, and thus physiological consequence, would be dependent upon the sensitivity of the tissue in question. The sensitivity of vascular tissue towards calcium will be discussed later in this chapter.

One possible contradiction in the hypothesis of increased paracellular permeability discussed herein is the increase in absorption of nutrients by solvent drag that would occur along with increased fluid absorption, and will probably depend upon the osmotic gradient present in the intestine. Under normal circumstances, substantial concentration and osmotic gradients exist in the intestinal lumen including those caused by local concentrations of glucose and bile acids. Despite the diffusional gradient, not all compounds are capable of passive diffusion and must be actively transported opposing the electrochemical gradient. If metformin increases paracellular permeability to water-soluble nutrient-sized molecules, but not to larger molecules with a strong osmotic pull, this may induce backflux of solutes and water, or simply diminish absorption in the first instance through paracellular channels. This may partly account for the watery-stool side effect of metformin therapy. Indeed, metformin has recently been reported to inhibit the absorption of glucose in perfused rat intestine (Ikeda *et al.*, 2000), although this has not been confirmed by others.

The effects of metformin upon vascular reactivity have been conflicting and may be dependent partly upon the anatomical location of the vessels investigated, along with the role of the vessel in terms of arterial resistance or conductance. Studies presented in chapter 5 provide evidence for the effect of metformin and cholesterol feeding on contraction and relaxation in conduit arteries. As stated at the beginning of this chapter, chronic metformin therapy resulted in both increased vascular contraction and relaxation in response to noradrenergic and cholinergic stimulation, respectively. Evidence exists linking the states of insulin resistance and diabetes to impaired vascular reactivity, resulting in enhanced reactivity to contractile agonists and a diminished vasodilatory response (Fleischhacker *et al.*, 1999). These effects appear to be evident prior to any gross changes in vessel morphology and as such represent pre-eminence to occlusive atherosclerosis. A recent study by Reil *et al.* (1999) provides evidence for diet-induced changes in endothelial-dependent relaxation in rat thoracic aorta. The diet used in this study was composed of approximately 40% fat with a similar value for carbohydrate; no effect was seen on the contractile properties of thoracic aorta. The study undertaken by Reil *et al.* (1999) included no additional cholesterol in the high fat diet yet Ach-induced relaxations remained significantly attenuated in the group receiving this diet.

Similarly, a recent study by Gerber *et al.* (1999) also demonstrated a diet high in saturated fat could result in reduced vascular relaxation in response to Ach. This effect was cholesterol-independent since high saturated fat intake in rats results in lowering of plasma cholesterol levels (Gerber *et al.*, 1999), contrary to the usual occurrence in man. Wong (1996) has shown that feeding rabbits a 2% cholesterol

diet for eight weeks increased aortic sensitivity to depolarising agents compared with controls. In a separate study, aorta from streptozocin-induced diabetic rats initially demonstrated enhanced sensitivity to noradrenergic stimulation, as the diabetic state progressed changes were seen in aortic sensitivity to agonists. At the end point of this study the sensitivity towards noradrenergic stimulation was again significantly heightened in diabetic rats compared with controls (Wong and Tzeng, 1992). These data suggest that a diet rich in saturated fat and/or cholesterol may result in the onset of vascular dysfunction and should be seen as an independent risk factor for the development of such disease.

Although no visible alteration in the composition of aortae could be identified following cholesterol feeding, many effects of vascular dysfunction occur prior to such gross alterations. An altered composition of aorta as a consequence of cholesterol feeding in mice could be a realistic possibility and may alter membrane-bound functioning of receptors or sensitivity to stimulation.

Insulin resistance is an independent risk factor for diabetes. Metformin has been shown to improve vascular function in insulin resistant rats (Katakam *et al.*, 2000). In this study, metformin was associated with improved mesenteric artery relaxation in response to Ach and is postulated to achieve this by agonist-stimulated-NO production. Interestingly, metformin, at very high concentrations, was shown to induce relaxation in vascular smooth muscle. This effect appeared to involve decreasing intracellular calcium levels, although no direct evidence from this study could unequivocally confirm or refute this.

Importantly, a recent study indicated that in human diabetes altered contractile and relaxant responses could be attributed to modified intracellular calcium distribution (Fleischhacker *et al.*, 1999). This study associated enhanced contraction of isolated smooth muscle cells with increased perinuclear calcium concentration in response to NA, thereby promoting the contractile process. Increased relaxation was associated with a reduction in the subplasmalemmal calcium concentration. Thus, the vascular smooth muscle cells themselves may provide an additional mechanism through which vascular reactivity may be impaired. In a separate study, experimentally induced diabetes in rats was associated with enhanced responses to NA in mesenteric arteries. This effect was believed to be associated with enhanced flux of calcium across the plasma membrane (White and Carrier, 1990).

Metformin has been shown to exert a wide range of effects in a variety of tissues (Wiernsperger, 1999). Thus, an effect upon vascular reactivity is not unanticipated, particularly if the drug alters the level of intracellular calcium. Such an effect could account for data generated in the experiments performed herein, particularly those relating to vascular compliance.

The enhanced contractile response to NA was present in cholesterol fed animals. This effect was also evident in metformin treated animals and was significantly greater than in the cholesterol fed group. This may be explained partly by the nature of the diet, since evidence has been presented regarding diets high in saturated fat or cholesterol inducing enhanced sensitivity to NA. The relatively low level of fat used in the studies herein (4%) may have been sufficient to

induce such changes in responsiveness, due in part to the chronic nature of the study. Since cholesterol deposition was not detected in any experimental group, alterations in vessel responsiveness are most probably cholesterol-independent. In similar studies mentioned previously, the dietary fat content tended to be much higher and the experimental time period much shorter.

Metformin may also induce the release of NA from sympathetic nerve terminals (Lee and Peuler, 1999). A study reporting such results was performed using rat tail artery, a tissue known to contain many adrenergic nerve terminals. Although conduit arteries are innervated by sympathetic nerves, they are fewer in number than those supplying resistance arteries. The abundance of receptors may influence this effect of metformin if its agonist secreting effects are indeed confirmed. The significantly greater contractile response of aorta from the metformin treated animals in the present studies suggests an increased sensitivity towards NA, this may be the result of increased transmitter release, yet remains unlikely due to the poor sympathetic innervation in this region.

The most attractive hypothesis accounting for metformin's mode of action on vascular smooth muscle is, I believe, linked to levels of intracellular calcium. Calcium is the universal regulator in vascular tissue responsible for driving both contraction and relaxation, and any effect on either parameter would likely effect the opposing parameter also, particularly if the second messenger systems involved displayed heightened sensitivity. Metformin, when acutely perfused across a bed of A7r5 vascular smooth muscle cells, resulted in a modest transient increase in intracellular calcium levels. This effect was marginal and relatively

short lasting, and should not be overstated in terms of importance. Nevertheless, an effect is clear and is in direct response to metformin perfusion.

The origin of the calcium responsible for this transient rise in intracellular calcium levels is unknown but may be from extracellular sources. Evidence for extracellular calcium influx stems from the increase in intracellular levels following the addition of thapsigargin. Thapsigargin, as previously stated, blocks the resequestration of intracellular calcium. Thus, any increase in intracellular levels of calcium must be a consequence of extracellular influx or displacement from intracellular stores (Thastrup *et al.*, 1990). The transient increase in intracellular calcium levels in A7r5 cells following noradrenergic challenge and during metformin perfusion may indicate some form of membrane leakage allowing extracellular calcium levels to rise. These results, and others (Cusi and DeFronzo, 1998), suggest chronic metformin therapy is necessary for any effect on enzyme systems to be significantly demonstrated, particularly in relation to glucose uptake. This does not necessarily concur with metformin's intestinal effect however, since the drug accumulates at high concentrations in this tissue.

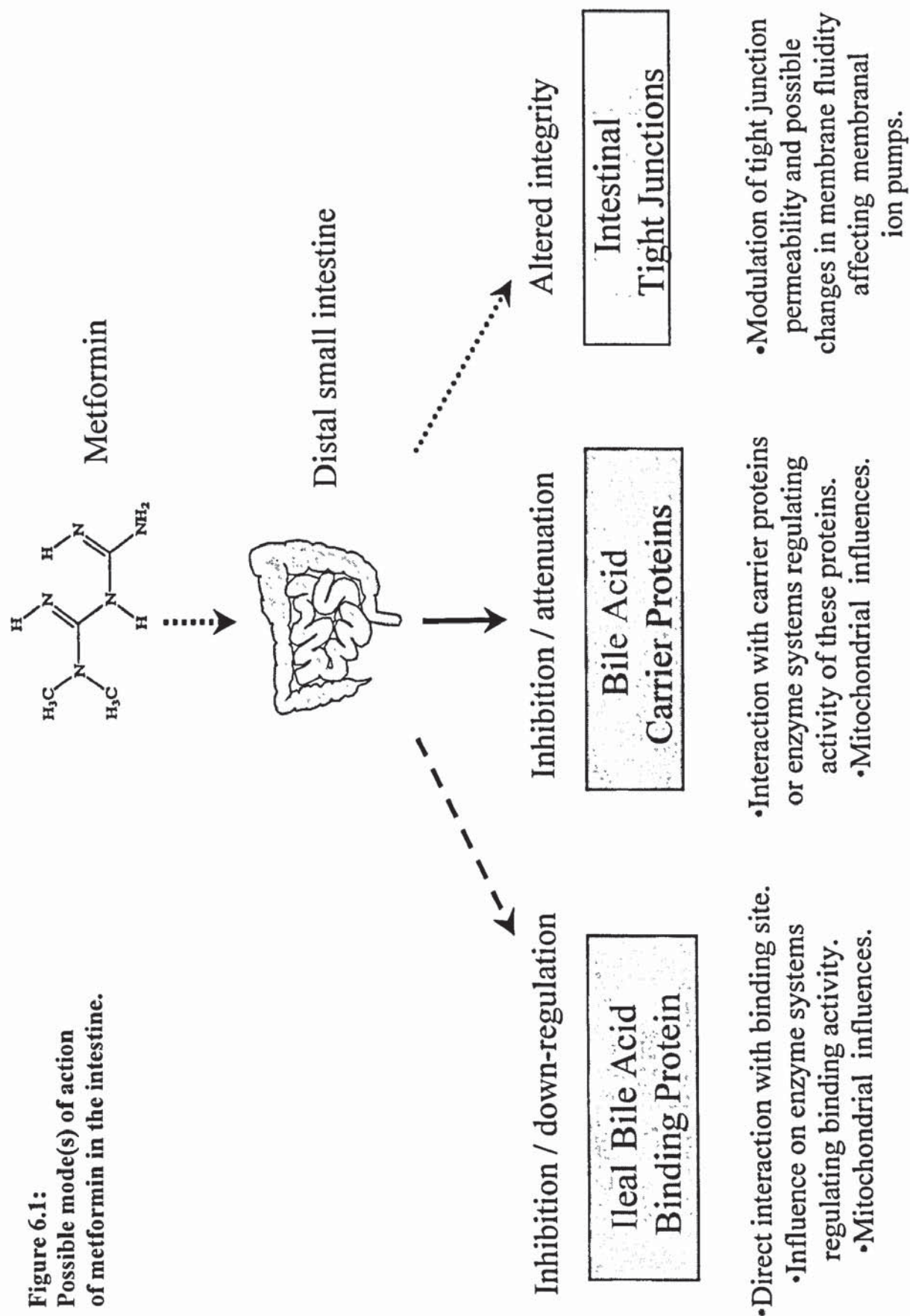
It is important to note that in the calcium imaging experiments only a small cluster of cells was selected to represent the larger cell population. In such situations not all cells respond with the same magnitude and will be affected by variables such as extent of maturity. Those cells in contact with surrounding cells may respond differently to entirely isolated cells and may be stimulated by adjacent cells. This situation was not best represented in the present culture model since most cells tested were not in direct contact with surrounding muscle

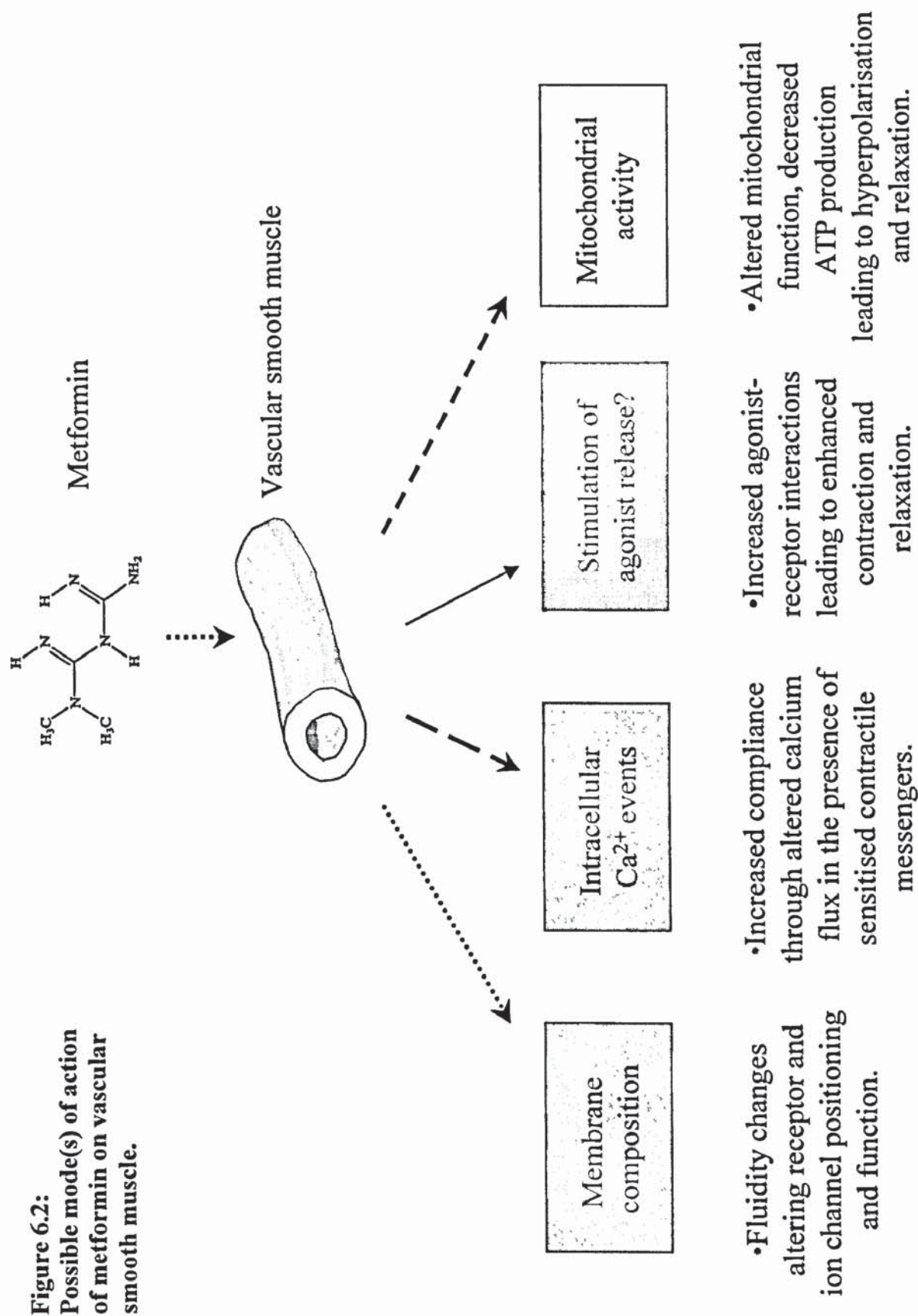
cells. Thus, any effect of metformin *in vivo* upon calcium flux may be expected to stimulate similar events in adjacent cells.

Sustained tonic contractions that occur in conduit arteries such as thoracic aorta are achieved by increased PKC sensitivity towards intracellular calcium levels (Ikebe and Brozovich, 1996). Approximately 5 minutes following noradrenergic stimulation in the smooth muscle cell model, metformin resulted in a transient intracellular calcium increase. If *in vivo* metformin induces similar spontaneous calcium rises, these would serve to increase contractile responses in the presence of sensitised PKC. In the cell culture model the calcium increase peaked after 11 minutes of metformin perfusion, before declining to basal levels. This calcium decrease in the presence of sensitised PKC, if I may be permitted to extrapolate to the situation *in vivo*, may result in increased relaxation following Ach release. The hypotheses generated from these studies and from current literature (for metformin's vascular and intestinal effects) are summarised in figures 6.1 and 6.2.

There are numerous reported sites of action of metformin on many physiological systems (Cusi and DeFronzo, 1998). In this general discussion I have attempted to summarise the significant findings of the studies undertaken in the present programme of research. I have explored the hypotheses raised in the introduction and the interpretations considered in the foregoing sections to account for the possible modes of action of metformin. The hypotheses detailed above were designed to give an assessment of current ideas in the literature and possible insights generated as a result of the present studies. One difficulty in forming a

working hypothesis for a compound such as metformin is that a range of effects have been reported not only upon vascular smooth muscle cells but also on the endothelium, possibly accounting for its vascular effects. Nevertheless, metformin therapy continues as the primary treatment for type 2 diabetes mellitus and to date is associated with the lowest incidence of micro- and macrovascular mortality in chronically treated type 2 diabetic individuals (UKPDS, 1998).





6.4 Concluding Remarks:

In conclusion, chronic metformin treatment in cholesterol fed mice resulted in a significant increase in vascular compliance. This effect could not be attributed to increases in cholesterol or glucose levels. These results are consistent with those recently published by the UKPDS (1998), and support the claim that metformin treatment may impose a vasoprotective effect in some individuals. Clearly, further research is required to elucidate the mechanisms involved in this effect.

Metformin, at high concentrations (250mg/kg), significantly inhibited the active unidirectional transport of ^{14}C sodium glycocholate *in vivo* and in cultured Caco-2 cells. Ouabain, a $\text{Na}^+\text{-K}^+\text{-ATPase}$ inhibitor, also inhibited active bile salt transfer in the Caco-2 cell model. Ouabain and metformin, in combination, exerted an additive inhibitory effect on bile salt transfer.

Both metformin and ouabain, whilst inhibiting the active transport of ^{14}C sodium glycocholate, simultaneously increased the flux of the non-transportable marker, ^3H mannitol, across Caco-2 monolayers. This suggests that both agents, individually or cumulatively, alter the integrity of the cell monolayer. This may provide an insight into a common locality for the action of these compounds and for the incidence of diarrhoea, which is a common side effect of metformin therapy.

This thesis has examined a potential mechanism through which metformin could reduce circulating cholesterol levels. The studies herein have clearly demonstrated that metformin imposes specific effects to increase jejunal uptake and decrease ileal uptake of bile salts. It has also been demonstrated that chronic

administration of metformin improves aortic compliance through increased contractile responses to noradrenaline and vasodilation to acetylcholine. The significant effects of metformin upon bile salt transfer *in vitro* and *in vivo* suggest a highly specific effect of this compound on the bile salt transfer system. This effect may be a possible route through which metformin might reduce circulating cholesterol levels, particularly in hypercholesterolaemic individuals.

List of References:

References:

- Aaronson P. I., Smirnov S. V. Membrane ion channels in vascular smooth muscle excitation-contraction coupling. In: *Pharmacology of Vascular Smooth Muscle*. Oxford University Press, Oxford. Chapter 6, pp 136-159, 1996.
- Adams C. W. M. A Perchloric acid-naphthoquinone method for the histochemical localisation of cholesterol. *Nature* **192**: 331-332, 1961.
- Adams D. J., Nonner W. Voltage-dependent potassium channels: gating, ion permeation and block. In: *Potassium Channels, Structure, Function and Therapeutic Potential*. Ed. Cook N. S. Halsted Press, New York. Chapter 2, pp 40-69, 1990.
- Adebe W., MacLeod K. M. Protein kinase C-mediated contractile responses of arteries from diabetic rats. *Br. J. Pharmacol.* **101**: 465-471, 1990.
- Adelstein R. S., Eisenberg E. Regulation and kinetics of the actin-myosin-ATP interaction. *Ann. Rev. Biochem.* **49**: 921-956, 1980.
- Åkerlund J. E., Reihner E., Angelin B., Rudling M., Ewerth S., Björkhem I., Einarsson K. Hepatic metabolism of cholesterol in Crohn's disease: effect of partial resection of ileum. *Gastroenterology*. **100**: 1046-1053, 1991.
- Allain C. C., Poon L. S., Chan C. S. G., Richmond W., Fu P. C. Enzymatic determination of total serum cholesterol. *Clin. Chem.* **20**: 470-475, 1974.
- Altan V. M., Karasu C., Özüari A. The effects of type-1 and type-2 Diabetes on endothelium-dependent relaxation in rat aorta. *Pharmacol. Biochem. Behav.* **33**: 519-522, 1989.
- Amelsberg A., Schteingart C. D., Ton-Nu H-T., Hofmann A. F. Carrier-mediated jejunal absorption of conjugated bile acids in the guinea pig. *Gastroenterology* **110**: 1098-1106, 1996.
- Andrews H. E., Bruckdorfer K. R., Dunn R. C., Jacobs M. Low-density lipoproteins inhibit endothelium-dependent relaxation in rabbit aorta. *Nature* **327**: 237-239, 1987.
- Ariëns R. A. S., Kohler H. P., Mansfield M. W., Grant P. J. Subunit antigen and activity levels of blood coagulation factor XIII in healthy individuals. Relation to sex, age, smoking and hypertension. *Arterioscler. Thromb. Vasc. Biol.* **19**: 2012-2016, 1999.
- Ariëns R. A. S., Standeven K., Whittaker P., Ashcroft A. E., Grant P. J. Cross-linking activity of blood coagulation factor XIII is inhibited by dimethylbiguanide and aminoguanidine. *Diabetic Med.* **17**: (Suppl 1) A9, 2000.

- Arrese M., Trauner M., Sacchiero R. J., Crossman M. W., Schneider B. L. Neither intestinal sequestration of bile acids nor common bile duct ligation modulate the expression and function of the rat ileal bile acid transporter. *Hepatology* 28: 1081-1087, 1998.
- Ashida T., Schaeffer J., Goldman W. F., Wade J. B., Blaustein M. P. Role of sarcoplasmic reticulum in arterial contraction: comparison of Ryanodine's effect in a conduit and a muscular artery. *Circulation Res.* 62: 854-863, 1988.
- Avogaro A., Toffolo G., Miola M., Valerio A., Tiengo A., Cobelli C., Del Prato S. Intracellular lactate and pyruvate-interconversion rates are increased in muscle tissue of NIDDM individuals. *J. Clin. Invest.* 98: 108-115, 1996.
- Bagdade J. D. HDL and reverse cholesterol transport in diabetes. *Diabetes Rev.* 5: 392-409, 1997.
- Bahar R. J., Stolz A. Bile acid transport. In: Bile Salts: Metabolic, Pathologic, and Therapeutic Considerations. *Gastroenterology Clinics of North America.* 28: (1) 27-57, 1999.
- Bailey C. J. Biguanides and NIDDM. *Diabetes Care* 15: 755-772, 1992.
- Bailey C. J. Metformin and its role in the management of type II diabetes. *Curr. Opin. Endocrin. Diabetes* 4: 40-47, 1997a.
- Bailey C. J. New drugs for the treatment of diabetes mellitus. In: *International Textbook of Diabetes Mellitus, Second Edition*. Eds. Alberti K. G. M. M., Zimmet P., DeFronzo R. A., Keen H. Wiley Publishers, Chichester. Chapter 38, pp 865-881, 1997b.
- Bailey C. J. Antidiabetic drugs. *Brit. J. Cardiol.* 3: 350-360, 2000.
- Balda M. S., Matter K. Tight junctions. *J. Cell Science* 111: 541-547, 1998.
- Balodimos M. C., Camerini-Dávalos R. A., Marble M. Nine years' experience with tolbutamide in the treatment of diabetes. *Metabolism* 15: 957-970, 1966.
- Bancroft J. D., Stevens A. Theory and practice of histological techniques. Fourth Edition. Churchill Livingstone, New York. pp 1-766, 1996.
- Barnard J. A., Ghishan F. K. Taurocholate transport by human ileal brush border membrane vesicles. *Gastroenterology* 93: 925-933, 1987.
- Baron A. D. Haemodynamic actions of insulin. *Am. J. Physiol* 267: E187-E202, 1994.
- Baron A. D., Brechtel G. Insulin differentially regulates systemic and skeletal muscle vascular resistance. *Am. J. Physiol.* 265: E61-E67, 1993.

Baron A. D., Brechtel G., Wallace P., Edelman S. V. Rates and tissue sites of non-insulin and insulin-mediated glucose uptake in humans. *Am. J. Physiol.* **255**: E769-E774, 1988.

Baron A. D., Quon M. J. Insulin action and endothelial function. In: *Insulin Resistance: The Metabolic Syndrome X*. Eds. Reaven G. M., Laws A. Blackwell Science, Oxford. Chapter 13, pp 247-265, 1999.

Baron A. D., Schaeffer L., Shragg P., Kolterman O. G. Role of hyperglucagonaemia in maintenance of increased rates of hepatic glucose output in type II diabetes. *Diabetes* **36**: 274-283, 1987.

Barthe L., Bessouet M., Woodley J. F., Houin G. The improved everted gut sac: a simple method to study intestinal P-glycoprotein. *Int. J. Pharmaceutics* **173**: 255-258, 1998.

Bates S. H. Investigation of potential intervention targets to improve insulin action: a therapeutic approach. Ph.D. Thesis Aston University. pp1-373, 1999.

Bean B. P. Classes of calcium channels in vertebrate cells. *Annu. Rev. Physiol.* **51**: 367-384, 1989.

Bellomo G., Maggi E., Poli M., Agosta F. G., Bollati P., Finardi G. Autoantibodies against oxidatively modified low-density lipoproteins in NIDDM. *Diabetes* **44**: 60-66, 1995.

Bergström S., Norman A. Metabolic products of cholesterol in bile and faeces of rat. *Proc. Soc. Exp. Biol. Med.* **83**: 71-74, 1953.

Berridge M. J. Inositol trisphosphate and calcium signalling. *Nature* **361**: 315-325, 1993.

Best J. D., Kahn S. E., Ader M., Watanabe R. M., Ni T-C., Bergman R. N. Role of glucose effectiveness in the determination of glucose tolerance. *Diabetes Care* **19**: 1018-1030, 1996.

Betteridge D. J. Lipid disorders in diabetes mellitus. In: *Textbook of Diabetes, Second Edition. Volume 2*. Eds. Pickup J. C., Williams G. Blackwell Science, Oxford. Chapter 55, 55.1-55.31, 1997.

Binder H. J., Rawlins C. L. Effect of conjugated dihydroxy bile salts on electrolyte transport in rat colon. *J. Clin. Invest.* **52**: 1460-1466, 1973.

Björkhem I. Mechanisms of bile acid biosynthesis in mammalian liver. In: *Sterols and bile acids*. Eds. Danielsson H., Sjövall J. Elsevier, Amsterdam. Chapter 9, pp 231-278, 1985.

Blais A., Bissonnette P., Berteloot A. Common characteristics for Na⁺-dependent sugar transport in Caco-2 cells and human fetal colon. *J. Membr. Biol.* 99: 113-125, 1987.

Blumenthal S. A. Stimulation of gluconeogenesis by palmitic acid in rat hepatocytes: evidence that this effect can be dissociated from the provision of reducing equivalents. *Metabolism* 32: 971-976, 1983.

Boden G., Chen X. Effects of fat on glucose uptake and utilisation in patients with NIDDM. *J. Clin. Invest.* 96: 1261-1268, 1995.

Bohr D. F. Vascular smooth muscle: dual effect of calcium. *Science* 139: 597-599, 1963.

Borgström B., Barrowman J. A., Lindström M. Roles of bile acids in intestinal lipid digestion and absorption. In *Sterols and Bile Acids* Eds. Dannielsson H., Sjövall J. Elsevier, Amsterdam. Chapter 14, pp 405-425, 1985.

Borin M. L., Tribe R. M., Blaustein M. P. Increased intracellular Na⁺ augments mobilisation of Ca²⁺ from SR in vascular smooth muscle cells. *Am. J. Physiol.* 266: C311-C317, 1994.

Boulanger C. M., Tanner F. C., Béa M-L., Hahn A. W. A., Werner A., Lüscher T. F. Oxidised low density lipoproteins induce mRNA expression and release of endothelin from human and porcine endothelium. *Circ. Res.* 70: 1191-1197, 1992.

Brophy C. M., Knoepf L., Xin J., Pollock J. S. Functional expression of NOS 1 in vascular smooth muscle. *Am. J. Physiol.* 278: H991-H997, 2000.

Brown M. S., Goldstein J. L. Lipoprotein receptors in the liver. Control signals for plasma cholesterol traffic. *J. Clin. Invest.* 72: 743-747, 1983.

Brown M. S., Goldstein J. L. A receptor-mediated pathway for cholesterol homeostasis. *Science* 232: 34-47, 1986.

Brownlee M., Vlassara H., Cerami A. Nonenzymatic glycosylation products on collagen covalently trap low density lipoprotein. *Diabetes* 34: 938-941, 1985.

Bülbring E., Tomita T. Catecholamine action on smooth muscle. *Pharmacol. Rev.* 39: 49-96, 1987.

Bünting C. E., Koschinsky T., Rütter R., Gries F. A. Metformin inhibits the growth of human vascular cells: a new potentially antiatherogenic drug effect. *Diabetologia* 29: 523A, 1986.

Busse, R. Stimulation of soluble guanylate cyclase activity by endothelium-derived relaxant factor: a general principle of its vasodilator and antiaggregatory properties. *Thromb. Res. (Suppl 7)*: 3, 1987.

- Caspary, W. F., Effect of biguanides on intestinal transport of sugars, amino acids and calcium. *Naunyn Schmiedeberg's Arch. Pharmacol.* **269**: 421-422, 1971.
- Caspary, W. F., Creutzfeldt, W. Inhibition of intestinal amino acid transport by blood sugar lowering biguanides. *Diabetologia.* **9**: 6-12, 1973.
- Caspary, W. F., Creutzfeldt W. Inhibition of bile salt absorption by blood-sugar lowering biguanides. *Diabetologia.* **11**: 113-117, 1975.
- Caspary W. F., Lücke H. Inhibition of bile acid and water absorption by phenethylbiguanide in rat ileum *in vivo*. *Digestion* **12**: 179-182, 1975.
- Cereijido M., Valdés J., Shoshani L., Contreras R. G. Role of tight junctions in establishing and maintaining cell polarity. *Ann. Rev. Physiol.* **60**: 161-177, 1998.
- Chait A., Bierman E. L., Albers J. J. Low density lipoprotein receptor activity in cultured human skin fibroblasts: mechanism of insulin-induced stimulation. *J. Clin. Invest.* **64**: 1309-1319, 1979.
- Chakrabarti R., Hocking E. D., Fearnley G. R. Fibrinolytic effect of metformin in coronary artery disease. *Lancet* **2**: 256-259, 1965.
- Chandler C. E., Zaccaro L. M., Moberly J. B. Transepithelial transport of cholytaurine by Caco-2 cell monolayers is sodium dependent. *Am. J. Physiol.* **264**: G1118-G1125, 1993.
- Chataigneau T., Félétou M., Huang P. L., Fishman M. C., Duhault J., Vanhoutte P. M. Acetylcholine-induced relaxation in blood vessels from endothelial nitric oxide synthase knockout mice. *Br. J. Pharmacol.* **126**: 219-226, 1999.
- Chen G., Cheung D. W. Characterisation of acetylcholine-induced membrane hyperpolarisation in endothelial cells. *Circ. Res.* **70**: 257-263, 1992.
- Chen G., Suzuki H., Weston A. H. Acetylcholine releases endothelium-derived hyperpolarising factor and EDRF from rat blood vessels. *Br. J. Pharmacol.* **95**: 1165-1174, 1988.
- Chen X-L., Panek K., Rembold C. M. Metformin relaxes rat tail artery by repolarisation and resultant decreases in Ca^{2+} influx and intracellular $[\text{Ca}^{2+}]$. *J. Hypertens.* **15**: 269-274, 1997.
- Cherrington A. D., Stevenson R. W., Steiner K. E., Davis M. A., Myers S. R., Adkins B. A., Abumrad N. N., Williams P. E. Insulin, glucagon, and glucose as regulators of hepatic glucose uptake and production *in vivo*. *Diabetes Metab. Rev.* **3**: 307-322, 1987.
- Chiang J. Y. L., Kimmel R., Weinberger C., Stroup D. Farnesoid X receptor responds to bile acids and represses cholesterol 7 α -hydroxylase gene (CYP7A1) transcription. *J. Biol. Chem.* **275**: 10918-10924, 2000.

- Chin J. H., Azhar S., Hoffman B. B. Inactivation of endothelial derived relaxing factor by oxidised lipoproteins. *J. Clin. Invest.* 89: 10-18, 1992.
- Chrisyensen O. Mediation of cell volume regulation by Ca^{2+} influx through stretch-activated channels. *Nature* 330: 66-68, 1987.
- Clemmons D. R. Growth factors and atherosclerosis. *Diabetes Rev.* 5: 353-364, 1997.
- Clissold S. P., Edwards C. Acarbose: A preliminary review of its pharmacodynamic and pharmacokinetic properties, and therapeutic potential. *Drugs* 35: 214-243, 1988.
- Cocks T. M. Endothelium-dependent vasodilator mechanisms. In: *Pharmacology of Vascular Smooth Muscle*. Oxford University Press, Oxford. Chapter 10, pp 233-251, 1996.
- Cohen R. A. Dysfunction of vascular endothelium in diabetes mellitus. *Circulation* 87: (Suppl V) V67-V76, 1993.
- Consoli A., Nurjhan N., Capani F., Gerich J. Predominant role of gluconeogenesis in increased hepatic glucose production in NIDDM. *Diabetes* 38: 550-556, 1989.
- Consoli A., Nurjhan N., Reilly J., Bier D., Gerich J. Mechanism of increased gluconeogenesis in NIDDM: role of alterations in systemic, hepatic, and muscle lactate and alanine metabolism. *J. Clin. Invest.* 86: 2038-2045, 1990.
- Cooper A. D. Role of The enterohepatic circulation of bile salts in lipoprotein metabolism. In: *Bile Salts: Metabolic, Pathologic, and Therapeutic Considerations. Gastroenterology Clinics of North America.* 28: (1) 211-229, 1999.
- Cox D. A., Cohen M. L. Effects of oxidised low-density lipoprotein on vascular contraction and relaxation: clinical and pharmacological implications in atherosclerosis. *Pharm. Rev.* 48: 3-19, 1996.
- Craddock A. L., Love M. W., Daniel R. W., Kirby L. C., Walters H. C., Wong M. H., Dawson P. A. Expression and transport properties of the human ileal and renal sodium-dependent bile acid transporter. *Am. J. Physiol.* 274: G157-G169, 1998.
- Crapo P. A. Dietary management. In: *Joslin's Diabetes Mellitus, Thirteenth Edition*. Eds. Kahn C. R., Weir G. C. Lea and Febiger, Philadelphia. Chapter 24, pp 415-430, 1994.

Cummings M. H., Watts G. F., Umpleby A. M., Hennessy T. R., Naoumova R., Slavin B. M., Thompson G. R., Sönksen P. H. Increased hepatic secretion of very-low-density lipoprotein apolipoprotein B-100 in NIDDM. *Diabetologia* 38: 959-967, 1995.

Cushing S. D., Berliner J. A., Valente A. J., Territo M. C., Navab M., Parhami F., Gerrity R., Schwartz C. J., Fogelman A. M. Minimally modified low density lipoprotein induces monocyte chemotactic protein 1 in human endothelial cells and smooth muscle cells. *Proc. Natl. Acad. Sci. USA* 87: 5134-5138, 1990.

Cusi K., DeFronzo R. A. Metformin: a review of its metabolic effects. *Diabetes Rev.* 6: 89-131, 1998.

Czyzyk A., Tawecki J., Sadowski J., Ponikowska, I., Szczepanik Z. Effect of biguanides on intestinal absorption of glucose. *Diabetes*. 17: 492-498, 1968.

Day C. Thiazolidinediones: a new class of antidiabetic drugs. *Diabetic Med.* 16: 179-192, 1999.

DeFronzo R. A. Glucose intolerance and aging: Evidence for tissue insensitivity to insulin. *Diabetes* 28: 1095-1101, 1979.

DeFronzo R. A. The Lilly Lecture. The triumvirate: β -cell, muscle, liver: A collusion responsible for NIDDM. *Diabetes* 37: 667-687, 1988.

DeFronzo R. A. Pathogenesis of type 2 diabetes: metabolic and molecular implications for identifying diabetes genes. *Diabetes Rev.* 5: 177-269, 1997.

DeFronzo R. A., Ferrannini E. Regulation of hepatic glucose metabolism in humans. *Diabetes Metab. Rev.* 3: 415-459, 1987.

DeFronzo R. A., Ferrannini E., Simonson D. C. Fasting hyperglycemia in non-insulin-dependent diabetes mellitus: contributions of excessive hepatic glucose production and impaired tissue glucose uptake. *Metabolism* 38: 387-395, 1989.

DeFronzo R. A., Gunnarsson R., Björkman O., Olsson M., Wahren J. Effects of insulin on peripheral and splanchnic glucose metabolism in noninsulin-dependent (type II) diabetes mellitus. *J. Clin. Invest.* 76: 149-155, 1985.

Del Prato S., Leonetti F., Simonson D. C., Sheehan P., Matsuda M., DeFronzo R. A. Effect of sustained physiologic hyperinsulinaemia and hyperglycaemia on insulin secretion and insulin sensitivity in man. *Diabetologia* 37: 1025-1035, 1994.

Demirel E., Rusko J., Laskey R. E., Adams D. J., Van Breemen C. TEA inhibits Ach-induced EDRF release: endothelial Ca^{2+} -dependent K^{+} channels contribute to vascular tone. *Am. J. Physiol.* 267: H1135-H1141, 1994.

- Dietschy J. M. Effects of bile salts on intermediate metabolism of the intestinal mucosa. *Fed. Proc.* **26**: 1589-1598, 1967.
- Dietschy J. M. Mechanisms for the intestinal absorption of bile acids. *J. Lipid Res.* **9**: 297-309, 1968.
- Dietschy J. M., Salomon H. S., Siperstein M. D. Bile acid metabolism: Studies on the mechanisms of intestinal transport. *J. Clin. Invest.* **45**: 832-846, 1966.
- Dix C. J., Hassan I. F., O Bray H. Y., Shah R., Wilson G. The transport of vitamin B₁₂ through polarised monolayers of Caco-2 cells. *Gastroenterology* **98**: 1272-1279, 1990.
- Dominguez L. J., Davidoff A. J., Srinivas P. R., Standley P. R., Walsh M. F., Sowers J. R. Effects of metformin on tyrosine kinase activity, glucose transport, and intracellular calcium in rat vascular smooth muscle. *Endocrinology* **137**: 113-121, 1996.
- Donovan J. M. Physical and metabolic factors in gallstone pathogenesis. In: *Bile Salts: Metabolic, Pathologic, and Therapeutic Considerations. Gastroenterology Clinics of North America* **28**: (1) 75-97, 1999.
- Drouet L. Atherothrombosis in diabetes: its evolution and management. *Diabet. Obesity and Metab.* **1**: (Suppl 2) S37-S47, 1999.
- Duckworth P. F., Vlahcevic Z. R., Studer E. J., Gurley E. C., Heuman D. M., Beg Z. H., Hylemon P. B. Effect of hydrophobic bile acids on 3-hydroxy-3-methylglutaryl-coenzyme A reductase activity and mRNA levels in the rat. *J. Biol. Chem.* **266**: 9413-9418, 1991.
- Duell P. B., Oram J. F., Bierman E. L. Nonenzymatic glycosylation of HDL resulting in inhibition of high affinity binding to cultured human fibroblasts. *Diabetes* **39**: 1257-1263, 1990.
- Eisenberg S. High density lipoprotein metabolism. *J. Lipid. Res.* **25**: 1017-1058, 1984.
- Elliot W. H. Metabolism of bile acids in liver and extrahepatic tissues. In: *Sterols and Bile Acids* Eds. Danielsson H., Sjövall J. Elsevier, Amsterdam. Chapter 11, pp 303-329, 1985.
- Emis J. J., Van Gent C. M., Van Sabben C. M. An enzymatic method for the histochemical localisation of free and esterified cholesterol separately. *Histochem. J.* **9**: 197-204, 1977.
- Faergeman O., Havel R. J. Metabolism of cholesteryl esters of rat very low density lipoproteins. *J. Clin. Invest.* **55**: 1210-1218, 1975.

Fantus I. G., Brosseau R. Mechanisms of action of metformin: insulin receptor and postreceptor effects *in vitro* and *in vivo*. *J. Clin. Endocrinol. Metab.* **63**: 898-905, 1986.

Felber J. P., Ferrannini E., Golay A., Meyer H. U., Theibaud D., Curchod B., Maeder E., Jequier E., DeFronzo R. A. Role of lipid oxidation in pathogenesis of insulin resistance of obesity and type II diabetes. *Diabetes* **36**: 1341-1350, 1987.

Félétou M., Vanhoutte P. M. Endothelium-derived hyperpolarising factor. *Clin. Exp. Pharmacol. Physiol.* **23**: 1082-1090, 1996.

Ferrannini E., Barrett E. J., Bevilacqua S., DeFronzo R. A. Effect of fatty acids on glucose production and utilisation in man. *J. Clin. Invest.* **72**: 1737-1747, 1983.

Fielding C. J., Fielding P. E. Cholesterol transport between cells and body fluids: Role of plasma lipoproteins and the plasma cholesterol esterification system. *Med. Clin. North Am.* **66**: 363-373, 1982.

Fine K. D., Santa Ana C. A., Porter J. L., Fordtran J. S. Effect of D-glucose on intestinal permeability and its passive absorption in human small intestine *in vivo*. *Gastroenterology* **105**: 1117-1125, 1993.

Firth R. G., Bell P. M., Marsh H. M., Hansen I., Rizza R. A. Postprandial hyperglycaemia in patients with Non-insulin-dependent diabetes mellitus. *J. Clin. Invest.* **77**: 1525-1532, 1986.

Fleischhacker E., Esenabhalu V. E., Spitaler M., Holzmann S., Skrabel F., Koidl B., Kostner G. M., Graier W. F. Human diabetes is associated with hyperreactivity of vascular smooth muscle cells due to altered subcellular Ca²⁺ distribution. *Diabetes* **48**: 1323-1330, 1999.

Flier J. S. Obesity. In: *Joslin's Diabetes Mellitus, Thirteenth Edition*. Eds: Kahn C. R., Weir G. C. Lea and Febiger, Philadelphia. Chapter 19, pp 351-362, 1994.

Fogh J., Wright D. C., Loveless J. D. Absence of HeLa cell contamination in 169 cell lines derived from human tumors. *J. Nat. Cancer Inst.* **58**: 209-214, 1977.

Forester G. P., Tall A. R., Bisgaier C. L., Glickman R. M. Rat intestine secretes spherical high density lipoproteins. *J. Biol. Chem.* **258**: 5938-5943, 1983.

Förstermann U., Mülsch A., Böhme E., Busse R. Stimulation of soluble guanylate cyclase by an acetylcholine-induced endothelium-derived factor from rabbit and canine arteries. *Circ. Res.* **58**: 531-538, 1986.

Fox P. L., Chisolm G. M., DiCorleto P. E. Lipoprotein-mediated inhibition of endothelial cell production of platelet-derived growth factor-like protein depends on free radical lipid peroxidation. *J. Biol. Chem.* **262**: 6046-6054, 1987.

Fukushima K., Ichimiya H., Higashijima H., Yamashita H., Kuroki S., Chijiwa K., Tanaka M. Regulation of bile acid synthesis in the rat: relationship between hepatic cholesterol 7 α -hydroxylase activity and portal bile acids. *J. Lipid Res.* **36**: 315-321, 1995.

Furchgott R. F. The role of endothelium in the responses of vascular smooth muscle to drugs. *Ann. Rev. Pharmacol. Toxicol.* **24**: 175-197, 1984.

Furchgott R. F., Zawadzki J. V. The obligatory role of endothelial cells in the relaxation of arterial smooth muscle by acetylcholine. *Nature* **288**: 373-376, 1980.

Gailly P., Gong M. C., Somlyo A. V., Somlyo A. P. Possible role of atypical protein kinase C activated by arachidonic acid in Ca²⁺ sensitisation of rabbit smooth muscle. *J. Physiol.* **500**: 95-109, 1997.

Galle J., Bassenge E., Busse R. Oxidised low density lipoproteins potentiate vasoconstrictions to various agonists by direct interaction with vascular smooth muscle. *Circ. Res.* **66**: 1287-1293, 1990.

Galle J., Mulsch A., Busse R., Bassenge E. Effects of native and oxidised low density lipoproteins on formation and inactivation of endothelium-derived relaxing factor. *Arterioscler. Thromb.* **11**: 198-203, 1991.

Gan L. S., Yanni S., Thakker D. R. Modulation of the tight junctions of the Caco-2 cell monolayers by H₂-antagonists. *Pharm. Res.* **15**: 53-57, 1998.

Garland C. J., McPherson G. A. Evidence that nitric oxide does not mediate the hyperpolarisation and relaxation to acetylcholine in the rat small mesenteric artery. *Br. J. Pharmacol.* **105**: 429-435, 1992.

Garland C. J., Plane F., Kemp B. K., Cocks T. M. Endothelium-dependent hyperpolarisation: a role in the control of vascular tone. *Trends Pharm. Sci.* **16**: 23-30, 1995.

Gerber R. T., Holemans K., O'Brien-Coker I., Mallet A. I., Van Bree R., Van Assche F. A., Poston L. Cholesterol-independent endothelial dysfunction in virgin and pregnant rats fed a diet high in saturated fat. *J. Physiol.* **517**: 607-616, 1999.

Gerich J. E., Mitrakou A., Kelley D., Mandarino L., Nurjhan N., Reilly J., Jenssen T., Veneman T., Consoli A. Contribution of impaired muscle glucose clearance to reduced postabsorptive systemic glucose clearance in NIDDM. *Diabetes* **39**: 211-216, 1990.

Gianturco S. H., Bradley W. A. Lipoprotein receptors. In: *Plasma Lipoproteins* Ed. Gotto A. M. Jr. Elsevier, Amsterdam. Chapter 6, pp 183-220, 1987.

- Golay A., Felber J. P., Jequier E., DeFronzo R. A., Ferrannini E. Metabolic basis of obesity and noninsulin-dependent diabetes. *Diabetes Metab. Rev.* 4: 727-747, 1988.
- Golay A., Munger R., Felber J-P. Obesity and NIDDM: the retrograde regulation concept. *Diabetes Rev.* 5: 69-82, 1997.
- Goldstein J. L., Brown M. S. Regulation of the mevalonate pathway. *Nature* 343: 425-430, 1990.
- Goldstein J. L., Ho Y. K., Basu S. K., Brown M. S. Binding site on macrophages that mediates uptake and degradation of acetylated low density lipoprotein, producing massive cholesterol deposition. *Proc. Natl. Acad. Sci. USA* 76: 333-337, 1979.
- Gonzalez A. M., Sochor M., Hothersall J. S., McLean P. Effect of aldose reductase inhibitor (sorbitol) on integration of polyol pathway, pentose phosphate pathway, and glycolytic route in diabetic rat lens. *Diabetes* 35: 1200-1205, 1986.
- González R. G., Barnett P., Aguayo J., Cheng H. M., Chylack L. T. Direct measurement of polyol pathway activity in the ocular lens. *Diabetes* 33: 196-199, 1984.
- Goodyear L. J., Smith R. J. Exercise and diabetes. In: *Joslin's Diabetes Mellitus, Thirteenth Edition*. Eds. Kahn C. R., Weir G. C. Lea and Febiger, Philadelphia. Chapter 26, pp 451-459, 1994.
- Gordon D. J., Probstfield J. L., Garrison R. J., Neaton J. D., Castelli W. P., Knoke J. D., Jacobs D. R., Bangdiwala S., Tyroler A. High-density lipoprotein cholesterol and cardiovascular disease: Four prospective American studies. *Circulation* 79: 8-15, 1989.
- Goyal R. K. Muscarinic receptor subtypes. Physiology and Clinical Implications. *New Engl. J. Med.* 321: 1022-1029, 1989.
- Green C. J. In: *Animal Anaesthesia*. Laboratory Animal Handbook 8. Laboratory animals Ltd., London. Chapter 7, pp 53-84, 1982.
- Grober J., Zaghini I., Fujii H., Jones S. A., Kliwer S. A., Willson T. M., Ono T., Besnard P. Identification of a bile acid-responsive element in the human ileal bile acid-binding protein gene. *J. Biol. Chem.* 274: 29749-29754, 1999.
- Grundy S. M., Ahrens E. H. Jr., Salen G. Interruption of the enterohepatic circulation of bile acids in man: comparative effects of cholestyramine and ileal exclusion on cholesterol metabolism. *J. Lab. Clin. Med.* 78: 94-121, 1971.
- Gryglewski R. J., Palmer R. M. J., Moncada S. Superoxide anion is involved in the breakdown of endothelium-derived vascular relaxing factor. *Nature* 320: 454-456, 1986.

- Gwynne J. T. High-density lipoprotein cholesterol levels as a marker of reverse cholesterol transport. *Am. J. Cardiol.* **64**: 10G-17G, 1989.
- Havel R. J., Hamilton R. L. Hepatocytic lipoprotein receptors and intracellular lipoprotein catabolism. *Hepatology* **8**: 1689-1704, 1988.
- Hidalgo I. J., Borchardt R. T. Transport of bile acids in a human intestinal epithelial cell line, Caco-2. *Biochim. Biophys. Acta.* **1035**: 97-103, 1990.
- Hirst G. D. S., Edwards F. R. Sympathetic neuroeffector transmission in arteries and arterioles. *Physiol. Rev.* **69**: 546-604, 1989.
- Hofmann A. F. Biliary secretion and excretion. The hepatobiliary component of the enterohepatic circulation of bile acids. In: *Physiology of the Gastrointestinal Tract, Third Edition, Volume Two*. Ed. Johnson L. R. Raven Press, New York. Chapter 44, pp 1555-1575, 1994a.
- Hofmann A. F. Intestinal absorption of bile acids and biliary constituents. The intestinal component of the enterohepatic circulation and the integrated system. In: *Physiology of the Gastrointestinal Tract, Third Edition, Volume Two*. Ed. Johnson L. R. Raven Press, New York. Chapter 55, pp 1845-1865, 1994b.
- Hofmann A. F., Mysels K. J. Bile salts as biological surfactants. *Colloids and Surfaces* **30**: 145-173, 1988.
- Hofmann A. F., Sjövall J., Kurz G., Radomska A., Schteingart C. D., Tint G. S., Vlahcevic Z. R., Setchell K. D. R. A proposed nomenclature for bile acids. *J. Lipid Res.* **33**: 599-604, 1992a.
- Hofmann C. A., Edwards C. W., Hillman R. M., Colca J. R. Treatment of insulin-resistant mice with the oral antidiabetic agent pioglitazone: Evaluation of liver GLUT2 and phosphoenolpyruvate carboxykinase expression. *Endocrinology* **130**: 735-740, 1992b.
- Hofmann C., Lorenz K., Colca J. R. Glucose transport deficiency in diabetic animals is corrected by treatment with the oral antihyperglycaemic agent pioglitazone. *Endocrinology* **129**: 1915-1925, 1991.
- Hogikyan R. V., Galecki A. T., Halter J. B., Supiano M. A. Heightened norepinephrine-mediated vasoconstriction in type 2 diabetes. *Metabolism* **48**: 1536-1541, 1999.
- Holt P. R. Intestinal absorption of bile salts in the rat. *Am. J. Physiol.* **207**: 1-7, 1964.
- Hopfner R. L., Gopalakrishnan V. Endothelin: emerging role in diabetic vascular complications. *Diabetologia* **42**: 1383-1394, 1999.

Hopfner R. L., Misurski D., Wilson T. W., McNeill J. R., Gopalakrishnan V. Insulin and vanadate restore decreased plasma endothelin concentrations and exaggerated vascular responses to normal in the streptozotocin diabetic rat. *Diabetologia* **41**: 1233-1240, 1998.

Horowitz A., Menice C. B., Laporte R., Morgan K. G. Mechanisms of smooth muscle contraction. *Physiol. Rev.* **76**: 967-1003, 1996.

Hoshita T. Bile alcohols and primitive bile acids. In: *Sterols and Bile Acids*. Eds. Daniellson H., Sjövall J. Elsevier, Amsterdam. Chapter 10, pp 279-302, 1985.

Howard B. V., Abbott W. G. H., Beltz W. F., Harper I. T., Fields R. M., Grundy S. M., Taskinen M-R. Integrated study of low density lipoprotein metabolism and very low density lipoprotein metabolism in non-insulin-dependent diabetes. *Metabolism* **36**: 870-877, 1987.

Howard B. V., Howard J. W. M. The pathophysiology and treatment of lipid disorders in diabetes mellitus. In: *Joslin's Diabetes Mellitus, Thirteenth Edition*. Eds. Kahn R. C., Weir G. C. Lea and Febiger, Philadelphia. Chapter 21, pp 372-396, 1994.

Howlett H. C. S., Bailey C. J. A risk-benefit assessment of metformin in type 2 diabetes mellitus. *Drug Safety* **20**: 489-503, 1999.

Hundal H. S., Ramlal T., Reyes R., Leiter L. A., Klip A. Cellular mechanism of metformin action involves glucose transporter translocation from an intracellular pool to the plasma membrane in L6 muscle cells. *Endocrinology* **131**: 1165-1173, 1992.

Hwa J. J., Ghibaudi L., Williams P., Chatterjee M. Comparison of acetylcholine-dependent relaxation in large and small arteries of rat mesenteric vascular bed. *Am. J. Physiol.* **266**: H952-H958, 1994.

Ignarro L. J., Buga G. M., Wood K. S., Byrns R. E., Chaudhuri G. Endothelium-derived relaxing factor produced and released from artery and vein is nitric oxide. *Proc. Natl. Acad. Sci. USA* **84**: 9265-9269, 1987.

Ignarro L. J., Kadowitz P. J. The pharmacological and physiological role of cyclic GMP in vascular smooth muscle relaxation. *Ann. Rev. Pharmacol. Toxicol.* **25**: 171-191, 1985.

Ikebe M., Brozovich F. V. Protein Kinase C increases force and slows relaxation in smooth muscle: evidence for regulation of the myosin light chain phosphatase. *Biochem. Biophys. Res. Comm.* **225**: 370-376, 1996.

Ikeda T., Iwata K., Murakami H. Inhibitory effect of metformin on intestinal glucose absorption in the perfused rat intestine. *Biochem. Pharmacol.* **59**: 887-890, 2000.

Inoue A., Yanagisawa M., Kimura S., Kasuya Y., Miyauchi T., Goto K., Masaki T. The human endothelin family: three structurally and pharmacologically distinct isopeptides predicted by three separate genes. *Proc. Natl. Acad. Sci. USA* 86: 2863-2867, 1989.

Jacobs M., Plane F., Bruckdorfer R. Native and oxidised low-density lipoproteins have different inhibitory effects on endothelium-derived relaxing factor in the rabbit aorta. *Br. J. Pharmacol.* 100: 21-26, 1990.

Janka H. U. Platelet and endothelial function tests during metformin treatment in diabetes mellitus. *Horm. Metab. Res.* 15: (Suppl. 1) 120-122, 1985.

Jarrett R. J. Cardiovascular disease and hypertension in diabetes mellitus. *Diabetes Metab. Rev.* 5: 547-558, 1989.

Jeanrenaud B. Central nervous system and peripheral abnormalities: clues to the understanding of obesity and NIDDM. *Diabetologia* 37: (Suppl. 2) S169-S178, 1994.

Jokl R., Colwell J. A. Arterial thrombosis and atherosclerosis in diabetes. *Diabetes Rev.* 5: 316-330, 1997.

Jörneskog G., Egberg N., Fagrell B., Fatah K., Hessel B., Johnsson H., Brismar K., Blombäck M. Altered properties of the fibrin gel structure in patients with IDDM. *Diabetologia* 39: 1519-1523, 1996.

Kamm K. E., Stull J. T. The function of myosin and myosin light chain kinase phosphorylation in smooth muscle. *Ann. Rev. Pharmacol. Toxicol.* 25: 593-620, 1985.

Kanda T., Foucand L., Nakamura Y., Niot I., Besnard P., Fujita M., Sakai Y., Hatakeyama K., Ono T., Fujii H. Regulation of expression of human intestinal bile acid-binding protein in Caco-2 cells. *Biochem. J.* 330: 261-265, 1998.

Kanda T., Niot I., Foucaud L., Fujii H., Bernard A., Ono T., Besnard P. Effect of bile on the intestinal bile-acid binding protein (I-BABP) expression. *In vitro* and *in vivo* studies. *FEBS Letters* 384: 131-134, 1996.

Kane J. P. Apolipoprotein B: structural and metabolic heterogeneity. *Annu. Rev. Physiol.* 45: 637-650, 1983.

Kannel W. B., McGee D. L. Diabetes and glucose tolerance as risk factors for cardiovascular disease: the Framingham study. *Diabetes Care* 2: 120-126, 1979.

Kasim S. E., Tseng K., Jen K. L. C., Khilnani S. Significance of hepatic triglyceride lipase activity in the regulation of serum high density lipoproteins in type II diabetes mellitus. *J. Clin. Endocrinol. Metab.* 65: 183-187, 1987.

- Katakam P. V. G., Ujhelyi M. R., Hoenig M., Miller A. W. Metformin improves vascular function in insulin-resistant rats. *Hypertension* **35**: 108-112, 2000.
- Kawano Y., Fukata Y., Oshiro N., Amano M., Nakamura T., Ito M., Matsumura F., Inagaki M., Kaibuchi K. Phosphorylation of Myosin-binding subunit (MBS) of myosin phosphatase by Rho-kinase *in vivo*. *J. Cell Biol.* **147**: 1023-1038, 1999.
- Khalil R. A., Lajoie C., Resnick M. S., Morgan K. G. Ca^{2+} -independent isoforms of protein kinase C differentially translocate in smooth muscle. *Am. J. Physiol.* **263**: C714-C719, 1992.
- Khan B. V., Fungwe T. V., Wilcox H. G., Heimberg M. Cholesterol is required for the secretion of very-low-density lipoprotein: *In vivo* studies. *Biochim. Biophys. Acta.* **1044**: 297-304, 1990.
- Khan N. A., Wiernsperger N., Quemener V., Havouis R., Moulinoux J. P. Characterisation of metformin transport system in NIH 3T3 cells. *J. Cell. Physiol.* **152**: 310-316, 1992.
- Kilpatrick E. V., Cocks T. M. Evidence for differential roles of nitric oxide (NO) and hyperpolarisation in endothelium-dependent relaxation of pig isolated coronary artery. *Br. J. Pharmacol.* **112**: 557-565, 1994.
- Kimes B. W., Brandt B. L. Characterisation of two putative smooth muscle cell lines from rat thoracic aorta. *Exp. Cell Res.* **98**: 349-366, 1976.
- Kimura K., Ito M., Amano M., Chihara K., Fukata Y., Nakafuku M., Yamamori B., Feng J., Nakano T., Okawa K., Iwamatsu A., Kaibuchi K. Regulation of myosin phosphatase by Rho and Rho-associated kinase (Rho-kinase). *Science* **273**: 245-248, 1996.
- King G. L., Johnson S. M. Receptor-mediated transport of insulin across endothelial cells. *Science* **227**: 1583-1586, 1985.
- Kita S., Taguchi Y., Matsumura Y. Endothelin-1 enhances pressor responses to Norepinephrine: involvement of endothelin-B receptor. *J. Cardiovasc. Pharmacol.* **31**: (Suppl 1) S119-S121, 1998.
- Kitazawa T., Eto M., Woodsome T. P., Brautigan D. L. Agonists trigger G protein-mediated activation of the CPI-17 inhibitor phosphoprotein of myosin light chain phosphatase to enhance vascular smooth muscle contractility. *J. Biol. Chem.* **275**: 9897-9900, 2000.
- Kitazawa T., Masuo M., Somlyo A. P. G. Protein-mediated inhibition of myosin light-chain phosphatase in vascular smooth muscle. *Proc. Natl. Acad. Sci. USA* **88**: 9307-9310, 1991.

Kitazawa T., Takizawa N., Ikebe M., Eto M. Reconstitution of protein kinase C-induced contractile Ca^{2+} sensitisation in Triton X-100-demembranated rabbit arterial smooth muscle. *J. Physiol.* **520**: 139-152, 1999.

Klip A., Guma A., Ramlal T., Bilan P. J., Lam L., Leiter L. A. Stimulation of hexose transport by metformin in L6 muscle cells in culture. *Endocrinology* **130**: 2535-2544, 1992.

Klip A., Leiter L. A. Cellular mechanism of action of metformin. *Diabetes Care* **13**: 696-704, 1990.

Komori K., Suzuki H. Heterogenous distribution of muscarinic receptors in the rabbit saphenous artery. *Br. J. Pharmacol.* **92**: 657-664, 1987.

Kramer W., Burckhardt G., Wilson F. A., and Kurz G. Bile salt-binding polypeptides in brush-border membrane vesicles from rat small intestine revealed by photoaffinity labelling. *J. Biol. Chem.* **258**: 3623-3627, 1983.

Kubota Y., Nomura M., Kamm K. E., Mumby M. C., Stull J. T. GTP γ S-dependent regulation of smooth muscle contractile elements. *Am. J. Physiol.* **262**: C405-C410, 1992.

Kugiyama K., Ohgushi M., Sugiyama S., Murohara T., Fukunaga K., Miyamoto E., Yasue H. Lysophosphatidylcholine inhibits surface receptor-mediated intracellular signals in endothelial cells by a pathway involving protein kinase C activation. *Circ. Res.* **71**: 1422-1428, 1992.

Laakso M. Epidemiology of diabetic dyslipidaemia. *Diabetes Rev.* **3**: 408-422, 1995.

Laakso M., Edelman S. V., Brechtel G., Baron A. D. Decreased effect of insulin to stimulate skeletal muscle blood flow in obese man. A novel mechanism for insulin resistance. *J. Clin. Invest.* **85**: 1844-1852, 1990.

Laakso M., Edelman S. V., Brechtel G., Baron A. D. Impaired insulin-mediated skeletal muscle blood flow in patients with NIDDM. *Diabetes* **41**: 1076-1083, 1992.

Laakso M., Lehto S. Epidemiology of macrovascular disease in diabetes. *Diabetes Rev.* **5**: 294-315, 1997.

Lack L., Weiner I. M. *In vitro* absorption of bile salts by small intestine of rats and guinea pigs. *Am. J. Physiol.* **200**: 313-317, 1961.

Lebovitz H. E. Oral antidiabetic agents. In: *Joslin's Diabetes Mellitus, Thirteenth Edition*. Eds. Kahn C. R., Weir G. C. Lea and Febiger, Philadelphia. Chapter 29, pp 508-529, 1994.

- Lee J. M., Peuler J. D. Acute vasorelaxant effects of metformin and attenuation by stimulation of sympathetic agonist release. *Life Sci.* **64**: 57-63, 1999.
- Lee M. R., Li L., Kitazawa T. Cyclic GMP causes Ca^{2+} desensitisation in vascular smooth muscle by activating the myosin light chain kinase phosphatase. *J. Biol. Chem.* **272**: 5063-5068, 1997.
- Levy R. I. Cholesterol, lipoproteins, apoproteins, and heart disease: Present status and future prospects. *Clin. Chem.* **27**: 653-662, 1981.
- Liao J. K., Clark S. L. Regulation of G-protein α_{i2} subunit expression by oxidised low-density lipoprotein. *J. Clin. Invest.* **95**: 1457-1463, 1995.
- Liao J. K., Shin W. S., Lee W. Y., Clark S. L. Oxidised low-density lipoprotein decreases the expression of endothelial nitric oxide synthase. *J. Biol. Chem.* **270**: 319-324, 1995.
- Lillienau J., Crombie D. L., Munoz J., Longmire-Cook S. J., Hagey L. R., Hofmann A. F. Negative feedback regulation of the ileal bile acid transport system in rodents. *Gastroenterology* **104**: 38-46, 1993.
- Lin M. C., Kramer W., Wilson F. A. Identification of cytosolic and microsomal bile acid-binding proteins in rat ileal enterocytes. *J. Biol. Chem.* **265**: 14986-14995, 1990.
- Lin M. C., Mullady E., Wilson F. A. Timed photoaffinity labelling and characterisation of bile acid binding and transport proteins in rat ileum. *Am. J. Physiol.* **265**: G56-G62, 1993.
- Lin M. C., Weinberg S. L., Kramer W., Burckhardt G., and Wilson F. A. Identification and comparison of bile acid-binding polypeptides in ileal basolateral membrane. *J. Membr. Biol.* **106**: 1-11, 1988.
- Lincoln T. M. Effects of nitroprusside and 8-bromo-cyclic GMP on the contractile activity of the rat aorta. *J. Pharmacol. Exp. Ther.* **224**: 100-107, 1983.
- Lincoln T. M., Cornwell T. L. Intracellular cyclic GMP receptor proteins. *FASEB J.* **7**: 328-338, 1993.
- Lincoln T. M., Komalavilas P., Boerth N. J., MacMillan-Crow L. A., Cornwell T. L. cGMP signalling through cAMP- and cGMP-dependent protein kinases. *Adv. Pharmacol.* **34**: 305-322, 1995.
- Lohmann S. M., Vaandrager A. B., Smolenski A., Walter U., De Jonge H. R. Distinct and specific functions of cGMP-dependent protein kinases. *Trends Pharm. Sci.* **22**: 307-312, 1997.

Longmore J., Weston A. H. The role of K⁺ channels in the modulation of vascular smooth muscle tone. In: *Potassium Channels: Structure, Classification, Function and Therapeutic Potential*. Ed. Cook N. S. Halsted Press, New York. Chapter 9, pp 259-278, 1990.

Lopes-Virella M., Mironova M., Virella G. LDL-containing immune complexes and atherosclerosis in diabetes. *Diabetes Rev.* 5: 410-424, 1997.

Lücke H., Stange G., Kinne R., Murer H. Taurocholate-sodium co-transport by brush-border membrane vesicles isolated from rat ileum. *Biochem. J.* 174: 951-958, 1978.

Madara J. L. Loosening of tight junctions: lessons from the intestine. *J. Clin. Invest.* 83: 1089-1094, 1989.

Madara J. L. Maintenance of the macromolecular barrier at cell extrusion sites in intestinal epithelium: physiological rearrangement of tight junctions. *J. Membr. Biol.* 116: 177-184, 1990.

Madara J. L., Moore R., Carlson S. Alteration of intestinal tight junction structure and permeability by cytoskeletal contraction. *Am. J. Physiol.* 253: C854-C861, 1987.

Makishima M., Okamoto A. Y., Repa J. J., Tu H., Learned R. M., Luk A., Hull M. V., Lustig K. D., Mangelsdorf D. J., Shan B. Identification of a nuclear receptor for Bile Acids. *Science* 284: 1362-1364, 1999.

Malarkey K., Aidulis D., Belham C. M., Graham A., McLees A., Paul A., Plevin R. Cell signalling pathways involved in the regulation of vascular smooth muscle contraction and relaxation. In: *Pharmacology of Vascular Smooth Muscle*. Oxford University Press, Oxford. Chapter 7, pp 160-183, 1996.

Martin W., Villani G. M., Jothianandan D., Furchgott R. F. Selective blockade of endothelium-dependent and glyceryl trinitrate-induced relaxation by haemoglobin and by methylene blue in the rabbit aorta. *J. Pharmacol. Exp. Ther.* 232: 708-716, 1985.

Matsuda M., Consoli A., Bressler P., DeFronzo R. A., Del Prato S. Sustained response of hepatic glucose production (HGP) to glucagon in type II diabetic subjects. *Diabetologia* 35: (Suppl. 1) A37, 1992.

McClintock C., Shiau Y. F. Jejunum is more important than terminal ileum for taurocholate absorption in rats. *Am. J. Physiol.* 244: G507-G514, 1983.

Mekhjian H. S., Phillips S. F., Hofmann A. F. Colonic secretion of water and electrolytes induced by bile acids: perfusion studies in man. *J. Clin. Invest.* 50: 1569-1577, 1971.

Mieyal P., Fulton D., McGiff J. C., Quilley J. NO-independent vasodilation to acetylcholine in the rat isolated kidney utilises a charybdotoxin-sensitive, intermediate-conductance Ca^{++} -activated K^{+} channel. *J. Pharmacol. Exp. Ther.* **285**: 659-664, 1998.

Miller K. W., Small D. M. Structure of triglyceride-rich lipoproteins: an analysis of core and surface phases. In: *Plasma Lipoproteins*. Ed. Gotto A. M. Jr. Elsevier, Amsterdam. Chapter 1, pp 1-71, 1987.

Moncada, S., Higgs A. The L-arginine-nitric oxide pathway. *New Engl. J. Med.* **329**: 2002-2012, 1993.

Montanari G., Bondioli A., Rizzato G., Puttini M., Tremoli E., Mussoni L., Mannucci L., Pazzucconi F., Sirtori C. R. Treatment with low dose metformin in patients with peripheral vascular disease. *Pharm. Res.* **25**: 63-73, 1992.

Mustard J. F., Packham M. A. Factors influencing platelet function: adhesion, release, and aggregation. *Pharmacol. Rev.* **22**: 97-187, 1970.

Muszbek L., Ádány R., Mikkola H. Novel aspects of blood coagulation factor XIII. I. structure, distribution, activation, and function. *Crit. Rev. Clin. Lab. Sci.* **33**: 357-421, 1996.

Myers P. R., Wright T. F., Tanner M. A., Ostlund R. E. Jr. The effects of native LDL and oxidised LDL on EDRF bioactivity and nitric oxide production in vascular endothelium. *J. Lab. Clin. Med.* **124**: 672-683, 1994.

Nagao T., Vanhoutte P. M. Hyperpolarisation as a mechanism for endothelium-dependent relaxations in the porcine coronary artery. *J. Physiol.* **445**: 355-367, 1992.

Nelson M. T., Patlak J. B., Worley J. F., Standen N. B. Calcium channels, potassium channels, and voltage dependence of arterial smooth muscle tone. *Am. J. Physiol.* **259**: C3-C18, 1990.

Nelson M. T., Quayle J. M. Physiological roles and properties of potassium channels in arterial smooth muscle. *Am. J. Physiol.* **268**: C799-C822, 1995.

Nguyen L. B., Shefer S., Salen G., Ness G. C., Batta A., Chowdhary I. R., Paroulek E., Hauser S. Regulation of 3-hydroxy-3-methylglutaryl-coenzyme A reductase activity in the rat ileum: effects of bile acids and lovastatin. *Metabolism* **43**: 1446-1450, 1994.

Ni Neill A. M., Moore U., Collins P. B., Johnson A. H., Tomkin G. H. Metformin mimics insulin action on cholesterol biosynthesis in cultured intestinal rat cells. *Diabetologia* **30**: 562A, 1987.

- Nicklin P., Keates A. C., Page T., Bailey C. J. Transfer of metformin across monolayers of human intestinal Caco-2 cells and across rat intestine. *Int. J. Pharmaceutics* **128**: 155-162, 1996.
- Niewiarowski S., Stuart R. K., Thomas D. P. Activation of intravascular coagulation by collagen. *Proc. Soc. Exp. Biol. Med.* **123**: 196-200, 1966.
- Northup J. K., Smigel M. D., Sternweis P. C., Gilman A. G. The subunits of the stimulatory regulatory component of adenylate cyclase. Resolution of the activated 45,000-Dalton (α) subunit. *J. Biol. Chem.* **258**: 11369-11376, 1983.
- Ohgushi M., Kugiyama K., Fukunaga K., Murohara T., Sugiyama S., Miyamoto E., Yasue H. Protein kinase C inhibitors prevent impairment of endothelium-dependent relaxation by oxidatively modified LDL. *Arterioscler. Thromb.* **13**: 1525-1532, 1993.
- Okumura K., Nishiura T., Awaji Y., Kondo J., Hashimoto H., Ito T. 1,2-Diacylglycerol content and its fatty acid composition in thoracic aorta of diabetic rats. *Diabetes* **40**: 820-824, 1991.
- Opdam F. J. M., Kamps G., Croes H., van Bokhoven H., Ginsel L. A., Fransen J. A. M. Expression of Rab small GTPases in epithelial Caco-2 cells: Rab 21 is an apically located GTP-binding protein in polarised intestinal epithelial cells. *Eur. J. Cell Biol.* **79**: 306-316, 2000.
- Owen M. R., Doran E., Halestrap A. P. Evidence that metformin exerts its anti-diabetic effects through inhibition of complex 1 of the mitochondrial respiratory chain. *Biochem. J.* **348**: 607-614, 2000.
- Palmer A. M., Thomas C. R., Gopaul N., Dhir S., Änggård E. E., Poston L., Tribe R. M. Dietary antioxidant supplementation reduces lipid peroxidation but impairs vascular function in small mesenteric arteries of the streptozotocin-diabetic rat. *Diabetologia* **41**: 148-156, 1998.
- Pappenheimer J. R. On the coupling of membrane digestion with intestinal absorption of sugars and amino acids. *Am. J. Physiol.* **265**: G409-G417, 1993.
- Pappenheimer J. R., Reiss K. Z. Contribution of solvent drag through intercellular junctions to absorption of nutrients by the small intestine of the rat. *J. Membr. Biol.* **100**: 123-136, 1987.
- Parkington H. C., Tonta M. A., Coleman H. A., Tare M. Role of membrane potential in endothelium-dependent relaxation of guinea-pig coronary arterial smooth muscle. *J. Physiol.* **484**: 469-480, 1995.
- Parks D. J., Blanchard S. G., Bledsoe R. K., Chandra G., Consler T. G., Kliewer S. A., Stimmel J. B., Willson T. M., Zavacki A. M., Moore D. D., Lehmann J. M. Bile Acids: natural ligands for an orphan nuclear receptor. *Science* **284**: 1365-1368, 1999.

- Parsons B. J., Smyth D. H., Taylor C. B. The action of phlorrhizin on the intestinal transfer of glucose and water *in vitro*. *J. Physiol.* **144**: 387-402, 1958.
- Parsons D. S., Wingate D. L. The effect of osmotic gradients on fluid transfer across rat intestine *in vitro*. *Biochim. Biophys. Acta.* **46**: 170-183, 1961.
- Patsch J. R., Gotto A. M. Jr. Metabolism of high density lipoproteins. In: *Plasma Lipoproteins* Ed. Gotto A. M. Jr. Elsevier, Amsterdam. Chapter 7, pp 221-259, 1987.
- Pérez M., Barber A., Ponz F. Modulation of intestinal paracellular permeability by intracellular mediators and cytoskeleton. *Can. J. Physiol. Pharmacol.* **75**: 287-292, 1997.
- Perris, A.D. Some effects of whole body X-Irradiation on intestinal function. Ph.D. Thesis Sheffield University. pp1-269, 1964.
- Peuler J. D., Miller J. A., Bourghli M., Zamman H. Y., Soltis E. E., Sowers J. R. Disparate effects of antidiabetic drugs on arterial contraction. *Metabolism* **46**: 1199-1205, 1997.
- Pfeifle B., Ditschuneit H. H., Ditschuneit H. Binding and biological actions of insulin-like growth factors on human arterial smooth muscle cells. *Hormone Met. Res.* **14**: 409-414, 1982.
- Pfeifle B., Ditschuneit H. Receptors for insulin and insulin-like growth factor in cultured arterial smooth muscle cells depend on their growth state. *J. Endocr.* **96**: 251-257, 1983.
- Phillips S. F., Giller J. The contribution of the colon to electrolyte and water conservation in man. *J. Lab. Clin. Med.* **81**: 733-746, 1973.
- Pieper G. M. Enhanced, unaltered and impaired nitric oxide-mediated endothelium-dependent relaxation in experimental diabetes mellitus: importance of disease duration. *Diabetologia* **42**: 204-213, 1999.
- Pieper G. M., Langenstroer P., Siebeneich W. Diabetic-induced endothelial dysfunction in rat aorta: role of hydroxyl radicals. *Cardiovasc. Res.* **34**: 145-156, 1997.
- Pinto M., Robine-Leon S., Appay M-D., Kedinger M., Triadou N., Dussaulx E., Lacroix B., Simon-Assman P., Haffen K., Fogh J., Zweibaum A. Enterocyte-like differentiation and polarisation of the human colon carcinoma cell line Caco-2 in culture. *Biol. Cell* **47**: 323-330, 1983.
- Plane F., Pearson T., Garland C. J. Multiple pathways underlying endothelium-dependent relaxation in the rabbit isolated femoral artery. *Br. J. Pharmacol.* **115**: 31-38, 1995.

- Playoust M. R., Isselbacher K. J. Studies on the transport and metabolism of conjugated bile salts by intestinal mucosa. *J. Clin. Invest.* **43**: 467-476, 1964.
- Putney J. W. A model for receptor-regulated calcium entry. *Cell Calcium* **7**: 1-12, 1986.
- Quinn M. T., Parthasarathy S., Fong L. G., Steinberg D. Oxidatively modified low density lipoproteins: a potential role in recruitment and retention of monocyte/macrophages during atherogenesis. *Proc. Natl. Acad. Sci. USA* **84**: 2995-2998, 1987.
- Rafter J. J., Branting C. Bile acids-interaction with the intestinal mucosa. *Eur. J. Cancer Prev.* **1**: (Suppl 2) 49-54, 1991.
- Rains S. G. H., Wilson G. A., Richmond W., Elkeles R. S. The effect of glibenclamide and metformin on serum lipoproteins in type 2 diabetes. *Diabetic Med.* **5**: 653-658, 1988.
- Rains S. G. H., Wilson G. A., Richmond W., Elkeles R. S. The reduction of low density lipoprotein cholesterol by metformin is maintained with long-term therapy. *J. Royal Soc. Med.* **82**: 93-94, 1989.
- Randle P. J., Garland P. B., Hales C. N., Newsholme E. A. The glucose-fatty acid cycle: its role in insulin insensitivity and the metabolic disturbances of diabetes mellitus. *Lancet* **I**: 785-789, 1963.
- Rapoport R. M., Draznin M. B., Murad F. Sodium nitroprusside-induced protein phosphorylation in intact rat aorta is mimicked by 8-bromo cyclic GMP. *Proc. Natl. Acad. Sci. USA* **79**: 6470-6474, 1982.
- Rasmussen H., Takuwa Y., Park S. Protein kinase C in the regulation of smooth muscle contraction. *FASEB J.* **1**: 177-185, 1987.
- Reaven G. M. Role of insulin resistance in human disease. Banting Lecture. *Diabetes* **37**: 1595-1607, 1988.
- Reaven G. M. The fourth musketeer: from Alexandre Dumas to Claude Bernard. *Diabetologia* **38**: 3-13, 1995.
- Reaven G. M., Hollenbeck C. B., Chen Y. D. I. Relationship between glucose tolerance, insulin secretion, and insulin action in non-obese individuals with varying degrees of glucose tolerance. *Diabetologia* **32**: 52-55, 1989.
- Reihner E., Angelin B., Rudling M., Ewerth S., Björkhem I., Einarsson K. Regulation of hepatic cholesterol metabolism in humans: stimulatory effects of cholestyramine on HMG-CoA reductase activity and low density lipoprotein receptor expression in gallstone patients. *J. Lipid Res.* **31**: 2219-2226, 1990.

Reil T. D., Barnard R. J., Kashyap V. S., Roberts C. K., Gelabert H. A. Diet-induced changes in endothelial-dependent relaxation of the rat aorta. *J. Surg. Res.* **85**: 96-100, 1999.

Resink T. J., Scott-Burden T., Bühler F. R. Endothelin stimulates phospholipase C in cultured vascular smooth muscle cells. *Biochem. Biophys. Res. Comm.* **157**: 1360-1368, 1988.

Revers R. R., Fink R., Griffin J., Olefsky J. M., Kolterman O. G. Influence of hyperglycaemia on insulin's *in vivo* effects in type II diabetes. *J. Clin. Invest.* **73**: 664-672, 1984.

Rinaldi G. J., Cingolani H. E. Effect of diabetes on fast response to norepinephrine in rat aorta. *Diabetes* **41**: 30-34, 1992.

Rock E., Malmud L., Fisher R. S. Gallbladder emptying in response to sham feeding. *Gastroenterology* **80**: 1263A, 1981.

Roda A., Cappelleri G., Aldini R., Roda E., Barbara L. Quantitative aspects of the interaction of bile acids with human serum albumin. *J. Lipid Res.* **23**: 490-495, 1982.

Root C., Smith C. D., Winegar D. A., Brieady L. E., Lewis M. C. Inhibition of ileal sodium-dependent bile acid transport by 2164U90. *J. Lipid Res.* **36**: 1106-1115, 1995.

Rosenzweig J. L. Principles of insulin therapy. In: *Joslin's Diabetes Mellitus, Thirteenth Edition*. Eds. Kahn C. R., Weir G. C. Lea and Febiger, Philadelphia. Chapter 27, pp 460-488, 1994.

Ross R. The pathogenesis of atherosclerosis-an update. *N. Engl. J. Med.* **314**: 488-500, 1986.

Rubanyi G. M. Vascular effects of oxygen-derived free radicals. *Free Rad.Biol. Med.* **4**: 107-120, 1988.

Ruderman N. B., Toews C. J., Shafrir E. Role of free fatty acids in glucose homeostasis. *Arch. Intern. Med.* **123**: 299-313, 1969.

Rudling M. J., Reihner E., Einarsson K., Ewerth S., Angelin B. Low density lipoprotein receptor-binding activity in human tissues: Quantitative importance of hepatic receptors and evidence for regulation of their expression *in vivo*. *Proc. Natl. Acad. Sci. USA.* **87**: 3469-3473, 1990.

Russell D. W., Setchell K. D. R. Bile acid biosynthesis. *Biochemistry* **31**: 4737-4749, 1992.

Salomaa V., Stinson V., Kark J. D., Folsom A. R., Davis C. E., Wu K. K. Association of fibrinolytic parameters with early atherosclerosis: The ARIC Study. Atherosclerosis risk in communities study. *Circulation* **91**: 284-290, 1995.

Scarborough N. L., Carrier G. O. Nifedipine and *alpha* adrenoreceptors in rat aorta. II. Role of extracellular calcium in enhanced *alpha*-2 adrenoreceptor-mediated contraction in diabetes. *J. Pharm. Exp. Ther.* **231**: 603-609, 1984.

Scarpello J. H. B., Hodgson E., Howlett, H. C. S. Effect of metformin on bile salt circulation and intestinal motility in type 2 diabetes mellitus. *Diabetic Med.* **15**: 651-656, 1998.

Schäfer G. On the mechanism of action of hypoglycaemia-producing biguanides. A re-evaluation and a molecular theory. *Biochem. Pharmacol.* **25**: 2005-2014, 1976a.

Schäfer G. Some new aspects on the interaction of hypoglycaemia-producing biguanides with biological membranes. *Biochem. Pharmacol.* **25**: 2015-2024, 1976b.

Scheck S. H., Barnard R. J., Lawani L. O., Youngren J. F., Martin D. A., Singh R. Effects of NIDDM on the glucose transport system in human skeletal muscle. *Diabetes Res.* **16**: 111-119, 1991.

Scherrer U., Randin D., Vollenweider P., Vollenweider L., Nicod P. Nitric oxide release accounts for insulin's vascular effects in humans. *J. Clin. Invest.* **94**: 2511-2515, 1994.

Schneider J., Erren T., Zofel P., Kaffarnik H. Metformin-induced changes in serum lipids, lipoproteins, and apoproteins in non-insulin-dependent diabetes mellitus. *Atherosclerosis* **82**: 97-103, 1990.

Schonfeld G. Diabetes, lipoproteins, and atherosclerosis. *Metabolism* **34**: 45-50, 1985.

Scott L. M., Tomkin G. H. Changes in hepatic and intestinal cholesterol regulatory enzymes: the influences of metformin. *Biochem. Pharmacol.* **32**: 827-830, 1983.

Secombe J. F., Pearson P. J., Schaff H. V. Oxygen radical-mediated vascular injury selectively inhibits receptor-dependent release of nitric oxide from canine coronary arteries. *J. Thorac. Cardiovasc. Surg.* **107**: 505-509, 1994.

Sharma R. V., Bhalla R. C. Metformin attenuates agonist-stimulated calcium transients in vascular smooth muscle cells. *Clin. Exper. Hypertension* **17**: 913-929, 1995.

Shaw A. M., McGrath J. C. Initiation of smooth muscle response. In: *Pharmacology of Vascular Smooth Muscle*. Eds. Garland C. J., Angus J. A. Oxford University Press, Oxford. Chapter 5, pp 103-135, 1996.

Simon F. R., Sutherland E., Sutherland J. Selective modulation of hepatic and ileal Na⁺-K⁺-ATPase by bile salts in the rat. *Am. J. Physiol.* **254**: G761-G767, 1988.

Sirtori C. R., Franceschini G., Gianfranceschi G., Sirtori M., Montanari G., Bosisio E., Mantero E., Bondioli A. Metformin improves peripheral vascular flow in nonhyperlipidemic patients with arterial disease *J. Cardiovasc. Pharm.* **6**: 914-923, 1984.

Somlyo A. P., Himpens B. Cell calcium and its regulation in smooth muscle. *FASEB J.* **3**: 2266-2276, 1989.

Somlyo A. P., Somlyo A. V. Signal transduction by G-proteins, rho-kinase and protein phosphatase to smooth muscle and non-muscle myosin II. *J. Physiol.* **522**: 177-185, 2000.

Somlyo A. V. Ultrastructure of vascular smooth muscle, In: *Handbook of Physiology, Section 2: The Cardiovascular System, Volume II: Vascular smooth muscle*. Eds. Bohr D. F., Somlyo A. P., Sparks A. V. Bethesda, Md, American Physiological Society. Chapter 2, pp 33-67, 1980.

Song Y. C., Sheng D., Taubenfeld S. M., Matsueda G. R. A microtiter assay for Factor XIII using fibrinogen and biotinylcadaverine as substrates. *Analytical Biochem.* **223**: 88-92, 1994.

Soulis T., Sastra S., Thallas V., Mortensen S. B., Wilken M., Clausen J. T., Bjerrum O. J. Petersen H., Lau J., Jerums G., Boel E., Cooper M. E. A novel inhibitor of advanced glycation end-product formation inhibits mesenteric vascular hypertrophy in experimental diabetes. *Diabetologia* **42**: 472-479, 1999.

Spellman S. J., Shaffer E. A., Rosenthal L. Gallbladder emptying in response to cholecystokinin. *Gastroenterology* **77**: 115-120, 1979.

Standl E. Cardiovascular risk in type 2 diabetes. *Diabetes Obesity Metab.* **1**: (Suppl. 2) S24-S36, 1999.

Stange E. F., Alavi M., Schneider A., Ditschuneit H., Poley J. R. Influence of dietary cholesterol, saturated and unsaturated lipid on 3-hydroxy-3-methylglutaryl CoA reductase activity in rabbit intestine and liver. *J. Lipid Res.* **22**: 47-56, 1981.

Stange E. F., Alavi M., Schneider A., Preclik G., Ditschuneit H. Lipoprotein regulation of 3-hydroxy-3-methylglutaryl coenzyme A reductase in cultured intestinal mucosa. *Biochim. Biophys. Acta* **620**: 520-527, 1980.

Stange E. F., Dietschy J. M. Cholesterol absorption and metabolism by the intestinal epithelium. In: *Sterols and Bile Acids*. Eds. Danielsson H., Sjövall J. Elsevier, Amsterdam. Chapter 5, pp 121-149, 1985.

Stange E. F., Suckling K. E., Dietschy J. M. Synthesis and Coenzyme A-dependent esterification of cholesterol in rat intestinal epithelium. *J. Biol. Chem.* **258**: 12868-12875, 1983.

Stein O., Stein Y. Bovine aortic endothelial cells display macrophage-like properties towards acetylated ¹²⁵I-labelled low density lipoprotein. *Biochem. Biophys. Acta.* **620**: 631-635, 1980.

Steinberg D., Parthasarathy S., Carew T. E., Khoo J. C., Witztum J. L. Beyond cholesterol: Modifications of low-density lipoprotein that increase its atherogenicity. *New Engl. J. Med.* **320**: 915-924, 1989.

Steinberg H. O., Cressman E., Wu Y., Hook G., Cronin J., Johnson A., Baron A. D. Insulin mediated nitric oxide production is impaired in insulin resistance. *Diabetes* **46**: (Suppl 1) 24A, 1997.

Stiehl A. Intestinal absorption of bile acids: effect of ursodeoxycholic acid treatment. *Ital. J. Gastroenterol.* **27**: 193-195, 1995.

Stout R. W. Insulin and atheroma: 20-year perspective. *Diabetes Care* **13**: 631-654, 1990.

Stull J. T. Phosphorylation of contractile proteins in relation to muscle function. *Adv. Cyclic Nucleotide Res.* **13**: 39-93, 1980.

Sugiura M., Inagami T., Hare G. M. T., Johns J. A. Endothelin action: Inhibition by a protein kinase C inhibitor and involvement of phosphoinositols. *Biochem. Biophys. Res. Comm.* **158**:170-176, 1989.

Surks H. K., Mochizuki N., Kasai Y., Georgescu S. P., Tang K. M., Ito M., Lincoln T. M., Mendelsohn M. E. Regulation of myosin phosphatase by a specific interaction with cGMP-dependent protein kinase I α . *Science* **286**: 1583-1587, 1999.

Tam E. S. L., Ferguson D. G., Bielefeld D. R., Lorenz J. N., Cohen R. M., Pun R. Y. K. Norepinephrine-mediated calcium signalling is altered in vascular smooth muscle of diabetic rat. *Cell Calcium* **21**: 143-150, 1997.

Taskinen M-R. Hyperlipidaemia in diabetes. *Baillière's Clinical Endocrin. Metab.* **4**: 743-775, 1990.

Taskinen M-R., Beltz W. F., Harper I., Fields R. M., Schonfeld G., Grundy S. M., Howard B. V. Effects of NIDDM on very-low-density lipoprotein triglyceride and apolipoprotein B metabolism. Studies before and after sulfonylurea therapy. *Diabetes* **35**: 1268-1277, 1986.

Taylor S. G., Southerton J. S., Weston A. H., Baker J. R. J. Endothelium-dependent effects of acetylcholine in rat aorta: a comparison with sodium nitroprusside and cromakalim. *Br. J. Pharmacol.* **94**: 853-863, 1988.

Taylor S. I., Accili D., Imai Y. Insulin resistance or insulin deficiency. Which is the primary cause of NIDDM? *Diabetes* **43**: 735-740, 1994.

Taylor S. I., Cama A., Accili D., Barbetti F., Quon M. J., Sierra M. L., Suzuki Y., Koller E., Levy-Toledano R., Wertheimer E., Moncada V. Y., Kadowaki H., Kadowaki T. Mutations in the insulin receptor gene. *Endocr. Rev.* **13**: 566-595, 1992.

Tesfamariam B., Brown M. L., Cohen R. A. Elevated glucose impairs endothelium-dependent relaxation by activating protein kinase C. *J. Clin. Invest.* **87**: 1643-1648, 1991.

Thastrup O., Cullen P. J., Drøbak B. K., Hanley M. R., Dawson A. P. Thapsigargin, a tumor promoter, discharges intracellular Ca^{2+} stores by specific inhibition of the endoplasmic reticulum Ca^{2+} -ATPase. *Proc. Natl. Acad. Sci. USA* **87**: 2466-2470, 1990.

Thiébaud D., DeFronzo R. A., Jacot E., Golay A., Acheson K., Maeder E., Jéquier E., Felber J.-P. Effect of long chain triglyceride infusion on glucose metabolism in man. *Metabolism* **31**: 1128-1136, 1982.

Tomkin G. H. Comparison of the effect of parenteral with oral biguanide therapy on vitamin B₁₂ and bile acid absorption. *Ir. J. Med. Sci.* **145**: 340-347, 1976.

Tomkin G. H., Hadden D. R., Weaver J. A., Montgomery D. A. D. Vitamin-B₁₂ status of patients on long-term metformin therapy. *BMJ* **2**: 685-687, 1971.

Torchia E. C., Cheema S. K., Agellon L. B. Coordinate regulation of bile acid biosynthetic and recovery pathways. *Biochem. Biophys. Res. Comm.* **225**: 128-133, 1996.

Trovati M., Massucco P., Mattiello L., Mularoni E., Cavalot F., Anfossi G. Insulin increases guanosine-3',5'-cyclic monophosphate in human platelets: A mechanism involved in the insulin anti-aggregating effect. *Diabetes* **43**: 1015-1019, 1994.

Tsien R. W., Ellinor P.T., Horne W. A. Molecular diversity of voltage-dependent Ca^{2+} channels. *Trends Pharm. Sci.* **12**: 349-354, 1991.

Turley S. D., Dietschy J. M. The Metabolism and Excretion of Cholesterol by the Liver. In: *The Liver: Biology and Pathobiology*. Eds. Arias I., Jakoby W. B., Popper H., Schachter D., Shafritz D. A. Raven Press, New York. Chapter 34, pp617-641, 1988.

Turner J. R., Angle J. M., Black E. D., Joyal J. L., Sacks D. B., Madara J. L. PKC-dependent regulation of transepithelial resistance: roles of MLC and MLC kinase. *Am. J. Physiol.* 277: C554-C562, 1999.

Turner J. R., Carlson S. L., Carnes D., Kerner R., Madara J. L. Permeability of intestinal epithelial tight junctions is regulated by Na⁺-glucose cotransport via myosin light chain phosphorylation. *Gastroenterology* 112: A413, 1997.

Turner J. R., Madara J. L. Physiological regulation of intestinal epithelial tight junctions as a consequence of Na⁺-coupled nutrient transport. *Gastroenterology* 109: 1391-1396, 1995.

UKPDS 16. Overview of 6 years therapy of type II diabetes: A progressive disease. *Diabetes* 44: 1249-1259, 1995.

UKPDS. Effect of intensive blood-glucose control with metformin on complications in overweight patients with type 2 diabetes (UKPDS 34). *Lancet* 352: 854-865, 1998.

Van Renterghem C., Vigne P., Barhanin J., Schmid-Alliana A., Frelin C., Lazdunski M. Molecular mechanism of endothelin-1 action on aortic cells. *J. Cardiovasc. Pharmacol.* 13: (Suppl 5) 186-187, 1989.

Van Tilburg A. J. P., De Rooij F. W. M., Van Blankenstein M., Van Den Berg J. W. O., Bosman-Jacobs E. P. Na⁺-dependent bile acid transport in the ileum: The balance between diarrhoea and constipation. *Gastroenterology* 98: 25-32, 1990.

Vazquez C. M., Molina M. T., Ilundain A. Role of rat large intestine in reducing diarrhoea after 50% or 80% distal small bowel resection. *Dig. Dis. Sci.* 34: 1713-1719, 1989.

Vidon N., Chaussade S., Noel M., Franchisseur C., Huchet B., Bernier J. J. Metformin in the digestive tract. *Diabetes Res. Clin. Pract.* 4: 223-229, 1988.

Vlahcevic Z. R., Heuman D. M., Hylemon P. B. Regulation of bile acid synthesis. *Hepatology* 13: 590-600, 1991.

Vlahcevic Z. R., Jairath S. K., Heuman D. M., Stravitz R. T., Hylemon P. B., Avadhani N. G., Pandak W. M. Transcriptional regulation of hepatic sterol 27-hydroxylase by bile acids. *Am. J. Physiol.* 270: G646-G652, 1996.

Vlahcevic Z. R., Pandak W. M., Stravitz R. T. Regulation of bile acid biosynthesis. In: Bile Salts: Metabolic, Pathologic, and Therapeutic Considerations. *Gastroenterology Clinics of North America*. 28: (1) 1-25, 1999.

Vodenlich A. D., Gong Y.-Z., Geoghegan K. F., Lin M. C., Lanzetti A. J., Wilson F. A. Identification of the 14 kDa bile acid transport protein of rat ileal cytosol as gastrotropin. *Biochem. Biophys. Res. Comm.* 177: 1147-1154, 1991.

Voyta J. C., Via D. P., Butterfield C. E., Zetter B. R. Identification and isolation of endothelial cells based on their increased uptake of acetylated-low density lipoprotein. *J. Cell Biol.* 99: 2034-2040, 1984.

Waldman S. A., Murad F. Biochemical mechanisms underlying vascular smooth muscle relaxation: the guanylate cyclase-cyclic GMP system. *J. Cardiovasc. Pharmacol.* 12: (Suppl 5) S115-S118, 1988.

Walker P. S., Ramlal T., Donovan J. A., Doering T. P., Sandra A., Klip A., Pessin J. E. Insulin and glucose-dependent regulation of the glucose transport system in the rat L6 skeletal muscle cell line. *J. Biol. Chem.* 264: 6587-6595, 1989.

Wang H., Chen J., Hollister K., Sowers L. C., Forman B. M. Endogenous bile acids are ligands for the nuclear receptor FXR/BAR. *Mol. Cell* 3: 543-553, 1999.

Way K. J., Chou E., King G. L. Identification of PKC-isoform-specific biological actions using pharmacological approaches. *Trends Pharm. Sci.* 21: 181-186, 2000.

Webb B. L. J., Hirst S. J., Giembycz M. A. Protein kinase C isoenzymes: a review of their structure, regulation and role in regulating airways smooth muscle tone and mitogenesis. *Br. J. Pharmacol.* 130: 1433-1452, 2000.

Wegener J. W., Gath I., Förstermann U., Nawrath H. Activation of soluble guanylyl cyclase by YC-1 in aortic smooth muscle but not in ventricular myocardium from rat. *Br. J. Pharmacol.* 122: 1523-1529, 1997.

Weinberg SL, Burckhardt G, Wilson FA. Taurocholate transport by rat intestinal basolateral membrane vesicles. Evidence for the presence of an anion exchange transport system. *J. Clin. Invest.* 78: 44-50, 1986.

Weir G. C., Leahy J. L. Pathogenesis of non-insulin-dependent (type II) diabetes mellitus. In: *Joslin's Diabetes Mellitus, Thirteenth Edition*. Eds. Kahn M. C., Weir G. C. Lea and Febiger, Philadelphia. Chapter 14, pp 240-264, 1994.

Westerbacka J., Vehkavaara S., Bergholm R., Wilkinson I., Cockcroft J., Yki-Järvinen H. Marked resistance of the ability of insulin to decrease arterial stiffness characterises human obesity. *Diabetes* 48: 821-827, 1999.

White R. E., Carrier G. O., Vascular contraction induced by activation of membrane calcium ion channels is enhanced in streptozotocin-diabetes. *J. Pharmacol. Exp. Ther.* 253: 1057-1062, 1990.

Wiernsperger N. F. Membrane physiology as a basis for the cellular effects of metformin in insulin resistance and diabetes. *Diabetes Metab.* 25: 110-127, 1999.

Wiernsperger N. F., Bailey C. J. The antihyperglycaemic effect of metformin. Therapeutic and cellular mechanisms. *Drugs* 58: 31-39, 1999.

- Wilcock C., Bailey C. J. Accumulation of metformin by tissues of the normal and diabetic mouse. *Xenobiotica* **24**: 49-57, 1994.
- Wilcock C., Wyre N. D., Bailey C. J. Subcellular distribution of metformin in rat liver. *J. Pharm. Pharmac.* **43**: 442-444, 1991.
- Wild G., Madsen K., Thomson A. B. R. Intestinal tight junctions and their importance in health and disease: role of dietary lipids. *J. Nutr. Biochem.* **8**: 2-12, 1997.
- Williamson J. R., Kreisberg R. A., Felts P. W. Mechanism for the stimulation of gluconeogenesis by fatty acids in perfused rat liver. *Proc. Natl. Acad. Sci. USA* **56**: 247-254, 1966.
- Wilson T. H., Wiseman G. The use of sacs of everted small intestine for the study of the transference of substances from the mucosal to the serosal surface. *J. Physiol.* **123**: 116-125, 1954.
- Witztum J. L., Fisher M., Pietro T., Steinbrecher U. P., Elam R. L. Nonenzymatic glucosylation of high-density lipoprotein accelerates its catabolism in guinea pigs. *Diabetes* **31**: 1029-1032, 1982.
- Wong K. K. Effect of a cholesterol-rich diet on the excitability of rabbit aorta. *Biochem. Mol. Biol. Internat.* **40**: 389-393, 1996.
- Wong K. K., Tzeng S. F. Norepinephrine-induced contractile responses in isolated rat aortae from different duration of diabetes. *Artery* **19**: 1-13, 1992.
- Woodcock S., Williamson I., Hassan I., Mackay M. Isolation and characterisation of clones from the Caco-2 cell line displaying increased taurocholic acid transport. *J. Cell Sci.* **98**: 323-332, 1991.
- Wu X., Somlyo A. V., Somlyo A. P. Cyclic GMP-dependent stimulation reverses G-protein-coupled inhibition of smooth muscle myosin light chain phosphatase. *Biochem. Biophys. Res. Comm.* **220**: 658-663, 1996.
- Yaffe D. Retention of differentiation potentialities during prolonged cultivation of myogenic cells. *Proc. Natl. Acad. Sci. USA* **61**: 477-483, 1968.
- Yanagisawa M., Inoue A., Ishikawa T., Kasuya Y., Kimura S., Kumagaye S-I., Nakajima K., Watanabe T. X., Sakakibara S., Goto K., Masaki T. Primary structure, synthesis, and biological activity of rat endothelin, an endothelium-derived vasoconstrictor peptide. *Proc. Natl. Acad. Sci. USA* **85**: 6964-6967, 1988a.
- Yanagisawa M., Kurihara H., Kimura S., Tomobe Y., Kobayashi M., Mitsui Y., Yazaki Y., Goto K., Masaki T. A novel potent vasoconstrictor peptide produced by vascular endothelial cells. *Nature* **332**: 411-415, 1988b.

Zeng G., Quon M. J. Insulin-stimulated production of nitric oxide is inhibited by wortmannin. Direct measurement in vascular endothelial cells. *J. Clin. Invest.* **98**: 894-898, 1996.

Appendices

Appendix I:

Figure a:

Confluent monolayer of the Caco-2 cell model (human) x 10

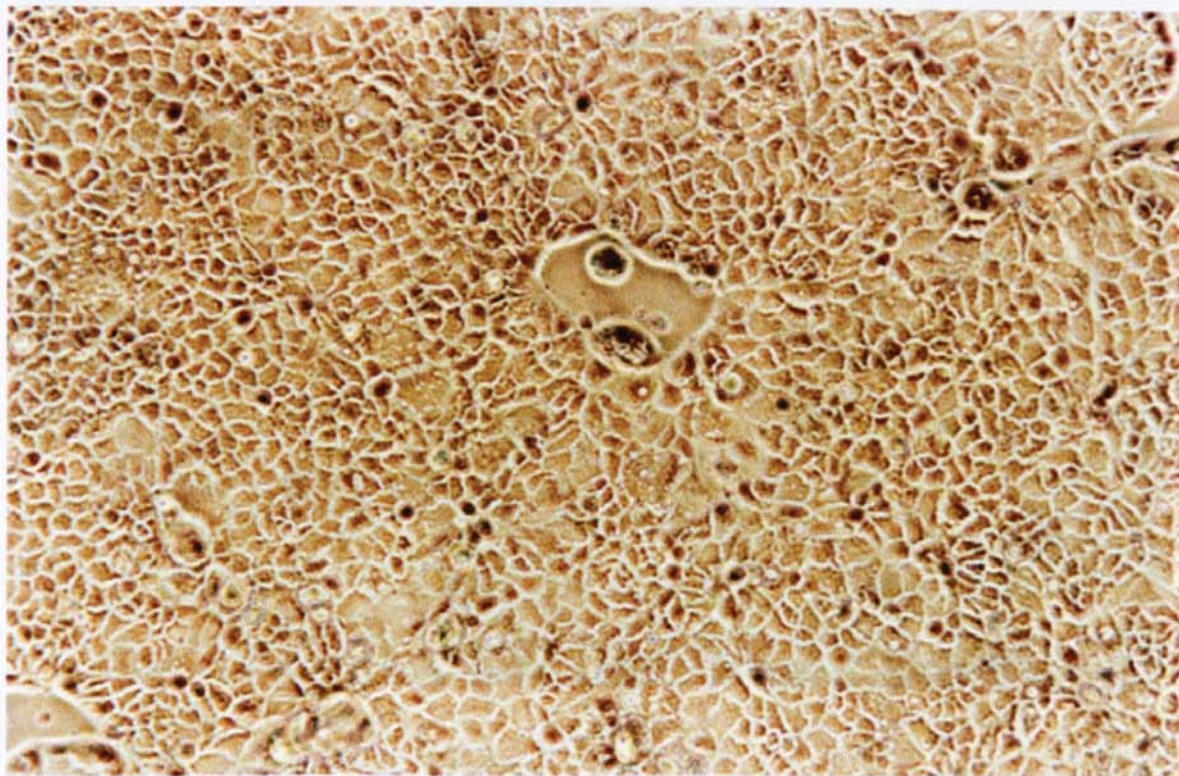


Figure b:

Confluent monolayer of the Caco-2 cell model (human) x 40

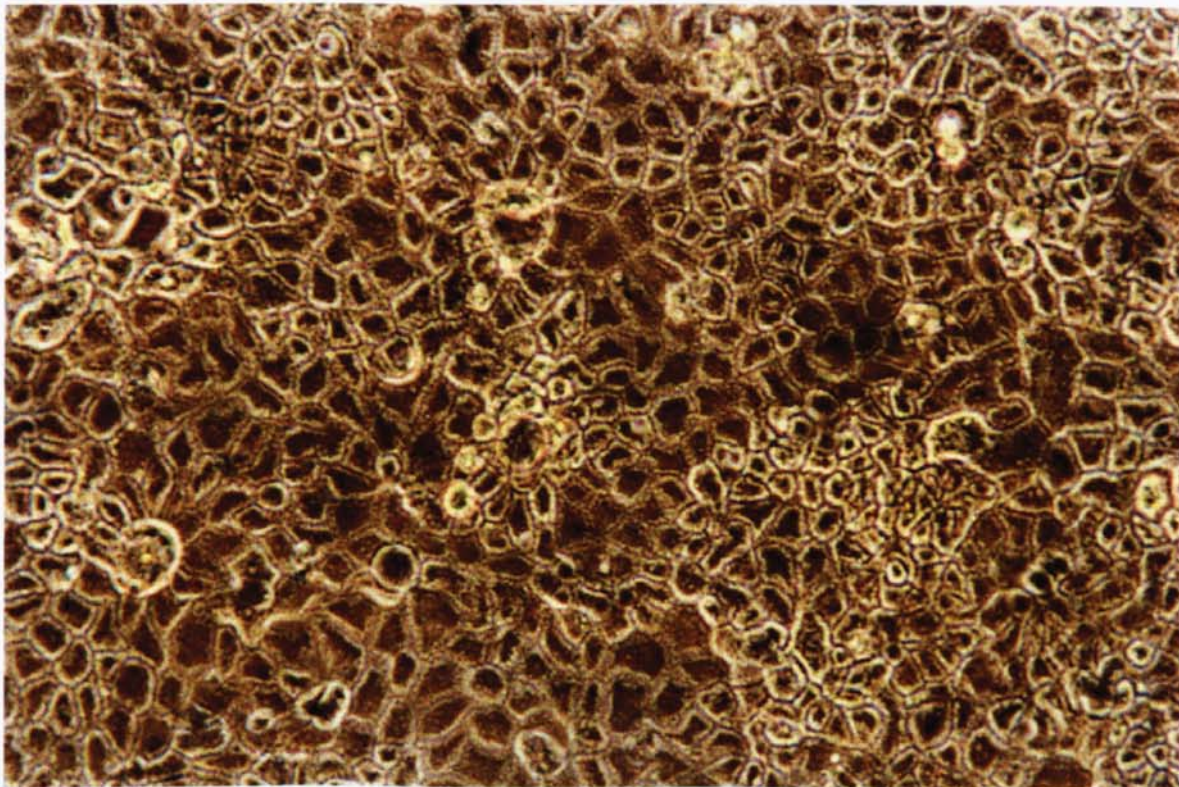


Figure c:



Multimyograph system used in the vascular compliance studies based on the Mulvany and Halpern design

Figure d:



Figure e:

Cryostat section ($12\mu\text{m}$) of thoracic aorta from a cholesterol and metformin treated mouse following an aneurism x 10 H + E. Yellow colouration represents oxidised haemoglobin

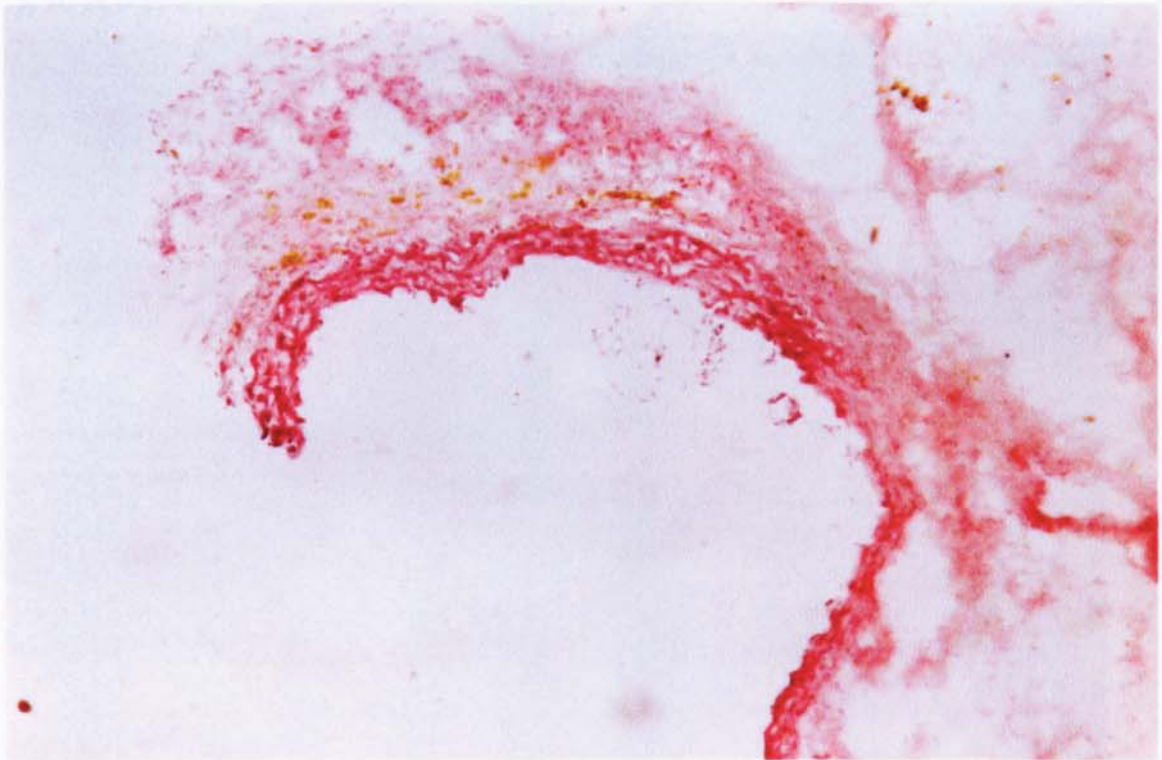


Figure f:

Cryostat section ($12\mu\text{m}$) of thoracic aorta from a cholesterol and metformin treated mouse following an aneurism x 40 H + E. Yellow colouration (arrow) represents oxidised haemoglobin

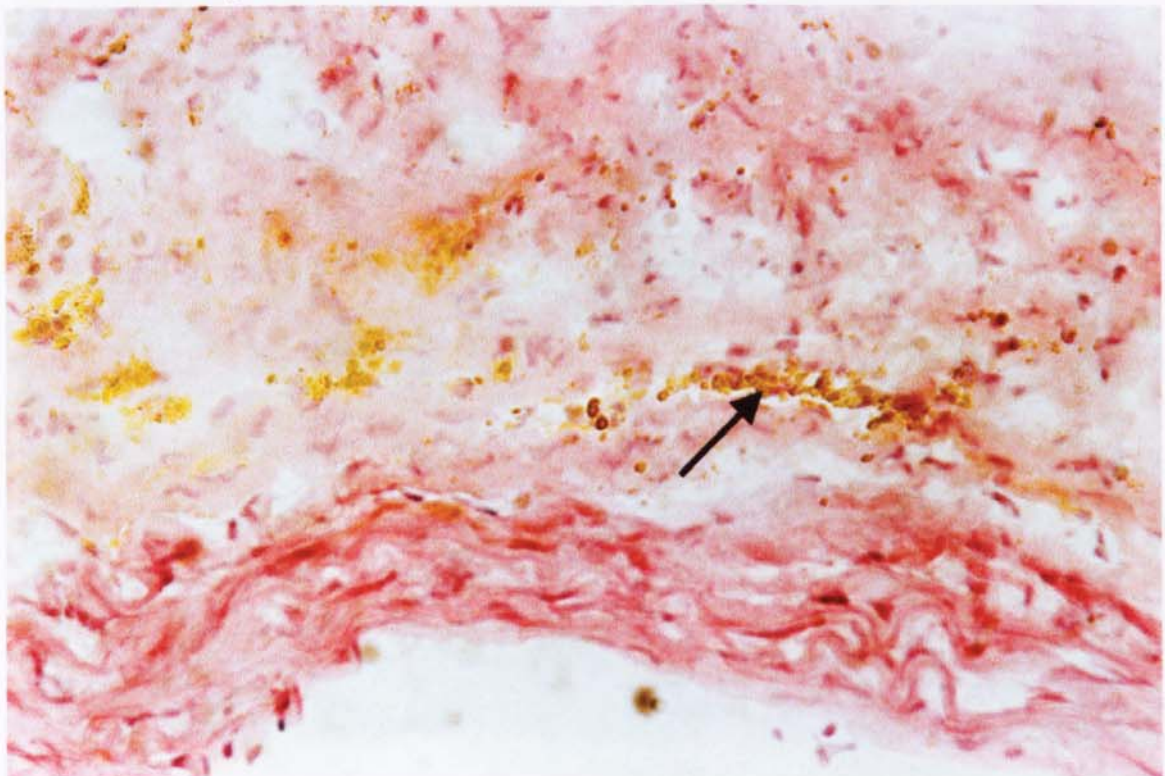


Figure g:

Cryostat section ($12\mu\text{m}$) of thoracic aorta from a control animal (standard diet)
 $\times 10$ H + E

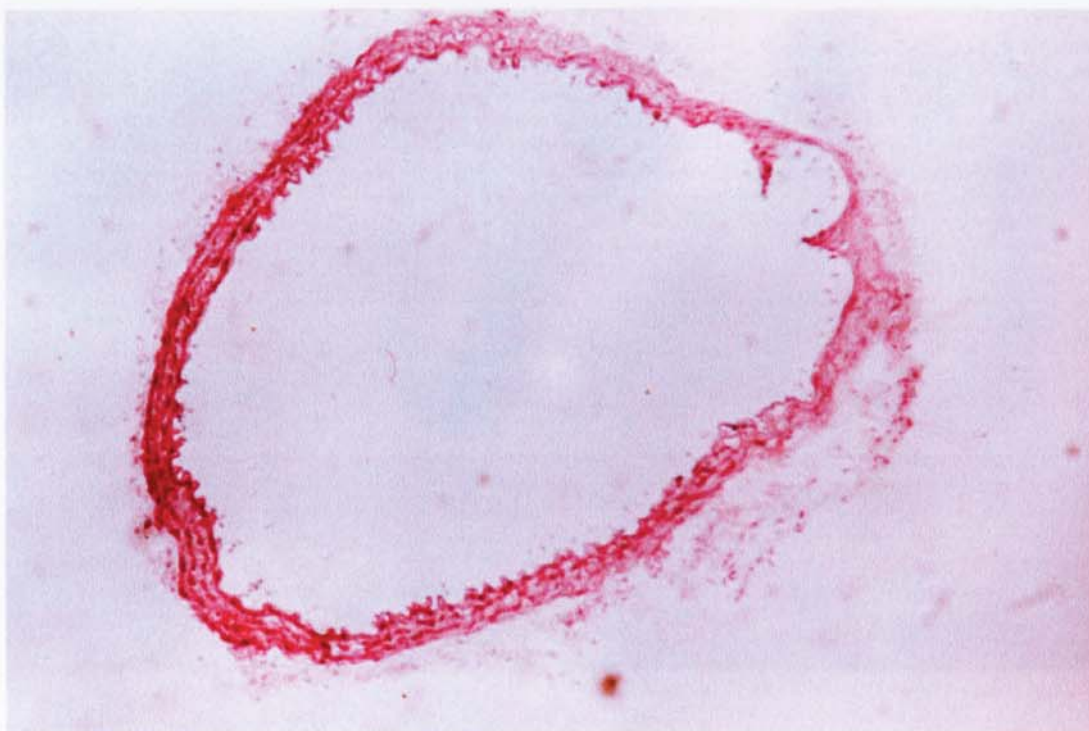


Figure h:

Cryostat section ($12\mu\text{m}$) of thoracic aorta from a control animal (standard diet)
 $\times 40$ H + E. Arrow identifies damage to the luminal surface of the vessel



Figure i:

Cryostat section ($12\mu\text{m}$) of thoracic aorta from a cholesterol fed mouse x 10 H + E

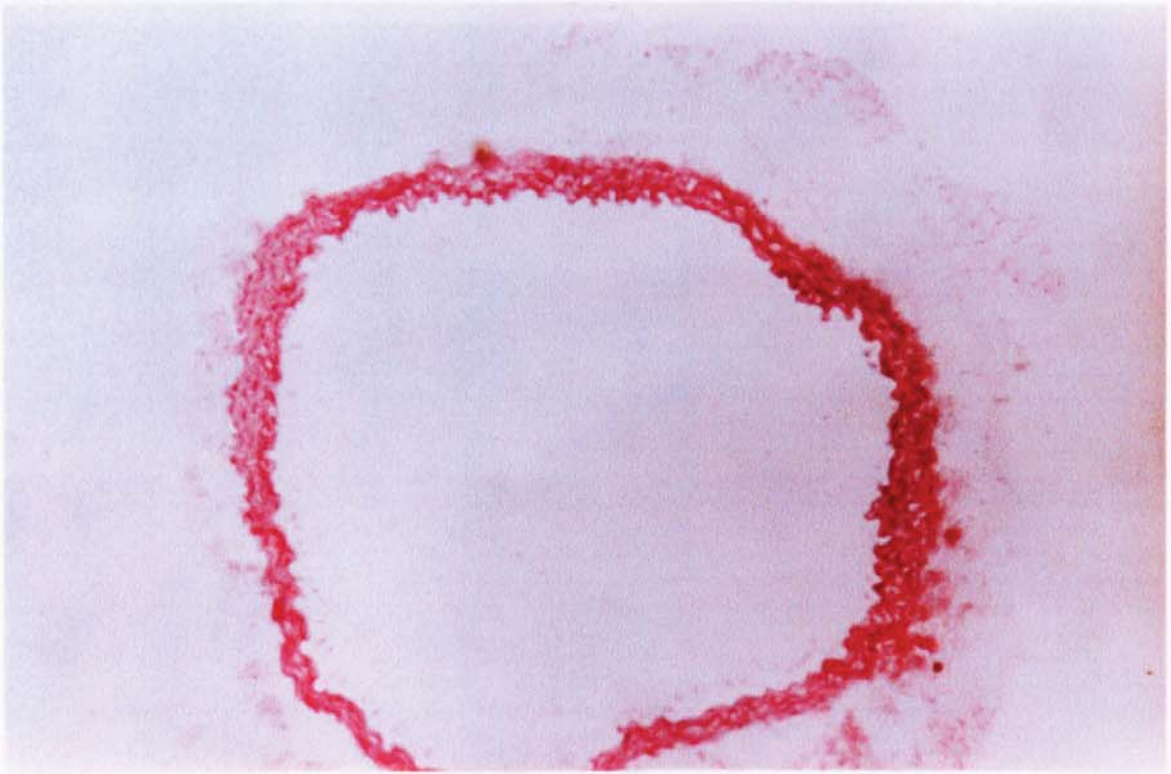


Figure j:

Cryostat section ($12\mu\text{m}$) of thoracic aorta from a cholesterol fed mouse stained using the method described by Emis *et al.*, 1977 x 10. Note insoluble brown colouration as indicated by the arrow depicting presence of cholesterol



Figure k:

Cryostat section ($12\mu\text{m}$) of mouse thoracic aorta stained with Sudan III + IV x 40

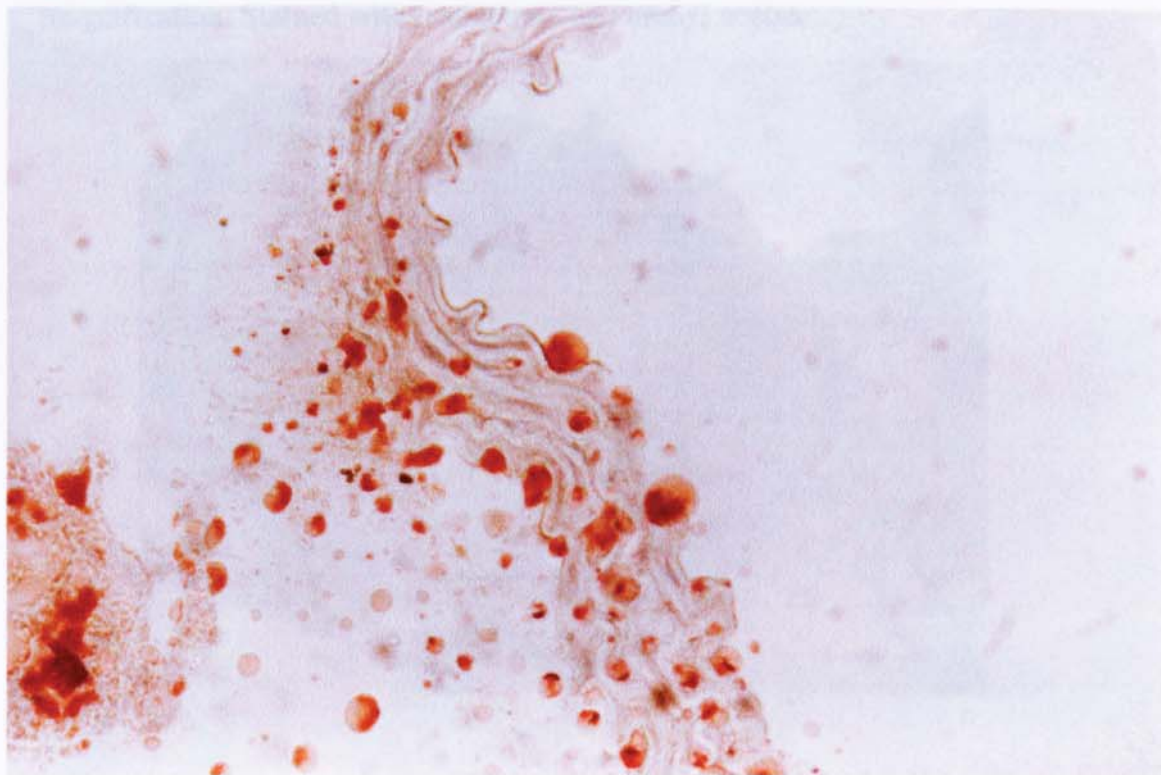


Figure l:

Cryostat section ($12\mu\text{m}$) of mouse thoracic aorta stained with Oil Red O x 40

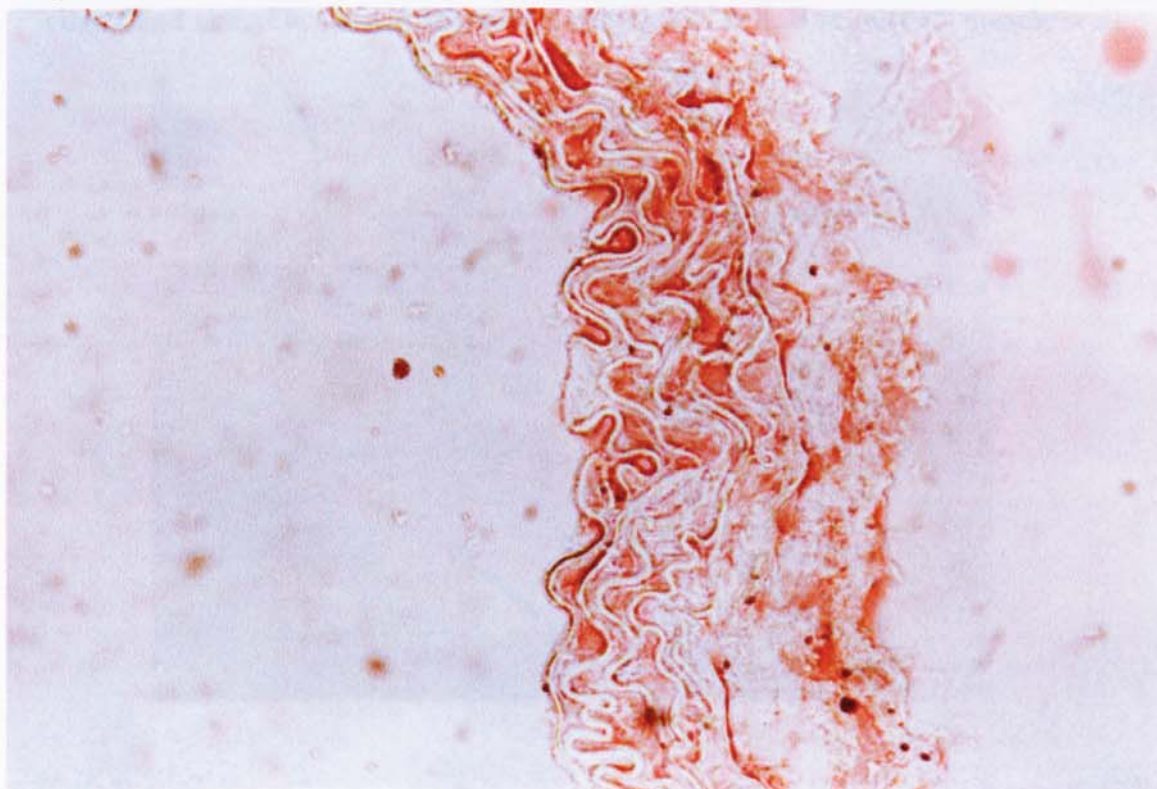


Figure m:

Transmission electron micrograph of mouse thoracic aorta detailing an endothelial cell attached to the luminal surface of the vessel x 15.000 magnification. Stained with lead citrate and uranyl acetate

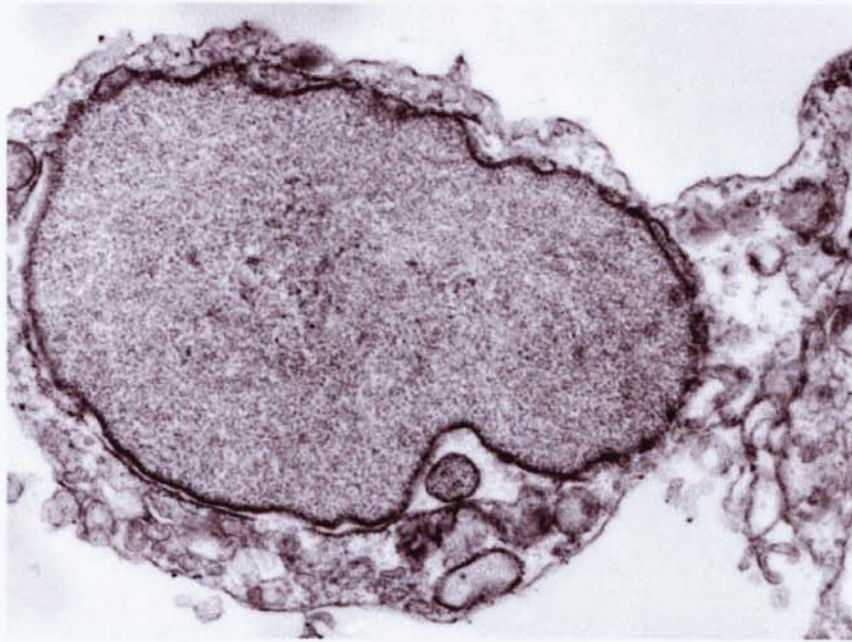


Figure n:

Transmission electron micrograph of mouse thoracic aorta detailing an endothelial cell and the luminal surface of the vessel x 12.000 magnification. Stained with lead citrate and uranyl acetate. A represents endothelial cell, B represents muscle wall

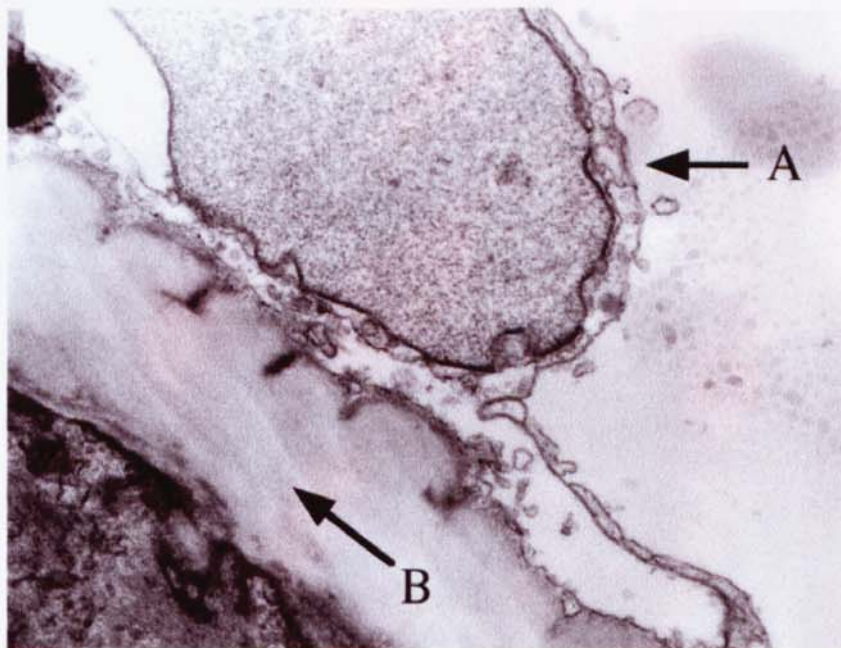


Figure 0:

Confluent monolayer of A7r5 smooth muscle cells (embryonic rat) x 40

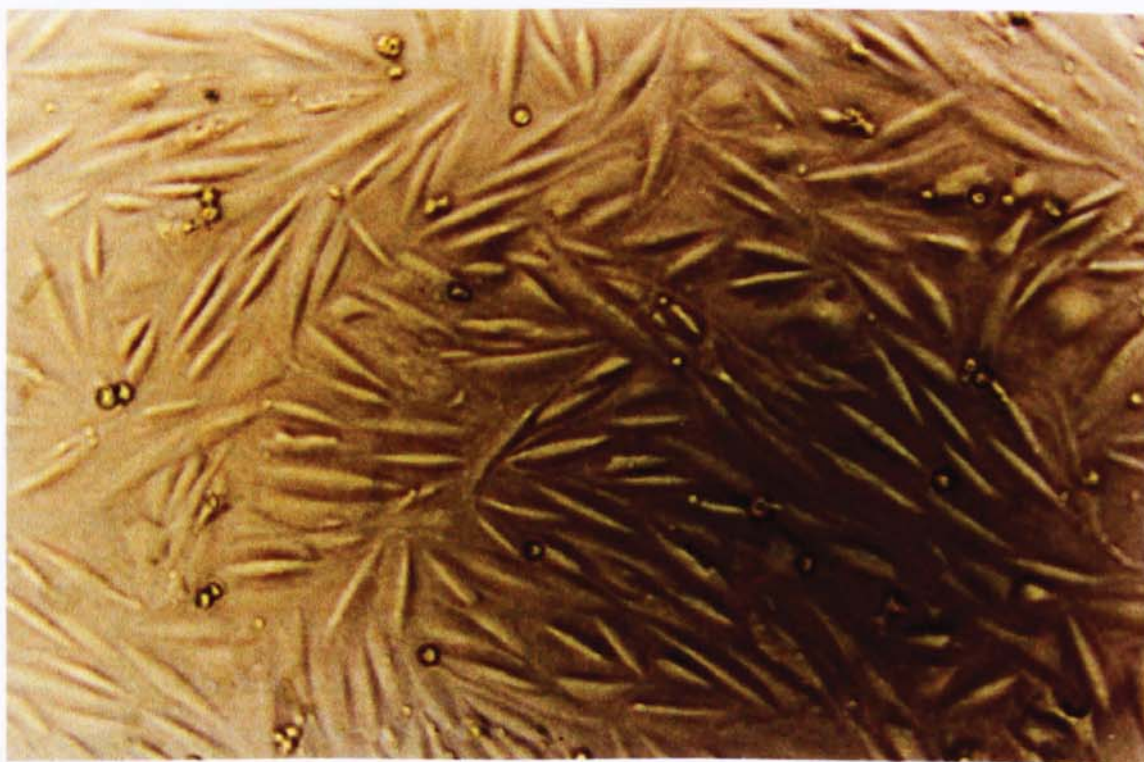
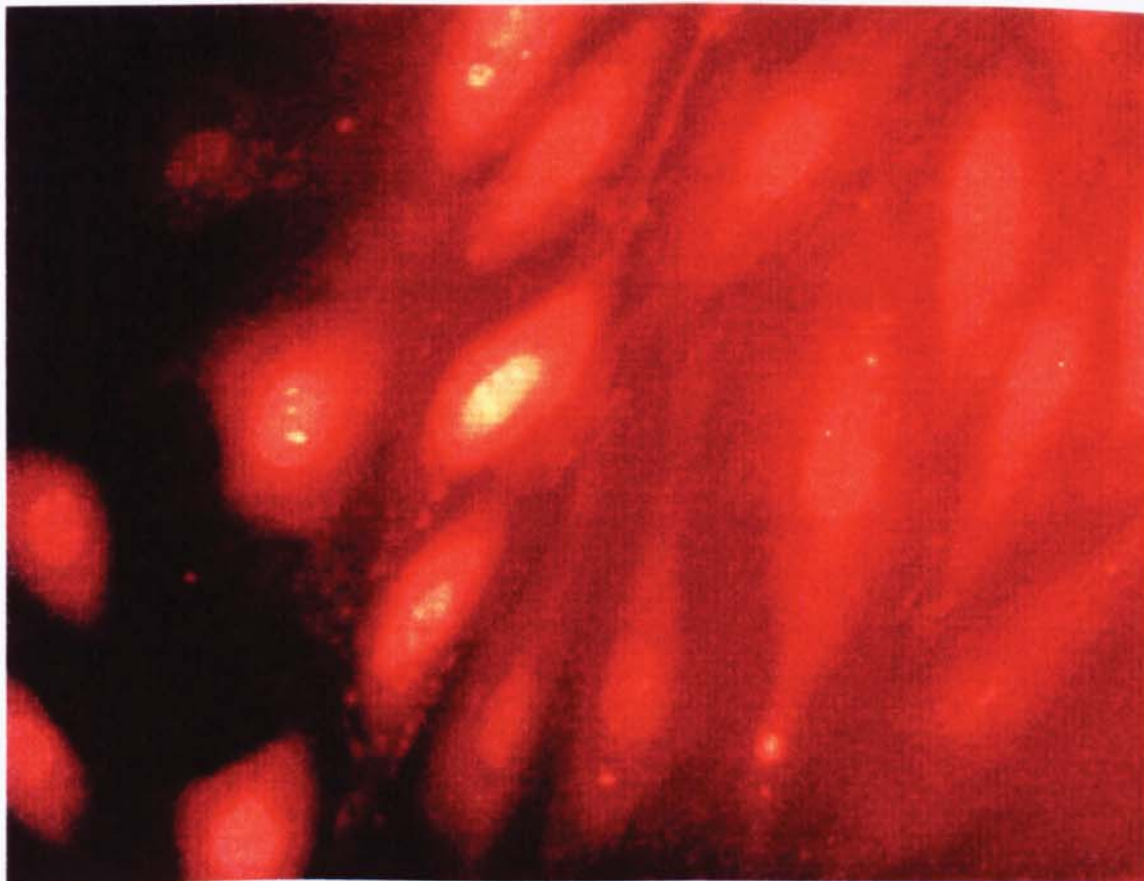


Figure p:

Cluster of confluent A7r5 smooth muscle cells (embryonic rat) incubated with Fura-2 and excited using the fluorescence ratio 360:380 nm (x 40 water immersion)



Appendix II: Physiological Buffers

Physiological salt solution:

Used as a bathing solution during arterial compliance studies.

Palmer A. M., Thomas C. R., Gopaul N., Dhir S., Anggard E. E., Poston L., Tribe R. M. Dietary antioxidant supplementation reduces lipid peroxidation but impairs vascular function in small mesenteric arteries of the streptozotocin-diabetic rat. *Diabetologia* 41: 148-156, 1998.

Compound	mmol/l	Molecular weight	g/litre
NaCl	119	58.44	6.9544
NaHCO ₃	25	84.01	2.1003
KH ₂ PO ₄	1.18	136.09	0.1606
MgSO ₄ (7H ₂ O)	1.17	246.48	0.2884
KCl	4.7	74.56	0.3504
EDTA	10	292.25	-
CaCl ₂ (dihydrate)	1.27	147	-
D-glucose	5.5	180.16	0.99088
Ascorbic acid	100	176.13	-
Propranolol	10	295.8	2.958

EDTA should be prepared as a 0.01M solution in 100ml PSS and 1ml added per litre of buffer.

Ascorbic acid should be prepared as a 0.1M solution in 100ml PSS and 0.5ml added per litre of buffer.

Calcium chloride should be prepared as a 1.27M stock solution and 1µl added per ml of buffer.

Krebs-Ringer Solution:

Used as a bathing and incubating solution during everted intestinal sac experiments. Also as an incubating solution for L6 cell culture experimentation.

*Biochem. Biophys. Acta.*4: 249, 1950.

Compound	mmol/l	Molecular weight	g/litre
NaCl	118	58.44	6.920
KCl	5	74.56	0.354
NaHCO ₃	25	84.01	2.100
MgSO ₄ (7H ₂ O)	1.18	246.48	0.290
KH ₂ PO ₄	1.17	136.09	0.324
D-glucose	10	180.16	1.802

Solution should be pre-gassed with 5% CO₂ and 95% O₂ for 20 minutes.

Calcium chloride should be prepared as a 1.27M stock and 1µl added per ml buffer.

Krebs-Henseleit:

Used as a bathing and incubating solution during everted gut sac experiments.

*Hoppe-Seyler's Z. physiol. Chem.*210: 33, 1932.

Compound	mmol/l	Molecular weight	g/litre
NaCl	117.55	58.44	6.87
KCl	5.36	74.56	0.4
MgSO ₄ (7H ₂ O)	0.568	246.48	0.14
CaCl ₂	1.905	147.02	0.28
NaH ₂ PO ₄	1.167	119.98	0.14
NaHCO ₃	24.99	84.01	2.1
Glucose	11	180.16	2

Physiological salt solution:

Used as a bathing and perfusion solution during calcium imaging experiments.

Borin M. L., Tribe R. M., Blaustein M. P. Increased intracellular Na⁺ augments mobilisation of Ca²⁺ from SR in vascular smooth muscle cells. *Am. J. Physiol.* 266: C311-C317, 1994.

Compound	mmol/l
NaCl	140
KCl	5.9
NaH ₂ PO ₄	1.2
NaHCO ₃	5
MgCl ₂	1.4
CaCl ₂	1.8
D-glucose	11.5
HEPES	10

Buffer should be adjusted to pH 7.4 using concentrated NaOH prior to use.

Appendix II: Staining Solutions

Carazzi's Haematoxylin.

Haematoxylin	5g
Glycerol	100ml
Potassium alum	25g
Distilled Water	400ml
Potassium Iodate	0.1g

Oil Red O.

Solution prepared by adding Oil Red O to 70% alcohol until supersaturated.

Oil Red O protocol: Bancroft J. D., Stevens A. Theory and Practice of Histological Techniques. Fourth Edition. Churchill Livingstone, New York. Chapter 11, pp213-242, 1996.

- 1) Sections should be air dried
- 2) Rinse in 70% alcohol
- 3) Stain in saturated Oil red O solution (maximum 2 hours)
- 4) Rinse in 70% alcohol
- 5) Rinse in running tap water
- 6) Counterstain with Carazzi's haematoxylin (3 minutes)
- 7) Blue in tap water
- 8) Rinse in distilled water
- 9) Mount in glycerine jelly

Sudan III and IV.

Solution prepared by adding 200ml 70% alcohol and saturating with equal parts of Sudan III and IV at 37°C. Add 200ml acetone. Allow to stand at room temperature overnight and then filter.

Sudan protocol: Bancroft J. D., Stevens A. Theory and Practice of Histological Techniques. Fourth Edition. Churchill Livingstone, New York. Chapter 11, pp213-242, 1996.

- 1) Freeze and cut tissue
- 2) Place in 30% alcohol followed by 70% alcohol (30 seconds)
- 3) Stain with filtered Sudan solution (1-2 minutes)
- 4) Rinse briefly in 70% alcohol (30 seconds)
- 5) Rinse in 30% alcohol (30 seconds –1 minute)
- 6) Counterstain with haematoxylin (maximum 30 seconds)
- 7) Rinse and blue in running tap water (10 minutes)
- 8) Mount using a aqueous mounting medium

Perchloric acid-naphthoquinone (PAN) method for cholesterol:

Adams C. W. M. A Perchloric acid-naphthoquinone method for the histochemical localisation of cholesterol. *Nature* **192**: 331-332, 1961.

1,2-naphthoquinone-4-sulphonic acid	40mg
Ethanol	20ml
Perchloric acid (60%)	10ml
Formaldehyde (40%)	1ml
Distilled water	9ml

Solution should be mixed and used within 24 hours.

PAN protocol: Bancroft J. D., Stevens A. Theory and Practice of Histological Techniques. Fourth Edition. Churchill Livingstone, New York. Chapter 11, pp213-242, 1996.

- 1) Sections should be air dried and treated with 1% ferric chloride for 4 hours
- 2) Rinse in distilled water

- 3) Sections are painted with the solution and heated at 60-70°C for upto 5 minutes
- 4) A blue colour should develop whilst heating
- 5) Add 1-2 drops of perchloric acid onto a cover slip and lower sections once colour has developed

Rapid Haematoxylin and Eosin for frozen sections:

Bancroft J. D., Stevens A. Theory and Practice of Histological Techniques. Fourth Edition. Churchill Livingstone, New York. Chapter 11, pp213-242, 1996.

- 1) Sections should be air dried and then fixed in formol-calcium (20 seconds)
- 2) Rinse in water
- 3) Stain in haematoxylin
- 4) Rinse in running tap water
- 5) Stain in eosin for 10 seconds
- 6) Rinse in running tap water
- 7) Dehydrate through 70% and 100% alcohol
- 8) Pass through xylene
- 9) Mount with DPX

Electron microscopy (TEM) specimen preparation:

Mollenhauer H. H. Plastic embedding mixtures for use in electron microscopy. *Stain technol.* 39: 111, 1964.

- 1) Carefully dissect tissue sample, ideally 1mm × 1mm × 2mm
- 2) Place sample in 2.5% glutaraldehyde (60 minutes)
- 3) Place in 1% osmium tetroxide (60 minutes)
- 4) Dehydrate samples through 70%, 90%, 3 × 100% ethanol (15 minutes per stage)
- 5) Pass samples through propylene oxide (15 minutes)
- 6) Repeat
- 7) Prepare mixture of propylene oxide and resin 1:1 (45 minutes)
- 8) Embed samples in epoxy resin under vacuum in plastic moulds (20 minutes)

- 9) Polymerise samples at atmospheric pressure for 24 hours at 60°C
- 10) Trim specimen
- 11) Deliver ultra-thin sections (70nm) onto electron microscope grids
- 12) Stain with uranyl acetate and Reynolds Lead citrate
- 13) Examine under transmission electron microscopy